DOE/WIPP 88-004

FACIES VARIABILITY AND POST-DEPOSITIONAL ALTERATION WITHIN THE RUSTLER FORMATION IN THE VICINITY OF THE WASTE ISOLATION PILOT PLANT, SOUTHEASTERN NEW MEXICO

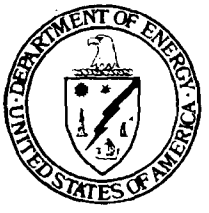

waste isolation pilot plant

DOE/WIPP-88-004

FACIES VARIABILITY AND POST-DEPOSITIONAL ALTERATION WITHIN THE RUSTLER FORMATION IN THE VICINITY OF THE WASTE ISOLATION PILOT PLANT, SOUTHEASTERN NEW MEXICO

AUTHORS

Robert M. Holt - IT Corporation

Dennis W. Powers - IT Corporation

January, 1988

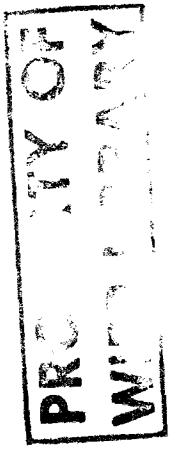

Any comments or questions regarding this report should be directed to the U.S. Department of Energy

WIPP Project Office

P.O. Box 3090

Carlsbad, NM 88221

or to the Manager

Engineering and Repository Technology

Westinghouse Electric Corporation

P.O. Box 2078

Carlsbad, NM 88221

This report was prepared for the U.S. Department of Energy by the Engineering and Repository Technology Department of the Management and Operating Contractor, Waste Isolation Pilot Plant Project, under Contract No. DE-AC04-86AL31950

Printed in the United States of America

Available from
National Technical Information Service
U.S. Department of Commerce
5285 Port Royal Road
Springfield, VA 22161
NTIS Price Codes: Printed Copy A04
Microfiche A01

FOREWORD

Over the history of the WIPP project, extraordinary properties have been attributed to "the halite that was" ... and wasn't in the Rustler. Halite is quite thick in some members of the Rustler east of the site; these same members are much thinner and are mostly mudstone at the WIPP site. A simple assumption was made that these halites continued laterally - after all, some of the beds above and below are continuous over very large areas. The mudstones then must be "dissolution residues," following this simple assumption. Still, we know that environments always change laterally, and halite (or mudstone or carbonate) must give way laterally to another rock or an area that isn't accumulating halite. Where were these transitions for the Rustler?

After our experience mapping the waste shaft, we felt strongly that we were seeing transitional area. The bedding, fossils, bioturbation, and sedimentary structures were convincing evidence to us that the shaft area had not undergone significant dissolution since the Rustler was deposited and that sufficient features were observable in shafts and cores to recontruct depositional environments. From this reconstruction, we expected that more realistic limits could be placed on the extent of salt dissolved from the Rustler since the Permian. Here we report our reconstructed depositional environments.

The initial response to our mapping experience varied, though much of it was skeptical. Some workers have felt strongly that expectations of lateral continuity outweigh specific evidence we presented such as continuity of bedding and primary sedimentary features. Very slow dissolution was postulated, so that sedimentary features and relationships can be preserved while 75 to 90% of the rock is removed. While we are reluctant to say that such a process cannot occur, we believe a more appropriate explanation is available.

Halite does appear and disappear in parts of the Rustler. But observable features and relationships in the Rustler indicate that it can disappear soon after it was deposited, as might be expected for one of the more soluble of evaporite minerals. It creates interpretable structures as it is dissolved, some of which are newly described in this report. We hope that other geologists who are interested in evaporites will benefit from our experience, too.

Many individuals have helped us during this investigation. Not all can reasonably be acknowledged, but some have been extensively involved: Mel Balderrama, David Frederick, Merrie Martin, Kathy Schiel, Mary Jane Graham, Linda Foster, and Judi Williamson. We thank them for persevering. The manuscript was reviewed by Steve Lambert, Sue Hovorka, Rick Deshler, Barb Deshler, Roy McKinney, Dwight Deal, and Ken Broberg, Mike Schulz, and Bennet Young. We especially thank Steve Lambert, Sue Hovorka, and Barb Deshler for their extra time and effort. We absolve all of the above for any mistakes we may have made.

The main thrust of this report is to describe and interpret sedimentological features in terms of depositional environments. It was written mainly for sedimentologists. A few obscure but useful words are explained in the text. We anticipate that geologists less familiar with evaporites and sedimentology will require occasional reference to the American Geological Institute Glossary of Geology, 3rd ed., ed. by R.L. Bates and J.A. Jackson.

Robert M. Holt

Dennis W. Powers

ABSTRACT

The late Permian Rustler Formation is the youngest of three evaporite-bearing formations in the Delaware Basin. The depositional environments which formed the Rustler and the post-depositional events which subsequently modified the Rustler have never before been investigated in a detailed, systematic way. The purpose of this study is to describe the detailed sedimentology and interpret the depositional environments of the Rustler. Another objective of this study is to reassess the extent of Rustler dissolution. The reconstructed depositional environments help to bound the extent and relative timing of dissolution. Existing literature was surveyed to distill criteria by which dissolution can be recognized. Microscopic examination of diagenetic alteration of the Rustler rounds out the evidence.

The Rustler was examined in detail in two shafts and many cores from the vicinity of the Waste Isolation Pilot Plant (WIPP) site in southeastern New Mexico. Nearly 600 geophysical logs from boreholes in southeastern New Mexico were interpreted, and the stratigraphy and lithology over a larger study area were related to units observed in cores and shafts from the WIPP site.

The Rustler consists of sulfates, carbonates, halite, and clastic rocks. Rustler sulfates and carbonates are areally extensive and vary little. Those zones containing halite and mudstone laterally change greatly in thickness and lithology. The Rustler thickens considerably toward a depocenter east and southeast of the WIPP site. Most of the variation in Rustler thickness is attributed to those stratigraphic intervals containing halite.

The depositional environments of the various units within the Rustler were reconstructed using a sedimentological approach. Carbonate and sulfate units were deposited subaqueously following a transgression or freshening event. Among the diagnostic features for subaqueous deposition are algal beds and laminations, bioturbation, fossils, gypsum growth textures, and cross-bedding sequences. Halite and mudstone units accumulated slowly due to repeated solution and reprecipitation of halite in salt pan and marginal mudflat environments. Subsidence in the depocenter allowed halite to accumulate and be preserved. Halite commonly was dissolved syndepositionally from parts of the halite and mudstone units. Small scale dissolution, often

reported in halite from both modern and ancient evaporite environments, was common, and, on a larger scale, syndepositional dissolution drastically modified the sedimentary sequence. Diagnostic features include pedogenic clay skins, incorporative gypsum, incorporative and displacive halite in various stages of growth and solution, and bedding. Smeared intraclast textures are a newly-described feature formed by repeated solution of halite in mudflat environments.

Several times during Rustler deposition, relatively fresh water transgressed rapidly over very low topography. Carbonate or sulfate formed subaqueously as evaporation proceeded. Salinity increased and the brine margins retracted as desiccation continued. Marginal clastics and a halite lens in the depocenter accumulated relatively slowly and were controlled by subsidence and cannibalism of soluble minerals at the margins. Deposition of these saline facies was abruptly ended by another freshening event. This style of deposition began with an initial marine transgression over the Salado and was repeated several times.

The Rustler in, and adjacent to, Nash Draw has been brecciated because of solution of the Salado. Breccias were superimposed on Rustler rocks, including clastic rocks exhibiting smeared intraclasts which are due to syndepositional dissolution. These breccias have a stratiform base, and the degree of brecciation diminished upwards. These features are consistent with post-depositional dissolution of a bed at depth as described in the literature. Some of these areas are now also being affected by karst processes (as at WIPP 33).

Most of the immediate site area is unaffected by large-scale post-depositional dissolution. Halite was removed from parts of the lower unnamed member, Tamarisk Member, and Forty-niner Member before overlying units were deposited. Minor brecciation at boreholes H-3 and H-11 indicates some dissolution and collapse after the Rustler was deposited. These boreholes are in marginal areas of the depositional environments where some halite precipitated in mudstone units. Part of the Tamarisk Member is brecciated in WIPP 13. Partial core from WIPP 13 limits interpretation of this anomaly. Halite is not predicted for the Tamarisk Member at this location, but the brecciation may have begun below the Tamarisk.

The Rustler has been altered extensively at the microscopic scale. Petrographic evidence demonstrates mainly volume-for-volume replacement of minerals, especially sulfates. Overgrowths on some clastic gypsum grains preserve shapes, suggesting the gypsum may never have inverted to anhydrite. These phenomena help limit hypotheses of the effects of the volume changes associated with sulfate mineral inversion.

TABLE OF CONTENTS

TABLE OF CONTENTS

(Continued)

TABLE OF CONTENTS
(Continued)

TABLE OF CONTENTS

(Continued)

TABLE OF CONTENTS

(Continued)

LIST OF TABLES

LIST OF FIGURES

LIST OF FIGURES
(Continued)

LIST OF PLATES

LIST OF PLATES
(Continued)

LIST OF APPENDICES

1.0 INTRODUCTION

The Late Permian Rustler Formation is the youngest of three Ochoan evaporite-bearing formations in the Delaware Basin, and it overlies the Salado Formation which contains the facility horizon of the Waste Isolation Pilot Plant (WIPP). The Rustler is being characterized in detail to understand the geological history of the strata overlying, and in the area surrounding, the WIPP. The long-term isolation of waste at the WIPP will be evaluated partly on our understanding of this geological history.

The Rustler must be characterized in two ways. First, the condition of the Rustler at the present time must be clearly understood. Hydrologic and water-quality data have been collected and synthesized to explain groundwater sources and movement in the Rustler. Second, data must be collected in order to interpret more precisely those events which formed the Rustler and subsequently modified it through geologic time. In this report, Rustler sedimentary features are reported and the depositional history of the Rustler is interpreted. Post-depositional history of the formation is partially assessed.

The WIPP project is a Department of Energy (DOE) research-and-development facility constructed to demonstrate the safe disposal of radioactive wastes derived from the defense activities of the United States. The WIPP site is located about 26 miles east of Carlsbad, New Mexico, in an area known as Los Medanos (Fig. 1.1).

1.1 GENERAL

The Late Permian Rustler Formation of the Delaware Basin in southeastern New Mexico and west Texas records, perhaps uniquely, the evaporitic end stages of a cratonic basin. The Rustler is unusual as it represents the transition from the thick bedded evaporites of the Salado Formation to the clastic dominated continental deposits of the Dewey Lake Redbeds (also called Dewey Lake Formation). Transitional deposits of this nature have not been widely investigated.

The depositional pattern of the Salado (thicker, laterally continuous beds of halite bounded by thinner, areally extensive beds of sulfate) did not continue in the Rustler. The Rustler lithology is more variable, consisting of interbedded sulfates, clastics, carbonates, and halite. The lower Rustler

contains principally clastic rocks with interbedded sulfates and halite. The upper Rustler consists of carbonates and thick sulfates which sandwich thinner units of clastics and laterally equivalent halite.

The depositional environments which produced the Rustler are poorly understood, as no attempt had been made until recently to collect and synthesize detailed sedimentological data into a depositional model (Holt and Powers, 1984, 1986a & b, 1987; Powers and Holt, 1984). Before this work, data on the Rustler came from studies of limited and highly disrupted outcrops (e.g. Vine, 1963), field examination of core, and general interpretations of geophysical logs. Most studies of ancient evaporites are based on observations of cores and interpretations made from geophysical logs. This is partially due to the fact that evaporites crop out poorly. Hydration and dissolution seldom leave original textures and features intact. Most core studies concentrate on recognizing features with modern analogs. In this study, an in situ sequence was directly observed and combined with detailed core description and geophysical log interpretation to yield a much better set of sedimentary features and more complete understanding of lateral lithologic relationships.

The Rustler at the WIPP site near Carlsbad, New Mexico, has been investigated recently in detail, providing unique lithologic data for this formation. The Rustler was directly observed, described, and geologically mapped in two shafts. The mapping revealed lateral relationships and sedimentary features that rarely are observed in core or surface outcrop. As the shafts displayed the entire Rustler section in situ, data from the shafts (Holt and Powers, 1984, 1986a) are superior to those collected by other means. Observations made in the WIPP shafts provided the impetus for further study; cores were also re-examined and redescribed, and lithologies were interpreted in some detail from geophysical logs. The purpose of this investigation is to synthesize the data collected from the northern Delaware Basin (WIPP site area) and surrounding areas into a detailed depositional model of the Rustler Formation. Once a detailed depositional model has been established, it becomes possible to separate depositional from diagenetic features and to more accurately access diagenetic models.

Jones and others (1973), Bachman (1974, 1976, 1980, 1984a), and Lambert (1983) have discussed dissolution or proposed models of dissolution for the Rustler in the vicinity of the WIPP. An improved understanding of the

depositional environments of the Rustler should enhance our understanding of any diagenetic events, including dissolution, that have affected the Rustler.

1.2 STUDY AREA

The Delaware Basin of southeastern New Mexico and west Texas is a major subdivision of the Permian Basin (Fig. 1.2). It is bounded on the west by the Diablo Platform, on the east by the Central Basin Platform, and on the north by the Northwestern Shelf. The areal extent of the basin is greater than 13,000 mi^2 (33,500 km^2), and it is filled with as much as 24,600 ft (7,500 m) of Phanerozoic sedimentary rocks (Hills, 1984). The Capitan reef almost completely surrounds the Delaware Basin. It is considered among the latest deposits immediately preceding deposition of the Ochoan evaporites. This study concentrates on the northern portion of the Delaware Basin and adjacent parts of the Northwestern Shelf and Central Basin Platform. The WIPP site lies among the vegetated dunes of the Los Medanos area, some 26 mi (42 km) east of Carlsbad, and is located in the northern part of the Delaware Basin between Nash Draw and San Simon Swale.

1.3 REVIEW OF PREVIOUS WORK

The depositional and diagenetic events which produced the Rustler Formation have not been investigated in any detailed, systematic way. Early workers (e.g. Lang, 1935; Adams, 1944) described the Rustler from outcrop and well data, but they provided little assessment of depositional environments or post-depositional events. Donegan and DeFord (1950) asserted that the Rustler was Permian in age on the basis of invertebrate fossils collected from the Culebra Dolomite Member of the Rustler in Culberson County, Texas. Walter (1953) further identified and examined these fossils, and he indicated that the environment was quite saline based on the restricted fauna. Vine (1963) described the Rustler outcrops in Nash Draw and the Rustler from a core south of the WIPP site as part of the geological work preparatory to Project Gnome, a nuclear device exploded in 1961 in the Salado Formation south of the WIPP site. Cooper and Glanzman (1971) and Gard (1968) provided final reports on hydrology and geology of the Project Gnome site that include considerable discussion of the Rustler stratigraphy and lithology as well as the effects of dissolution. Geologists from the U.S. Geological Survey prepared several reports in the early 1970s as part of broad site selection

activities for radioactive waste disposal that resulted in investigation of the Los Medanos area. Jones and others (1973) interpreted the regional thinning of the Rustler as the result of an eastward migrating wedge of dissolution.

Eager (1983) broadly described a core through the Rustler in Culberson County, Texas, and related lithology to geophysical logs. Six stratigraphic units were identified by Eager (1983): the four formal members and two informal members below the Culebra Dolomite Member. The basal 96 ft (29 m) was called the "siltstone member" and includes about 22 ft (6.7 m) of dolomite. The "lower gypsum and mudstone member" of Eager (1983) is between the "siltstone member" and the Culebra and is about 50 ft (15.2 m) thick. Eager (1983) attributes the Rustler to eolian, supratidal carbonate flats, brine pan and mud flat environments based on the general lithologic similarities to evaporites of the Palo Duro Basin as reported by Handford (1981), Handford and Fredericks (1980), McGillis and Presley (1981), and Presley and McGillis (1982).

Field investigations began in 1974 in the Los Medanos area to locate a site for the WIPP, and the present site was located in 1975. The site was investigated in detail to validate it based upon established criteria. The Rustler was deemed of importance to the WIPP as it overlies the Salado and contains two water-bearing units (the Magenta and Culebra Dolomite Members). The hydrology of the Rustler has been characterized extensively to help determine the likelihood of the Rustler acting as a conduit for radioactive materials to the biosphere. As part of the site investigations, a number of Rustler cores were taken. The initial field descriptions of those cores appear in basic data reports for each hole (e.g. Jones and Gonzalez, 1980). Data and interpretations of the hydrology of the Rustler have been presented in several WIPP documents (e.g. Mercer and Orr, 1979; Gonzales, 1982; Mercer, 1983). Ferrall and Gibbons (1980), Lambert (1983), and Powers and others (1978) discussed dissolution within the Rustler. The WIPP site location and design met all established criteria and the site validation report was published in 1983.

In 1984 and 1985, two shafts were enlarged or newly constructed through the Rustler to the WIPP facility level. These shafts were mapped in their entirety (Holt and Powers, 1984, 1986a), giving special attention to the Rustler. The Rustler exhibited none of the features that would be expected

if recent dissolution had occurred. Holt and Powers (1984) state that:

> "Post-depositional dissolution features were not observed in any stratigraphic horizons in the waste shaft. In fact, several zones previously identified as dissolution residues in nearby boreholes (e.g., ERDA-9) contain pronounced primary sedimentary features. This is of great significance since dissolution has, historically, been considered as an important process that has greatly modified the Rustler Formation in this area."

The authors were subsequently given the task to study in detail the sedimentology, depositional environments, and subsequent modifications of the Rustler, building on their unique experience in mapping and describing the Rustler in the waste handling and exhaust shafts. This report is the consequence of that task.

Several of the intervals within the Rustler were modified by diagenetic processes. Based upon examination of four cores and one geophysical log, Lowenstein (1987c) discussed post-depositional alteration within the Rustler. Bachman (1987b) reported on evaporite karst, culminating years of study of the processes and features in Ochoan rocks, including the Rustler. Diagenetic alterations are assessed in this study as they pertain to both the depositional environments and dissolution.

1.4 METHODS OF ANALYSIS OR APPROACH TO EVAPORITE STUDIES

As previously discussed, the surface outcrops of most ancient evaporites provide little or no significant data concerning the depositional environment which formed the evaporites or subsurface geologic processes that modified them. In turn, the majority of evaporite-related studies rely on two types of data from the subsurface: geophysical logs and core. Among the most common tools available for evaporite studies are geophysical logs. The geophysical log itself is data about the physical properties of the rocks that must be interpreted. The interpretations are sometimes not unique and are frequently based upon a factor which cannot be quantified - experience. Geophysical logs become more useful when the logs from holes containing core are compared with descriptions of that core. This procedure allows for better extrapolation of rock types away from a data area.

Geophysical log interpretations are limited. No information can be collected or inferred beyond that which is inherent in each specific logging tool. In the best of cases, geophysical logs individually may yield general or semi-quantitative information concerning density, water content, natural radioactivity, acoustic velocity, conductivity, resistivity, spontaneous potential and dip. As one type of geophysical log data does not usually yield a unique interpretation of lithology, geophysical log types are combined in a manner in which the data collected allows unique, or nearly so, interpretations of parameters of interest. At best, these interpretations can reveal general information concerning rock type, mineralogy and pore fluid type. Geophysical logs normally cannot provide any information concerning sedimentary features (although the dip log may indicate crossbedding). Therefore, it is improper to rely on geophysical logs for the interpretation of anything they are not designed to provide. The value of geophysical logs lies in their availability across the region of interest. Thus, vertical and lateral lithologic and stratigraphic relationships can be inferred from logs of boreholes without core, providing much greater range to interpret geological history for the Rustler.

In most cases, geophysical logs cannot provide the types of data most needed for accurate and detailed reconstruction of depositional and diagenetic models. Just as it is impossible, using geophysical logs, to differentiate directly between sulfate deposited in a sabkha and that deposited in a saline lagoon or lake, it is also generally impossible to distinguish between a clastically deposited mudstone and a mudstone residue left after the removal of salt. The features and fabrics we rely on for the interpretation of depositional environment and diagenetic history (including dissolution) come from direct observation of rock.

This can be done in one of two ways. First, rock samples collected by coring can easily be described and allow for the direct observation of sedimentary features. The surface of evaporite core is frequently less than ideal for detailed observations, so it is often desirable to cut a slab from the core. Another advantage of cores is that they can be taken from holes over a wide area relatively cheaply, providing a larger view of the unit. One disadvantage of the study of core is that the data are limited by core size and the chance of coring and preserving specific features of importance. Second, <u>in situ</u> observations of rock can be done in manmade underground openings such as shafts and drifts. Observation of the rocks <u>in</u>

situ has distinct advantages over observation of core, although it may be orders of magnitude more expensive than core. The entire sequence may be observed without interruption. Larger scale features may be readily observed and relationships not clear in core may be obvious. Thus the features observed in core can be understood with greater confidence.

Nevertheless, the surface of underground excavations is usually rough, and some of the details which are readily distinguishable in core may not bevisible. This is especially true for sulfate rocks. It is clear that the best approach toward collecting direct observational data is to use both core and observations from underground excavations, as one's weakness is the other's strength.

Other types of direct observations on evaporite cores or samples can be made. These include thin sections, X-ray diffraction, and other chemical and microscopic techniques.

As geophysical log data are more common and of greater areal extent than data collected from direct observations, it is important to integrate the data types. One can compare the direct observations from core with the geophysical logs and determine what geophysical log signatures correspond with the observed rocks. One can reasonably expect to extrapolate lithologies between direct data points via geophysical logs. Those interpretations become less valid when they are not bounded by directly observed data and lose validity further from a direct observation. It is best to use caution when using geophysical logs alone.

Once the data have been collected and compiled, features with easily recognizable modern depositional analogs should be identified. The sequence of occurrence of those features in both the lateral and vertical sense should be analyzed and lithofacies should be determined. As few ancient examples exactly mimic modern analogs, it is not necessary to find an exact environmental match. The processes which formed the sedimentary features are commonly recognizable. It is the assimilation of those processes and their inherent limitations that yields a range of possibilities of original depositional environment. Further narrowing of the field is then done by determining which of the possible models is inconsistent with the lateral and vertical lithofacies relationships. Once this process is completed on a small scale, it should then be reapplied to the larger scale. The most reasonable interpretation should be selected and tested.

Data have been compiled on several types of maps and diagrams for interpretation. Lithofacies are identified, and their lateral variations assessed. By comparing the features and facies relationships of the Rustler to modern analogs, depositional models have been generated for various parts of the Rustler and integrated to create a composite depositional model of the Rustler Formation.

2.0 GEOLOGIC HISTORY OF THE DELAWARE BASIN

2.1 PRE-PENNSYLVANIAN

Prior to the Late Mississippian, Paleozoic depositional patterns in the Delaware Basin reflect migrations of epeiric seas over the region and the structural development of the Tobosa Basin, the predecessor to the Permian Basin. From the Late Cambrian/Early Ordovician until the Late Mississippian, a nearly continuous record of sedimentation is preserved as the region was, for the most part, tectonically stable during that time. Carbonates deposited under shallow shelf conditions dominate the rock record. However, carbonate deposition was interrupted by shale sedimentation during the Middle Ordovician, Late Devonian, and Early Mississippian.

During and immediately following the Late Mississippian, the Delaware Basin began to develop structurally by vertical movement along pre-existing structural trends (Hills, 1984). A thick sequence of basinal shales was deposited in the Delaware Basin during the Late Mississippian.

2.2 PENNSYLVANIAN PERIOD

The tectonic processes that were initiated during the Mississippian continued into the Early Pennsylvanian, and clastic materials derived from the Pedernal uplift in central New Mexico, the exposed Central Basin Platform, mountains in the Ouachita-Marathon area, and the Matador Arch filled the growing Delaware Basin (Hills, 1984; Powers and others, 1978).

During the Middle to Late Pennsylvanian, tectonic activity increased in the region (Ross, 1986). Broad carbonate shelves grew concurrently along the margins of the Delaware Basin (Hills, 1984). Carbonate bank development began in Atoka time and persisted through the Late Pennsylvanian and much of Permian time (Mazzulo, 1981). For the most part, clastic input from the north was trapped behind the carbonate banks, thus starving the Delaware Basin of sediment (Adams and others, 1951).

By early Permian (mid-Wolfcampian) time, tectonic activity had ceased (Ross, 1986), and the entire region subsided, deepening the Delaware Basin and establishing the major features of the Permian Basin.

2.3 PERMIAN PERIOD

2.3.1 Wolfcampian Epoch

In the Early Permian, the last stages of the Marathon orogeny thrust

Guadalupian sediments. The Castile is restricted to the Delaware Basin, because Lang (1939, 1942) redefined the base of the Salado as the base of the Fletcher anhydrite that rests on the Capitan reef in the subsurface.

Following the deposition of the Castile, the basin desiccated to an areally extensive salt-pan/saline mudflat. Surface topography was essentially nonexistent and the laterally continuous desiccating-upward cycles of carbonate - sulfate - halite were deposited (Jones, 1972; Lowenstein, 1982, 1987a). Locally, over 2300 ft (700 m) of the Salado evaporites, mostly halite, were deposited in the basin. Salado deposition extended over the margins of the then buried Capitan reef.

Rustler time was marked by a major freshening of the basin. Clastic sediments were introduced into a deeper, somewhat less saline lagoonal type environment which later desiccated to a saline mudflat/salt pan. Rapid transgressions followed by desiccation deposited carbonates, sulfates, and halite rocks during the remainder of Rustler time.

Near the end of the Permian, nearly 650 ft (200 m) of siltstones and sandstones were deposited over Rustler evaporites. Earlier studies of the Dewey Lake Redbeds have been limited in scope (e.g., Miller, 1955, 1957). Miller (1966) interpreted the Dewey Lake as having been deposited in a shallow marine environment. Oriel and others (1967) followed Miller (1966), while Eager (1983) suggested that the Dewey Lake originated as prodeltaic sediments. Schiel (1987), as part of a continuing study, suggests the Dewey Lake is a continental deposit, in contrast with previous marine interpretations.

2.4 POST-PERMIAN

Following the deposition of the Dewey Lake Redbeds, most of southeastern New Mexico and west Texas were subject to erosion. The uplift and/or tilting that caused erosion was minor as the unconformity between the Late Triassic Dockum Group and the Late Permian Dewey Lake Redbeds is minimal. By the Late Triassic, southeastern New Mexico was reduced to a broad peneplain (Kelley, 1971). A northwesterly draining flood-plain basin formed in the Late Triassic and was not contained by the Delaware Basin (Hills, 1963; Brokaw and others, 1972; McGowen and others, 1983). Source areas to the south provided detrital material for the Santa Rosa and Chinle Formations (McGowan and others, 1983).

The Jurassic was a period of uplift and erosion of Triassic and possibly Permian rocks in the western part of the Delaware Basin. Southeastern New Mexico was a source area for Jurassic rocks in central and northern New Mexico (Powers and others, 1978).

By Cretaceous time, earlier erosion had exposed Precambrian to Permian rocks in the region. From late in the Early Cretaceous until early in the Late Cretaceous, southeastern New Mexico was covered by shallow shelfal seas (Hills, 1984). Thin deposits of limestone and coarse sandstone and conglomerate were deposited. In the Delaware Basin, the Cretaceous rocks were removed by later erosion, save isolated slump blocks of limestone and shale associated with karst features (Bachman, 1974). Late in the Cretaceous or early in the Tertiary, the Guadalupe Mountains were uplifted and tilted to the northeast. Mild tectonism affected the Northwestern Shelf (Kelley, 1971).

Regional uplift and tilting of southeastern New Mexico and west Texas to the east and southeast occurred in the late Tertiary. Tectonic activity to the west increased, resulting in the uplift of the Delaware, Guadalupe, and Sacramento Mountains. Eastward flowing streams drained the recently elevated highlands forming coalescing alluvial systems. These systems eventually produced an extensive blanket of sands and gravels called the Ogallala Formation. The Ogallala represents the first preserved sedimentary record since the Cretaceous (Bachman, 1974). Ogallala deposition ended in the Pliocene with the advent of additional regional uplift and warping (Powers and others, 1978). The surface became stabilized, and soil forming processes began that resulted in the formation of an extensive caliche caprock (Bachman, 1980).

A major uplift of the Guadalupe Mountains occurred in the late Pliocene and early Pleistocene. Subsequent erosion and coalescence of subsided areas removed Ogallala sediments (Nicholson and Clebsch, 1961; Mercer and Orr, 1979). During the early to middle Pleistocene, Nash Draw, the Clayton Basin, and San Simon Swale underwent subsidence (Bachman, 1974).

The middle Pleistocene was relatively humid, and the conditions were right for the fluvial reworking and deposition of earlier sediments as the Gatuna Formation. Gatuna time was followed by a much more arid environment. The arid conditions coupled with a tectonic and an erosionally stable surface permitted the formation of the Mescalero caliche. During the late

Pleistocene to Holocene, eolian reworking of detrital materials formed the extensive dune fields which now blanket large portions of southeastern New Mexico.

3.0 STRATIGRAPHY

3.1 OCHOAN STRATIGRAPHY

The Ochoan Series in the Delaware Basin was named by Adams and others (1939) for the Ochoa Post Office (T.24S., R.34E., Lea County). It includes four formations, three of which consist primarily of evaporites. They are, in ascending order, the Castile, Salado, and Rustler Formations, and the Dewey Lake Redbeds (or Formation)(Fig. 3.1).

3.1.1 Castile Formation

Richardson (1904) named the Castile Formation for outcrops near Castile Spring in Culberson County, Texas. The Castile was divided into a "lower" and an "upper" salt series until Lang (1935) named the upper salt series the Salado Formation.

The Castile Formation consists of thick units of laminated anhydrite/carbonate and halite. The sulfatic beds dominate. Halite is thin or absent in the western part of the Delaware Basin. The change is usually attributed to dissolution of halite (Anderson and others, 1972, 1978; Anderson, 1978, 1981, 1982; Bachman, 1984b; Lambert, 1983).

Anderson and others (1972) divided the Castile into additional informal members from the base upwards: basal limestone, anhydrite I, halite I, anhydrite II, halite II, anhydrite III, halite III, and anhydrite IV. Bachman (1984b) reported additional halite within anhydrite IV and called it halite V (sic). The informal framework provided by Anderson and his co-workers is in regular usage by investigators of the Castile Formation.

The basal contact of the Castile with the underlying Bell Canyon Formation of the Delaware Mountain Group is poorly exposed at best. Geophysical logs display a sharp transition based on natural gamma, acoustic, density, and other parameters. The contact has been considered unconformable based on these signatures. Cys (1978) reviews the evidence from a core of the transition in Winkler County, Texas, and concludes that the contact is clearly transitional. Cys (1978) placed the contact at the first lamina of anhydrite. He indicates that the sharp log signature is due to the thinness of the transitional contact relative to the resolution of the log. Anderson and others (1972) report a thin limestone unit at the base of the Castile. More recently, Robinson and Powers (1987) examined cores of the contact from numerous boreholes along the western edge of the Delaware Basin, and

geophysical logs from a larger area. Cores show the transition over a few tens of centimeters, and the logs display sharp transitions. In addition, there appears to be an intertonguing of limestone and sulfate near the base of the Castile forming what has been called "false Lamar" (Powers and Robinson, in prep.). The intertonguing occurs east of Whites City over several miles. While the Bell Canyon/Castile contact is transitional over an interval of < 3 ft (1 m) and the log signature is distinctive, some marginal variation in the contact is demonstrable.

The upper contact with the Salado is less clear. Lang (1939, 1942) placed the base of the Salado at the base of the Fletcher Anhydrite Member which rests immediately on the Capitan Limestone. Jones (1954) and Jones and others (1973) included the Fletcher Anhydrite Member in an anhydrite unit considered part of the Castile in the Delaware Basin. This anhydrite was informally designated anhydrite III or IV, or a combination of III/IV, by Anderson and others (1972).

Bachman (1984b) reviewed the nature of the Castile/Salado contact in some detail. He generally confirms (p. 8) the conclusion of Jones (1954) that "the contact between the Castile and Salado is gradational and interfingering."

Bachman (1984b) interprets the contact as generally sharp, but modified in part by dissolution resulting in a residue resting on the Castile.

The Castile has been the subject of many well-known studies. Anderson and others (1972) relate studies of the anhydrite/carbonate laminations begun by Udden (1924), carried on by Adams (1944), and extended by Anderson and co-workers. The Castile Formation is usually considered an example of a deep-water evaporite basin; the characteristics attendant with such deposits are discussed more fully by Schmalz (1969), Dean and others (1975), and Kendall (1984).

The Castile Formation is dominated lithologically by thick units of sulfate (mainly anhydrite) or thinly laminated anhydrite and carbonate. Near the center of the basin, thick units of relatively pure halite are interbedded to intertonguing with the sulfate units. The thickness of beds within the Castile can be consistent over considerable distances, interrupted only by intraformational deformation or by dissolution. Anderson and Powers (1978) report on deformation of parts of the Castile from several areas within the Delaware Basin buried no more than about 4000 ft (1200 m) deep at

present. Borns and others (1983) and Borns and Shaffer (1985) examined deformation in the Castile near the WIPP site and in larger areas of the basin. Borns and Shaffer (1985) concluded that the structures outlined by Anderson and Powers (1978) were smaller than originally conceived and were similar to salt flowage/deformation structures near the WIPP site.

Some investigators report basin margin effects, including submarine fan deposits of gypsum or anhydrite (Billo, 1986), along the eastern and northern basin margin. Robinson and Powers (1987) report a fan-like deposit of sulfate clasts approximately equivalent to halite I (Anderson and others, 1972) along the western margin of the basin. Details of the sedimentological processes for the Castile are still being profitably studied.

3.1.2 Salado Formation

The term Salado was originated by Lang (1935) for the upper, salt-rich part of the Castile gypsum of Richardson (1904). An informal threefold division of the Salado Formation is utilized here: an unnamed upper member, a middle member locally designated the McNutt potash zone, and an unnamed lower member. As each of the members contains similar amounts of halite, anhydrite, and polyhalite (Jones, 1972), the members are distinguished by their content of other potassium and magnesium-bearing minerals. The upper and lower members generally lack these minerals, while the middle member (McNutt potash zone) contains a relative abundance of potassium and magnesium-bearing minerals. Due to the abundance of laterally persistent beds, the middle and upper Salado are also subdivided on a much finer scale. A system of numbering individual beds of anhydrite and polyhalite (marker beds) was introduced by geologists of the U. S. Geological Survey (Jones and others, 1960). The marker bed system is used extensively by mining companies in the Carlsbad potash mining district.

The Salado consists of halite, anhydrite, and polyhalite with varying amounts of other potassium-bearing minerals. About 85-90% of the Salado is halite (Jones and others, 1973). Beds of anhydrite and polyhalite alternate with thicker beds of halite throughout the Salado section.

Halite in the Salado is rarely pure and often contains minor amounts of clay, polyhalite, and anhydrite. The halite is generally white to clear, but it may be tinted orange, reddish-brown, and gray by varying amounts of interstitial polyhalite or clay (here used mainly as a textural term as the

finest grain sizes include clay and other minerals). Halite may also occur in some argillaceous beds and anhydrites as displacive crystals. Halite replacements of sulfate are common; the most recognizable are halite pseudomorphs after gypsum swallowtail crystals.

In the Salado, argillaceous halite is reddish-brown to gray. In an argillaceous halite, clay minerals may occur as matrix material, interstitial material, and intercrystalline material. The clay mineral content of the Salado (Bodine, 1978) and most individual argillaceous halites increases upward (Lowenstein, 1982, 1987a).

Most sulfate units in the Salado consist of finely crystalline polyhalite and anhydrite. During geologic mapping in the exhaust shaft, various classic sulfate sedimentary structures were observed in the anhydrites and polyhalites of the Salado, including nodular structures, enterolithic structures, and swallowtail structures. Some of the anhydrite and polyhalite beds are visually structureless. The majority of the polyhalite and anhydrite beds are underlain by thin beds of gray carbonate-rich claystone. Polyhalite and anhydrite may also occur in halite beds as disseminated, irregularly shaped blebs or as stringers.

Unlike the Castile, the Salado is not confined to the Delaware Basin. North and east of the WIPP site Salado deposition passed well beyond the Capitan reef and occurred on the Northwestern Shelf and the Central Basin Platform. The Salado has been erosionally removed from the west and south sides of the Delaware Basin leaving a horseshoe-shaped rim of brecciated insoluble material.

The upper contact of the Salado with the Rustler within the central part of the basin is marked consistently on geophysical logs by a relatively large increase in natural gamma over an interval as thick as 100 ft (30 m). This log signature immediately overlies successively deeper Salado marker beds to the west (Jones and others, 1960; Bachman, 1974), usually attributed to solution or leaching of salt from the upper Salado (Vine, 1963). Jones and others (1973) argue that this zone is partly attributable to the Rustler and partly to the Salado Formation. Holt and Powers (1984) described erosion and channeling very near the base of the Rustler that indicates processes other than late dissolution may contribute part of the apparently unconformable relationship between Salado and Rustler.

3.1.3 Rustler Formation

The Rustler Formation is the youngest of three Ochoan evaporite-bearing formations in the Delaware Basin (Fig. 3.1). Richardson (1904) named the Rustler for outcrops in the Rustler Hills, Culberson County, Texas. Lang (1939) clarified the term "Rustler" to stratigraphically define the interval between the Pierce Canyon Redbeds (abandoned term; now recognized in part as the Dewey Lake Redbeds) and the Salado Formation. Lang (1939; in Adams, 1944) recognized and named two laterally extensive dolomite units. The lower is named the Culebra Dolomite Member, and the upper is named the Magenta Dolomite Member.

Vine (1963) introduced the presently used fivefold stratigraphic subdivision of the Rustler (Fig. 3.2). Vine named the interval above the Magenta the Forty-niner Member, and the interval between the Culebra and the Magenta the Tamarisk Member. The interval between the Rustler/Salado contact and the Culebra was not named and is referred to as the unnamed lower member.

The Rustler Formation in this area is characterized by a variable lithology consisting of interbedded sulfates, carbonates, clastics, and halite. Jones (1972) reported the Rustler as consisting of 10% carbonate rocks, 30% sulphate rocks, 43% chloride rocks, and 17% clastic rocks.

The Rustler varies in thickness from tens of feet, where exposed and subjected to solution and erosion, to nearly 560 ft (170 m) in the northeastern part of the Delaware Basin. The western margin of the Rustler has been removed by erosion. The Rustler crops out along the Pecos River Valley, within Nash Draw, and in an arcuate pattern near the southwestern edge of the Delaware Basin. It has been extensively altered by near-surface ground water in Nash Draw.

Outcrops of the Rustler are poor at best. Solution and/or hydration of the soluble rocks within the Rustler, and frequently the solution of halite from the underlying Salado Formation, extensively modify and disrupt any primary sedimentary features. Rustler units may be displaced from their expected position. Where dissolution of the underlying Salado is complete, Rustler outcrops may consist only of broken blocks of less soluble rocks.

The upper contact of the Rustler with the Dewey Lake Redbeds has been reported as conformable (e.g., Bachman, 1984b). Within the shafts of the WIPP site, Holt and Powers (1984, 1986a) report local minor erosional relief on the contact.

3.1.4 Dewey Lake Redbeds

The Dewey Lake Redbeds are the uppermost of the four Ochoan formations and represent the close of the Paleozoic in the Delaware Basin. The assignment of the Dewey Lake to the Permian is somewhat arbitrary as it is not supported by radiometric dating or fossil evidence in the Delaware Basin. Fracasso and Kolker (1985) provide Permian radiometric ages from the Quartermaster Formation, the Dewey Lake equivalent in the Texas panhandle. The Dewey Lake was named by Page and Adams (1940) based on samples from the Penn Oil, Habenstreit #1 well, Glasscock County, Texas. The term "Dewey Lake" superseded the term "Pierce Canyon" originally proposed by Lang (1935) for redbeds in the Delaware Basin. The term "Pierce Canyon" was used as late as 1963 by Vine in his descriptions of the Permian redbeds in Nash Draw. However, the U.S.Geological Society later abandoned the term "Pierce Canyon" and adopted the term "Dewey Lake," as it was more widely accepted by geologists, and "Pierce Canyon," as defined, included rocks of the Pleistocene Gatuna Formation.

The Dewey Lake conformably overlies the Rustler Formation on a large scale (with local minor erosional relief) and underlies Late Triassic and younger rocks. The Dewey Lake thins to the northwest as the result of pre-Late Triassic erosion. The Dewey Lake is often assumed to be laterally equivalent to the Quartermaster Formation or Group of the Texas panhandle and Oklahoma (Hills and Kottlowski, 1983). However, the age of the Quartermaster is not consistently stated, and the relationship with the Dewey Lake is not clear (Hills and Kottlowski, 1983).

The Dewey Lake is characterized by its reddish-orange to reddish-brown color and varying sedimentary structures. The Dewey Lake consists almost entirely of mudstone, claystone, siltstone, and interbedded sandstone. Abundant sedimentary structures are characteristic of the Dewey Lake (Holt and Powers, 1984, 1986a) and include horizontal laminations, fine cross-laminations of varying size, rip-up clasts, silt-filled mud cracks, interbasinally derived pebble conglomerates, fining upward sequences, and soft sediment deformation features. Locally, greenish-gray reduction spots are abundant, and a few beds may have a gray color. Schiel (1987), in a continuing study of the Dewey Lake, has also provided initial interpretations of geophysical logs indicating generalized lithologic trends within the Dewey Lake.

With the exception of the upper portion, the Dewey Lake is characterized by locally abundant gypsum-filled fractures. The majority of the fractures are filled with fibrous gypsum, although granular gypsum fracture fillings do occur in the upper portion of the Dewey Lake. The significance of the first occurrence (from the surface) of gypsum-filled fractures at various localities is not clear. It informally has been considered a possible indicator of the depth and extent of infiltration of recent meteoric water, though this is certainly not a unique interpretation. Preliminary comparisons of data gathered from the waste handling and exhaust shafts with data gathered from boreholes around the WIPP site indicate that the first occurrence of gypsum fracture fillings does not occur in the same stratigraphic interval laterally (Holt and Powers, 1986a).

The majority of all fractures in the Dewey Lake are horizontal to subhorizontal and follow bedding planes. High angle fractures are the least common fracture type in the Dewey Lake. At least three separate episodes of fracturing and subsequent filling with gypsum have been reported from the Dewey Lake at the exhaust shaft (Holt and Powers, 1986a).

3.2 RUSTLER STRATIGRAPHY

The stratigraphy of the Rustler Formation at the WIPP site is discussed in the following sections. Vine's (1963) fivefold subdivision of the Rustler is used as the stratigraphic framework for the Rustler data in later chapters (e.g., sedimentological data in Ch. 5). Some units of the Rustler vary considerably beyond the area of the WIPP site. These variations, including hydration and alteration of sulfates near the surface, are not considered here.

3.2.1 Unnamed Lower Member

The unnamed lower member consists of clastic sediments with subordinate amounts of bedded halite, anhydrite, and polyhalite (Fig. 3.2). The lower member is roughly 130 ft (40 m) thick. The basal contact with the Salado, as observed in the shafts, indicates neither significant erosion nor dissolution (Holt and Powers, 1984, 1986a).

The lowermost 65 ft (20 m) of the lower member consists of siltstone with minor amounts of sandstone. Two halite-rich sequences overlie the siltstone. These sequences are in turn overlain by a 10 ft (3 m) thick,

bedded anhydrite sequence. The top of the unnamed lower member is marked by roughly 10 ft (3 m) of claystone.

3.2.2 Culebra Dolomite Member

The Culebra consists of brown, finely crystalline, locally argillaceous and arenaceous dolomite with rare to abundant vugs with variable gypsum and anhydrite filling (Fig. 3.2). The Culebra is about 27 ft (7 m) thick. Frequently, the upper 4 inches to 1 ft (0.1 to 0.3 m) consists of organic-rich, thinly to micro-laminated claystone and carbonate.

3.2.3 Tamarisk Member

The Tamarisk Member varies from about 100 to 170 ft (30 to 50 m) thick in normal sections. It consists of a lower and an upper anhydrite separated by either a thin 6.5 to 10 ft (2 to 3 m) thick claystone or a thicker interval of halite (Fig. 3.2).

3.2.4 Magenta Dolomite Member

The Magenta is a light gray to dark brown gypsiferous and arenaceous dolomite roughly 25 ft (8 m) thick (Fig. 3.2). It displays abundant primary sedimentary structures including wavy and lenticular bedding, cross-stratification, climbing ripple structures, and nodules of gypsum. The Magenta assumes a purplish cast after surficial weathering or in the shallow subsurface.

3.2.5 Forty-niner Member

The Forty-niner is similar to the Tamarisk as it consists of a lower and an upper anhydrite which sandwiches claystone or a laterally equivalent halite (Fig. 3.2). The contact with the Dewey Lake Redbeds is sharp and undulatory within the WIPP shafts; it is regionally conformable.

4.0 LATERAL RELATIONSHIPS WITHIN THE RUSTLER FORMATION

Lateral relationships will be described at two different scales: local (WIPP site area) and regional. The local geology reported here is strongly influenced by previous shaft descriptions (Holt and Powers, 1984, 1986a) and redescribed cores from WIPP boreholes, emphasizing sedimentary features and relationships important in interpreting the depositional history and subsequent events. Geophysical logs of these boreholes have been correlated to details from shaft and core descriptions. The local sedimentary features and relationships are presented elsewhere in detail (Ch. 6); here, we summarize briefly the site relationships as a prelude to a regional synthesis. The regional lateral relationships are based principally on our interpretation of geophysical logs, tied to the stratigraphy and lithology of the site area. A variety of isopach maps and structure contour maps will be used in conjunction with cross sections to provide the basis for lateral relationships in the Rustler at both scales.

The regional information serves mainly to illustrate important stratigraphic and sedimentologic relationships. These relationships are best preserved from the vicinity of the site to the east, north, and south, limited by the state boundary. Outcrops of the Rustler west of the site have not been examined in detail for stratigraphic and sedimentologic data for reasons outlined by Vine (1963). West of the site, logs are increasingly difficult to interpret as they are near the surface and have been disrupted by erosion and solution of both Rustler and Salado. For this report, which concentrates on depositional and dissolution features in the vicinity of the WIPP site, the region includes the site (see Fig. 4.20) and areas west, but usable information is from the site area to the east, north, and south.

Several distinctive, widespread lithostratigraphic units may be correlated. This kind of correlation does not require synchronous deposition or bounding isochronous surfaces (Hedberg, 1976), although widespread beds of similar mineralogy and geochemistry in an evaporite basin are often, at least implicitly, assumed to be isochronous or nearly so. Within parts of the Rustler, the vertical sequence of beds is similar to lithofacies developed laterally in evaporite deposits, and thus they may generally be interpreted as prograding or retrograding deposits. Mildly disjunct facies, somewhat similar in arrangement to punctuated aggradational cycles (PACs) of Goodwin and Anderson (1980) and Anderson and others (1984), indicate rapid relative

changes in sea level or regional base level (Ch. 6).

The framework for lateral relationships is the five member lithostratigraphic designation of the Rustler (Vine, 1963). Individual beds within these members are described in some detail in shafts and cores (Ch. 5). These beds, as far as geophysical characteristics permit (Fig. 4.1), are traced laterally across the region. Some lithologies (e.g., Tamarisk halites) occur regionally, as interpreted from geophysical logs, and do not occur in cores from the site area. These lithologies vary within well-defined members, however, and are easily assigned to lateral lithofacies variations in most areas. The region well north and east of the site demonstrates some changes within the lower Rustler requiring considerable care in interpretation. Some of these lateral changes are briefly mentioned, as they are beyond the areal scope of this report and are not resolved.

The isopach and structure contour maps may be used to infer considerable information about the depositional history and structural evolution of the late stages of the Delaware Basin and immediate surroundings. Section 4.3 summarizes that information, part of which is also used to interpret the depositional history section.

4.1 WIPP SITE

Within the site area, all members are clearly defined and change little in thickness and general lithology. The Tamarisk and Forty-niner Members vary most in thickness and lithology due to the presence or absence of halite.

4.1.1 Unnamed Lower Member

The lower contact of the unnamed lower member is at the base of a section of reddish-brown to greenish-gray siltstones, above a halitic and sulfatic section of the Salado. Within the shafts, this boundary is sharply defined. Cores also show sharp differentiation of the boundary, and these boundaries are closely related to natural gamma increase (from the underlying Salado Formation), and changes in the sonic, density, or neutron character (Fig. 4.2).

To the west, this basal contact has been considered less definable. Jones and others (1973) have stated that the argillaceous clastics above

halitic Salado include the residue from dissolution of the upper Salado, meaning that the Rustler/Salado contact may not always be located at the base of the natural gamma bulge characteristic of the lower Rustler. Some of the evidence for this conclusion is observable near the site. In the Nash Draw area, Salado halite can be demonstrated to have been removed sometime after Rustler deposition on the basis of brecciation of much of the Rustler (Ch. 7; see also Mercer, 1983). Within the site, however, there is very clear evidence of erosive channeling and fill near the base of the Rustler (Holt and Powers, 1984), and the Salado/Rustler contact is variable within the region in areas that have not undergone post-Rustler dissolution. Channeling, fossils, and bioturbation in the basal Rustler are clear indicators of much less saline water compared to the Salado brines (Holt and Powers, 1984, 1986b; Ch. 5, 6). It is reasonable to suppose that this water caused dissolution and/or erosion of the upper Salado, though the amount is yet undetermined. The extent of this early process may be obscured in the western part of the study area by later solution and collapse of the Rustler and upper Salado.

The upper boundary of the unnamed lower member is placed at the base of the Culebra Dolomite Member, specifically at the contact with a gray claystone unit. This contact is among the clearest and most easily interpreted both in the site area and the region (Fig. 4.2). The correspondence between shafts, cores and logs is excellent. This boundary is used as a baseline in profiles for correlation purposes in this report (Fig. 4.3 - 4.6).

Within the lower unnamed member are two main anhydrite beds. These beds are traceable regionally as well as through the eastern part of the site area, providing a tie within the lower section. The lower, thinner sulfate thins or disappears in the western part of the site.

4.1.2 Culebra Dolomite Member

The upper contact of the Culebra within the site area was poorly preserved and described prior to shaft excavation. Within both shafts, a waxy organic-rich, well-laminated carbonate and clay bed occurs. It is cored with difficulty, probably washes out during drilling, and can be associated with a gamma spike and low density, low acoustic velocity signature on logs (Fig. 4.2). This signature carries through much of the region and is the

basis for interpreting its regional extent. In this chapter of the report, the contact of the Culebra has been placed at the base of this organic unit because of the variable thickness in the organic-rich unit. In many previous reports, the Culebra boundary was placed above the organic-rich beds on the basis of gamma logs. For the discussion of sedimentary features (Ch. 5) and depositional environments (Ch. 6), the organic-rich unit is included in the Culebra. Some of the systematic variation in Culebra thickness in the site area between this and other reports can be attributed to this interpretive difference.

Within the site, the Culebra is slightly variable in thickness. It is present throughout the site and is an important regional marker.

4.1.3 Tamarisk Member

The upper contact of the Tamarisk with the Magenta Dolomite Member is distinctive in shafts, cores, and logs throughout the site and region (Fig. 4.2). It is a transitional boundary spanning a few feet (1-2 m) between the upper sulfate of the Tamarisk and the carbonate, including algal structures, of the basal Magenta.

The most laterally continuous unit of the Tamarisk Member is the upper sulfate. A sulfate above the basal organic claystone and carbonate (see 4.1.2) is regionally continuous, though it is absent in WIPP 19, a borehole about 0.5 mi (0.8 km) north of the site center.

The beds between these sulfates are among the most variable units in the Rustler. Even within the site area, the interval between these sulfates varies in thickness from about 15 to about 115 ft (4.6 to 35 m). A polyhalite bed occurs within this interval in the eastern part of the site area; the polyhalite can be traced through a part of the region as well especially in the Rustler depocenter southeast of the site (e.g. log of H01, Fig. 4.2, 4.3, 4.5, 4.6).

4.1.4 Magenta Dolomite Member

The upper contact of the Magenta is transitional over a small thickness, resulting in easy identification in the site area and easy correlation within the region (Fig. 4.2). As with the Culebra, the Magenta varies slightly in thickness within the site area, though it is continuous throughout the site area and the region.

4.1.5 Forty-niner Member

The upper contact of the Forty-niner is sharp in shafts, core, and logs (Fig. 4.2). The transition from the sulfate of the Forty-niner to the clastics of the overlying Dewey Lake Redbeds has local relief of a few inches (a few cm) in shafts and cores.

The sulfate beds at the base and top of the Forty-niner are persistent throughout the site area as well as the region. The thickness of these sulfates varies only slightly within the site area. However, the thickness of the clastic/halitic beds between the sulfates varies greatly both locally and regionally. The thickness varies mainly with the volume of halite present.

4.2 REGIONAL LATERAL RELATIONSHIPS

Important regional relationships have been defined by correlating geophysical logs with cores and shaft descriptions. In addition, certain units of the Rustler vary considerably within the region studied, providing evidence of facies changes.

4.2.1 Lower Unnamed Member

The basal contact of the Rustler a few tens of miles east and southeast of the site appears very much like the contact at the site (Fig. 4.2). At the fringes of the study area, the basal contact may exhibit a variable position with respect to Salado marker beds (e.g., MB 103 and 109) and the Culebra. At the eastern and northern edges of the region, the log character indicates that the part of the section equivalent to the lower silts and clays of the Rustler is very similar to, and perhaps continuous in deposition from, the Salado; it could possibly be considered part of the Salado. The natural gamma bulge is much diminished, indicating less clay in a thinner unit, and acoustic velocities are similar to halite (Fig. 4.2). Because the basal gamma signature appears continuous though diminished, we consider this interval part of the Rustler. A further study of the regional character of this boundary is obviously warranted, though not a part of this report.

Two anhydrite beds within the lower unnamed member are prominent in the site area and to the east (Fig. 4.3 - 4.6). These distinctive units occur in the upper part of the member at the site but are lower in the member to the

east and south. Further to the south, these two anhydrites are again high in the member, and a sulfate/carbonate which is not present at the site appears near the base of the member. The position of these anhydrites is variable with respect to the base of the Rustler and with respect to the base of the Culebra. Their position generally relates to the thickness of halite in the member. As halite decreases above the anhydrites, their position is closer to the Culebra. As halite decreases below the anhydrites, their position is closer to the base of Rustler. These changes do not occur at the same locations along the constructed profiles (Fig. 4.3 - 4.6), indicating the cause of position change is not common to both sections of the member. In addition, clastics between the upper anhydrite and Culebra vary in thickness, but the variation does not appear to directly relate to thinning or absence of halite. The position changes and relationships appear to be due to variations in depocenter for a saline pan and attendant clastic deposits.

Halite below the two anhydrite markers is thickest to the east of the site area. The relationships within the lower unnamed member (as well as the rest of the Rustler) are somewhat unclear due to a lack of data in the immediate vicinity of the buried Capitan reef margin east and north of the site. The thickness of this lower part of the member does not appear to vary greatly across the reef at the north, though it may be significantly thinner along some areas southeast of the site. The proportion of halite in the member is greater over the Central Basin Platform, and the lithologic sequence is similar to the Salado. The Central Basin Platform area may have formed a semi-independent depocenter dominated by a saline pan during this time.

The lower unnamed member is thickest (550 ft; 168 m) east and south of the site, both within the Delaware Basin and across the margin of the Capitan reef to the east (Fig. 4.7). Though data are few over the reef, the areas east of the reef are clearly equivalent in maximum thickness.

Borns and Shaffer (1985) also found the thickest part of the upper Salado to the south and east of the site area. Within that area, the Salado/Rustler contact usually varies slightly in position above distinctive beds above MB 103. The contact is not perfectly concordant even in these areas, indicating erosion and/or solution of the uppermost Salado with the influx of water with much lower salinity to begin Rustler deposition.

4.2.2 Culebra Dolomite Member

The Culebra varies moderately in thickness, from about 10 to 35 ft (3 to 11 m), through the region (Fig. 4.8). The Rustler dolomites are reported to be oolitic (Lang, 1935; Adams, 1944) but we have not confirmed this. Limited field observations and core descriptions from sulfur exploration in Culberson County, Texas, indicate that the Culebra is richer in clastics to the south and southwest of the site.

The distinctive Culebra log signature within the Delaware Basin begins to fade at about T15S. The Culebra thins to the north, appears to become increasingly sulfatic, and then disappears as a distinctive unit. It is not clear whether the Culebra disappears entirely by pinching out or merges with the upper anhydrite of the Tamarisk Member. Along the western edges of the Rustler (outcrops in T17S, R28E), a very thin unit of mottled to color-laminated clastics with no distinctive anhydrite occurs between the Culebra and Magenta. The lower Magenta shows probable algal laminations and thin breccia zones bounded by zones of continuous bedding. Geophysical logs east of this outcrop show the upper anhydrite of the Tamarisk Member. This important question of the lateral relationship of the Culebra to Tamarisk is still unresolved.

At the southeastern corner of the regional study area, the Culebra underlies a single anhydrite. The lower Tamarisk anhydrite has pinched out or perhaps combined with the upper Tamarisk anhydrites. This relationship on the Central Basin Platform is similar to that north of T15S.

The eastward extent of the Culebra has not yet been determined in this study, but the Culebra appears to be thinner (about 10 to 15 ft; 3 to 4 m) over the Central Basin Platform. A few of the available logs suggest the Culebra becomes sulfatic and combines with the upper Tamarisk anhydrite in the northeastern part of the study area.

4.2.3 Tamarisk Member

The Tamarisk has a maximum thickness of about 270 ft (82 m) in the region (Fig. 4.9), while in the site area it is commonly about 90 ft (72 m) thick. The difference is mainly attributable to a thick section of halite within the Tamarisk depocenter (Fig. 4.9).

The organic-rich carbonate and clay bed immediately overlying the Culebra has good continuity within most of the region. It varies locally in

thickness and may also be absent in a few wells (Fig. 4.3 - 4.6). At this time, no apparent trend in either thickness variations or rare absences of the bed has been observed.

The lower anhydrite of the Tamarisk is generally about 20 to 25 ft (6 - 6.7 m) thick in R32-34E. It thins away from this zone and disappears entirely north of the study area. Within the thicker zone, the unit is divided by a clastic, and probably carbonate-rich, zone into two beds approximately equal in thickness (Fig. 4.10). The separating bed is considered to be the lateral equivalent of a persistent thin claystone observed in shafts, some cores, and most logs. The clastic/carbonate bed is 5 to 10 ft (1.5 - 3 m) thick in parts of the area where the anhydrite is thickest. Eastward, onto the Central Basin Platform, only about 10 ft (3 m) of anhydrite, undivided by other beds, is usually present. It appears that the upper part of the unit pinches out depositionally toward the east and northeast. Local variations, such as the lack of this anhydrite bed immediately north of the site center (WIPP 19), have not been demonstrated on the regional scale.

The beds between the anhydrites of the Tamarisk are laterally traceable, but are among the most variable lithologically in the Rustler. Within the region, the beds vary from 0 to about 200 ft (0 - 61 m) thick. Its thickest area is east of the site, along the Delaware Basin margin and on the Central Basin Platform. The beds consist largely of halite where they are thickest. The interbeds thin to the north, west, and south (Fig. 4.3 - 4.6, 4.11), and are dominantly clastics when less than 20 to 30 ft (6 - 9 m) thick. North of R18S, this unit may be entirely missing, as the Culebra appears to underlie the upper Tamarisk anhydrite or even the Magenta (4.2.2). Clastic zones in the Tamarisk are also generally traceable laterally within parts of the halite unit; in some areas southeast of the site, halite clearly surrounds a clastic or mudstone unit (e.g., C04, Fig. 4.10; Fig. 4.5).

A polyhalite or polyhalite/anhydrite bed is associated with the halite between the two sulfates of the Tamarisk. This bed, which occurs along the eastern part of the WIPP site, is very distinct because of the high natural gamma and associated high acoustic velocity and/or density (Figs. 4.2, 4.10). The polyhalite exists within the Delaware Basin as well as on both the Central Basin Platform and Northwest Shelf areas. Within the Tamarisk depocenter, it maintains a rather constant position above the lower anhydrite

of the Tamarisk, but its position is more variable with respect to the upper anhydrite. Where halite is thickest in this member, the polyhalite is about 100 ft (30 m) below the upper anhydrite. As this halite thins, the polyhalite approaches the upper anhydrite base, and, in T25S, R33E for example, the polyhalite immediately underlies the upper anhydrite of the Tamarisk without any evidence of intervening halite or clastics (Figs. 4.3, 4.5, 4.6). Where this occurs, the polyhalite may be underlain either by halite or by clastics overlying halite. Snyder (1985, p. 4) reports "...that no polyhalite is present where all halite has been removed from the Tamarisk Member".

This marker is important evidence of the lateral depositional variations within the Delaware Basin during this depositional episode. Polyhalite overlies halite or halitic units east of the WIPP site. Polyhalite also overlies clastic zones (mudrocks) in several boreholes around the margins of the halitic areas. The clastics are lateral equivalents to the halitic zones. This relationship of polyhalite over clastics indicates that solution did not remove halite from the clastics after formation of the polyhalite, or the polyhalite would have been dissolved. Polyhalite is very soluble, and it is usually considered a secondary or diagenetic mineral.

Through much of the basin area east of the WIPP site, polyhalite underlies a thick, relatively pure halite that laterally thins and disappears. In several boreholes around the margins of this halite lens, polyhalite directly underlies anhydrite. There is no log evidence of either clastics or erosional plane between polyhalite and anhydrite in these holes. If there is any "dissolution residue" present in these holes, it would have to be anhydrite in good contact with the overlying anhydrite. The presence of the polyhalite indicates that any removal of halite (laterally equivalent to the halite lens) must have taken place before formation of the polyhalite.

When did the polyhalite form? There is no direct evidence. Reasoning suggests it formed early, perhaps nearly coeval with the original sulfate (assuming this polyhalite is not primary). As the polyhalite thickness is about the same whether it underlies anhydrite or halite, it is unlikely that the polyhalite originated as a replacement or alteration of anhydrite or gypsum by downward percolating fluids. Within the basin, under the halite lens, polyhalite is unlikely to have formed from solutions percolating downward through much halite as permeability is plugged quite early

(Lowenstein, 1987) and the halites indicate no diagenetic alternation by potassium-rich solutions (no increase of natural gamma). If polyhalitization was driven by brines from the underlying zones, these fluids passed equally effectively through halitic and clastic zones. There is no gamma log evidence of alteration by potassium-rich solution in halitic zones, and they are usually plugged very early.

The polyhalite within the Tamarisk is present in locations where it limits the timing of any removal of halite from adjacent units. Halite is not believed to have been dissolved from any zone adjacent to extant polyhalite since polyhalite formed. Though the absolute age of the polyhalite is not known, the polyhalite occurs in areas where adjacent halites should show very little permeability to brines that would alter original sulfate minerals to polyhalite. The polyhalite is thought to have formed very early, showing in its lateral extent and relationships effects of the basin margins and limiting the timing, at least, of any dissolution of halite in clastic units laterally equivalent to halitic zones.

Two thin anhydrites (possibly mixed anhydrite and halite or carbonate) occur within the halite, above and parallel to the polyhalite (Fig. 4.10). These two anhydrites are easily traceable outside the Delaware Basin, providing evidence of continuity of both depositional process and lithology for this unit (Fig. 4.3, 4.5, 4.6). As the halite above these thin beds thins and disappears laterally, the halite between these two beds does not thin. The thin anhydrites in turn disappear or merge with the upper anhydrite of the Tamarisk. It is possible these two beds are successively truncated by the upper anhydrite of the Tamarisk, but borehole well log locations are not appropriately located to resolve this question.

The upper thick anhydrite of the Tamarisk is persistent throughout the study area. It is persistent beyond the extent of the Culebra and lower part of the Tamarisk. This anhydrite usually varies moderately in thickness, as where the polyhalite merges with the base of the anhydrite. Laterally, the high gamma spike of the ^{40}K in the polyhalite disappears, and the thickness of anhydrite is similar to the combined thickness of anhydrite and polyhalite. Local thickening in the site area has also been noted, as in WIPP 13. West of the site area and in parts of the site area, Snyder (1985) attributes thickening to gypsification and the attendant volume increase.

Within the upper Tamarisk Member anhydrite (A3 of Ch. 5), laterally

continuous features occur in logs throughout the basin (Fig. 4.12). From core descriptions (Ch. 5), lithologies and sedimentary features from this anhydrite in the site area can be grouped into broad units. A three part division of the anhydrite core features appears to correspond well to the geophysical log features (Fig. 4.12).

Within the upper Tamarisk anhydrite, the basal log unit displays breaks in the acoustic velocity attributed mostly to carbonate; there is a probable higher organic content and a few thin argillaceous intervals. This unit may be as much as 40% of the bed thickness, though it is more commonly 25-30%. On many logs, natural gamma is noticeably higher in this lower part of A3 than in the upper parts. This corresponds to the carbonate plus organic/argillaceous content apparent in some cores. Within the site area, decreased neutron activity from this part of the sulfate bed has been attributed to gypsification (Snyder, 1985). Gypsification of these units can be demonstrated petrographically, but it is an inadequate explanation for the observations as similar log features occur throughout the basin. Both organic and clay content also affect neutron log signatures in a way similar to hydrated minerals. And this lower unit is clearly discernible in the basin overlying halite. That is inconsistent with the hypothesis of gypsification by circulating water removing halite.

The middle log unit of the upper Tamarisk anhydrite generally has a very low background natural gamma and a consistently high acoustic velocity, indicating high purity anhydrite. This log unit is about 35-40% of the thickness of A3. Within cores, this segment corresponds to a zone of anhydrite pseudomorphs and crushed pseudomorphs after gypsum growth textures as well as crushed nodular textures. Only the great continuity of this subunit can be observed in the logs, not the presence of specific textures.

The upper subunit of A3 is thinner than the lower subunits, usually representing about 20-25% of A3. Natural gamma activity is usually slightly above, and acoustic velocity is more variable than, the middle subunit. A persistent, thin zone of lower acoustic velocity is taken as the base of this subunit. The cores corresponding to this zone are dolomitic and also partly nodular. The transition to Magenta is gradual within both cores and log signatures over a few ft (1 - 2 m).

4.2.4 Magenta Dolomite Member

The Magenta is a carbonate sandwiched between two anhydrite layers (Fig. 4.1, 4.2) and it is marked by a characteristic high gamma associated with relatively low densities and acoustic velocities. It can be traced throughout the study area (Fig. 4.3 - 4.6). The Magenta thins across the Central Basin Platform and may be absent or dominantly sulfatic along the eastern margin of the study area.

An outcrop of the Magenta from T17S, R28E, shows that the Magenta appears well-laminated from algal growth. The Magenta thins to the north and northeast of the site; there is little variation to the south and east in the study area. Within the site area, algal features appear near the base of the Magenta. Along the western edge of Nash Draw, algal structures are more common near the middle of the Magenta. Specific algal features are discussed in Chapter 5.

An isopach map of the Magenta is not presented. The thickness is not great, but the variability is significant. Normal contouring is not possible, nor is it seemingly fruitful.

4.2.5 Forty-niner Member

The sulfate beds of the Forty-niner are the most widespread units of the Rustler Formation. The upper sulfate is easily traced and is frequently called "first anhydrite" by oil companies working in the area. Though details have not been worked out, it appears that this unit may onlap older rocks (Salado?) to the north of the study area. The maximum apparent thickness of the Forty-niner is 104 ft (32 m) (Fig. 4.13).

The lower anhydrite of the Forty-niner maintains its thickness immediately north of the study area. The upper anhydrite thins by 50% or more by T8S and T9S. These units are consistently detectable near the Texas-New Mexico border this far north (T8-9S). To the west, the units are either eroded or thin to the point of not being consistently detected.

Between the two anhydrite beds is a bed of clastics and halite. In the shafts at the WIPP site, the clastic unit displays clear bedding and cut and fill, showing detrital origin. The halite is apparently restricted to the Delaware Basin proper from the eastern part of the WIPP site to the east and south. When halite is present in the halite/mudstone, it is present at the base. In some boreholes, this basal halite is overlain by a clastic bed or

alternating clastic-halite beds. The exception is in the southeastern part of the study area where borehole DO4 (Fig. 4.5) shows halite sandwiched between possible clastic layers. The thickness of the bed without salt varies little over the study area, and it is traceable as far as the sulfate units. Its fullest extent has not been determined.

The upper anhydrite of the Forty-niner Member southeast of the site is interpreted to enclose a halite lens (Fig. 4.14, 4.6). The best evidence is in a borehole (B06) in Sec. 6, T24S, R34E, where the acoustic travel time indicates halite less than 10 ft (3 m) thick. The natural gamma is at background levels, consistent with halite. Several logs in the vicinity also show a distinct lowering of acoustic velocity, usually much less than halite acoustic velocities. As the gamma is not elevated in most of these logs halite is interpreted to be present. Acoustic logs are normally corrected for borehole diameter. It is believed that the low acoustic velocity in this zone is probably due to inadequate correction for highly enlarged borehole diameters caused by drilling with undersaturated fluids. A few logs indicate a modest increase in gamma, probably due to clay content.

About 10 ft (3 m) below the top of the upper anhydrite, many borehole logs exhibit a thin zone of increased natural gamma, accompanied sometimes by a slight decrease in acoustic velocity (Fig. 4.14). This zone is detectable mainly along the western and northern parts of the general Rustler depocenter, and it is probably indicative of increased carbonate/organic content. This zone in cores is generally laminar.

The upper contact of the Rustler is placed at the top of the upper anhydrite of the Forty-niner Member throughout the study area. As the bed is consistently present and only thins significantly well north of the main study area, there is no evidence of real unconformity at the contact within this area. There may be disconformity. The Dewey Lake Redbeds have been studied petrographically (Miller, 1966), and some sedimentary features are reported (Holt and Powers, 1984, 1986a). Its internal stratigraphic relationships and depositional environments remain to be determined (Schiel, 1987).

4.3 REGIONAL STRUCTURAL RELATIONSHIPS

The isopach map of the Rustler Formation (Fig. 4.15, 4.27), and those of members or parts of members (Fig. 4.7 - 4.9, 4.11, 4.13, 4.22 - 4.26),

consistently indicate a general depocenter east and south of the site. Perhaps the most significant observation is that the depocenter includes areas behind the Capitan reef, on the Central Basin Platform or adjacent Northwest Shelf. The data are few close to the reef, but it appears that the Rustler does not diminish in thickness over the reef, indicating a common depocenter and that the reef and former basin margin affected deposition of the Rustler little, if at all. Preliminary data, beyond the area of study, indicate that the Rustler is considerably thinner outside the map area. There does not appear to be a secondary or equal depocenter in the region. In the Midland Basin, the Rustler is thinner and clastic-dominated.

All of the structure contour maps, from base to top (Fig. 4.16-4.19, 4.28 - 4.31), of the Rustler show similar features. The depocenter area from isopach maps also is a structurally low area. A basin form trends from south to north, apparently turning to the northeast to cross the Capitan reef margin. This structure is considered to have developed at an equal rate or pace with the Rustler, as it coincides with the depocenter for all of the members.

Superimposed on the basin structure are two important post-Rustler structures. A fault, downthrown on the west side, is interpreted to account for the large structural differences on various Rustler beds along the approximate western margin of the Central Basin Platform. This fault trends slightly east of south, from the northern edge of the map toward the southeastern map area. Its southern extent in the Rustler is indeterminate based on the information available to us at this time. In addition, a significant structural low exists west from this fault to the approximate area of the Capitan reef. The western margin of this wedge-shaped structural low could be a fault or a monoclinal fold. It is left as a fold in the absence of closer-spaced data demanding a fault interpretation.

In addition to the fault and the fold, smaller structural lows and highs exist. In addition to the low coinciding with the depocenter, a conspicuous high exists along the eastern margin of the fault in the area of T19-20S, R36-37E. North of this bulge, the structure on both sides of the fault is reversing. No simple interpretation of the fault mechanism exists, though adjacent strike-slip faults have been known to produce adjacent highs and lows across faults (R. Dyer, pers. comm.). Hills (1984) infers two parallel right-lateral strike-slip faults underlying the faulted Rustler section on

Precambrian basement. It is not clear if there is a relationship between faults in the Rustler and this much earlier trend.

Aside from the form of the deformation of the Rustler in this area, it is important to note that the deformation clearly indicates post-Rustler tectonics along the Central Basin Platform margin, later than previously suspected (Hills, 1984). Continuing study of the Dewey Lake Redbeds (Schiel, 1987) should clarify the extent of deformation during or after the Dewey Lake.

5.0 RUSTLER SEDIMENTOLOGY

The Rustler sedimentology is described in considerable detail from shafts and cores (Fig. 5.1) because some features have not been described previously in the literature and because prior core descriptions include few sedimentary features. The sedimentary structures and lithologic features and their associations are the principal framework for interpreting depositional environments. The depositional environments for the Rustler, in turn, will provide a framework for interpreting the degree to which the absence of certain evaporite minerals is due to non-deposition or syngenetic dissolution versus epigenetic dissolution.

5.1 UNNAMED LOWER MEMBER

The unnamed lower member of the Rustler Formation is by far the most lithologically variable stratigraphic unit within the Rustler (Figs. 5.2a and b). Rock types vary laterally within the unnamed lower member, and are obvious even within the limited core study area. In the WIPP site area, the unnamed lower member consists dominantly of siliciclastic rocks interbedded with lesser amounts of halite and sulfate.

5.1.1 Rustler/Salado Contact

In the WIPP site area, the Rustler/Salado contact is arbitrarily assigned to the base of a thin, stratigraphically distinct sulfate unit immediately underlying siliciclastics of the lower Rustler. Although this unit is more genetically related to Salado deposition than to Rustler, it is used in cores and shafts for its stratigraphic continuity. This sulfate unit consists of anhydrite and occasionally, polyhalite. It commonly is laminated and can show textures similar to swallowtail gypsum. The lower part of the sulfate is generally argillaceous, while the upper portion is commonly free of clay. Both the upper and lower contacts of the sulfate are sharp and readily distinguishable.

Within Nash Draw, the Rustler/Salado contact is often disturbed and the lower portion of the unnamed lower member is brecciated (Pl. 1). Where this is the case, the Rustler still retains a general sense of stratigraphic organization and the general location of the lower contact can be inferred. The lower contact area is distinguished by an upward matrix color change from reddish-brown to gray. The contact between the Rustler and Salado in cores

from Nash Draw is arbitrarily placed at the highest occurrence of gypsum clasts in a reddish-brown matrix. These clasts are assumed to be the brecciated remnant of the lowermost sulfate assigned in cores and shafts to the Rustler (see above).

Two or more reddish-brown clastic units commonly overlie the sulfate unit. The thickness of the combined reddish-brown zone rarely exceeds a few feet (about 1 m). The units are usually mudstone or siltstone and are frequently separated by an erosional surface exhibiting several feet (1 - 2 m) of relief (Holt and Powers, 1984, 1986a). Soft sediment deformation enhances erosional relief on the contact and modifies bedding adjacent to the erosional surface. In both the waste handling and exhaust shafts at the WIPP site and in several nearby cores, the erosional surface is capped by a siltstone and/or sandstone pebble/cobble conglomerate containing fossil bivalve fragments (Holt and Powers, 1984, 1986a). The lowermost units are commonly sulfatic and can exhibit tabular mudstone clasts flattened parallel to bedding. The lowermost unit of WIPP 19 exhibits cracks that may be due to desiccation. In some cases, the bedding in these lower units becomes more distinct upward. The upper unit(s) (those above the sharp, undulatory contact marked by a conglomerate) commonly contains coarser-grained clastic material. Near the top of the reddish zone, gypsum or anhydrite nodules are abundant. Thin laminations are common throughout the reddish-brown zone and often show cross-cutting relationships. Cross-laminations are rare. The size of sedimentary structures generally decreases upward.

The bedding is partly modified by soft sediment deformation, though this is less intense and less common upward; it is most common above and below the erosional surface. The upper contact of this basal zone is marked by a color change from reddish-brown to gray and is erosional in many cores.

5.1.2 Clastic-Bioturbated Interval

The gray zone in the lower part of the unnamed lower member contains interbedded mudstone, siltstone, and locally very fine sandstone. The coarser grain sizes occur at the base and near the top of the gray zone, and these coarser grained beds are well lithified. The middle part of the gray zone within the WIPP area is soft and slightly argillaceous. This middle interval becomes more calcareous and less clastic to the south (borehole H-12). Anhydrite or gypsum nodules are abundant near the base of the gray

zone; nodules occur near the top of the unit in a few cores (e.g., DOE 2). Horizontal to subhorizontal stratification and cross-stratification are locally common and some show the effects of soft sediment loading. Light to dark gray mottling results from bioturbation. Stratification is poorly preserved in mottled zones, and is very irregular, wavy, and discontinuous. Subhorizontal to subvertical burrows, about 1/4 to 1/2 inch (6 to 12 mm) diameter, are very common throughout the entire interval and they are observed cutting across poorly preserved strata. Casts and molds of fossils, mostly bivalves, were preserved in the bioturbated interval of WIPP 19. Halite-replaced fossils and fossil fragments occur through the equivalent section in H-12. Possible coated grains and oolites were found in the lower calcareous portion of H-12 . Near the top of the bioturbated zone, the grain size increases as does the degree of preservation of stratification. The upper contact is gradational and is usually assigned to the first occurrence of a reddish or reddish-brown interbeds.

The equivalent to the lower bioturbated zone, in Culberson County, Texas, consists of siltstone, calcareous siltstone, and carbonate. The lower zone commonly exhibits thin, parallel laminae which can be disrupted locally and display some wavy to lenticular bedding. Bioturbation and burrowing are common within the upper dolomitic equivalent to this upper bioturbated zone observed in cores from Texas.

5.1.3 Clastic-Transition Interval

A color transition zone of alternating gray to reddish-brown and brownish-gray siltstone and very fine sandstone overlies the gray zone (clastic bioturbated interval). Gray is dominant near the base, while reddish-brown predominates near the top. Well preserved laminations, local cross-laminations, and rare erosional scour and fill structures characterize this interval. Within the exhaust shaft, interpretable paleocurrent directions mostly trend toward the south. Burrows are common near the base, but do not occur higher in the section. Subhorizontal laminations and cross-laminations become more distinctive upward as the grain size increases. In some cores, the upper portion exhibits gray, possibly anhydrite-rich, interbeds and very small clasts or nodules of gypsum or anhydrite. In general, the upper 3 to 4 ft (0.9 - 1.1 m) of this unit exhibits wavy to contorted and convoluted to lenticular laminations. Soft

sediment deformation is common in this interval. In the upper one to two ft (30 - 60 cm), the sulfate content increases upward, and displacive halite crystals occur in some cores. The upper contact is gradational, showing a marked increase in the content of sulfate.

A gypsiferous or anhydritic sandstone, between one and two ft (< 1 m) thick, tops the transition zone. It contains gray to dark gray interbeds and a few reddish-brown interbeds. The unit is microlaminated to thinly laminated, convoluted to contorted, and was deformed as a soft sediment. Structures interpreted to be either fluid escape structures or polygonal cracks are found consistently in this interval. A nodular to somewhat enterolithic texture marks some interbeds. The upper contact of the sulfatic bed is sharp to gradational.

5.1.4 Halite/Mudstone Interval 1 (H-1/M-1)

In the WIPP site area, a zone containing halite (H-1) and laterally equivalent mudstone (M-1) overlies the sulfatic zone at the top of the clastic-transition interval. The halite can be subdivided into three distinct intervals. The lower (H-1a) and the upper (H-1c) intervals consist primarily of a mix of clastics and halite. Relatively clean halite and traces of sulfate characterize the middle interval (H-1b). As a whole, the first halite zone (H-1) in the unnamed lower member varies in thickness from 34 ft (10 m) to a maximum of 50 ft (15 m) in H-12 and 48 ft (14.6 m) in AEC 8. Where mudstone is laterally equivalent to halite, the mudstone interval can be subdivided into an upper and a lower part separated by one sulfatic interbed. The overall thickness of this interval is about 19 ft (5.8 m) in those cores where the lower contact was cored. The thickness of the upper half varies between 3 and 6 ft (0.9 - 1.8 m).

5.1.4.1 Lower Halite Bearing Zone (H-1a)

In most WIPP cores examined, the sulfatic unit is normally overlain by the first halite bearing zone (H-1a) within the Rustler. This interval thickens to the south and east, reaching the thickest point observed in core at H-12. The basal part of H-1a consists primarily of slightly halitic siltstone which may be sandy in some places. The siltstone is commonly microlaminated to laminated and can be wavy to slightly contorted. White, anhydritic laminae and zones are commonly wavy to distorted. At H-12,

sulfate is more prevalent near the base of this zone than in other boreholes. A few small incorporative halite crystals occur near the base of the zone, and, in general, the halite content increases upward. Halite crystal size varies; some incorporative crystals are up to one inch (2.5 cm) on a side. A halite-filled prismatic crack (possibly due to desiccation) occurs near the top of H-1a in core from the borehole WIPP 19. The upper portion of the first halitic zone (H-1a) is dominated by clastics and anhydrite-rich laminae and zones.

5.1.4.2 Middle Halite Bearing Zone (H-1b)

The lower halite-bearing zone (H-1a) is overlain by a much purer halite interval (H-1b) that varies in thickness from 5 ft to 8 ft (1.5 to 2.4 m) in WIPP cores. Sulfate (anhydrite to gypsum) occurs as stringers and laminae to thick beds with thinly laminated internal structure. Irregular zones of halite occur within some of the sulfates. Anhydrite is more common near the base and top of H-1b. Thin laminae to laminae of clastic material separate beds of halite. The halite is medium to coarsely crystalline, clear to orange tinted with traces of intercrystalline and interstitial sulfate and clastic material and thinly to medium bedded. Vertically oriented, elongate crystals due to competetive growth (Shearman, 1978) occur locally, some exhibiting zones of fluid inclusions. Cloudy halite, due to fluid inclusions and indicating primary origins, is not abundant, but it does occur.

5.1.4.3 Upper Halite-Bearing Zone (H-1c)

The middle halite zone (H-1b) is overlain by an upper, more clastic-dominated halite-bearing interval (H-1c) that varies from 11 to 18 ft (3.4 to 5.5 m) thick. It is thinnest in the area of DOE 2 and WIPP 34 and thickens to the east and south with the thickest section at AEC 8 and the next thickest interval at H-12. The transition from H-1b to H-1c is marked by a sharp increase in the clastic content. The clastic content in H-1c fluctuates, with maxima near the middle and top of the unit. The clastic material consists mostly of siltstone and in H-1c is typically reddish-brown with some greenish-gray reduction spots and zones and white to gray sulfatic zones. The uppermost bed of H-1c is an anhydritic mudstone which exhibits thin laminae, sulfate nodules, and locally, clasts of mudstone.

5.1.4.4 Textures and Fabrics in Clastic-Rich Halite

The fabric of these halite-bearing rocks is quite variable; the most notable variations of fabric are type and amount of halite. Incorporative halite crystal fabric varies from isolated individual crystals (Pl. 2), to tightly packed locally touching crystals (Pl. 3). Interstitial matrix boundaries vary from planar to irregular. Displacive/incorporative overgrowths on halite crystals occur along the contact between aggregate halite and matrix material. Skeletal crystals occur in more clastic zones. Zones of partly incorporative halite crystals occur in distinct zones at the top of, and parallel to, well-defined clastic interbeds. Many of these crystals exhibit euhedral crystal faces oriented upward. Some zones of halite crystals display irregular to poorly defined bases with well defined upper boundaries. In these cases, planed-off crystals mark the upper boundaries. Some of these surfaces exhibit euhedral overgrowths oriented upward. Halite also occurs in zones and pods containing interlocking mosaics of crystals with some interstitial clastic material or sulfate (Pl. 4). These pods may be surrounded by clastic material or argillaceous halite. Where halite is abundant, crude stratification is common. Channel forms were reported in both intervals in the waste handling shaft and the exhaust shaft (Holt and Powers, 1984; 1986). These channel forms may be filled with dominantly clastic material or with halite.

The fabric of the rock is also controlled by the distribution of the clastic material. Clastic material occurs as matrix, intercrystalline material, interstitial material, and isolated pods or blebs within a dominantly halite rock. In most cases, the clastic material is relatively structureless, exhibits wavy to contorted to smeared thin laminae to thin beds, or contains smeared/deformed intraclasts showing no evidence of transport (Pl. 5). Some laminae surrounding incorporative halite crystals are contorted or displaced by those crystals.

5.1.4.5 Mudstone Interval (M-1)

Mudstone, claystone, and minor amounts of siltstone (M-1) are laterally equivalent to the halitic zone H-1. Where the lower contact was cored, this zone rests conformably upon the transition zone. This zone (M-1) is preserved in WIPP cores from Nash Draw and in the core from WIPP 30. M-1 is subdivided into an upper and a lower part by a medium to thick bed of

sulfate. The thickness of the lower part can not always be determined as the lower contact with the transition zone is not always preserved, or may be difficult to recognize, in the core. The upper part of M-1 varies in thickness from 3 to 6 ft (.9 to 1.8 m).

The mudstone commonly exhibits a smeared intraclast/laminae texture similar to that seen in halite clastic rocks. This texture consists of deformed or smeared intraclasts showing no evidence of transport and in some cases, irregular, poorly preserved, discontinuous laminae. The intraclasts and laminae appear to be squashed together while soft (Pl. 6, 7). Smeared laminae and intraclasts may be well preserved and distinct. In other cases, indistinct mottling is present. The mudstone may be structureless where the grain size is more uniform. M-1 has irregularly distributed and oriented slickensides. A few small nodules or clasts of gypsum and anhydrite occur within M-1. Some cores of this interval have a characteristic lumpy or corrugated surface indicative of the preferential removal of matrix or pseudomatrix by drilling fluids during coring. A few nodules and clasts of gypsum and anhydrite occur within M-1.

The lower contact of M-1 with the transition zone is generally well preserved. The mudstone (in some cores siltstone or very fine sandstone) is ordinarily thinly laminated to laminated within the first few ft (1 - 2 m) of the lower contact. The zone may also be slightly gypsiferous. The laminated zone is overlain by a zone exhibiting the smeared intraclast/laminae texture with varying amounts of clasts versus laminae. Zones containing well preserved (i.e., not disrupted) depositional fabrics occur in the lower part of M-1 and can bound zones exhibiting the smeared intraclast/laminae texture. Smeared intraclast/laminae textures are more abundant upward within the section and dominate the textures in the upper few feet of the lower part of M-1. Near the base of the lower part of M-1, gypsiferous interbeds may occur. Near the top of the lower part of M-1, small nodules of gypsum/anhydrite may occur. A medium to thick bed of mostly gypsum separates the upper part of M-1 from the lower part. The gypsum is thinly laminated to laminated and may locally exhibit swallowtail structures or nodules. The strata within the gypsum may be disrupted near the base of the bed. The gypsum contains laminae or very thin interbeds of claystone in some cores. The upper part of M-1 principally consists of claystone exhibiting the smeared intraclast/laminae texture. It is mostly reddish-brown with gray

smeared intraclasts of siltstone. The upper contact of M-1 is sharp to gradational with the overlying gypsum.

Within Nash Draw, portions of M-1 as well as most of the entire Rustler are disturbed and brecciated. In some cores (e.g., WIPP 25, WIPP 28, and WIPP 32), subangular to subrounded clasts of sulfate may be found near the top of both the upper and lower parts of M-1. In some cases, these gypsum clasts are derived from gypsum fracture filling (Pl. 8). Often these clasts are associated with breccia clasts and clay filled fracture-bounded blocks of mudstone exhibiting the smeared intraclast/laminae texture (Pl. 9). Some blocks are bounded by possible clay skins. Some zones exhibit well preserved stratification, now dipping. M-1 is not the only stratigraphic unit disturbed. In all cases, when M-1 is disturbed both the overlying and underlying rocks exhibit similar disturbance.

5.1.5 Anhydrite (A-1)

The first major sulfate unit of the Rustler overlies the halite zone and consists of anhydrite and gypsum. It varies in thickness from about 7 to 10 ft (2.1 to 3 m) to a maximum of 13 ft (4 m) in cores from WIPP 25 and WIPP 29. The increase in thickness in the Nash Draw boreholes is probably attributable to local dip (up to 25^{o}) and lengthening of the section due to downdropping, rotation of blocks, and brecciation within the section. The core of WIPP 32 exhibits only broken rotated blocks in this interval. The section there is considerably thinner than in other Nash Draw holes, as a block probably representing the lower portion of A-1 occurs 5 ft (1.5 m) below the base of the anhydrite surrounded by clastic matrix material.

The lowermost few inches (cm) of this bed appear nodular to enterolithic. Much of the section is thinly laminated to laminated. Laminae are commonly slightly wavy and some may be slightly contorted. A few stylolites occur within the laminated portion of A-1. Halite and anhydrite pseudomorphs after gypsum swallowtail crystals 1/4 inch to 6 inches (6 mm - 1.5 cm) high, are locally common in A-1 (Pl. 10). Swallowtails are most abundant and largest in the lower 2 to 3 ft (0.6 to 0.9 m). A second zone of swallowtails occurs near the middle of A-1 in several cores. It, too, may show an upward decrease of crystal size. A-1 in some of the WIPP cores exhibits the collapsed pseudomorph texture described elsewhere in this report. The upper 1 to 2 ft (30 to 60 cm) of A-1 is a stratigraphically

persistent pink-colored that shows in some cores a nodular texture, irregular/discontinuous laminae, and/or disturbed stratification/nodules. Clay content increases in the uppermost few inches (cm) of A-1. The upper contact is slightly gradational and irregular with the transition from sulfate to clastic material occurring over 1 to 2 inches (2.5 - 5 cm).

5.1.6 Mudstone/Halite Interval 2 (M-2/H-2)

A clastic zone (M-2), above A-1 in the WIPP site area, is partially equivalent to a halite-bearing interval (H-2) as much as 50 ft (15 m) south and east of the WIPP site center (Figs. 4.5, 4.6). The halite-bearing equivalent of this zone is not contained within any WIPP cores. However, its presence to the east is confirmed by both the cuttings and geophysical logs from the borehole P-18; the halitic zone is about 30 ft (9 m) thick there. The upper portion of interval M-2/H-2 has a widespread and characteristic gamma log signature regardless of the underlying material. The geophysical log signature suggests that this upper unit is generally argillaceous; it is up to 20 ft (6 m) thick east of the site (Figs. 4.5, 4.6). In the vicinity of the WIPP site, the thickness of M-2 varies slightly but averages about 10 ft (3 m).

In cores M-2 can be subdivided into two lithologically distinct zones: an upper gray zone and a lower reddish-brown zone. The gray upper zone is usually only about 2 ft (60 cm) thick in cores while the lower reddish-brown zone is about 7 to 8 ft (2.1 to 2.4 m) thick.

The reddish-brown lower zone commonly consists of mudstone and siltstone. It may be either calcareous or gypsiferous or both. Interbeds of gypsum, argillaceous gypsum, and carbonate are common. These interbeds and other distinct color changes within the clastic material have been reported as continuous, albeit undulatory, around the circumference of two shafts at the WIPP site (Holt and Powers, 1984, 1986a). Small clasts/nodules of gypsum up to 2 inches (5 cm) in diameter exist near the base of the lower zone. Sediment-incorporative gypsum crystals are found locally throughout the lower zone (Pl. 11). They are often euhedral to subhedral with a stubby-equant to bladed, or rarely stellate, habit. The clastic sediment in some cores contains gray zones or greenish-gray reduction spots. It can be structureless, or it can exhibit irregular and discontinuous laminae and thin laminae. Angular to sub-rounded clasts of siltstone and mudstone are

abundant and are often associated with zones exhibiting a smeared-interclast-laminae texture. Slickensides are common in the lower interval. Thin sections from this interval reveal oriented clay skins and possibly cutans (Pl. 12). In the core of WIPP 25, dolomite clasts believed to have originated from the overlying Culebra occur in this interval and are intermixed within the mudstone.

The upper gray zone is ordinarily about 2 ft (60 cm) thick and it consists of calcareous claystone and mudstone. The contact between the upper gray and lower reddish-brown zones is distinct. It can be structureless or micro to thinly laminated with flat to wavy strata. Light gray to tan carbonate clasts are abundant in this interval and vary in size from coarse sand-size to pebble-size (Pl. 13). These clasts can be well rounded to angular, and many were deformed while soft. In most cases, clasts are overlain by well preserved stratification. This interval locally exhibits slickensides. The upper contact with the Culebra Dolomite shows no clear break in deposition. The upper contact is undulatory in the exhaust shaft at the WIPP site (Holt and Powers, 1986a) and shows the effects of differential loading and subsequent settling of the Culebra. Similar features exist along this contact in outcrops east of Artesia, New Mexico (T17S, R28E). The upper interval is poorly preserved and/or deformed in some of the Nash Draw cores.

Holt and Powers (1986a) report a disrupted zone (discussed below) at the upper contact of this interval in the exhaust shaft at the WIPP site.

5.2 CULEBRA DOLOMITE MEMBER

The Culebra Dolomite Member of the Rustler Formation is the lowermost of two areally extensive dolomite units within the Rustler. The thickness of the Culebra varies from 20 to 30 ft (6.1 to 9.1 m) within the cores described (Figs. 5.4 and 5.5). The Culebra consists mainly of micritic dolomite.

The Culebra often cores poorly because of fractures. Holt and Powers (1986a) report that the Culebra is extensively fractured in the exhaust shaft at the WIPP and that mapping units were selected partly, if not wholly, on the basis of fracture patterns. Holt and Powers (1986a) also note an apparent relationship between the degree of induration, competency, and fracture patterns of mapping units and the amount of clay-rich interbeds and the apparent clay content of the dolomite. They generally correlate the abundance of broken, fractured beds and the overall content of clay.

The lowermost foot (30 cm) of the Culebra locally is thinly laminated to laminated with alternating light and dark brown laminae. This zone is rarely preserved in core. Within the exhaust shaft at the WIPP site, Holt and Powers (1986a) report that this zone is extremely undulatory and locally dips up to 45°. Deformational space problems manifest themselves as locally contorted and displaced laminae. Holt and Powers (1986a) report that this zone is brecciated in the vicinity of one of the major downwarps of this lowermost Culebra unit. The breccia consists of roughly 80% angular to subangular clasts of dolomite within a dolomite matrix. The units described and mapped within M-2 in the exhaust shaft parallel the lower contact of the Culebra. Directly below the downwarp and associated breccia, the upper units of M-2 are also downwarped and cut by the breccia. The middle and upper part of the Culebra is unaffected by the brecciation.

The bulk of the Culebra is microlaminated to thinly laminated. The strata may be flat to wavy to locally contorted and discontinuous. Portions of the Culebra appear macroscopically devoid of depositional fabric. The dolomite is mottled in some zones. With the exception of the upper and lower contact zones, there is very little variation of depositional sedimentary features throughout most of the Culebra.

The uppermost few inches to 1 ft (30 cm) of the Culebra often differs radically from the underlying dolomite. The gamma ray signature of this zone is unique and is present throughout the Delaware Basin (Ch. 4). Within the WIPP site area, this interval consists of waxy golden-brown carbonate, dark brown to black highly organic claystone, and locally coarser grained clastic material including siltstone. The interval exhibits microlaminated to thinly laminated strata that are usually subhorizontal, irregular, contorted on a fine scale, and discontinuous. Small gypsum nodules often occur flattened parallel to stratification. Holt and Powers (1984) report details of this interval in the waste handling shaft at the WIPP site. They describe moundlike or domal structures in this interval and assign a probable algal origin. Cornell (pers. comm., 1984) reported that material from this zone is rich in organic carbon.

Both open and filled porosity occur in the Culebra (Holt and Powers, 1984; 1986a). Gypsum is the major pore-filling mineral. Three porosity types were observed: vuggy porosity, intercrystalline porosity, and fracture porosity. Vuggy porosity varies in size from fractions of an inch to two

inches (up to 5 cm). Many large vugs are interconnected by fractures, and when unfilled, vugs and fractures commonly contain clay rims. When vugs and fractures are filled with gypsum, a portion of some vug-filling material may be optically continuous with adjacent fracture filling. Vug-filling gypsum is often polycrystalline, exhibiting two or more crystals with different optical positions. Twinning is common, and extensively twinned crystals may exhibit a somewhat undulatory extinction. Many filled vugs have one optically continuous, yet extremely undulose, crystal as a partial and imperfect rim with two other crystals constituting the bulk of the vug filling. Laminae often are terminated abruptly at the vug/dolomite contact. However, laminae in the dolomite also appear displaced around some vugs. Smaller vugs appear to have some depositional control, as they occur in distinct sub-horizontal zones.

Biogenic features have been observed in and reported from the Culebra at several localities, including the WIPP. Fossils in the Culebra were first reported by Donegan and DeFord (1950) and were studied further by Walter (1953). The authors have also observed gypsum-replaced bivalves in Culebra core from Texas. Some thin sections of the Culebra from WIPP 19 and H-12 contain fecal pellets and possible shell fragments. Burrows and mottling occur near the top of the Culebra in H-12. Holt and Powers (1984) suggest the organic-rich carbonate and clay at the top of the Culebra is algal in origin.

5.3 TAMARISK MEMBER

The Tamarisk Member of the Rustler Formation is divided into three parts: a lower sulfate (A-2), a middle halite/mudstone zone (H-3/M-3), and an upper sulfate (A-3) (Figs. 5.4 and 5.5). The Tamarisk thickens toward the south and east of the WIPP site. The Tamarisk within the WIPP cores described varies in thickness from 82 ft (25 m) at WIPP 19 to 121 ft (36.9 m) in H-12 and 120 and 119 ft (36.6 and 36.3 m) respectively in WIPP 13 and WIPP 25.

5.3.1 Anhydrite (A-2)

The lower anhydrite of the Tamarisk Member is an areally extensive unit. Several geophysical logs within the Delaware Basin of New Mexico indicate that A-2 is locally absent. This is also the case within the WIPP site area as A-2 is not present at WIPP 19. The maximum thickness of A-2 in cores is

21 ft (6.4 m) in WIPP 25. A-2 can be subdivided consistently into an upper and a lower part by a bed of mudstone. This mudstone bed occupies a stratigraphically distinct position and is areally extensive (Ch. 4). The lower part of A-2 varies in thickness within WIPP cores from a minimum of 6 ft (1.8 m) in the core of WIPP 12 to a maximum of 16 ft (4.9 m) in the core of WIPP 25. The average thickness of the lower part is about 9 to 10 ft (2.7 to 3 m). The upper part varies in thickness from 3 ft (0.9 m) at boreholes B-25 and H3-b3 to a maximum of 8 ft (2.4 m) at borehole H-11b3.

The sulfate consists of anhydrite in many cores but can be part gypsum. The most common sedimentary structure is stratification ranging from microlaminate to laminate. The strata are commonly wavy, may be locally contorted, or discontinuous, and in some extreme cases, can exhibit dipping strata (up to 80^{o} in WIPP 13). The laminae consist of sulfate interbedded with carbonate and/or claystone. The strata locally become convolute to crenulate with a small wavelength and amplitude. Stylolites are locally common within the laminated parts of A-2.

Both anhydrite and halite pseudomorphs after gypsum swallowtail crystals occur within the laminated sulfate of A-2. They are most abundant in the upper part of A-2. Zones where the size of swallowtails decreases upward are common in the upper part of A-2. In H-12, a similar zone of halite pseudomorphs after gypsum swallowtail crystals overlies a core that clearly does not retain a swallowtail morphology. The basal part of this zone exhibits a "pile of sticks" morphology; the "sticks" are similar to the intercrystalline laminae-like inclusions preserved in large swallowtail crystals, but are not arranged in any pattern reflecting swallowtail morphology. The base of this unit is in turn overlain by clearly more regular and vertically oriented halite pseudomorphs after gypsum that are up to 3 inches (7.6 cm) high. These larger pseudomorphs are followed vertically by smaller pseudomorphs and thinner laminae. The laminae within this zone become more horizontal, and the halite pseudomorphs become better aligned upward. Because of the clearly gradational sequence of textures from "pile of sticks" to pseudomorphs, this "pile of sticks" texture is interpreted as crushed pseudomorphs.

The sulfate of A-2 can also be nodular, especially near the upper and lower contacts and near the claystone which subdivides the unit. These poorly formed nodules are distributed unevenly within argillaceous anhydrite.

Within an argillaceous zone that is laterally equivalent to the subdividing claystone of A-2, an irregular vertically-oriented prism crack occurs which is filled with less argillaceous gypsum. (This prism crack appears similar to desiccation cracks in other sediments.)

The basal contact of A-2 is gradational. In the core of WIPP 13 a deformed calcareous mudstone at the base contains clasts and interbeds of gypsum. The core of WIPP 25 exhibits zones of breccia clasts of gypsum contained within a clear gypsum cement. The upper contact of A-2 may be slightly brecciated and irregular, and fractures displacing strata locally occur in this stratigraphic position. A small prism-crack is developed in the core of H-12 at the upper contact of A-2 with H-3. The upper contact of this zone is extremely undulatory and erosional in WIPP shafts (Holt and Powers, 1984, 1986a).

5.3.2 Halite (H-3) and Mudstone (M-3)

An interval containing halite (H-3) and laterally equivalent mudstone (M-3) occurs above the lower anhydrite (A-2) of the Tamarisk Member. Only the core of borehole H-12 contains halite (H-3) in this interval. H-3 in the core of H-12 is 40 ft (12.1 m) thick. M-3 varies from 9 ft (2.7 m) in DOE 2 to 17 ft (5.2 m) in WIPP 19. The halite is subdivided into lower (H-3a) and upper (H-3b) units by an areally extensive sulfate bed composed of polyhalite in much of the region (see Ch 4). Where the interval H-3 is thinned, the sulfate commonly directly underlies the upper anhydrite of the Tamarisk Member. Where this occurs, the upper part of H-3 (H-3b) has pinched out leaving no evidence of a clastic-rich stratigraphic equivalent (e.g., H-12) or disrupted or interrupted section. The halite represented in the core of H-12 is the lower part of the halite interval (H-3a). West of H-12, the stratigraphic equivalent of H-3a thins considerably and consists of mudstone (M-3) in the remaining WIPP cores described. This interval (M-3) is usually overlain by a sulfate sequence similar to the sequence preserved in the interval overlying the halite interval (H-3a) at H-12.

5.3.2.1 Tamarisk Member Halite (H-3)

H-3 forms a lens-shaped body with its thickest area (207 ft; 63 m) located in T22-24S, R33-35E (Fig. 4.4). It is subdivided into a lower (H-3a) and an upper (H-3b) part by a 1 to 3 ft (0.3 to 0.9 m) thick bed of

polyhalite. The thicknesses over much of the study area of H-3a and H-3b vary independently of one another, and one may occur where the other does not. However, H-3a is the more laterally extensive bed; H-3b is laterally more confined and pinches out near the eastern margin of the WIPP area (Ch. 4). The only core containing any halite in this stratigraphic interval is from borehole H-12, and only part of the interval H-3a exists there.

The lower part of H-3 (H-3a) can be subdivided on the basis of geophysical logs into lower and upper clean zones (low natural gamma, not argillaceous) separated by a clastic-rich/argillaceous zone (Ch. 4). The upper clean zone is restricted to the Rustler depocenter of the Delaware Basin. The middle clastic-rich/argillaceous zone occurs at the top of H-3a around the margins of the depocenter and is generally thinner toward the center of the basin. The core from H-12 is complete through the stratigraphic interval between the lower (A-2) and the upper (A-3) anhydrites of the Tamarisk; within this interval at H-12, the upper clean zone of H-3a does not occur while both the lower clean zone and the middle argillaceous zones are present. The upper clean zone pinches out east of H-12. The sulfate unit which separates H-3a from H-3b is present at H-12 at the top of the halite interval (H-3a) and converges with the upper anhydrite of the Tamarisk (A-3) to the west.

The lower clean halite zone from H-3a in the core of H-12 is nearly pure halite. Halite crystals from this zone may be equidimensional and, rarely vertically elongate. Zones of cloudy halite occur but are rare. Clay and sulfate occur as minor intercrystalline material and irregular blebs. The halite is mostly thin to medium bedded with strata separated by irregular laminae of anhydrite or (rarely) claystone and thin color bands, usually brown from disseminated clay. The surfaces under both sulfate and claystone beds are marked by dissolution; small trough-shaped dissolution pits filled with claystone or sulfate also occur. Some erosional surfaces are marked by thin crusts of sulfate. Laminae of claystone are more abundant near the top of this zone.

The middle argillaceous halite zone of H-3a is the uppermost zone of H-3a in the core of H-12 as the upper clear zone pinches out east of H-12. The lower contact is gradationally overlain by increasingly argillaceous halite which is in turn overlain by halitic siltstone. The clastic content decreases dramatically above the halitic siltstone and then increases

upward. The upper contact is marked by a halitic, anhydritic claystone with deformed, discontinuous, irregular laminae and halite containing blebs of claystone. Planar halite crystal boundaries are not common through this interval as most crystals do not exhibit a cubic form. Some incorporative crystals of halite do occur. Smeared intraclast/laminae textures occur in clastic sediments. As the clay content decreases, the fabric becomes more irregular.

The polyhalite which is so continuous in the center of the basin (Ch. 4) directly underlies the anhydrite (A-3) with no clastic unit separating them, as is the case at H-12 (Snyder, 1987). The upper part of H-3 (H-3b) does not occur within the core of H-12.

5.3.2.2 Tamarisk Member Mudstone (M-3)

Mudstones occur within a rough ring around a regionally extensive lens of halite (H-3). Most of the cores fall into this ring. Lateral variations within this mudstone ring are evident in cores of this interval in the vicinity of WIPP. The Tamarisk Member mudstone (M-3) thickens and thins on a local scale, and some variations reflect a controlled areal distribution or pattern of occurrence.

The term mudstone, as used here, allows for a range of lithologies including claystone and siltstone. M-3 is sulfatic and somewhat calcareous. The interval is predominantly reddish-brown with an uppermost gray zone. The color relationship was described by Holt and Powers (1984, 1986a) in both the waste handling and exhaust shafts as a reduction/oxidation contact. The gray zone may have associated pyrite and/or marcasite (Holt and Powers, 1986a).

The contact of M-3 with the lower anhydrite of the Tamarisk (A-2) is sharp and very undulatory. This contact undulates over four feet in the waste handling shaft and three feet in the exhaust shaft, and it is erosional (Holt and Powers, 1984; 1986a) (Pl. 14). At WIPP 19, the lower anhydrite (A-2) does not occur; M-3 is thicker, and directly overlies the Culebra with a sharp lower contact.

Unmodified sedimentary structures indicating clastic transport are rare within M-3, although subhorizontal laminae do occur. The most common texture is the smeared intraclast/laminae texture. Soft sediment deformation is a common feature where stratification is preserved. As deformation becomes more extreme, soft sediment deformation grades into the smeared

intraclast/laminae texture. Some subangular to subrounded clasts of mudstone and siltstone are included. Where the grain size and the color is uniform, as in most claystone intervals, the rock may appear structureless. Many surfaces of unslabbed core of M-3 exhibit a corrugated or lumpy appearance. This is associated with the smeared intraclast/laminae texture and is caused by removal of less well indurated matrix and pseudomatrix material during coring. M-3 has many slickensides, and slickensides may show differing orientations within several inches (cm).

Some sulfate occurs in M-3 as cements, incorporative crystals, gypsum pseudomorphs after anhydrite nodules, nodular anhydrite pseudomorphs after gypsum crystals, angular to subrounded clasts, local fibrous gypsum fracture fillings and overgrowths on detrital gypsum grains (Pl. 15). Incorporative gypsum crystals may be lenticular, subhedral, or euhedral, and both isolated crystals and stellate aggregates are common. Incorporative gypsum occurs in the following boreholes: WIPP 30, WIPP 34, WIPP 13, WIPP 33, DOE 2, AEC 8, and WIPP 12. Nodules and clasts of gypsum may be disseminated through M-3 but most commonly occur near the base (Holt and Powers, 1984; 1986a). Fibrous gypsum fracture fillings are locally common within M-3 and in the shafts (Holt and Powers 1984; 1986a); several generations of fracturing and subsequent filling are evident. The fractures may exhibit arcuate patterns possibly parallel with zones exhibiting slickenside partings. The fibrous fillings within fractures are variably oriented with some exhibiting a perpendicular relationship to the wall rock while others have a tilted to sigmoidal morphology.

The core of WIPP 19 is unique through this interval as the lower anhydrite of the Tamarisk Member (A-2) does not occur and the clastic rocks of M-3 directly overlie the Culebra Dolomite. The organic-rich stromatolitic zone at the top of the Culebra is overlain by smeared irregular strata and rip-up clasts. A thinly laminated claystone above the clasts is in turn overlain by deformed and contorted gray laminae. A claystone and siltstone clast conglomerate follows vertically the contorted laminae (Pl. 16). This clast-supported conglomerate consists of subangular to rounded granule- to pebble-sized clasts of gray and reddish-brown siltstone and rare clasts of gypsum. The average clast size appears to decrease upward. Some of the reddish-brown clasts have been deformed and form a pseudomatrix The conglomerate is overlain by a very thin bed of gypsum with an undulatory

base. Above the gypsum is a sequence of mudrocks that is similar to M-3 in other cores. The smeared intraclast/laminae texture is common, and local nodules/clasts of gypsum occur. A few carbonate clasts have been observed in this interval.

The upper contact of M-3 is sharp (Pl. 17). A distinctive 1 to 3 ft (0.3 to 0.9 m) zone of sulfate overlain by thinly laminated claystone overlies M-3 and is commonly preserved intact. However, the upper contact of M-3 is not everywhere distinct and undisturbed. The contact is disrupted in cores from Nash Draw and in several cores outside Nash Draw (WIPP 13, H-3b3, and H-11b3). Within these disrupted zones, the overlying stratigraphy is preserved to varying degrees. Extreme brecciation occurs at the upper contact of M-3 at WIPP 13. Allochthonous blocks of the overlying laminated anhydrite float within a claystone matrix. Block sizes increase upward until they occur as rotated blocks separated by thin stringers of claystone. Finally, the claystone does not occur and the blocks are in direct contact. Throughout the brecciated lower zone, recognizable clasts of well-laminated claystone occur. At borehole H-3b3, the sulfate and thinly laminated claystone which usually overlie M-3 do not occur, and a large rotated gypsum block floats within claystone near the top of the claystone. A 1.6 ft (0.5 m) thick breccia with clast size increasing upward and consisting of sulfate and laminated claystone occurs at the upper contact of M-3 in core from borehole H-11b3.

5.3.2.3 Polyhalite-Equivalent Sulfate

A 1 to 2 ft (30 to 60 cm) thick anhydrite or gypsum bed overlies M-3 in cores that have been disrupted along the upper contact of M-3 and H-3a. It is apparently stratigraphically equivalent to the polyhalite that separates H-3a from H-3b east and south of the WIPP site. This sulfate in most cores has a horizontal to subhorizontal fabric with hints of laminations, nodules, convulate stratification, and anhydrite pseudomorphs after vertically-oriented gypsum crystals. The sulfate may be argillaceous and consist of nodules surrounded by claystone within the lower part. Neomorphic gypsum commonly surrounds angular zones of anhydrite and some fractures are filled by fibrous gypsum. The upper contact with the thinly laminated claystone is sharp but does not appear erosional.

5.3.2.4 Claystone

Claystone, described as limestone in some core, overlies the polyhalite-equivalent sulfate. This bed is less than 1 ft (30 cm) thick, calcareous, locally organic-rich, and interbedded with some gypsum. The claystone is distinguished by parallel and predominantly flat microlaminations and thin laminations with alternating light and dark gray. Soft sediment deformation (slumping, contortion, and/or microfaulting) in this claystone is similar in appearance to the synsedimentary non-tectonically brecciated sediments of Brodzikowski and Van Loon (1985). Micronodules of gypsum are overlain by thin laminae of claystone. Fibrous gypsum-filled fractures are abundant within this zone. An en echelon pattern of gypsum-filled fractures reported in this zone in the waste handling shaft (Holt and Powers, 1984) indicates a shear along a subhorizontal or horizontal plane with displacement of the upper zone to the south. One fracture in this interval in the DOE 2 core demonstrates thrusting. The upper contact of this zone is gradational. The stratigraphic significance of this interval toward the center of the basin is not known as it is not distinguishable on geophysical logs, but it is a stratigraphically continuous and significant zone within the core-study area.

5.3.3 Tamarisk Member Upper Anhydrite (A-3)

The Tamarisk Member upper anhydrite (A-3) can be subdivided into three stratigraphically distinct zones which grade upward from one to another. These zones are, in ascending order, as follows: a lower laminated zone (A-3a), a middle zone (A-3b) exhibiting a crushed prismatic texture, and an upper bedded nodular zone (A3-c). Within the A-3, other distinct beds are present. For example, a very thin bed of claystone occurs 20 ft (6.1 m) up from the base of A-3 in the shafts . This claystone is usually washed out of core during drilling. Geophysical logs reveal it in those boreholes. Other stratigraphically distinct zones are evident in geophysical logs of this interval throughout the Delaware Basin (Ch. 4). In WIPP cores, the thickness of A-3 varies from 57 ft (17.4 m) at H-3b3 to 93 ft (28.4 m) at WIPP 13. Some general relationships can be inferred by comparing the combined thickness of the middle (A-3b) and the upper (A-3c) zones to the thickness of the lower zone (A-3a). A-3b and A-3c are combined as they are vertically quite gradational. It varies from 33 to 40 ft (10 to 12.2 m) and averages

about 35 ft (10.7 m). A-3a varies in thickness from 19 ft (5.8 m) at H-3b3 to 47 ft (14.3 m) at WIPP 25. For the most part, the thickness of A-3 varies with the thickness of A-3a.

5.3.3.1 Lower Laminated Zone (A-3a)

The lower laminated portion (A-3a) of the upper Tamarisk Member anhydrite (A-3) consists of anhydrite with minor gypsum. Near the lower contact, the anhydrite is interbedded with carbonate. Poorly preserved ripple cross-laminae occur within both carbonate-rich and anhydrite interbeds, and cross-cutting relationships are evident. Microlaminae to laminae predominate and may be flat and parallel but are wavy or contorted to crenulate. Anhydrite halite pseudomorphs after gypsum are common in borehole H-12. Pseudomorphs after vertically oriented prismatic gypsum crystals are abundant locally and occur in genetically related zones exhibiting an upward decrease in crystal size. The height of the prisms varies from less than 1/4 to 4 inch (6 mm to 10 cm). These pseudomorphs are not all oriented perpendicular to the substrate and may be tipped over to one side, crushed, slumped, smeared, and disrupted (Pl. 18). Carbonate and gypsum laminae locally drape pseudomorphs. In many cases, pseudomorphs after prismatic gypsum contain microlaminae to thin laminae of carbonate or fine grained anhydrite oriented parallel to crystal growth planes. Pseudomorphs after epitaxial gypsum prisms are rare but do occur. Probable stylolites through this interval are distinguished by a crenulate zone parallel to stratification and marked by a dark concentration of clay and carbonate. The upper contact of A-3a is gradational with A-3b.

5.3.3.2 Middle "Crushed Prism" Zone (A-3b)

The middle zone (A-3b) within the Tamarisk upper anhydrite is characterized by the "crushed prism" texture (Pl. 19, 20 and 21). This texture is created by modifying the volume of an originally laminated sediment containing large or small prismatic gypsum crystals. Some to all of the volume originally occupied by the crystals was lost to create the characteristic texture. The genesis of the texture will be described later.

The most prominent feature of the crushed prism texture is irregularly shaped masses of sulfate that are vertically elongate. These may be lighter in color than the sulfate between these masses. The masses have parallel

internal stratification, though it is not continuous between masses. The stratification indicates displacement or rotation of the mass relative to adjacent masses. The stratification can also be disk-shaped. Anhydrite pseudomorphs after tiny prismatic gypsum crystals may be preserved. Boundaries between these vertically elongate masses are commonly v-shaped and may have angles of 45^{o} or more. As further evidence of the origin of this texture, a portion or ghost of an original prismatic gypsum crystal is visible in some of the v-shaped darker sulfate between masses.

This texture might initially be confused with nodular textures. It can be separately diagnosed in the absence of ghost or remnant prismatic gypsum by the irregular vertically elongate shape, v-shaped boundaries, and the lack of an exclusionary margin. A strong sub-horizontal pattern, to be confused with bedded-nodular texture, is not seen though it is possible that the original size and space of prismatic gypsum could vary such that the crushed prism texture would appear similar.

The textures preserved in A-3b indicate that the rock was originally dominated by prismatic gypsum crystals. One or more sequences are present where crystal size decreases upward. Some of the crystals grew to be at least 1 ft (30 cm) high. Strata size is proportional to crystal size. The crushed prism texture is increasingly developed, and apparently becomes more mature, upward from the base of the zone. Prismatic crystals are present, although visibly reduced in volume at the base. Crystal preservation decreases upward until no relic or ghost prisms remain.

5.3.3.3 Bedded Nodular Zone (A-3c)

The upper zone of A-3 is stratified with a superimposed nodular texture (bedded nodular zone - A-3c). The lower contact of A-3c is gradational, and locally A-3c exhibits the crushed prism texture. The sulfate is interbedded with carbonate, and the carbonate content increases upward. Anhydrite is increasingly altered to gypsum upward.

The bedded-nodular fabric results from an exclusive nodular fabric superimposed on stratified sulfate rock (Pl. 22). Internal layering is traceable from nodule to nodule. In general, nodules occur in distinct horizontal zones with similar nodule sizes, reflecting bedding control on size and distribution. Some nodules exhibit anhydrite pseudomorphs after prismatic gypsum crystals. Unlike the crushed prism texture, the

commonly, irregular organic-rich laminations occur in groups or zones and are very common at and near the base of the Magenta. This lower zone exhibits very low-amplitude laterally-linked hemispheroids. Within the core of WIPP 19, probable small vertically oriented prismatic gypsum crystals occur within an algal laminated zone of low-amplitude laterally-linked hemispheroids.

The subhorizontal laminae are overlain by a zone containing closely spaced, microlaminated to thinly laminated algal hemispheroids. These hemispheroids may be laterally linked by laminations. In some cases, the laminae within hemispheroids retain the same radius and thus appear vertically stacked. The basal radius varies from 4 to 8inches (10 to 20 cm). These hemispheroids are similar to algal biscuits observed by Gebelein (1969).

A zone dominated by wavy laminations and lenticular-shaped, very thin beds overlies the hemispheroids. Draping laminae are common through this zone. Lens shaped or lenticular interbeds often thicken in the trough and thin over the tops of the underlying wavy strata. The amplitude of the wavy strata decreases upward while the wavelength appears to increase upward. Dark organic-rich interlaminae are common through this zone.

Gypsum nodules near the base of the algal-dominated unit decrease in size and abundance upward. Subhorizontal gypsum-filled fractures are common throughout the algal-dominated unit but are most common in the wavy to lenticular bedded zone where there are abundant clay interbeds and partings.

5.4.2 Cross-Laminated Unit

The upper of the Magenta is dominated by horizontal to subhorizontal, wavy to lenticular beds exhibiting cross-laminations and cross-laminated bedforms. The cross-laminated unit was subdivided into six mapping units during the mapping of the Magenta in the exhaust shaft (Holt and Powers, 1986a). Those mapping units can be identified in cores of the Magenta. The vertical sequence of sedimentary structures will be discussed later.

The clastic sedimentary structures observed within the upper unit include: ripple cross-laminations; ripple drift cross-laminations, starved ripples; both erosional stoss and depositional stoss climbing ripples; wavy and lenticular bedding; flaser bedding; erosional scour marks; clay drape; soft sediment loading; probable rip-up pebbles; pebbles at base of cross-laminations; local cross-bedding; and structureless beds. These

sedimentary features are most common within subhorizontal, very thin and thin beds that are laterally continuous.

At the base of the cross-laminated unit, grain sizes are more homogeneous and clay-rich interbeds are less common than in the underlying unit. Wavy bedding with low-angle cross-stratification is very common. The amount of cross-laminations and ripple forms and the average set size increases upward as does the grain size. Nearly structureless very thin interbeds are common near the top of the cross-laminated unit. Gypsum nodules become more common and an areally persistent, very thin bed containing abundant gypsum nodules occurs within the upper 2 ft (60 cm). The uppermost contact with the overlying Forty-niner Member is gradational as the carbonate fraction decreases and is interbedded with gypsum. Small nodules of gypsum are common both within the gypsum-rich interbeds and the carbonate interbeds.

5.5 FORTY-NINER MEMBER

The Forty-niner Member of the Rustler Formation is similar to the Tamarisk Member as it consists of a lower (A-4) and an upper (A-5) sulfate unit separated by a mudstone unit (M-4) and laterally equivalent halite (H-4) unit (Figs. 5.4 and 5.5). Within the upper anhydrite (A-5), a second halite unit present at the depocenter of the basin (Ch. 4) does not occur near the WIPP site.

5.5.1 Anhydrite (A-4)

The lower sulfate unit (A-4) within the Forty-niner is an areally extensive unit that varies from 15 to 21 ft (4.6 to 6.4 m) thick in cores. The sulfate mainly consists of anhydrite with some gypsum and carbonate. The carbonate interbeds are most abundant at the base of A-4 and decrease upward. The uppermost foot (30 cm) of A-4 is partly argillaceous. Small nodules of sulfate are abundant in the lower interbeds. Bedded nodular textures locally occur, and nodules may be superimposed upon nodules. Chicken-wire nodular and enterolithic textures are present. The nodular texture becomes better developed and larger upward as the more mature nodular features dominate. The upper few feet (m) of A-4 may be in part laminated to thinly laminated, and the laminae may be wavy to slightly contorted. The upper contact of A-4 is sharp.

5.5.2 Mudstone (M-4) and Halite (H-4)

The mudstone interval of the Forty-niner Member is laterally equivalent to an argillaceous halite and halite toward the depositional center of the Delaware Basin. Of the WIPP cores examined, only H-12 contained halite in this unit. Geophysical log interpretations suggest that halite occurs within this zone in boreholes from the eastern site area (e.g., P-18, P-19, P-20). The M-4/H-4 interval consistently thickens toward the depositional center of the basin as the halite content appears to increase.

5.5.2.1 Forty-niner Member Mudstone (M-4)

M-4 varies from a minimum of 6 ft (2 m) at AEC 8 to a maximum of 17 ft (5.2 m) at WIPP 25. In addition to mudstone, M-4 may consist of siltstone, claystone, and locally some sandstone. It is commonly gypsiferous and/or calcareous. Thin sections from this interval at WIPP 19 show a halite cement and incipient displacive halite crystals (Pl. 23). Both large and small scale primary sedimentary structures are common through this interval. In the waste handling shaft, large scale cross-cutting relationships were observed in M-4 as a wedge-shaped unit bounded by erosional surfaces (Holt and Powers, 1984).

M-4 was subdivided into five mapping units in the exhaust shaft, and they are recognizable in the cores as three reddish-brown units between upper and lower gray beds. The lowermost unit within M-4 is gray siltstone 2 to 3 ft (0.6 to 0.9 m) thick. It is locally gypsiferous and contains irregular gypsum-rich laminae and some gypsum nodules. The lower gray unit has well defined and preserved horizontal to subhorizontal thin laminae to very thin beds. It may locally be structureless. The lower reddish-brown unit is the thickest and usually varies from 5 to 6 ft (1.5 to 1.8 m) in thickness. The stratification within this unit is less distinct than that of the underlying and overlying units. Stratification is more abundant near the top of the unit and occurs as discontinuous, wavy to irregular, locally slightly contorted thin laminae to very thin beds. Interbeds are white to gray. The lower part of this unit displays small granule to small pebble sized clasts of mudstone and exhibits smeared intraclast textures. Greenish-gray reduction spots are common. The middle and upper reddish-brown units are not always distinguishable from one another in core. The middle reddish-brown unit is about 1 ft (30 cm) thick. It is separated from the underlying unit

by a relatively large scale erosional surface that is continuous around the circumference of the exhaust shaft. As in the underlying unit, the stratification is distinguished by color and consists of irregular to discontinuous wavy laminations to thin beds. The unit is locally gypsiferous. The upper reddish-brown unit is also about 1 ft (30 cm) thick. It has subhorizontal to horizontal, slightly wavy thin laminations to laminations. In general, stratification is more continuous and better preserved than in the underlying units. The uppermost gray bed has sedimentary structures similar to the upper reddish-brown unit. The upper contact of M-4 with the overlying anhydrite (A-5) is sharp and distinct (Pl. 24). Gypsum nodules and gypsum crystals appear to be areally restricted, as they are most common in WIPP 12, WIPP 19, B-25, exhaust shaft, waste handling shaft, H-3, H-11, and H-12.

5.5.2.2 Forty-niner Member Halite (H-4)

Within the cores examined, only H-12 contained halite in the stratigraphic unit equivalent to M-4. The halite interval (H-4) there is argillaceous and not very thick. Geophysical log interpretations suggest that the amount of clay in this unit decreases and the overall thickness of H-4 increases eastward toward the depositional center of the basin. At borehole H-13, the stratigraphic sequence described for the interval M-4 is present. Five ft (1.5 m) of halite-bearing sediment occurs within the 12 ft (3.7 m) section of H-4. The halite is in a stratigraphic position equivalent to the lower part of the lower reddish-brown unit of M-4.

The lower contact of the halite-bearing zone with the lateral equivalent of the lower gray unit of M-4 is sharp. Siltstone and claystone matrix is abundant near the upper and lower contacts where incorporative halite crystals are common. Aggregates of halite crystals are associated with irregular blebs of siltstone within the remainder of the halite section. The upper contact of the halite-bearing interval is gradational and is overlain by the lateral equivalent of the upper part of the lower reddish-brown unit. The remainder of the sequence at H-12 is similar to the sequence observed in M-4 in other cores and the shafts and preserves the middle and upper reddish-brown units and the upper gray unit.

5.5.3 Anhydrite (A-5)

The uppermost sulfate within the Rustler Formation is areally extensive and is locally subdivided into two parts by a thin halite unit (see Ch.4: Lateral Relationships). The thickness of the sulfate varies from 28 to 37 ft (8.5 to 11.3 m) in the core study area.

The sulfate bed consists of anhydrite, gypsum, and carbonate. The anhydrite is usually thinly laminated to laminated, wavy to slightly contorted, with locally abundant anhydrite pseudomorphs after vertically oriented prismatic gypsum crystals up to two inches high. Pseudomorphs after prismatic gypsum can be tipped over, smeared, or vertically oriented. Some reflect epitaxial gypsum growth. Pseudomorphs in some zones become smaller upward. Very carbonate-rich interbeds occur. Horizontal to subhorizontal stylolites within laminated intervals are common. The anhydrite may locally exhibit nodules and/or the bedded nodular fabric. Possible prism cracks occur locally. The upper contact is sharp and erosional.

energy of the depositional system was high or the sulfate content was low enough to prevent incorporative gypsum development. Instead, gypsum was precipitated during the desiccation phase following flooding. After flooding, the base level or water table was at the surface of the mudflat. Evaporative pumping concentrated the sulfate at the surface where gypsum was precipitated within void spaces, forming a gypsum cement or incipient gypcrete within one to several laminae. Further evaporation drove the water table deeper. This resulted in desiccation of the muds and upon the next flooding event, reworking and deposition of fragile rip up clasts from desiccation. This clastic interval records an initial increase of the potential and kinetic energy of the basin.

6.1.2 Lagoonal Environment

An unconformity with a documented local relief of over 3 ft (1 m) marks the beginning of perhaps the greatest variation of depositional style and environment within the Delaware Basin since the Guadalupian/Ochoan transition. Once again, the waters within the basin were, for at least a short period of time, directly connected with marine waters. The unconformity was described in shafts within a few ft (1 to 2 m) of the base of the Rustler. The presence of fossil bivalve fragments within a thin conglomerate locally overlying the unconformity suggests that a basin-wide freshening to at least near-marine conditions had already occurred and may have been quite rapid. Presumably, the source of the water and fauna was to the south through the Hovey Channel. The transgression was rapid, leaving only isolated occurrences of conglomerate as record of its passing. Consistent with the rapid nature of the transition, grain size and sedimentary structure size within the rocks overlying the unconformity indicate a decrease of system energy upward. Within a few feet of the unconformity, the system's energy reached a relative steady state as burrowing and bioturbation become prevalent within a near-marine to marine lagoon-like environment.

Clastic deposition continued under shallow lagoonal conditions, and clastic depositional fabrics were subsequently modified by burrowing organisms. Most bedding fabrics are not the result of migrating bedforms. However, cross-laminations do occur and are more abundant higher in the section. During quiescent times of little or no deposition of clastic

materials, bioturbation and burrowing were prevalent and in some cases so complete as to completely eradicate any sedimentary structure and leave only mottled siltstone. This mottled appearance formed during periods when the substrate was relatively stable (i.e., limited addition of clastics), and in general, the degree of completeness of the bioturbation reflects of the length of time that the substrate was stable. In other instances, when the energy of the system was higher, clastics were deposited more rapidly, essentially eliminating bioturbation or, at the least, diluting its effect. This is represented by those zones containing well preserved stratification with no or few burrows.

The presence of a lagoon with water of near-marine salinity has important implications. A direct connection to marine waters can be implied by the presence of marine to near-marine fossils. This is important as it represents the first and only documented near-marine episode within the Delaware Basin during the Ochoan Epoch. (There is growing evidence that the Dewey Lake is not marine (Schiel, 1987, in progress) contary to earlier suggestions.) Several possible events could result in such a marine incursion. First, a rapid change of absolute sea level could result in such a rapid transgression. However, there is no direct evidence to support it, and such an event would be likely to have longer lasting and broader effects. More than likely, whatever had barred the Delaware Basin during the preceding portion of the Ochoan was breached, and marine water rapidly transgressed over a large area with very low relief. Such a breach could have easily resulted from a local tectonic event resulting also in subsidence. It is clear that the marine invasion and the subsequent shallow lagoonal system yielded a higher overall base level, and the effect of a raising of base level is to decrease the hydrologic gradient in the depositional basin. However, for coarse clastic material to continue to be supplied to the lagoonal setting, the gradient within the basin must rise to counter the decrease caused by a rising base level. In the face of a rising base level, the gradient could only increase as the result of tectonic activity. As the distribution of clastic material seems to decrease somewhat to the south (Ch. 4), the source areas for clastic materials within the northern part of the Delaware Basin were probably to the north and northwest. Whatever tectonic activity increased the potential for clastic deposition must have affected those areas to the north and northwest.

Although separate tectonic events could have resulted in local subsidence and uplift of potential clastic source areas, one tectonic event could be envisioned that could account for both the breach of a southern barrier and yet could keep the energy of the basin at or near the same level in the north. A southerly tilting of the Delaware Basin and possibly a portion of the Northwestern Shelf could account simultaneously for both situations. Figures 4.3 and 4.6 display thicker basal clastics to the south consistent with this proposal.

6.1.3 Fresh to Saline Transitional Facies

The transition between marine or near-marine lagoonal deposition and playa-like deposition of evaporites is recorded by several ft (2 - 3 m) of dominantly clastic rock about 35 - 40 ft (10.7 - 12.2 m) below the Culebra at the WIPP site. This zone contains no obvious erosional surfaces of any magnitude and is not very thick, so it is likely that deposition was nearly continuous with no major hiatus. Thus, the transition itself must have been rapid. As the size of both sedimentary structures and clastic grains increases upward within the section, both the potential and kinetic energy of the system increased with time. This is consistent with shallowing upward in near-shore or shallow marine systems.

Near the top of the sequence, groups of carbonate-rich interlaminae occur and are followed vertically by groups of gypsiferous interlaminae. Their presence indicates that solutes were being concentrated within the ground/depositional waters. Less indurated laminae commonly bound the calcareous or gypsiferous laminae that stand out as resistant zones in cores of this interval. The tops of laminae commonly contain the most cement. These laminae have been preferentially cemented by the precipitation of either carbonate or sulfate without affecting the overlying laminae and with minimal effect on the underlying strata. It is very unlikely that this cement is the result of a much later pervasive diagenetic process as porosity and permeability do not vary significantly from lamina to lamina. Therefore, the cements must be related to an early process. Did these cements form by the concentration of solutes at the sediment/air interface on a subaerially exposed mudflat, or did they form subaqueously?

In subaerially exposed gypsum saline mudflats in Death Valley, Saline Valley and Bristol Dry Lake, California, most clastic laminae are very

irregular in both thickness and shape. These irregularities are in part due to very early diagenetic growth of gypsum within the sediment. Efflorescent crusts are commonly found at the surface of an active saline mudflat and also contribute to the formation of irregular stratification. Eolian sediment is trapped within the efflorescence crust and on the lee side of irregularities (e.g. polygonal cracks) on the surface of the crust. The efflorescent crust is ephemeral and dissolves with the next rainfall or flooding event. The trapped sediment is then deposited on the underlying clastic material creating very irregular, discontinuous pockets of sediment and laminae. If a flooding event causes the dissolution of the efflorescent crust, the sediment carried with the flood is deposited over a rapidly dissolving irregular surface. Should the crust be dissolved before sediment is deposited, an irregular surface forms from freshly freed eolian sediment. Once the water evaporates or infiltrates, another efflorescent crust forms and displacive growth within the crust further disrupts the sediment. Preservation of efflorescence crust is highly unlikely, and none was observed within the sediment sections in any of the California examples. The laminae in this section of the Rustler are, however, regular in nature and do not resemble those observed in subaerially exposed mudflats. It is unlikely, then, that the cements observed within the laminae originated at the sediment/air interface.

The cements are clearly early, but did not originate due to subaerial exposure; they must have occurred early in a subaqueous environment. The laminae have a regular morphology. They are somewhat wavy and locally contorted, but this deformation is due to soft-sediment loading. As the tops of the laminae contain the most cement, it is likely that deposition of the clastic laminae was followed by a period of nucleation of carbonate and/or gypsum on and within the substrate. During this time, little or no reworking of clastic sediment could have occurred. The cement effectively stabilized the substrate preserving the laminae. Early cementation of laminae at the bottom of a saline body has been reported for both modern and ancient examples by other workers (e.g. Garrison and others, 1978, for Messinian gypsum; Warren, 1982a, for Holocene gypsum in salinas). Clastic deposition resumed and either a freshening or the mechanical energy of the system prevented further precipitation of cement. As long as the system remained energetic, cement did not precipitate. This type of laminae can be used to

indicate subaqueous depositional environments

Sulfate within the sediment is more concentrated up section until sulfate laminae are common forming a 1 to 2 ft (30 to 60 cm) thick zone about 30 to 35 ft (9.1 to 10.7 m) below the Culebra in the WIPP site area. In most cores, clastics are still present. Most of the laminations are regular and suggest a subaqueous origin. However, the stratification may be very convoluted to contorted. Soft sediment shear and loading are in part responsible for this deformation. Enterolithic and nodular structures locally are present. These formed by expansive growth within the soft sediment and partially deformed some laminae. Irregular to prismatic vertical features are abundant in the zone containing enterolithic and nodular textures and are interpreted as possible desiccation cracks.

The sulfate-rich interval represents the final stage of the transition from the near-marine lagoonal deposits to playa-like deposits. This interval may be a silica-rich version of Warren's (1982a) gypsarenite, which he uses without genetic connotation. Warren (1982a) defines gypsarenite as "gypsum which contains at least 50% sand-sized gypsum grains." From the preserved sediment record, it has not been possible to determine the original grain size of the gypsum due to diogenesis. However, it is likely that depositional processes similar to these suggested by Warren produced the sulfate interval. Laminated gypsarenite (after Warren, 1982a) consists of laminae of mechanically deposited gypsum and/or gypsum formed in situ. In this interval, most of the gypsum was probably reworked mechanically and deposited with some clastic material. The gypsum converted to anhydrite during burial and/or early diagenetic growth of gypsum within the sediment probably destroyed all of the original gypsum textures but the laminations. Arakel (1980) observed similar sediments in the Hutt and Leaman Lagoons of western Australia and found that early diagenesis of gypsum (less than 6,000 years old) had obliterated most primary crystal fabrics.

The desiccation cracks and enterolithic to nodular structures within the sulfate are consistent with subaerial exposure. The prismatic cracks found within this stratigraphic zone may be parts of large scale polygonal cracks. Several authors (e.g. Neal and others, 1968; Tucker, 1981; and Lowenstein and Hardie, 1985) have discussed the possible origins of these features. These prismatic cracks are clear evidence of subaerial exposure. Nodular and enterolithic structures, however, are not unique indicators of subaerial

exposure; syndepositional diagenetic growth of sulfate is common in both the subaqueous and subaerially deposited sediments. Enterolithic and nodular structures, when observed within some stratigraphic sequences, are often interpreted to have formed in a subaerially exposed environment (e.g., a sabkha: Shearman, 1978). Other examples of enterolithic and/or nodular sulfate are interpreted to have formed diagenetically in sediments in subaqueous environments (e.g., the Castile Formation: Dean and others, 1975). Dean and others (1975) suggest that nodular and enterolithic structures are not diagnostic of either subaerial exposure or subaqueous deposition.

During subaerial exposure of the sulfate interval, sulfate was precipitated and disseminated throughout the soft sediment, including those rocks associated with the marine transgression. When the potentiometric surface of the water table is at or below the surface of the sediment, the salinity of the groundwater became much higher than the maximum salinity of the previously standing body of water due to capillary evaporation. This would be the optimal time to develop early diagenetic gypsum. Cody and Hull (1980) demonstrated that primary anhydrite could nucleate in the presence of certain types of macromolecular organic compounds at temperatures and salinities expected in hot, arid regions. It is possible that some of the sulfate originated as primary anhydrite.

The sulfate interval meets Warren's (1982a) hydrologic criteria for a continental playa: 1) the hydrologic system depositing the sulfate interval was clearly separated from large volumes of saline water (e.g., marine water), and 2) the sulfate was deposited on a clastic (clayey) substrate. Further, Warren reports that the gypsum within the central part of the paleopond area of continental playas in Australia is usually less than 3 ft (1 m) thick, nearly the same thickness as the sulfate interval in the Rustler. Clastic material was brought into the basin during episodic flooding. Both cementing processes (previously discussed) and precipitation and reworking of gypsum on the substrate account for the presence of sulfate in this interval. Analogous sediments with a similar origin are reported in Hutt Lagoon, western Australia (Arakel, 1980). The variable depositional style and lack of larger, more stable forms of gypsum reflect the dynamic chemical and mechanical nature of the small, precipitating brine body.

Any connection with marine waters must have been blocked prior to the deposition of this zone as the transition appears to have taken little time and an overall salinity change occurred rapidly. Potential evaporation rates were apparently high as saturation with respect to gypsum was reached easily and quickly. As Warren (1982) points out in his discussion concerning salinas in Australia, rapid changes of salinity cannot occur within fluid well connected with a large (for all practical purposes, infinite) body of fluid with a constant salinity. Rapid changes of salinity can, therefore, most reasonably occur within small volumes of fluid. The preservation of the transitional sequence indicates continued relative subsidence through the period of deposition while the sedimentary features indicate a rapid shallowing upward. If the basin were not effectively sealed from marine waters, subsidence would not be reflected within the sediment as shallowing upward. Instead, lagoonal-type sediment deposition would have begun again or continued. The rapid increase of the kinetic energy of the system and the concentration of solutes within the water resulted in the death of burrowing organisms. The ease of gypsum saturation, the increase of grain size (potential energy), the increasing-upward occurrence of sedimentary structures showing the migration of bedforms, and the presence of probable polygonal/desiccation structures are all consistent with a transition from a near-marine lagoon, via a rapid shallowing upward due to evaporation, to a subaerially exposed sulfatic saline mudflat.

Such a transition is rarely preserved geologically. Usually, the evident transitions between widely differing depositional environments are erased by one or more erosional events. The time between preserved depositional events is unknown, and those events whose records were erased by, and the amount of time unrecorded by, the hiatus cannot be determined. The complete transition between near-marine conditions and the deposition of halite in a saline mudflat is preserved here. These sediments recording the transition were preserved because of continued subsidence through the transition. Subsidence prevented reworking of sediment within the basin during a time of decreasing base level and allowed nearly continuous deposition to occur.

6.1.4 Halite (H-1) and Mudstone (M-1) Deposition

The fresh to saline transitional facies are overlain by a sequence of rock dominated by halite and laterally equivalent mudstone. The lateral

relationships between the halite-bearing zone and the mudstone zone are in part depositionally controlled. The halite sequence (H-1) appears to be the product of the interaction between halite saline mudflat, mud-rich salt pan, and mud-poor salt pan environments (see section 6.2). Marginal subenvironments consisting of gypsum saline mudflats and mudflats existed around the periphery of the halite depositing environments (see section 6.2). Halite was further concentrated in the depositional center of the basin by the syndepositional dissolution of halite from marginal environments and relocation of solutes toward the center during episodic subsidence of the depocenter center. The WIPP site and Nash Draw area are located along the margin of the depocenter center of the basin, and the rocks present in the H-1/M-1 stratigraphic interval in the study area formed as the result of the interaction of halite depositional environments with marginal nonevaporitic environments.

Above the transitional facies, clastics continued to be deposited. Groundwater salinity increased by evaporation, and halite reached saturation. Displacive crystals nucleated and precipitated within the clastic sediment in a halite saline mudflat. An increasing upward content of displacive crystals suggests that the salinity was also increasing with time. A standing brine body developed in the depocenter and a mud-rich to mud-poor halite pan developed. The halite pan occupied the lowest topographic areas. The mud-rich part of the salt pan was affected more by syndepositional dissolution as it was closer to the margin. Within the WIPP area, unit H-1a was deposited by the interaction of both saline mudflat and mud-rich salt pan environments. A minor transgression or flooding event halted the deposition of H-1a. The input of clastic material was stopped by the sudden rise of base level. Sulfate was locally deposited as the standing body of water was concentrated through evaporation. As evaporation and attendant concentration continued, halite saturation was again reached. A large mud-poor salt pan developed and H-1b was deposited. Minor freshening events did not bring much clastic material into the system but did precipitate thin layers of gypsum. Subsidence increased, and the base level was lowered. Flooding associated with subsidence again introduced clastic material into the system. The size of the mud-poor salt pan decreased considerably, and mud-rich salt pan deposition dominated the system throughout the deposition of H-1c.

Cores of M-1 suggest that it was deposited by the interaction of mudflat, saline mudflat, and possibly mud-rich salt pan environments and with intermittent syndepositional dissolution resulting from flooding events and vadose exposure. Halitic facies of H-1 extended beyond their present boundaries before being partially removed by syndepositional dissolution. Some flooding or transgressive events inundated the margins. Subaqueous gypsum deposition followed resulting in widespread sulfate units that extend beyond the bounds of the salt pan and associated environments.

6.1.5 Anhydrite (A-1)

A rapid, nearly instantaneous transgression of fresher water, of possible marine origin abruptly terminated halite deposition and further planed a very broad, topographically low area. Syndepositional dissolution similar to that reported by Hovorka (1983b, in press), Hovorka and Granger (in press), and Fraccasso and Hovorka (1986) for halites underlying anhydrite and carbonate rocks of the San Andres Formation in the Palo Duro Basin affected the upper part of the H-1 sequence. The top of the syndepositional dissolution residue represents a time-line or the base of a punctuated aggradational cycle (e.g., Goodwin and Anderson, 1980). A thin gypsum unit, now anhydrite (A-1), was deposited over the H-1 sequence. The nearly uniform thickness of A-1 suggests that rapid deposition of the sulfate occurred as there is no thickening of the section attributable to subsidence of the depositional center of the basin. The sedimentary structures preserved in the anhydrite confirm that the deposition was rapid and the result of one major transgressive pulse with minor fluctuations of base level. One thicker, and in some areas a second thinner, zone of anhydrite and halite pseudomorphs after vertically oriented gypsum crystals occurs within a wavy-laminated to ripple-laminated anhydrite. Vertically oriented selenite crystals and their pseudomorphs are commonly reported features in both modern sediment and ancient rocks, respectively (e.g., Schreiber, 1978; Warren, 1982; Vai and Ricci Luchi, 1977). They are usually interpreted to have formed in a subaqueous setting. The size of pseudomorphs after selenite decreases upward. Both Warren (1982b) and Vai and Ricci Luchi (1977) interpret similar sequences as shallowing upward. Wavy-laminated to ripple laminated anhydrite overlies the pseudomorph zones, and in some cores the top of the anhydrite is nodular. A-1 is interpreted to have been rapidly deposited in a shallowing upward subaqueous environment. Slight base-level fluctuations are recorded

by the presence of more than one zone of decreasing upward pseudomorph size. The base level dropped considerably at the end of A-1 deposition, and subaerial exposure of some of the sulfate in the western part of the study area may have occurred, but the evidence is equivocal.

6.1.6 Halite (H-2) and Mudstone (M-2) Deposition

Once A-1 was deposited and the base level lowered, clastic material could again be transported into the study area. Either an increase of the subsidence of the depositional center, or a decrease in the rate of evaporite deposition, increased the potential for clastic transport. Minor tectonic activity outside of the study area may have added to the potential energy of the basin. Evaporitic conditions remained, and siltstone, mudstone, and claystone were deposited in mudflat, saline mudflat, and mud-rich halite pan environments in marginal environments (including the study area) while mud-free halite pan environments existed in the depositional center. Along the margins of the depositional center, repetitive displacive growth of evaporite minerals and subsequent dissolution, driven by a fluctuating water table, churned the clastic sediment. The original clastic texture was disrupted, mixing intraclasts of various grain sizes within a very poorly sorted matrix. Subsidence in the depositional center of the basin lowered the base level, and subsequently, lowered the protective water-table on the margins of the deposition center exposing the evaporite minerals to dissolution by meteoric waters. Halite was remobilized, transported to the depositional center, and redeposited leaving a very churned and haloturbated muddy sediment free of halite (Smith, 1971, p. 229: "... repeated re-solution and re-precipitation of ... salts ... might ... cause ... the almost total lack of sedimentary structures in the clastic parts ... for which the term haloturbation would seem appropriate..."). This muddy sediment developed incipient soil textures (clay cutans or argillaceous), as meteoric fluids percolated downward toward the phreatic zone. Gypsum nodules and crystals and possibly anhydrite nodules grew within the vadose zone. When the water table was at or below the top of the sulfate A-1, some leaching of sulfate may have occurred. Interbeds of gypsum were deposited following episodic flooding events when the salinity of the water was decreased. The areal extent of these gypsum interbeds was several times greater than that of halite as the size of the brine pond increased considerably following flooding. Gypsum saline mudflats formed locally on

the margins of the basin, and displacive gypsum and anhydrite grew within the sediment.

Subsidence was probably episodic, and during periods of no subsidence, the pattern of depositional environments was shifted outward like an expanding bullseye as the depression within the depositional center was filled, causing the available fluid to spread outward. Once again, the clastic marginal sediments were churned by the displacive action of evaporite minerals. When subsidence resumed, syndepositional dissolution again removed the halite from the marginal clastic sediments, leaving behind a syndepositional dissolution residue. Near the end of the deposition of the H-2/M-2 interval, very little halite remained within the interval in the WIPP site area.

6.1.7 Culebra Transgression and Deposition

Halite deposition and the deposition and subsequent modification of related muddy sediments was halted by a transgression of waters with near-marine salinity. Marine waters transgressed across an extremely low relief area. Both dissolution of underlying halite as waters of low salinity came into contact with the halite and erosional reworking of clastic material further flattened the topography. The upper gray zone of M-1 records the transgression and subsequent reworking of muddy sediments and some carbonates. Nontectonic deformation, similar to that described by Brodzikowski and Van Loon (1985) for sediments deformed as ice melts, occurred as the underlying halite continued to be dissolved after the initial deposition of the gray claystone. Erosion, transport, and deformation of soft clasts of carbonate occurred. Once the transgression was complete, a stable substrate developed and carbonate deposition began.

A low-energy, productive carbonate lagoon developed following the transgression. Pelletal carbonate mud was deposited along with a minor amount of clastic material, mostly clay. Water depth was great enough to allow only minimal reworking of pelletal mud and clay and fine silt sized material into bedforms. However, the energy of the system occasionally increased, and migrating bedforms developed. The substrate was often stable and shows evidence of locally extensive bioturbation. Algal mats developed episodically on the substrate. These were, however, very thin and were usually choked and covered by rapid deposition of pelletal material and clay. Reworking of the algal mats was minimal. Near the end of Culebra

deposition, the marine connection was blocked and the salinity of the water increased. Grazing invertebrates apparently decreased, and algal mats and stromatolitic forms developed on the substrate. Shallowing occurred, and some clastic material was carried into the basin.

Algal features are commonly reported in evaporite settings (e.g., Carozzi, 1962; Kendall and Skipwith, 1968; Friedman and others, 1973; Peryt and Piatkowski, 1977; Shearman, 1978; Butler and others, 1982; Warren, 1982a; Toomey, 1985). They have been interpreted to indicate: a) subaerial exposure in a subtidal environment (after Logan, 1961; Kendall and Skipwith, 1968), b) subtidal settings (e.g., Gebelein, 1969), and c) deep water (e.g., Hoffman, 1974; Playford and Cockbain, 1969). The occurrence of algal features is not unique to any environment. Desiccation cracks and chips are evidence of subaerial exposure, but none were found in the Culebra. No head or club-shaped forms indicating subaerial exposure (e.g., Logan, 1961) were observed, and fenestral fabrics do not occur. Instead, algal mat, biscuit, and dome-shaped features similar to those described in subtidal environments by Gebelein (1969) were found.

During and shortly following Culebra deposition, halite within the M-2/H-2 interval continued to be partially dissolved. Further soft sediment deformation occurred, and the lower beds of the Culebra slumped partially in those zones affected by the dissolution.

Regional isopachs of the Culebra show a thickening in the depositional center indicating that Culebra depositional conditions existed long enough to be affected by the subsidence of the depositional center.

6.1.8 Anhydrite (A-2) Deposition

The connection with marine waters that existed during the initial Culebra transgression became more restricted during the later stages of Culebra deposition. This restriction continued after the end of the Culebra time. The water continued to increase in salinity, becoming saturated with respect to gypsum. Gypsum and carbonate algal material were interlayered. The environment was sufficiently energetic to locally rework the fine-grained gypsum and carbonate into low relief bed forms. Local subaerial exposure occurred. Once gypsum saturation was reached, gypsum crystals nucleated and grew displacively within the still soft carbonate of the Culebra.

Sulfate was deposited rapidly, and was subaerially exposed. Some clastic material and possibly some halite were deposited over the nearly exposed to exposed surface of the sulfate. Halite, if present, was dissolved by another rapid transgression. The transgressive waters concentrated quickly and sulfate saturation was again reached. A more stable substrate existed and vertically oriented selenitic gypsum grew at the sediment water interface. Shallow conditions are implied by the lack of large vertically oriented selenite prisms.

The sulfate was deposited in a shallowing upward environment. Subaerial exposure of sulfate along the margins of the depocenter resulted in the dissolution and erosion of sulfate by meteoric waters.

6.1.9 Halite and Mudstone (H-3/M-3)

The deposition of clastic materials and halite followed the lowering of the water table after the deposition of A-2. The standing body of water was reduced in size by evaporation, solutes were concentrated, and the sediment along the margins of the depocenter was exposed to erosion and dissolution. Local channels developed among the margins dissolving or eroding into A-2. The absence of A-2 at WIPP 19 is interpreted to be the result of syndepositional channeling. Halite began to be deposited within the lowest areas. The saline pan was largely desiccated and then flooded to bring clastics across the basin. The following depositional environments were recognized, from the margin to the middle of the depocenter: gypsum-saline mudflat, halite-saline mudflat, mud-rich saltpan, and mud-poor saltpan. The size of depositional environments changed in response to changes in the relative position of base level and surficial hydrologic system. Subsidence controlled the basin geometry and subsequent facies distribution. During episodic subsidence, syndepositional dissolution of soluble minerals occurred during subaerial exposure of the marginal sediments. This remobilized soluble minerals and relocated them toward the depocenter. During the exposure, these marginal sediments were affected by soil-forming processes which translocated and reoriented clay-sized particles in microscopic fractures and as cutans.

Initially, nearly pure halite was deposited in the depocenter, and the depositional environments remained stable for some time with no large scale facies migration. After the initial halite deposition within the depocenter, clastic materials were brought into the study area during episodic flooding

events. Clastics were sedimented along the margins of the depocenter and rarely were deposited within the depocenter. Later, subsidence and fluctuating base levels were conducive to the continued deposition and dissolution of saline minerals in the saline mudflat areas, further churning the sediment.

Clastic deposition increased after the initial period of uniform conditions. A more clastic-rich halite was deposited in the depocenter. Depositional facies migrated inward toward the depocenter. Subsequently, the size of the mud-poor salt pan decreased while the size of the mud-rich pan increased. The mud-rich and mud-poor salt pan environments interfingered with one another, with the mud-rich facies dominating. The source of clastic material was interrupted and clastic material, once again, could not reach the depocenter. Subsidence in the depocenter accelerated, and clear halite was deposited in the depocenter in a mud-poor salt pan environment. Further base-level drops associated with the increased subsidence exposed additional margin areas and allowed more syndepositional dissolution of those soluble minerals, particularly halite, in the newly created vadose zone. The base level stabilized or rose, and clastic deposition decreased dramatically in the depocenter. Mud-poor salt pan deposition once again dominated, depositing relatively clear halite in the depocenter.

A basin-wide freshening occurred following the deposition of a second clear halite unit in the depocenter. Minor amounts of halite dissolved from the interaction of halite with the fresher fluids. Laminated to nodular gypsum was deposited in a thin blanket over the underlying halite. The base of this sulfate probably represents a nearly isochronous event. The sulfate was rapidly deposited following the freshening event as it shows little evidence of thickening in the depocenter.

The fluids concentrated, and the areal extent of the standing body of water decreased, in response to evaporation. Sulfate deposition ceased in the depocenter, and mud-free salt began to precipitate. The underlying sulfate unit locally consists of polyhalite, suggesting that extreme salinities were reached during evaporation. The polyhalitized sulfate extends in some areas beyond the overlying halite This suggests that extremely saline fluids affected a larger area than is indicated by the halite. Clastic materials were no longer contributed to the basin in any large amount, and clastic facies are nonexistent. Subsidence was relatively rapid, and deposition was confined to a smaller area. A thick, lenticular

unit of nearly mud-free halite with two thin sulfate interbeds was deposited. Nondeposition prevailed along the margins of the salt pan, including much of the study area. This marginal area is apparently quite complex, and there are no cores to examine from the northern and eastern part of the study area to resolve some critical concepts. It was argued in Ch. 5 that the polyhalite probably formed early and halite was not dissolved late because: 1) permeability is usually low in halite zones, 2) polyhalite is about equal thickness whether adjacent to halite, mudstone, or anhydrite, and 3) removing halite should affect adjacent polyhalite. If polyhalitization occurred very early, there is still no direct evidence of specific mechanism, such as percolation of overlying brines, lateral migration of polyhalitizing fluids within unlithified sulfate, or evaporative pumping of brines associated with lateral migration. Within all of the cores described, this time is represented by a hiatus. A freshening event terminated halite deposition.

6.1.10 Anhydrite (A-3)

Fresher water, of possible marine origin, transgressed rapidly across the low topography. The base of the sulfate is nearly a time-line. The transgressive waters overlaid halite in the depocenter and the thin sulfate unit on the margins. Some halite within the depocenter area undoubtedly dissolved by direct contact with the transgressive fluids. Initially, thin laminae of carbonate-rich claystone were deposited by settling out of the transgressive waters. Locally, small stromatolitic algal forms grew. The water was fairly deep but probably not below storm-wave base. The salinity of the waters increased, and sulfate began to deposit. Fine-grained gypsum was deposited in thin laminae over the claystone. Vertically oriented crystals of selenitic gypsum grew along the substrate. Carbonate-rich interbeds were deposited with the gypsum. A thin rip-up breccia was deposited locally. It consists of thin, tabular clasts of anhydrite and carbonate in a gypsum matrix. Hardie and Eugster (1971) and Garrison and others (1978) report similar rip-up breccias. Hardie and Eugster (1971) interpret them to be the result of wave reworking of subaerially hardened crusts. It is possible that the rip-up breccias formed in that manner, although no other evidence of subaerial exposure (e.g., desiccation cracks) was found. Regardless of whether the clasts were derived from sediment hardened or lithified by subaerial exposure or in a subaqueous environment,

the breccias were deposited in a shallow subaqueous setting as infrequent storm events locally ripped up parts of the laminated gypsum, redepositing them as thin beds of tabular clasts. Dissolution continued to affect the underlying halite resulting in slumping and soft sediment deformation of the overlying sediment in a manner similar to the slumping and deformation of glacial and related sediments during the melting of ice, as described by Brodzikowski and Van Loon (1985). Vertically oriented selenitic gypsum crystals were disrupted by slumping due to dissolution and isolated storm events (e.g., Schreiber and Schreiber, 1977; Schreiber, 1978). The water depth decreased and low-angle slipface migration of bedforms became common. Vertically oriented selenitic gypsum continued to be deposited when the substrate was stable. Sequences of vertically oriented selenitic gypsum crystals with size decreasing upward were deposited as the water depth decreased. In at least one case, a shallowing upward sequence reached or nearly reached subaerial exposure and was accompanied by clastic deposition. Slumping of the overlying beds suggests that halite may have originally been present and dissolved soon after the deposition of the overlying gypsum beds (e.g., Schreiber and Schreiber, 1977; Schreiber, 1978).

After the deposition of the thick section of gypsum (A-3a), the substrate became very stable, and large vertically oriented selenitic gypsum crystals grew competitively upward and eventually became interlocking. The size of these crystals decreased upward indicating a shallowing upward (e.g. Warren, 1982a). Some of the large selenite crystals were syndepositionally dissolved. All or part of the coarsely crystalline gypsum was preferentially dissolved and removed to create a characteristic "crushed prism texture." The fine grained crystalline matrix deformed in response to the partial to complete removal of the selenitic gypsum. The size and number of prismatic selenite crystals controlled the morphology of the texture. Undeformed anhydrite above zones exhibiting the crushed prism texture indicates that the texture was fully developed prior to the deposition of the overlying material. The upper contact of the zones exhibiting the crushed prism texture (A-3b) is gradational.

Following the deposition and partial syndepositional dissolution of vertically oriented selenitic gypsum crystals in A-3b, the energy of the system gradually increased and more carbonate was deposited during the deposition of A-3c. The vertical change of bedforms reflects a change in energy, a shoaling upward. A fairly low energy depositional environment

producing subhorizontal to slightly wavy bedforms gradually became more energetic and dominated by wavy to lenticular bedded gypsum and carbonate. The amplitude and size of the cross-laminations increases upward reflecting shoaling conditions. Small, vertically oriented selenitic gypsum crystals were deposited during quiescent periods and, in some cases, were reworked. A nodular fabric was superimposed over laminated sediment. Similar bedded nodular textures have been reported by Hovorka (in press) who recognized that textures indicative of subaqueous deposition were preserved within the nodules. However, Hovorka (in press) did not assess the origin of the texture, and it has not been interpreted elsewhere. The texture is probably early and developed prior to, or synchronous with, the replacement of gypsum with anhydrite. Near the end of the deposition of A-3c, algal mats and stromatolites grew on and stabilized the gypsum and carbonate substrate. Algal forms are not persistent vertically through the section as they were short-lived and effectively swamped by overlying carbonate and gypsum.

6.1.11 Magenta Dolomite

Carbonate material rapidly dominated the clastic grain type at the onset of Magenta deposition, and both gypsum and carbonate sand and mud were interbedded. Subaqueous algal forms similar to those reported by Gebelein (1969) developed on the shallow sea floor. Algal mats, biscuits, and domes have all been observed. Algal mats stabilized the substrate providing a protective cover from erosion (e.g., Neuman and others, 1970). The sedimentation rate governed the morphology, with the biscuits and domes being deposited in areas with higher sedimentation rates (Gebelein, 1969). The lack of rip-up clasts of algal material indicates that wave energy never exceeded the strength of the mat. During quiet periods, vertically oriented prismatic gypsum crystals grew on the substrate. Algal biscuits and domes (laterally linked hemispheroids, after Logan and others, 1964) were deposited over carbonate and mat sediments. Over the algal biscuits and domes, carbonate sand and silt were deposited in wavy beds. The amplitude of the wavy beds decreases while the wave length increases upward, indicating a decrease in energy.

Gypsum and carbonate silt, sand, and mud were deposited in a cross-laminated unit which overlies the algal unit. The cross-laminated unit commonly exhibits lenticular and wavy bedding (after Reineck and Singh, 1980). Erosional scour and fill and drape features are common. Wavy and

lenticular bed forms become more abundant upward, while cross-laminated carbonate and gypsum of a more uniform grain size occurs near the base of the unit. Some small, tabular rip-up pebbles occur near the base of ripples and cross-laminae. The cross-laminated unit records an increase of energy over the algal unit. As both the grain size and the sedimentary structure size increase up the section, the kinetic energy of the depositional system is interpreted to have increased through time. This is consistent with shallowing upward. Unequivocal evidence of subaerial exposure has not been found. However, the presence of tabular rip-up clasts is consistent with subaerial exposure. Most of the deposit is interpreted to have formed within the subtidal environment. Deposition and accumulation was periodically rapid, depositing local climbing ripples. Near the end of Magenta deposition, gypsum again became a more common grain type as gypsum and carbonate laminae and beds alternated.

Several authors report cross-laminated carbonate deposits within various evaporite depositional environments (e.g. Eugster and Hardie, 1975, for sedimentation related to a playa lake complex; Demicco, 1983, for sedimentation in a transgressive, shallow subtidal to intertidal zone associated with a sabkha). Wavy and lenticular bedded carbonates described and interpreted by Demicco (1983) are similar to the Magenta. Demicco (1983) presented and interpreted an ideal cycle within the Conococheague Limestone of the central Appalachians. The ideal cycle consisted of, from bottom to top, with description (interpretation): intraformational conglomerate (sheet storm deposits); thrombolitic bioherms (subtidal algal patch-reefs); cross-stratified grainstone (subtidal ooid-peloid sand shoals); ribbon rock (intertidal-subtidal mixed sand-mud flats); prism-cracked laminate (high intertidal algal mud flat); mud-cracked laminated dolostone (sabkha). The Magenta does not totally fit Demicco's (1983) ideal Conococheague cycle. However, there are clear similarities. No intraformational conglomerate occurs at the base of the Magenta, as the base of the Magenta appears to be gradational with the underlying anhydrite. The next unit Demicco reports is a thrombolitic bioherm. This is somewhat similar to the Magenta as subtidal algal mats and stromatolitic forms occur at the base of the Magenta. The next Conococheague unit is a cross-stratified grainstone which is followed by a ribbon-rock unit (Demmico, 1983). Demmico's ribbon-rock unit displays wavy to lenticular bedding similar to that of Reineck and Singh (1980). The sedimentary structures contained within those two units are similar in

occurrence and distribution to the cross-laminated unit of the Magenta. Prism-cracked and mud-cracked units do not occur at the top of the Magenta.

The Magenta is not exactly analogous to a Conococheague cycle, which Demicco (1983) interprets as a shallowing upward sequence. It is not exactly analogous to either playa lake carbonates (Eugster and Hardie, 1975) or shallow, clastic marine evaporites proposed for sandstones of the Upper Miocene Solfera Series of Sicily (Hardie and Eugster, 1971). Yet the algal forms and bedding suggest relatively high energy in a shallow tidal shelf to lagoon environment. In the case of the Magenta, there is no specific evidence in cores to suggest the site area was subaerially exposed to any extent. The WIPP site apparently remained subtidal through the Magenta, and did not accumulate intertidal or supratidal deposits. Outcrops of Crow Flats (T17S, R28E) display thin brecciated zones within the algal laminated zone, indicating syngenetic dissolution and probably subaerial exposure. The Magenta was probably shallower than the underlying (A-3) sulfates; it was certainly a higher energy environment.

6.1.12 Anhydrite (A-4)

Gypsum and carbonate deposited subaqueously with intermittent subaerial exposure followed Magenta deposition. Crystals of gypsum and/or nodules of anhydrite grew displacively in the soft sediment during subaerial exposure. Chicken wire nodular and enterolithic textures developed near the end of A-4 deposition as subaerial exposure times increased. During subaerial exposure, nodules grew within the underlying soft sediment, including the Magenta. The bedded-nodular texture in A-3c developed during this time. During episodic floods, the water level increased, allowing the deposition of laminated gypsum sediment. Near the end of A-4 deposition, the water level dropped due to evaporation and sulfate deposition ceased as halite saturation was reached.

6.1.13 Mudstone/Halite (M-4/H-4)

Following the deposition of A-4, evaporation decreased the size of the standing body of water and subsequently initiated halite deposition. Salt pan halite was deposited in the lowest parts of the basin. Within the WIPP area, the margin was subaerially exposed and clastics were eroded and deposited. The basin flooded once again, bringing clastic material across gypsum at the basin margin and across halite in the depocenter. Halite

deposition resumed and the following facies were present, from basin margin to depocenter: mudflat, gypsum saline mudflat, halite saline mudflat, mud-rich and, episodically, mud-poor halite pans. Subsidence within the depocenter again controlled the vertical and lateral distribution of facies. Subsidence followed and the syndepositional dissolution of halite from halite saline mudflat facies along the basin margins occurred. A mud-poor halite pan developed within the depocenter. A second major flooding event again distributed clastic material to the depocenter of the basin. The facies were redistributed toward the depositional center. Minor subsidence within the depocenter followed and a nearly mud-free halite pan developed at the depocenter.

Within the WIPP site area, M-4/H-4 records the interaction between mudflat, gypsum saline mudflat, halite saline mudflat, and mud-rich halite pan environments. M-4 in the waste handling shaft and several cores resembles gypsum-rich mudflats at Saline Valley, California (Pl. 25, 26, 27 and 28). Syndepositional dissolution caused by water table variations is recorded near the base of the sequence in cut and fill deposits.

6.1.14 Anhydrite (A-5)

A basin wide transgression caused the halite and mudstone associated with M-4/H-4 to cease deposition. Minor syndepositional dissolution may have occurred within those areas containing abundant halite. Gypsum saturation was reached very quickly, and subaqueous laminated gypsum with minor amounts of carbonate began forming. Minor amounts of slipface migration occurred as low relief ripples migrated across the substrate. The substrate was occasionally capable of supporting the growth of vertically oriented selenite crystals. The standing body of water decreased in size and halite was deposited in the vicinity of the depocenter at least once during the deposition of the A-5 interval. Clastic material did not accompany halite deposition. Halite was not preserved within that interval in the vicinity of the WIPP. However, evidence of subaerial exposure occurs within the WIPP cores. A second transgression occurred, and gypsum and carbonate deposition resumed as before.

6.1.15 Rustler Formation/Dewey Lake Formation Contact

The contact between Rustler and Dewey Lake Formations is erosional at the scale of cores and shafts. However, the thickness of the upper Rustler anhydrite (A-5) varies little across the basin indicating a limited hiatus. Little or no localized tectonic activity occurred during the hiatus as there is no apparent angular component to the unconformity.

6.2 HALITE/MUDSTONE (H/M) DEPOSITIONAL MODEL

All of the zones now containing or previously containing halite within the Rustler exhibit several of the facies attributed to a halite/mudstone depositional model. Five major facies are recognized, including mudflat, gypsum saline mudflat, halite saline mudflat, mud-rich halite pan, and mud-poor halite pan (Fig. 6.1). The facies distribution is controlled by chemical and physical parameters associated with pan and mudflat environments. The H/M zones throughout the study area exhibit vertical as well as lateral mineralogical zonation within some units. This is the consequence of salinity zonations within the depositional environments, with the least saline ground waters and surficial waters at the margins or near sources and the most concentrated at the depocenter. This distribution contrasts with sabkha other environments marginal and connected to the sea. The distribution of facies is also constrained by the potential for clastic deposition, a function of the capacity and competence of the hydrologic regime within a particular depositional setting. Clastic material is introduced into the depositional environment only when the hydrologic system can carry it.

Modern marine evaporite deposits and saline continental playas are known to be chemically zoned (e.g., Hardie, 1968; Hardie and others, 1978; Eugster and Hardie, 1978; Till, 1978; Kendall, 1984). In most marginal marine-derived evaporites, seawater is the main source of fluid. Concentrations increase from the seawater to a maximum, usually in the supratidal area, and finally the concentration decreases further landward as nonmarine ground water dominates. The zonal pattern of mineralogies of the marginal marine environment records these salinity variations. Inland playa lakes are very commonly chemically zoned (Eugster and Hardie, 1978; Hardie, and others, 1978). Fluids move from their source at the margins of the basin to the center of the basin. Ground water increases in solute concentration toward the center of the basin. The least soluble minerals precipitate

first, along the margins, and the most soluble minerals deposit last, at the basin center. Rustler H/M sediments are similarly zoned and are considered to have formed in a setting very similar to inland playa lakes, though there was some marine influence on Rustler deposition.

The relief within the depositional area was extremely low, and clastic material should therefore show a relatively simple distribution pattern.

Although clay-sized material could probably be transported in suspension across the basin, the distance that coarser clastic material can be transported into the system is limited by the capacity and competence of the hydrologic system feeding the basin. In a basin with an extremely broad and flat topography and distant clastic sources, the maximum limits of clastic deposition probably varied little. Following the flooding stage (which may have been a gradual rising water level/not necessarily a sudden and energetic went), the base level raise further, pushing the limit of clastic deposition away from the depocenter.

Claystone, mudstone, and siltstone were deposited in marginal mud-rich environments. The marginal mud-rich environments were areally less extensive than the mud-poor salt pan. Evaporite minerals grew displacively within both the vadose and phreatic zones in the saline mudflat environments. Gypsum grew from less saline fluids further from the depocenter while halite precipitated from more concentrated brines near the halite pan environments. The halite salt pan deposits are subdivided into two parts: a mud-rich salt pan and a mud-poor salt pan. The mud-rich saltpan received more clastic input during the flooding stage. The mud-poor salt pan is the zone that was minimally affected by clastic deposition during flooding events. The primary distinguishing characteristic of halite deposited within the mud-rich salt pan is displacive growth of cements on multicrystalline seeds or relicts of halite crust. Mud-poor salt pan sediments are recognized by the classic void-filling cements with little or no displacive growth into muddy sediment. The terms mud-rich and mud-poor only reflect the ability of the hydrologic system to transport clastic material during flood episodes. The style of halite deposition is the same from one to another. However, the early diagenetic growth styles of halite are different. Episodes of flooding following desiccation brought clastic material out onto the mud-free salt pan environments creating mudstone and/or claystone interbeds within mostly clear halite.

6.3 SYNDEPOSITIONAL DISSOLUTION

Syndepositional dissolution plays an important role in the formation of evaporite sequences. Many authors have reported or interpreted the occurrence of syndepositional dissolution in both modern and ancient evaporite depositional environments (e.g., Schreiber and Schreiber, 1977; Schreiber, 1978; Powers and Hassinger, 1985; Lowenstein and Hardie, 1985; Shearman, 1970; Arthurton, 1973; Hovorka, 1983a, 1983b, in press; Hovorka and Granger, in press; Wardlaw and Schwedtner, 1966; Adams, 1969; Fracasso and Hovorka, 1986). Primary depositional fabrics within evaporites often are extensively modified by syndepositional dissolution. Three models for syndepositional dissolution have been created. Syndepositional dissolution fabrics are unique, and several criteria for their identification have been presented.

6.3.1 Syndepositional Dissolution Mechanisms

Soluble minerals can be exposed to undersaturated fluids in a variety of ways. Three hydrologic situations can cause syndepositional dissolution of evaporites. These include raising of the water table, lowering of the water table, and varying of the positions of fresh and saline ground water zones. In many respects, it is remarkable that evaporites are well preserved within the rock record at all. Halite deposition can be extremely rapid, but it is mostly ephemeral within the depositional setting.

The most commonly recognized and reported dissolution process occurs with the raising of the base level during flooding or transgressive events. Voids caused by the dissolution of halite during minor flooding events are considered to be unique to, and diagnostic of, salt pan deposition of halite (Lowenstein and Hardie, 1985). These voids are recognized petrographically by the abrupt termination of zones of fluid inclusions with a depositional origin. In some cases, very little primary depositional fabric is preserved within the halite. In mud-free halite, clear halite cements and void fillings bound those crystals exhibiting primary inclusion zoning. In mud-rich halite, displacive overgrowths on relict salt pan halite seed crystals exhibiting growth zonation are characteristic textures indicating syndepositional dissolution due to minor flooding. Large scale flood events result in the dissolution of a greater volume of salt, sometimes the entire existing sequence (Fig. 6.2). This style of dissolution has occurred in the Great Salt Lake and has been discussed by Hardie and others (1978). Hovorka

(in press) reports ancient analogues of dissolution due to major flooding during transgressions of less -saline water in the San Andres Formation of the Texas panhandle. Dissolution related to a major freshening or transgression can occur below the immediate sediment fluid interface. This results in the slumping and soft sediment deformation of the overlying, recently deposited sediment. The textures observed in the overlying sediment could resemble those formed by the melting of ice in periglacial sediments (e.g., Brodzikowski and Van Loon, 1985). Some authors (e.g., Schreiber, 1978; Schreiber and Schreiber, 1977) attribute deformation of evaporite beds to nearly syndepositional dissolution of underlying halite. One feature that is easy to diagnose is disrupted, tilted and slumped zones containing vertically oriented selenite crystals. These deformational textures develop before the overlying sediment is lithified. If a large body of low salinity water overlies a zone containing soluble material, or the sediment overlying the soluble material, for an extended period of time, a relatively thick vertical section of soft sediment can be deformed by dissolution.

The second major dissolution style is caused by the lowering of the water table. When the water table is lowered, those soluble minerals occurring within the newly created vadose zone are susceptible to dissolution by downward percolating meteoric water and surface runoff (Fig. 6.3). Erosion can also play a role in the process. Regardless of the composition of the fluids below the water table, the soluble minerals within the vadose zone will continue to dissolve until the water table, with fluids of sufficient concentration, is again raised. If no less-soluble or insoluble material is contained within the soluble rock, then no record of the dissolution is preserved, unless the dissolution is incomplete. If this is the case, then filled void space within rock will attest to the dissolution. This dissolution style accounts for some of the void space developed in salt pans following complete desiccation. In addition, this style of dissolution has been observed within the dominant halite sediments of the Devil's Golf Course in Death Valley, California and the muddy sediments of Bristol Dry Lake, California. If the water table remains lowered for an extended period of time, soluble minerals from the vadose zone are completely dissolved. A considerable thickness of soluble material could be dissolved if the water table dropped sufficiently. The water table can be lowered by a general reduction of the volume of fluid within the basin with little or no basin configuration change; vadose dissolution would then affect a distinct stratigraphic zone.

Tectonic activity can also produce a widespread water table drop. Subsidence within the depositional center lowers the water table along the margins (Fig. 6.4). This allows for the dissolution of soluble materials and subsequent redistribution of the solutes to the depositional center. The soluble minerals are effectively cannibalized from the margin. This type of syndepositional dissolution can cut across facies tracts significantly modifying their lateral distribution. Essentially, a new facies type is created by the dissolution and superimposed over the preexisting facies pattern.

The third hydrologic regime conducive to syndepositional dissolution is the result of changes in the lateral salinity distribution. Fresher water may be driven by higher potentiometric surfaces from the margins toward the solute sink, allowing a fresher groundwater to interact with the soluble minerals.

Within a basin or playa setting, this process is controlled by the size and density of the body of saline groundwater. As the areal extent of the saline groundwater and surface body responds to outside controls (evaporation, subsidence, and rates of precipitation), the freshwater zone moves and changes the maximum distribution of soluble minerals. Similar interactions of fresher groundwater are reported by Butler (1969) in the sabkhas along the Persian Gulf. Fresh groundwater from the landward side of the sabkhas dilutes the saline groundwaters derived from the lagoon (Butler, 1969).

6.3.2 Syndepositional Dissolution Fabrics

Fabrics representing all stages of syndepositional dissolution have been recognized or interpreted by a number of authors for both gypsum and halite (e.g., Lowenstein and Hardie, 1985 for incomplete dissolution of halite; Hovorka, 1983a, 1983b, in press; Hovorka and Granger, in press, for complete syndepositional dissolution of halite). Where halite is partially preserved, syndepositional dissolution terminates or truncates original depositional textures within a soluble material. When the most soluble minerals are entirely removed, less-soluble or insoluble constituents of the sediment are characteristically disrupted.

Syndepositional textures within halite from modern environments have been recognized and described in detail by Lowenstein and Hardie (1985). These textures are primarily voids and dissolution surfaces which truncate primary

fluid inclusion zones. Lowenstein and Hardie (1985) attribute some depositional fabric control to the orientation of voids, and they consider that the presence of these dissolution fabrics are unique to salt pan environments. These dissolution textures form during Lowenstein and Hardie's (1985) desiccation stage. During this stage, the water table is at or below the surface. If the water table is below the surface, the halite within the vadose zone is subject to dissolution by meteoric water. In either case, dissolution will occur during the next flooding event when the base level is raised and fresh water is brought in to contact with the halite.

Those sediments consisting of a high percentage of mud will also record the effects of syndepositional dissolution. Smith (1971) coined the term "haloturbation" for the repetitive disruption of muddy sediment by the expansive growth and dissolution of halite. Haloturbated sediments show a smeared intraclastic texture. Clasts and strata from the zone of removal will be smeared, distorted, and disrupted proportionally to the net volume of material precipitated and removed by haloturbation. Hovorka (1983a) implies that the matrix material will be poorly sorted due to the mixing of material derived from various clast types. Surviving clasts will retain their sorting. If the soluble material dissolves above the water table in the vadose zone, then soil or ped textures indicating the downward percolating water may be present. Complete soil development is not expected. However, incipient soils should be common and can be diagnosed by translocated clays and cutans. The degree of disruption is a factor of the number of growth and solution episodes that have occurred and the length of time above the phreatic zone. Mixing of intraclast types, without evidence of post-lithification brecciation of the overlying material suggests a syndepositional origin.

6.4 SEDIMENTATION AND TECTONICS

The depositional setting of the Rustler was controlled largely by the tectonic setting. Other authors (e.g., Valyashko, 1972) have discussed the relationship between evaporite deposition and tectonic history, particularly with respect to continental or continentally-influenced evaporite environments. The Rustler provides an excellent record of the tectonic end stages of a continental basin. The depositional style of the Rustler, evaporite pan/playa deposits with episodic transgressive deposits (the bases of which are essentially time lines), creates a picture of the subtle tectonic events that occurred during Rustler time.

The depositional style of the Rustler initially reflects a change in the local tectonic setting from Salado time. The Salado Formation was deposited in a setting influenced by little or no tectonic activity. Sedimentation kept up with subsidence, and the base level of the basin remained relatively constant with respect to the surrounding topography and underwent no major fluctuations. Minor changes in the base level caused by episodic flooding and subsequent desiccation are recorded by the Salado as areally extensive vertical changes in lithology. As the clastic content of the Salado is small and clastic materials were brought into the basin mainly following desiccation, the maximum potential energy of the system or the ability of the system to supply clastic material to the basin was quite low.

The lower portion of the Rustler consists predominantly of clastic materials. The presence of these clastic rocks suggests that the maximum potential energy level of the basin increased during Rustler time. As the transition from Salado evaporites to Rustler clastics is quite abrupt, the change of potential energy must have also been abrupt. The situation is compounded further when the depositional environments that produced the clastic rocks are assessed. Bioturbation, preserved fossils fragments, and fossils casts and molds in the lower Rustler indicate that those rocks were deposited in near-marine conditions. This implies that at the start of Rustler time the local to regional base level or sea level was much higher than that which produced the Salado. When the base level of a system rises, the potential energy of the system decreases. So base-level rise or decrease of potential energy must have been more than offset by a much greater increase of potential energy yielding a relatively thick Rustler clastic section.

Local and possibly regional tectonic activity increased during Rustler time. This provided the potential energy change that initiated Rustler deposition. Tectonic events which could produce such a change include uplift of clastic source areas, basin-wide subsidence and/or tilting, and subsidence of local depocenters. Of the possible tectonic events mentioned, only subsidence of local depocenters can be supported by direct evidence. Isopach maps of the total Rustler thickness and unnamed lower member (Fig. 4.7, 4.15) show evidence of thickening in the area of those depocenters. It can be generalized, however, that if either uplift of clastic source areas or basin-wide subsidence and/or tilting had occurred, the effect and, therefore, the actual extent of those processes was minor.

Zones containing halite and the bittern salts and their stratigraphic equivalents are especially useful for paleotectonic investigations. Halite and the bittern salts will be concentrated in the lowest topographic area within the basin. If the topography is very flat, then halite can be deposited over a large area. As the topography changes in response to tectonic influences, the distribution of halite also changes. Should differential subsidence occur, older halite will be exposed along the margins of the developing basin. Soluble minerals will be cannabilized. Halite will be dissolved from the margin of the basin, transported in groundwater or surface runoff, and redeposited in a halite pan. Thus, the halite section develops a lenticular shape with the thickest section at the point of greatest subsidence. The distribution of halite will record the shape of the subsiding area. It, therefore, becomes imperative that one can distinguish between halite removed by syndepositional processes related to tectonic activity and later dissolution unrelated to the depositional environment. In this report, halite is demonstrated to have been dissolved syndepositionally from specific facies tracts laterally adjacent to halitic rocks. The features that show this process can be used to better differentiate such processes from much later dissolution that has also affected some of these Rustler rocks.

Nearly instantaneous freshening events or transgressions create an effective time line or isochronous surface. The sediments deposited over the time line represent punctuated aggradational cycles (e.g., Anderson and others, 1984; Goodwin and Anderson, 1980). Within the Rustler, transgressions and freshening events are recorded by carbonates, gypsum, and anhydrite. The thickness does not vary much, indicating that either subsidence slowed during the deposition of these units or, perhaps more reasonably, the units were deposited rapidly enough not to greatly reflect ongoing subsidence. Where these units thicken slightly in the depocenter, it is reasonable to assume that they were more slowly deposited.

Evaporite beds of differing composition can have contacts that are fairly sharp and show no evidence of a hiatus or subaerial exposure between them. Over the lateral extent of such a contact, the standing body of water must have changed chemistry nearly uniformly by mixing. These contacts can be considered nearly isochronous planes. Chemically gradational contacts between carbonate and sulfate are an example of this type of isochronous surface. One example of this type of isochronous surface within the Rustler

is the contact between the Culebra and A-2. This contact appears to be gradational within the WIPP site area, and no evidence of subaerial exposure between the two units has been found. Thus, the lithologic change is interpreted to be the result of gradually increasing salinity causing biogenic activity within the waters to cease and sulfate saturation to be reached. Sulfate saturation and deposition was not absolutely isochronous everywhere, but in terms of Rustler events, it can be considered isochronous.

Isochronous events can readily occur within continental evaporitic depositional environments. Subtle changes in the tectonic development of the area can be reflected by these boundaries.

7.0 REVIEW OF DISSOLUTION

7.1 INTRODUCTION

From the time bedded salt was initially recommended (NAS, 1957) as the preferred rock type for the disposal of radioactive waste, part of the concern in selecting specific sites has been the role of dissolution. Thick sections of evaporites, including halite, in basins around the world clearly attest to the fact that circulating water has played little or no role in these parts of the basins. No halite section could long remain in the presence of circulating fresh, or even moderately saline, fluid in any quantity. Nevertheless, some basins, such as the Delaware Basin, that have evaporite rocks include areas in which outcrops and/or beds at depth contain no halite or appear to have greatly reduced sections of halite compared to other parts of the basin. These areas are frequently interpreted, with or without additional criteria, as the result of the dissolution of halite or other soluble evaporites from the section.

Within this chapter, many studies of rocks are reviewed; the examples range from modern to ancient and surficial to subsurface. The objective of this chapter is to summarize at least a portion of the evidence and collective wisdom that may be used to interpret rock units that are subject to solution. Some criteria are also distilled from the literature to use in separating processes and establishing relative ages, though these will no doubt be refined or rejected with experience.

Walters (1977) describes the circumstances in which halite is dissolving in central Kansas, causing continuing subsidence and collapse. Landes (1945), for example, describes features that he attributes to dissolution of halite and collapse of overlying beds, all occurring before the end of the Devonian. However, a number of studies concern basins where evidence may be mixed between modern and ancient (perhaps unrelated) episodes of dissolution. So too, the Delaware Basin continues to be examined for evidence of dissolution and the processes, rates and ages of such dissolution. The discussion and search for evidence continues partly because opinions vary as to the effects such dissolution might have on the long-term isolation of radioactive waste in the Waste Isolation Pilot Plant (WIPP). The extent and processes of dissolution are of industrial interest as well, as the dominant theory explaining the origin of native sulfur in world-class deposits such as the Pennzoil (formerly Duval) Culberson mine includes circulating water dissolving salt within the Castile Formation (Smith, 1978).

Evaporites are generally considered to dissolve when the factors of source, solution, pathway, and sink are present (Johnson, 1981). That is, a soluble material needs to be present, a fluid capable of dissolving the soluble rocks exists, a pathway for movement is provided, and a sink is available to permit continuing drainage from the area of solution. Lambert (1983) used slightly different terminology for these factors, using five terms (trigger, path, continuity, source, and sink) to be more explicit about initiating events (trigger), lateral or vertical extent of soluble rock (continuity), and the nature of the fluid (source). Though these factors are usually invoked in discussion of dissolution interpreted to take place at some depth within the rock column, they are certainly applicable as well for surficial or near-surface dissolution such as that which occurs in karst terrains. For the Rustler study, there is concern about the factors of continuity and trigger. More fundamental questions, however, override the discussion of these factors:

What is the real extent of dissolution in the Rustler Formation?

What is the timing of dissolution in the Rustler Formation?

What are the criteria by which we separate depositional variation, modern or continuing dissolution, and ancient dissolution?

The focus to this time has been to provide reasonable or possible explanations of relatively conservative estimates (that is, assuming the maximum) of the extent and effects of dissolution. Through re-examination of the extent, timing, and nature of the dissolution products, a better hypothesis or set of hypotheses should emerge which is applicable to southeastern New Mexico as well as other basins. There has been, within the discussion of the hypothesized processes and observable features of dissolution in southeastern New Mexico, an implicit notion of the scale of effects and features of significance. The features generally attributed to dissolution in this area are features observable at the scales effective for geophysical logs, perhaps mappable at scales ranging up to 1:100,000 or even 1:250,000, and visible in hand specimen without magnification. It is clear from this study (Ch. 8) that minerals and rock fragments have also been dissolved in the microscopic range. At all of these scales, the same factors are critical, as mentioned previously. The fundamental, observable difference in scale is due to the relative volume of material dissolved and whether the solutes were transported out of the system (at whatever scale of

observation). For example, a large relative volume may be removed from a microscopic volume without necessarily affecting operations or isolation of waste on the scale of a repository. These microscopic diagenetic alterations to the sediment are important in the history of the sediment, and will be examined. But the major focus of the review and discussion of dissolution phenomena and processes in this chapter is on scales that are nearer repository size.

7.1.1 Dissolution in Southeastern New Mexico

Dissolution of rocks in southeastern New Mexico has long been described and discussed. Lee (1925) discussed solution and fill related to the Pecos River valley and gypsum terrains here. Maley and Huffington (1953) described stratigraphic relationships of evaporite beds near and under the Pecos River valley; dissolution of some of the units was considered the source of thinned beds and the observable stratigraphic relationships. Olive (1957) described surficial troughs on a surface of Castle gypsum in the Yeso Hills/Gypsum Plain area; he concluded that subsidence had occurred as a result of dissolution of gypsum. More recently, Anderson and several co-workers, in a series of papers (Anderson, 1978, 1981, 1982; Anderson and others, 1972, 1978), discussed data and interpreted dissolution of the Castile and Salado Formations. These authors generally conclude that about 50% of the halite in the Delaware Basin has been dissolved and that a major part dissolved in the late Tertiary. Bachman (1974, 1976, 1980, 1981, 1984a,b) extends the period of possible dissolution, mainly for the Rustler and Salado Formations, back to Triassic, and possibly Permian, time. Lambert (1983) extensively reviewed the data and hypotheses concerning the existence, processes, and rates of dissolution for evaporites of the northern Delaware Basin. He has modified dissolution hypotheses previously presented by Anderson (1978). Holt and Powers (1984, 1986b) demonstrated the presence of abundant depositional features in the Rustler Formation at the WIPP site, including some zones that have been interpreted as dissolution residues. They concluded that dissolution of the Rustler was less extensive than had previously been interpreted. Sares and Wells (1984) present some of the details of dissolution associated with karsting of evaporites in their study of the Gypsum Plains.

While this section does not provide an exhaustive account of the study of dissolution in the Delaware Basin, it does indicate the range of studies that bear on the general problem of dissolution of evaporite units in this area. As part of a better approximation of the extent of dissolution of the Rustler, the sedimentology of the Rustler was examined and presented in detail in previous chapters. The features of several zones previously attributed to dissolution are interpreted as depositional phenomena, albeit with synsedimentary dissolution for some areas. Within this chapter, the features that have been attributed in other studies to dissolution, both surficial and at depth, from modern examples as well as ancient, are summarized. These features, as summarized, indicate relative timing as well as the nature of the process. These are compared to the explicit features of the Rustler Formation attributable to dissolution (Ch. 8).

7.1.2 Objective of the Rustler Dissolution Study

The principal objective of the Rustler study is to reassess the limits to which the Rustler has suffered solution. A better understanding of the depositional environments, as described in other chapters, provides an important step. Beyond that, other research on the effects of dissolution and the diagnostic features has been extensively reviewed. To this review and understanding of depositional environments are added direct observations of shafts, cores, and logs in order to better determine the extent to which dissolution has altered the Rustler Formation.

7.2 REVIEW OF DISSOLUTION

Dissolution processes and features are reviewed to set the stage for further analysis. In addition to the data and hypotheses concerning southeastern New Mexico and the Rustler Formation, the wider literature has been examined for related discussions. Some of the opposing viewpoints and some of the assumptions and/or background information and implications for southeastern New Mexico will be stated out as they may not always be explicit or familiar to some readers. Certainly, some of the details are not reviewed here, as that has frequently been done before (e.g., Anderson, 1978, 1981, 1982; Anderson and others, 1972, 1978; Anderson and Kirkland, 1980; Bachman, 1974, 1976, 1980, 1981, 1984a,b; Bachman and others, 1973; Lambert, 1983; Powers and others, 1978), particularly in these references with some emphasis

on the suitability of the northern Delaware Basin or the WIPP site for the disposal of radioactive waste. Several authors (e.g., Anderson, 1982; Bachman, 1984b; Lambert, 1983) have reviewed various hypotheses to account for some of the features in southeastern New Mexico.

This review begins with the features and characteristics from a number of studies in the literature and summarizes the evidence and processes hypothesized to account for them. It will become evident that there are processes which may occur at or near the surface (karst) as well as those hypothesized to occur at some depth within the sedimentary pile ("deep" dissolution or stratabound dissolution resulting in solution breccias). In addition, there will be features attributed to "early" and "late" stages; early may mean synsedimentary (e.g., Powers and Hassinger, 1985), or it may mean that the dissolution is geologically old and has been succeeded by some length of time with no evidence of dissolution. Late usually means that dissolution has occurred within the Quaternary or may be active. Neither of these terms has necessarily been used consistently with depth of process, so that near-surface ("shallow") and deep are also used as modifiers to describe the relative position of the sediments when dissolution took place.

Within this chapter, dissolution features or processes are grouped according to implicit or explicit interpretation of the location of the solution process: a) karst, if the dissolution occured at or near the surface, or b) solution breccia beds, if dissolution occurred at sufficient depth (undefined) to result in brecciation of the units.

7.2.1 Karst

The literature on near-surface dissolution or karst is very extensive for carbonates. Excellent reviews of karst and their hydrologic systems have been provided by Herak and Stringfield (1972), Boeglie (1980), Sweeting (1972), Jennings (1971), and in Dilamarter and Csallany, eds. (1977). Examples of paleokarst in carbonates are becoming more commonly reported.

Evaporite rocks dissolving at and near the surface by karst processes are much less frequently treated in the literature, partly because sulfates and halite, especially, are more soluble and do not crop out well. Among the reports of research on karst in evaporites in the southeastern New Mexico area are those by Sares and Wells (1984) and Bachman (1973, 1974, 1976, 1980, 1981, 1984, 1985, 1987a,b). These reports largely follow carbonate karst

terminology, as carefully reviewed in Bachman (1985), though additional terms have been introduced (Bachman, 1980). The processes by which karst is formed in evaporites are differentiated from carbonate karst by Bachman (1985), following Pfeiffer and Hahn (1972, p. 211); he considers the dissolution and corrosion of evaporites as dominantly physical processes in contrast to the chemical activity where meteoric water combines with CO_2 to form acid which dissolves carbonate. Though the processes by which karst is formed might be differentiated, most of the resulting landforms and near surface features are described by the same terminology and will not be described here.

Two new terms, karst mounds and karst domes, are applied by Bachman (1980) to evaporite karst features from southeastern New Mexico. Karst mounds are slightly elevated topographic features consisting of brecciated material attributed to solution-collapse and subsequent erosion of less resistant surrounding rocks. Karst domes are also slightly elevated topographic features, apparently domal in structure, and attributed to solution of surrounding evaporites at shallow depths and subsidence of these areas to leave the domal features. Some karst domes may be resistant to shallow solution due to a collapsed core from earlier dissolution. Extreme examples of this, from rather deep-seated earlier dissolution and collapse, have been reported from southeastern New Mexico (e.g., Elliot, 1976; Anderson, 1978; Bachman, 1987a,b) and elsewhere (e.g., Landes, 1945; Bowles and Braddock, 1963; Wenrich, 1985); among the names applied to these features are breccia pipes, breccia chimneys, and transformational breccias.

Modern surfaces on which evaporite-related karst has formed, or is forming, exhibit a variety of karst features. Pfeiffer and Hahn (1972) report large depressions as well as sinks as a consequence of evaporite dissolution in Germany. In the Swabian Alps, Pfeiffer and Hahn (1972) report karst as deep as 6,400 ft (2000 m) with fresh water. Few details of features are provided, though it is clear that open fracture and cavernous porosity must be present in highly productive karst zones. Pfeiffer and Hahn (1972) relate basins or dolines in evaporite karst to "regular salt leaching" from outcrop down along dip. They expect sinks and marginal tensional gashes to reflect "irregular salt leaching," solution at greater depth where water circulates in zones of deformation and disruption. Belloni and others (1972) report karst in Miocene gypsum along the Central Apennines of Italy and in Sicily, but they provide no details of internal features. Glazek and others

Mississippian (Chesterian) to Pennsylvanian age. He separated the karst in process and time from the solution breccia beds.

Sando (1974) examined the Madison Limestone of north-central Wyoming, generally equivalent to the Madison Group of Montana, and described several features he attributed to paleokarst. Enlarged joints, marked by a filling of red clastics, are interpreted as fractures enlarged by meteoric water percolating down from the surface. Large cavities, with angular blocks of carbonate and clastic fill, occur at the top of the Madison and extend to as much as 90 ft (30 m) below the surface of the Madison. Sando (1974) interprets these cavities as sinkholes, as he did not find evidence of collapse of caves. Caves are also common in this part of the Madison. Sando (1974) differentiates pre-Amsden caves, filled with red clastics, from open cavities which may be Tertiary or Holocene in age. The older caves lack flowstones and dripstones, and are interpreted to have occurred below the vadose zone during the time of exposure in the late Mississippian; the limit to the vadose zone is also indicated by the deepest local base levels for erosion of the surface. Breccia zones that are stratigraphically limited and have a clastic matrix were also reported by Sando (1974). He follows McCaleb and Wayhan (1969) in interpreting these forms as having originated as another phase of the same process that formed caves, sinkholes, and enlarged joints during the Mississippian. In this respect, these authors differ from the interpretation by Roberts (1966) of breccia beds caused by solution at depth (see below).

The Carrara Formation and overlying Bonanza King Limestone in southern Nevada display angular breccia blocks, varying in size, that are grossly stratiform. The lithologies are distinctive and can be attributed to specific units, revealing that rough stratigraphic order is preserved in the breccia. Gillett (1983) proposes this breccia unit as a "healed" early Tertiary age cave. The hypothesis of collapse due to evaporite dissolution was rejected by Gillett (1983); he follows Middleton (1961), Roberts (1966), and Vaughn (1978) (see below) in expecting a planar basal contact and strongly stratiform body to form from evaporite dissolution. No direct evidence of evaporites was found and Gillett (1983) cites work by Palmer and Halley (1979) suggesting open-shelf, unrestricted marine environments. Gillett (1983) did not record flowstone features or speleothems commonly attributed to vadose zone caves. It is inferred here that Gillett (1983)

considers evaporite dissolution as a process that occurs at depth, though he did not directly state conditions.

Bretz (1950) describes features called circle deposits from Missouri. He attributes these to collapsed caves. Bretz also reports filled caves which "are so obviously solution caves that there never have been other interpretations of their origin" (p. 831).

7.2.2 Solution Breccia Beds

Several features, including solution breccia beds or rough equivalents and transformational breccias or breccia pipes, have been described by a variety of authors, most of whom have attributed the phenomena to dissolution of a bed, especially evaporite rock, at some depth under saturated (phreatic) conditions. The descriptions of these features yield some comparisons with the apparently karst-related phenomena. The Madison Group and MVT deposits are important areas displaying these features.

Landes (in Landes and others, 1945) extensively describes the Mackinac Breccia, brecciated equivalents to several Silurian to Devonian age formations of northern southern Michigan. Landes divides the breccia into three types: megabreccia, intra-formational breccia, and trans-formational breccia. Megabreccia consists of very large inclined blocks with random orientations. Stages of brecciation range from "let-down" to severely shattered and disturbed. Intra-formational breccia occurs in layers surrounded by non-brecciated rock. Landes always associates intra-formational breccias with megabreccias. Stages range from extensive fissuring to complete brecciation. Trans-formational breccias cut through several stratigraphic units, occurring as vertical bodies to several hundred feet in width. Landes estimates the vertical thickness to be as much as 1500 ft (500 m). Fragments are nearly all very angular. Some trans-formational breccias are well-indurated, forming prominent stacks or other features due to higher resistance to recent erosion than the surrounding rocks. More commonly, these breccias are porous and non-indurated to partially indurated and do not stand out as an erosion-resistant rock.

Landes (in Landes and others, 1945) concludes that brecciation occurred before deposition of the overlying Devonian Dundee Limestone. "Irregularities" (not further described) in the Dundee are attributed to later settling, but not to the episode of brecciation.

Based on relationships to the Silurian Salina Group, Landes interprets the Mackinac Breccia to have formed from collapse of overlying units when salt was dissolved from the Salina Group. He envisions solution and collapse as the Salina was exposed during early Devonian around the margin of the basin. Brines created by the solution may be the source of the central basin salts of the lower Devonian Detroit River Formation. The surface was eroded and smoothed, and the Dundee Limestone was deposited unconformably over the Mackinac Breccia and related formations. Recent erosion has re-exposed these breccias.

This report by Landes and others (1945) is the earliest extensive report of evaporite dissolution and collapse features not attributed partially or wholly to Pleistocene or later activity. The variety of breccia types are clearly distinguished, though the underlying mechanism is considered the same for all. Internally, breccias are consistently angular, though the degree of brecciation varies. The relationship to overlying beds, starting with the Dundee Limestone, is a clear feature to differentiate age. Landes clearly places the brecciation process as pre-Dundee based on the lack of breccia-related features in overlying rocks. It is not clear from review whether some breccias should be attributed to karst or not; most are clearly associated by Landes with solution at depth.

The Mississippian Boone Formation of the area around the Kansas-Oklahoma border near Missouri is a dominantly carbonate unit that hosts lead and zinc deposits and displays solution/subsidence features (McKnight and Fischer, 1970). Slump pipes are brecciated, irregularly cylindrical masses 100 to 300 ft (33 - 100 m) in diameter with a vertical displacement of several tens of feet along bounding vertical faults. Slump breccias are chert nodules to fragments of rock in a clay residuum in the Boone Formation. Later Mississippian units overlying the Boone have slump breccias with large limestone blocks and angular fragments in a residual material. McKnight and Fischer (1970) infer that these slump breccias are basal parts of slump pipes.

McKnight and Fischer (1970) also report on breccias formed tectonically within the Joplin Member of the Boone Formation. There, carbonate layers may be less competent structurally than chert zones. Along with brecciation, McKnight and Fischer (1970) report, for example, a large block of chert plucked from the lower part of the overlying unit and pulled laterally under

the unbroken part of the unit. Small thrusts and normal faults with low angles in the incompetent beds also signal this horizontal slippage even though the region has suffered only slight structural warping.

Ohle (1985) reviewed breccia types and probable breccia-producing processes for a variety of districts in North America hosting MVT Pb-Zn and related deposits. The breccia bodies are considered by Ohle (1985) to comprise two broad types: strata-bound (or mantos) and breccia columns or chimneys (or breccia bodies transecting strata boundaries). With some exceptions, the breccias are attributed principally to gravity-induced collapse associated with solution. Most of the solution and collapse is attributed to passage of hot fluids related to ore deposition, though some has been attributed to true karst. The breccias may consist of very large to very small, angular clasts that tend to be equidimensional rather than slab-like blocks associated with cave fillings. Ohle (1985) believes this shape factor, combined with unusual, often very narrow, breccia body dimensions, may indicate additional forces beyond gravity-induced collapse of dissolution zones. He proposes that tectonic forces may have been responsible for rockburst-like fragmentation of solution cavities in carbonates. As either an alternative or additional force, Ohle (1985) considers chemical brecciation (Sawkins, 1969; Lemish, pers. comm. cited by Ohle, 1985) a possible means of producing smaller breccia fragments consistent with these Mississippi Valley-type deposits.

Ohle (1985) also briefly mentions breccias of minor extent probably caused by sedimentary processes or syndepositional slides. Snyder and Odell (1958), as reviewed below, consider some of the breccia bodies to be syndepositional slides.

Rogers and Davis (1977) reviewed the geology of the Buick mine, a Pb-Zn mine along the Viburnum Trend of southeast Missouri formed in carbonate breccias. The setting is considered by Rogers and Davis (1977) to have been consistent with a carbonate-evaporite margin, and they attribute the brecciation as having been initiated through solution of evaporites and subsequent collapse. No direct evidence of evaporites was presented.

Beales and Hardy (1977) have summarized the indirect evidence for evaporites in the Viburnum Trend of southeastern Missouri. The "white rock facies" is associated with algal carbonates and minor redbeds, and the lateral relationships are similar to marginal carbonate-evaporite settings.

Beales and Hardy (1977) have also found small amounts of tiny gypsum crystals, including swallowtail twins, in impervious breccias which they conclude is direct indication of the former, more general presence of evaporites. These authors propose that evaporites may have been much more widespread, leading to much of the brecciation in the region now hosting abundant Pb-Zn ore bodies. The problem of "occult" evaporites was also discussed by Schreiber and Schreiber (1977) in a study of Mediterranean Messinian evaporites and modern solar salt works. On a very small scale (mm), halite layers between layers of gypsum crystals grown vertically on the sediment surface have disrupted normal epitaxial growth. The halite layers are absent laterally, due probably to dissolution. Thick units of Messinian gypsum consisting of thin beds with breaks in crystal growth are therefore considered suggestive that very thin beds of halite formerly existed.

Middleton (1961) also describes breccias within the Mission Canyon Formation of the Madison Group in Montana. He reports that the fragments are variable in size (microscopic to 10 ft or 3 m) and very angular to slightly rounded on edges. Limestone is the common lithology, but clasts are sometimes polymictic. Breccias of former breccias indicate multiple episodes. Fragments of different strata may be mixed, though a crude stratigraphy may be preserved. Middleton (1961) states that "the lower boundary of almost every breccia is well defined" (p. 191), though the breccias do not have the same extent upward. He describes well the upward transitions (p. 191):

> "A gradual transition may take place upwards from a breccia consisting of mixed, rotated fragments into one in which there is demonstrably little movement of the fragments and the rock has been brecciated in place."

Middleton suggests brecciation may have taken place before the Amsden Formation was deposited, but he is careful to point out he did not have evidence to support or refute this hypothesis. Finally, as the overlying units are not extensively brecciated, Middleton (1961) believes that "a thick breccia usually indicates an original zone of thin interbeds or interlaminations of limestone and anhydrite" (p. 194). Roberts (1966) investigated the Mission Canyon Formation as well, finding both paleokarst (see above) and solution breccia beds. Roberts found that solution breccia beds have a sharp, well-defined, and laterally continuous lower boundary. Roberts (1966) reported, as did Middleton (1961) and Severson (1952), a vertical progression of breccia fabrics from small heterogenous unsorted

fragments upward to slightly fractured and displaced roof rocks. Some wells in the area show anhydrite that is considered stratigraphically in the same position as the solution-breccias. Roberts (1966) considers this solution at depth to have occurred during or after Laramide orogeny.

Evaporites from the Williston Basin and surrounding areas are interpreted by Parker (1967) to have been partially dissolved. Beds overlying the evaporites are thickened by additional sedimentation to compensate for the salt removal and indicate the time of removal. Parker (1967) interprets these changes of thickness and lateral loss of halite mainly on the basis of geophysical logs. An important (and arguable) inference is that "thin regionally persistent sedimentary units directly above, between, and below the salt beds prove that locally there was little depositional change of salt thickness." In the Dillinger Ranch field (Wyoming), an estimated 100 ft of salt loss resulted in 38 to 93 ft (11.6 to 28.4 m) of thickening of Morrison and Dakota Formations in adjacent wells. From the Hurd area of North Dakota, 160 ft (48.8 m) of salt in a 200 ft (61 m) section is correlated laterally with 60 ft (18.3 m) of reported rubble/breccia. The cross-section accompanying this shows about 250 ft (76.2 m) of apparent compensation. Also from North Dakota (Fryberg field), salt was removed from Permian rocks resulting in complete compensation by the end of the Jurassic (Swift Formation), though elsewhere in the area, Parker (1967) cites Anderson (1966) to indicate that collapse may affect Jurassic and Cretaceous rocks. In the Outlook field in Montana, Parker (1967) shows that solution of the Lower Devonian Prairie Formation is completely compensated by sedimentation during the late Devonian.

In a review of features and processes related to dissolution of the Upper Devonian Leduc Formation from the South Sturgeon Lake field, Alberta, Stanton (1966) concluded that the late features were indistinguishable from the Mission Canyon solution breccias and the Mackinac Breccia. Stanton (1966) reports successive stages of primary evaporite, breccia composed of evaporite matrix with floating dolomite clasts, and evaporite-free breccia. The lithologies are dolomite clasts with anhydrite or dolomite matrix; the clasts range from sand to cobble size, are unsorted and angular. Anhedral dolomite clasts have sharp, straight edges while sucrosic dolomite is crumbly. Clasts may be fractured, brecciated and displaced. Stanton lists four features he considers important:

1) angular, unsorted, unbedded clasts; broken fragments displaced within breccia,
2) clasts often float in anhydrite matrix,
3) complete sequence: breccia with clasts floating in anhydrite --> breccia with more closely packed clasts and anhydrite matrix --> breccia without anhydrite,
4) fractures are rare beneath breccia; breccia grades upward into highly fractured rock.

Stanton (1966) considered four processes in the development of the Leduc breccias:

a) solution brecciation causing settling of evaporites, plastic deformation, concentration of fine clasts up against clast surfaces,
b) change in volume as gypsum --> anhydrite; lower strength from water in the rock,
c) simultaneous clasts and evaporite "deposition"; no bedding or rounding,
d) selective replacement of carbonate by anhydrite to explain anhydrite matrix.

Of these mechanisms, Stanton (1966) considers solution brecciation to account for all features observed. He also concludes that the solution brecciation is probably common at very shallow depths and that "gradual subsidence, brecciation, small-scale solution precipitation, and evaporite flowage occur simultaneously with the evaporite solution."

The Elk Point Group evaporites of the Prairie Provinces, Canada, are considered Devonian in age. The Prairie Formation, part of the Upper Elk Point Subgroup, consists of sulfates and halite; it overlies the Winnepegosis Formation, a limestone unit. Gorrell and Alderman (1968) review evidence of salt solution from the Prairie Formation in Saskatchewan. On the basis of geologic data, solution began as early as late Devonian. Salt springs in the area are considered evidence that salt solution is continuing.

Salt solution of the Elk Point Group locally has resulted in collapse features (DeMille and others, 1964; Christensen, 1971; Gendzwill and Hajnal, 1971), similar to breccia pipes reported for southeastern New Mexico (Snyder and Gard, 1984; Bachman, 1987a; Davies, 1983) as well as broader structural lows and unit thinning. Compensating thicknesses of overlying units may be used to infer ages of solution and, in some circumstances, differentiate

solution from tectonic or depositional features. Gorrell and Alderman (1968) distinguish depositional from dissolution edges on the basis of the configuration of the underlying units versus dip on the salt units (Fig. 7.1). Sharp changes in halite with reversal of dip are associated with dissolution. The underlying units change little. Consistent dip directions and changes in dip of underlying units are associated with depositional changes. The Palo Duro Basin of the Texas panhandle is one of the potential sites for the first repository to dispose of high-level radioactive waste. As the rocks of interest are evaporites, various geological and geomorphological studies examine the extent, nature, and timing of dissolution.

Gustavson and others (1980) recognize salt dissolution based on: 1) high solute loads, especially chlorides, in streams; 2) salt sequences that abruptly disappear between relatively closely spaced wells, as well as abrupt thinning of stratigraphic sequences away from salt units; 3) zones with abrupt salt thinning that also truncate facies tracts; 4) cores that show poorly consolidated to unconsolidated red-brown mud overlying salt beds; and 5) folds, collapse chimneys, breccia blankets, and sinkholes on Permian outcrops.

Criteria 2 and 3 are not easily reconciled with the figures referred to in Gustavson and others (1980) as the "relatively close spaced wells" usually appear to be 5 miles or more apart, and it is not clear, on the basis of the natural gamma ray logs presented, how the presence/absence of halite is always interpreted. Criterion 4 could be consistent with syn-sedimentary dissolution.

A playa, Lake McConnell, overlies an area where about 165 ft (50 m) of salt appears to have been removed. Gustavson and others (1980) question if the relationships are clear in indicating cause and effect between lake and salt dissolution. The origin of other playas appears to be different, in that some do not show any evidence of salt dissolution in underlying formations. Modern collapse is occurring in Hall County as sinks and depressions have been formed and attributed to salt dissolution.

Collapse chimneys in different areas of the Texas panhandle range in probable age from late Cretaceous to as late as Quaternary. Boundaries are nearly vertical with slickensides. Bedding may be vertical, and breccias may be cemented or uncemented. The breccia chimneys are located over areas

identified as actively being dissolved or of possible paleodissolution of salt.

Dissolution is considered also to have caused fracturing of Permian mudstones and filling of fractures with gypsum. Goldstein and Collins (1984) describe in some detail the fault and fracture sets in outcrops of Permian formations overlying areas believed to have undergone or be subject to salt dissolution.

Portions of the Permian age evaporite-bearing section in the Palo Duro Basin area have been described as having undergone dissolution, and salt springs and chloride loads in drainages demonstrate salt is still being dissolved (e.g., Gustavson and others, 1980). Gustavson (1986) has re-examined evidence of salt deposition and dissolution in the vicinity of the Canadian River valley to test the hypothesis that the river developed in response to solution and collapse. As evidence of dissolution of evaporites, Gustavson (1986) cites the following:

a) "abrupt" lateral loss of subjacent salt associated with "structural collapse" of overlying units (emphasis added);

b) brecciated zones, fractures with slickensides, extension fractures filled with gypsum, insoluble residues of soft mudstone, anhydrite, or dolomite overlying salt;

c) folds, breccia-filled chimneys, and systems of gypsum-filled fractures in Permian outcrops along the Canadian River Valley;

d) sodium chloride brines in some wells above salt; and

e) high chloride in the Canadian River.

Gustavson concludes there "is strong evidence that Permian salts formerly extended farther to the north, northeast, and northwest beneath the valley of the Canadian River" (p. 463). Gustavson (1986) concludes also that a few salt units show lateral facies changes, generally without change in thickness or structural complications. Gustavson (1986) relates the Canadian River valley to salt dissolution based on several factors: the river trend is not that of the Ogallala system; the trend follows the structural trend on the Alibates, overlying the zone attributed to dissolution; and the plain north of the valley is about 250 ft (75 m) lower than to the south. This difference is also attributed to dissolution. Gustavson (1986) infers that the age of dissolution may be as early as Miocene.

Residues or breccias are reported by Smith (1972) as textural evidence of more extensive or "mature" near surface dissolution of the Upper Magnesian Limestone of England. Beds of the Upper Magnesian Limestone have variously collapsed or foundered as a consequence of dissolution of the underlying anhydrite beds. The residue from the anhydrite consists of carbonates and clay minerals with some gypsum and quartz and traces of detrital heavy minerals. It has been estimated that the original anhydrite might have been 100 to 200 ft (30 to 60 m) thick based on the insoluble content of the equivalent anhydrite elsewhere.

The degree of brecciation reported by Smith (1972) is highly variable. The clasts may vary from angular to subangular. The clast margins and the matrix from the Upper Magnesian Limestone are enriched in calcite relative to the center of clasts; this "dedolomitization" is attributed to the reaction between groundwater and the rock at the time of the dissolution of the underlying anhydrite and collapse of the limestone. Smith (1972) attributes the brecciation to "a number of rapid collapses separated by a long period of relative stability" (p. 264). In addition, broader scale foundering of strata is interpreted by Smith (1972) to be the result of gentle and slow sagging, and the process is considered to cause only slight brecciation. Along with this gentle foundering, the Upper Magnesian Limestone in the area displays "a gentle warping (not found in beds underlying the evaporites) into innumerable domes and basins of up to 10 metres (sic) amplitude and 25 to 200 metres (sic) diameter" (p. 266).

7.2.3 Other Breccia Sources

The Bonneterre Dolomite of Late Cambrian age is a Pb-Zn ore-bearing unit in southeast Missouri interpreted by Snyder and Odell (1958) to include breccias of approximately syndepositional origin. The breccias lie laterally adjacent to carbonate bars or banks and possible reef deposits. The breccias vary from very small clasts to large blocks >3 ft (>1 m); "locally within the disturbed mass, beds may be crumpled and folded without fracturing..." (p. 906). Snyder and Odell (1958) report that fragments are angular and there is little evidence of abrasion. The matrix is dolomite with other constituents, and it encloses breccia blocks. In addition to carbonate breccias, dolomitic shale breccias occur with carbonate matrix. Both types of breccia are tight, with rare cavities or open spaces.

The breccias are interbedded with undisturbed beds. The bodies of breccia may be >2 mi (3 km) wide, >100 ft (300 m) wide, and as thick as 80 ft (25 m). Later breccias can truncate earlier breccias. The basal contact may also be concordant or gradational with soft sediment to more brittle deformation marking the contact. While the units are adjacent to carbonate banks and reefs, they also tend to accumulate in areas where the carbonates are thin (and the depositional surface was presumably lower). Internal structures include small thrust faults and drag folds.

Snyder and Odell (1958) believe the breccia bodies moved and formed during early diagenetic and lithification stages. A bed on the margin of a carbonate was subjected to increased slope by greater compaction of the basin facies. A glide plane forms in more indurated units as the unconsolidated material near the surface-water interface from higher on the slope begins to move. More lithified beds are brecciated, and drag folds and thrust faults are created by the slumping mass. The glide planes and different brecciation styles within the breccia masses have been used by Snyder and Odell (1958) to separate breccia masses into distinct events.

Important diagnostic characters used by Snyder and Odell (1958) were:

a) localization and shape of breccia bodies,
b) interbedded undisturbed units,
c) position relative to carbonate banks or reefs,
d) different degrees of brecciation within masses, and
e) glide planes.

An individual mass, encountered in a core, for example, would reveal angular fragments within a matrix. It is possible the undisturbed units would also be properly interpreted. But the interpretation reached by Snyder and Odell (1958) would not have been reached without the extensive three-dimensional data available within the Pb-Zn mines.

Smith and others (1961) describe limestone breccia in a calcareous siltstone matrix and small shale and sandstone masses in the Mississippian St. Louis Limestone in Indiana. The breccia and clastic masses have dimensions of a few to tens of feet (m). The breccia body is "crudely funnel shaped". Breccia fragments range from very angular to subangular and up to about 6 ft (2 m) in length. Some fragments are reported to have stylolitic surfaces. Matrix displays contorted to sinuous bands of siltstone and sandstone that are even vertical in some places. Smith and others (1961)

suggest these breccias formed, probably during the Pennsylvanian, by folding and slumping due to movement on the Mt. Carmel fault. Other origins may not be eliminated, given the limited data, though Smith and others (1961) consider tectonic breccia, glacial loading, cave collapse, and evaporite solution and collapse as less likely alternatives. Evaporites in the St. Louis occur at or above the zone of breccias, and the thickness of evaporite is small in undisturbed areas. Undisrupted lateral beds also suggest that evaporite solution-collapse is not applicable.

The sandstone and siltstone masses are interpreted by Smith and others (1961) to have formed by filling small caverns on a paleokarst terrain now reactivated on a modern karst surface.

7.2.4 Delaware Basin Features

Anderson and others (1972), in a now classic paper on the laminated Castile Formation of the Delaware Basin, discussed the relationships between beds of anhydrite breccia and laterally equivalent halite units. During earlier work, Anderson and Kirkland (1966) and Kirkland and Anderson (1970) reported that short, selected thin intervals of laminated couplets from a few cores across the basin showed high correlation coefficients ($r = 0.99$). Anderson and his coworkers have concluded that there is a near one-to-one correspondence of laminae couplets across the basin, as well as of larger units, nodular zones, and other features. They concluded that lateral facies changes did not occur within the basin. Around the western margin of the basin, Anderson and others (1972) reported finding breccia beds in positions stratigraphically equivalent to halite units in the eastern part of the basin. Anderson and others (1972, p. 70ff) recorded some of the details of the arrangements of breccias in these beds:

> "Beds of laminated anhydrite as thin as one foot thick within halite beds more than 50 ft (15.2 m) thick are also present as unbrecciated layers within correlative breccia units, involve approximately the same number of laminae, and maintain their identity and remain undisturbed within overlying and underlying breccia beds despite the removal of salt. The presence of thin anhydrite beds within halite members can also be inferred from sonic logs, and these beds can be correlated with breccia zones in the University of New Mexico-Phillips no. 1 core...."
> "The breccia generally consists of rectangular-shaped, subangular fragments of single laminae or groups of laminae embedded in a matrix of anhydrite... The fragments, generally less than one cm in length, occur

in various orientations, but most occur with stratification, if visible, and long dimension near the horizontal. Many of the fragments appear to have been only slightly displaced."
"In some of the blanket breccia beds it is difficult to correlate the upper contact because of solution collapse that resulted in a collapse-type breccia...consisting of larger, more angular fragments than the blanket solution breccia, and with little matrix. Good examples of collapse-type breccia have been observed at the top of the Halite II Member (sic) and in the upper part of the Anhydrite IV Member (sic) above blanket solution breccia."

Along the eastern margin of the Delaware Basin, Anderson and others (1972) report the relationships within halite of the Union-University "37" core:

"The Winkler County core, however, revealed that thin anhydrite beds of only a few decimeters thick within more massive halite units maintained their position and character after halite solution. This fact (sic), and the observation that single anhydrite laminae, once separated by several centimeters of halite, were sometimes little disturbed upon solution, showed that the withdrawal of halite was a very gentle process."

Anderson and others (1972) consider dissolution most likely to have taken place after Salado time.

Both in Anderson and others (1972) and Anderson and others (1978), geophysical logs were used in conjunction with core to conclude that dissolution accounted for the lateral thinning of units from thick halite to thin breccia beds. It was concluded that each of the halite units is represented by a breccia bed. Interpreted geophysical logs also yielded thickness information for halite and sulfatic units indicating differing thickness patterns for these units, unlike models of deep water deposition.

Anderson and others (1978) recognize two different types of breccias within the breccia beds: dissolution breccias and collapse breccias. Within dissolution breccias, Anderson and others (1978) see textures similar to those described above, having fragments oriented generally parallel to bedding in units above and below. In addition, they also report that some fragments "are quite small (less than 0.5 cm), rounded, and suspended in random orientations within a matrix that comprises more than half the volume of material." The matrix is an impure anhydrite matrix. Anderson and others (1978) report that the dissolution breccias may be as much as a few tens of feet (several m) thick and "are approximately proportional to the thicknesses of correlative salt beds." These authors estimate that the ratios of breccia

to salt thickness is about .03 to .05 within the examples available to them. Collapse breccias are angular fragments of anhydrite often overlying the dissolution breccias. "The angular fragments are fitted together in a tight interlocking pattern with little or no fine-grained anhydrite matrix. The fragments range in size from a few millimeters to blocks of more than 30 cm, with a definite tendency for fragments of similar size to be found together." These authors describe this type of breccia as forming "at apparently random positions in overlying anhydrite beds" as a consequence of dissolution chambers collapsing resulting in "a diminishing chain reaction above."

In addition to the features of the breccia beds, Anderson and others (1972, 1978) consider that solution and subsidence/collapse caused, or is related to, the Big Sinks dissolution area, troughs with Gatuna-age sediments at the surface (Maley and Huffington, 1953), and breccia pipes, castiles (Kirkland and Evans, 1976; Anderson and Kirkland, 1980) and other collapse structures (Vine, 1960, 1963).

Anderson and others (1978), as well as Anderson (1978), attribute dissolution around the margins of the basin to probable effects of contact with the Capitan reef. Anderson and others (1978) are somewhat vague about the general process of dissolution, referring to an advancing front in the subsurface, probably preceded by caverns and tunnels at the leading edge developing an uneven front. They also attribute part of the dissolution to breccia pipes and other collapse structures. Anderson (1978) and Anderson and Kirkland (1978) described more specific roles for intrusion of water from the underlying Delaware Mountain Group through fractures, resulting in collapse structures or breccia pipes. Anderson and others (1978) suggest some blocks and fragments may have moved laterally into voids between separated horizontal laminae of anhydrite, and that fluids or slurries may have helped move brecciated rock.

More recently, Robinson and Powers (1987) report a fan-shaped "breccia" unit in the Castile near the western margin of the Delaware Basin as a gravity-driven clastic deposit. Multiple cores from a relatively small area reveal bedding in clast units, graded clasts, clasts in an anhydrite matrix or cement, and intermittent normal laminated beds similar to those described by Anderson and others (1972, quoted above). Robinson and Powers (1987) interpret this unit as a Permian-age gravity-driven clastic unit, not as a

dissolution breccia. It is not clear that Halite I of the Castile was deposited west of this area.

In many publications (e.g., Jones and others, 1973), the Rustler and upper Salado have been described as having undergone dissolution, resulting in complicated surficial features. However, specific features of the breccia beds have not generally been presented. Basic data reports for WIPP boreholes variously present general to detailed descriptions of material attributed to "dissolution residue"; the information from redescribed cores (Ch. 5) and interpretations (Ch. 6, 8) differ in many ways from those in the basic data reports. Lambert (1983) describes the relationships among several features related to dissolution or hydration in the vicinity of Nash Draw; he indicates that geophysical log signatures in the area of Nash Draw may be guides to units that have been partially dissolved.

Core from the Permian in Culberson County, Texas, is described by Eager (1983) as exhibiting breccia within parts of the Rustler and Salado Formations, but no details are given of the nature of the breccia or extent. Natural gamma ray and neutron logs accompanying the lithologic log do not indicate any signatures diagnostic of the breccia, and Eager (1983) did not report any difficulties in reconstructing the stratigraphic sequence within the cores.

7.3 DISCUSSION OF LITERATURE REVIEW

The review of the literature reveals several points and areas that may be inferred to be common. Various authors clearly differentiate between those solution events that occur from the surface downward, either at or near the surface, and those events which took place after some amount of burial and which begin at the bed. These concepts have been paralleled by the discussion of dissolution in southeastern New Mexico, where a dichotomy has been constructed between "deep dissolution" and near surface (generally related to karst processes) dissolution. It is not possible to assign specific depths to these phenomena, for the various authors appear to have different, sometimes unspecified, criteria for deep and near-surface. However, we may here differentiate these two end members of a probable general continuum as follows:

Surficial to near-surface processes show clear and relatively direct connection to meteoric water sources from the surface downward, with soluble material dissolving as meteoric water passes through. "Deep dissolution" shows an indirect connection to meteoric water with dissolution initially generally confined stratigraphically and not immediately affecting the superjacent rocks except by brittle deformation as a consequence of removal of material from the affected bed.

These two kinds of processes, in the reviewed literature, result in grossly different features as they are preserved in the geological record. Near-surface, karst-related processes will result in a sequence of brecciated material with sharp boundaries at the upper surface (Fig. 7.2a) as deposition covers karst and ends the process. The lower extent of dissolution may be controlled at a water table or at some chemical boundary, but, unless the dissolution proceeds to a very mature stage, the lower boundary is likely to be poorly defined and irregular. By dissolving a bed buried to some depth, a lower boundary will usually be much sharper, defined by an insoluble or much less soluble underlying rock. The breccia is likely to be more continuous laterally, and brecciation will propagate upward to a variable distance (Fig. 7.2b) in response to the removal of soluble rock. The upward boundary will generally, in this process, be more diffuse and undefinable, unless so much material is removed that fracturing propagates uniformly to the surface. We should still expect, however, that the brecciation, as described well by Middleton (1961) and others, will decrease upward as the fractures become hairline cracks to microcracks and may disappear.

The time of dissolution can be well-defined in some cases. It is clear that there are rocks in which dissolution has occurred, but in which the process has long ceased to operate. Landes (1945) and Parker (1967) provide two differing kinds of evidence of dissolution episodes from the geologic past. The criteria by which these authors decided the issue are that deposits overlying a surface that had been brecciated were unaffected and that compensation in the form of deposition had taken place by a particular point in geologic time. Present day geomorphic and sedimentologic adjustments may not easily be interpreted to determine if dissolution is contributing to the adjustment or not. It may be in a developmental stage or have been completed without a unique stage being assignable. Gustavson

(1986) and other authors describing the Palo Duro Basin have compiled criteria they believe indicate continuing dissolution. Among these criteria, local subsidence and water carrying a large chloride content are the clearest, most easily accepted evidence of continuing dissolution.

A particular problem, largely unaddressed at this time, is assessing the effects and extent of early or synsedimentary dissolution. Among the papers surveyed, few reveal any consideration of early or synsedimentary dissolution of evaporites. Of these, Powers and Hassinger (1985) relate synsedimentary dissolution in one horizon from the Salado as exposed in workings at the WIPP site. Hovorka (1983a, in press) provides evidence of synsedimentary dissolution of halite to produce disturbed textures within parts of the San Andres Formation of the Palo Duro Basin. Of the papers known to consider dissolution of these most soluble of rocks, only these present significant evidence of synsedimentary dissolution (other papers consider mainly microscopic evidence of very minor removal; e.g., Schreiber and Schreiber, 1977). Lowenstein (1985, 1987a) proposes that early diagenesis cements and plugs halite units before the sediment is buried deeper than a few tens of feet (several m). Early dissolution features as they are presently known are tied very closely to the sedimentation surface by observation, consistent with the proposal by Lowenstein. It seems clear that the rocks demand an examination of modern analogs for evidence of significant dissolution.

The extent of dissolution has been assessed largely by extrapolation from areas with evaporites to areas without evaporites or with a decreased section. Parker (1967) presents an early example based nearly exclusively on geophysical log interpretations. This approach, supplemented by some core information, was also used by Anderson and others (1972, 1978) and by other authors attempting to understand the extent and nature of dissolution in the Delaware Basin. As reviewed in several sources, the principal justification for this practice is that underlying and overlying units are laterally extensive from areas with salt to areas without salt; it is believed that lateral facies changes within salt beds did not occur over short distances either. Gustavson (1986), Anderson and others (1972, 1978), and Parker (1967) clearly follow this line of reasoning. Anderson and others (1972) utilized the correlation of limited sequences of anhydrite/carbonate couplets within the Castile to bolster their belief that sulfatic and chloride beds extended virtually from side to side of the Delaware Basin. This provides a

conservative, upper limit to the extent of salt dissolution within the basin. It is also clear, however, that within salt pan environments (Lowenstein and Hardie, 1985) lateral facies changes may occur over rather short distances, enhanced by the depositional changes that bring clastics to the margins and remove soluble materials. In addition, as water evaporates from basins, the brine is restricted to well-defined areas, again resulting in lateral facies changes over short distances. Within the Rustler Formation, as previously discussed, and in the San Andres (Hovorka, 1983a, in press), significant changes in environments and/or relative sea level may occur rapidly, resulting in the rapid covering of an area with a carbonate from much higher and fresher water. These units may extend laterally far beyond the extent of a previous saline pan, and they should not be considered direct evidence of the extent of the most saline facies. As in some previous types of evidence, the extent of evaporites will have to be evaluated basin by basin and case by case.

The rate at which evaporites dissolve is not easy to evaluate. The criteria and examples provided by Parker (1967) may be as clear as any. In the Williston Basin, sedimentary units which adjust to dissolution have lower and upper bounds well defined in geologic time. The adjustment within parts of the Fryberg field of North Dakota clearly took place during the latest Jurassic, bounded by the deposition of the Swift Formation. Approximately 100 ft (30 m) of compensating sediments were deposited within a few million years. Within the Delaware Basin, different authors have attributed dissolution to widely varying lengths of time as far back as Permian. Significant amounts of evaporites have been considered dissolved even as early as the time of the end of Castile deposition (Anderson and others, 1972; Bachman, 1974, 1976, 1980). In contrast, Anderson (1978, 1982) and Anderson and Kirkland (1980) attribute most dissolution to Cenozoic or later Cenozoic time.

The forms which the dissolution residues take are often considered rate-dependent. Breccia and brecciation are considered consequences of evaporite solution and subsidence/collapse. However, several authors (e.g., Anderson and others, 1972, previously quoted) have also interpreted dissolution to occur under some circumstances so gradually that thin, laminated anhydrite beds within halite beds may be undisturbed while large volumes and percentages of halite are removed; at the same time breccias are

formed around the undisturbed thin anhydrite beds. Though this process is not advocated in this report, it may be important from a risk assessment view to question whether such a slow, gradual process would, even if it occurs, be of any consequence to a waste repository.

Following this last point, it is appropriate to comment on the scale of events and processes that may be said to involve the dissolution of rock materials. Within the sedimentary sequence, several types of processes, sometimes given various names, may involve small or large amounts of dissolved rocks with transport distances of solutes ranging from microns to kilometers. Pressure solution from grain-grain contact and the creation or destruction of porosity is near one end of this scale. Hardly any sedimentary rock is free from the minute effects of diagenesis, including for some the effects of weathering immediately following deposition. These well-known, if imperfectly understood, phenomena are not reviewed here, though their effects are seen even in the Rustler (Ch. 8) and are reported. Near the other end of the scale, relatively high proportions of rocks of considerable volume may be removed completely from the system. This scale of process and consequent features are of principal concern within the previous review as these are the scale of processes and features that are hypothesized and reported, respectively, to occur in the Rustler as well as in the underlying evaporite formations.

It is important also to note a distinction in timing for the processes normally attributed to dissolution. It is quite clear, from published studies of dissolution of the Rustler and other evaporites in the Delaware Basin, that dissolution is a term used for processes occurring long after the deposition of the affected units. The term is used in the same sense in this report. These are phenomena associated with very early, approximately synsedimentary solution of evaporites from the Rustler, occurring before burial and lithification. In that sense, part of the reported sedimentary process includes the effects of early removal of evaporites from some of the same units interpreted by others as dissolution having occurred after burial and lithification. Synsedimentary processes are distinguised from late-stage dissolution in this report by calling it early or synsedimentary dissolution. Such features and processes clearly are associated with the sedimentary history of the units, differentiating them as well because they may be eliminated from the calculations of the consequences of dissolution affecting the WIPP at some future time.

The general features that are most widely accepted as evidence of later dissolution at depth are angular breccias that have propagated upward but with diminishing strain. These have lower bounds that locally are well defined. Early, synsedimentary dissolution or dissolution before subsequent burial reveals an upper boundary that is stratiform. Some of these relationships are applied to the physical features apparent in cores, shafts, and geophysical logs in the next chapter.

8.0 POST-DEPOSITIONAL ALTERATION

The late Permian Rustler Formation has a complex post-depositional history. Diagenetic reactions and mechanical responses to various stress fields have altered and in some cases have drastically changed the appearance and the nature of Rustler rocks. Although the origin and history of any one of the post-depositional alterations within the Rustler may be very complex, each feature is the result of one or more simpler mechanisms. These mechanisms or processes must be understood and kept in perspective. All post-depositional modifications or alterations are the driven by disequilibrium. Chemical disequilibrium causes either the addition of solutes or the subtraction/removal of solutes. Disequilibrium between a stress field and the rock may result in a mechanical adjustment toward equilibrating the system. In general, chemical reactions cause what are considered to be diagenetic features, while mechanical reactions to stress fields cause most of the remaining post-depositional alterations. Regardless of the complexity of the genesis of any one individual diagenetic feature, they can all be attributed to the operation of one or both of the following chemical reactions: the addition of solutes to, and/or the removal of solutes from, a particular site of reaction. Likewise, all of those post-depositional features that can be attributed to a mechanical process are the result of a mechanical, albeit ductile or brittle, response to various non uniform stress fields. Non uniform stress fields can result from the action of either tectonic processes or chemical diagenesis.

Numerous studies of evaporites report, interpret, or infer the occurrence, and recognize the importance, of early/syndepositional chemical diagenesis, including solute addition (e.g., Arakel, 1980; Butler and others, 1982; Eugster & Hardie, 1978; Gornitz and Schreiber, 1981; Hardie, 1968; Kinsman, 1976; Lowenstein and Hardie, 1985; Shearman, 1970, 1978; and Smith, 1971) and solute removal (e.g., Schreiber and Schreiber, 1977; Hardie and others, 1978; Hovorka, 1983a, in press; Lowenstein and Hardie, 1985; and Powers and Hassinger, 1985). As early diagenetic reactions are common within the depositional settings of most evaporites and, in fact, are responsible for the formation of many of the diagnostic evaporite sedimentary structures unique to a particular depositional setting, it is necessary to differentiate between those early/syndepositional diagenetic reactions and those late stage diagenetic reactions not related to the original depositional setting. So,

for the purpose of this study, early/syndepositional diagenetic reactions will not be considered in the same context as later diagenetic reactions, and the following definition of late stage diagenetic features will hold. Late stage diagenetic features originate in a system not closely tied by time or original ground-water conditions to the host material. In other words, features formed within the ground water system at or near the time of deposition of the host material are considered to be part of the depositional system and will not be discussed in context with late-stage diagenetic features.

8.1 CEMENTS

Several cements were observed at various locations throughout the Rustler section. The clastic rocks near the base of the bioturbated clastic interval and within H-1, H-3, and H-4, and locally M-4 contain halite cement. Most halite cements appear poikilitic. Halite cements are common within halite-bearing rocks, but as yet, no clear method exists for uniquely distinguishing between halite cement precipitated in the near surface environment and that precipitated during burial (Lowenstein and Hardie, 1985). This being the case, no interpretation of timing of halite cement in H-1, H-3, or H-4 can be made. However, halite cements within the lowermost part of the Rustler clearly have a diagenetic origin as halite was not associated with the depositional setting of that unit. As halite occurs within the intervals both above (H-1) and below (the Salado) this zone, it is likely that the solutes that formed the cement were derived from one of these zones. Halite cements within M-4 probably have an early or syndepositional origin. Thin sections from M-4 at WIPP 19 show halite-filled voids. Some of these voids are morphologically similar to skeletal and displacive halite crystals, while other voids are irregularly shaped. Poikilitic halite is an intergranular cement in the vicinity of the halite-filled voids. The halite-filled voids are relicts of displacive and skeletal halite crystals which have suffered syndepositional dissolution. The cements formed after the partial dissolution of the halite crystals, probably sometime during early burial (e.g., Lowenstein, 1987a).

Gypsum cements are common within some of the clastic units of the Rustler. Gypsum cements have been observed in the transition zone, the Magenta, M-2, and M-3. A syndepositional origin has been assigned to the

gypsum cemented part of the transition zone and it will not be discussed here. Gypsum cement occurs as an alteration of anhydrite within the Magenta Dolomite Member. The gypsum contains relics of large poikilitic anhydrite crystals. The fabric locally appears to be expansive. It is likely that much of the sulfate originated as transported grains; evidence of those grains has been destroyed by one or more episodes of replacement/alteration of gypsum with/to anhydrite and back to gypsum. Some poikilitic gypsum cement occurs within the coarser parts of some of the mudstone (M) units. However, no anhydrite precursor was observed.

Gypsum cements occur locally within M-2 and M-3. Some are poikilitic while others are not so coarsely crystalline. The cements are not pervasive throughout the mudstone units. They are most common near the top and the base of the mudstones and near sulfate interbeds.

8.2 OVERGROWTHS

Overgrowths on clastic transported grains are found within some zones in the Rustler. Silt and very fine sand-sized quartz grains, within the Culebra and some of the mudstone (M) units, exhibit euhedral terminations and dark, irregular, and roughly elliptical rims of foreign material within the crystal. These euhedral crystals are interpreted to be detrital grains with quartz overgrowths. Many of the quartz grains have corroded boundaries. These grains and their overgrowths were present prior to the dolomitization of the ground mass. Euhedral rhombohedrons of carbonate with M-3 and M-4 display thin, roughly elliptical zones of dark material which are interpreted to be the original clast boundaries prior to overgrowth development. The volume of the overgrowth is usually much greater than the original grain. The margins of the carbonate grains frequently display evidence of corrosion.

Large gypsum overgrowths on fine sand-sized grains of gypsum are found in thin sections from the M-3 internal of WIPP 19. These grains have not been replaced by, or altered to, anhydrite since their deposition and subsequent overgrowth. The grain margin might have survived the replacement of gypsum by anhydrite, but it could not have survived the conversion to anhydrite. The anhydrite-to-gypsum conversion would have destroyed the original grain margin.

8.3 STYLOLITES AND PRESSURE SOLUTION

Stylolites demonstrate pressure solution within the Rustler anhydrites. The stylolites within the anhydrites are subhorizontal to horizontal and only occur within laminated sulfate. Clay and carbonate mark the stylolite surface. They are extremely common within the upper Rustler anhydrites. Pressure solution within the Rustler occurred in response to a stress-field with the maximum principal stress in the vertical. Calcium sulfate was liberated by the pressure solution and removed from the site of reaction.

8.4 REPLACEMENT

Replacement occurs when the processes of solute addition and removal are simultaneous and balanced. Pseudomorphs are interpreted to be replacements. The most common replacement is anhydrite after gypsum as pseudomorphs. Sometime prior to maximum burial and the development of stylolites, anhydrite replaced gypsum on a volume for volume basis. Conversion or dehydration of gypsum did not occur, as a volume reduction is associated with that reaction and no evidence of volume change is found. Conversion or dehydration of gypsum to anhydrite would cause a loss of original depositional textures.

Secondary gypsum after anhydrite occurs throughout the anhydrite (A) units. Where both gypsum and anhydrite are present, the gypsum crystals usually crosscut the anhydrite crystals. The volume of gypsum observed within the anhydrite (A) units is at a minimum near the centers of the A-units and a maximum near the margins. Relationships between the gypsum and anhydrite fabrics cannot be determined when gypsum is the main constituent. However, disruption of the fabric caused by a volume increase during the conversion of anhydrite to gypsum was not observed when gypsum occurred within anhydrite. So, the gypsum is interpreted to be a volume for volume replacement of anhydrite when anhydrite is the major constituent. The relationship between what is converted to gypsum and what is replaced by gypsum becomes less distinct as the percentage of gypsum increases.

Gypsum-filled vugs within the Culebra are interpreted to be partly displacive as early syndepositional nodules and partly replacive. Stratification within the carbonate surrounding some of the gypsum-filled vugs appears to have been displaced away from the vug. This supports an early syndepositional displacive origin for the vugs. The majority of the vugs, however, do not have definite expansive textures preserved within the surrounding carbonate. In fact, stratification within the carbonate often

terminates abruptly at the vug-carbonate margin indicating that some of the carbonate was removed. No evidence of crystal growth inward into a void was found within the vug fillings. This suggests at least a partly replacive origin of the sulfate vug filling with no evidence of passive pore filling. Relict crystals of anhydrite are preserved as centers within some gypsum vug fillings at H-12. Petrographic relationships indicate that anhydrite once entirely filled the vugs and is now partially replaced by gypsum. Once again, as late stage expansive textures are not commonly associated with or attributed to the development of the vugs, gypsum did not result from the hydration of anhydrite, but is instead, the volume for volume replacement of anhydrite with gypsum.

Gypsum is a major constituent within the Magenta and is at least partly replacive of anhydrite. Relict crystals of anhydrite occur within the Magenta. Gypsum appears to crosscut optically continuous anhydrite crystals. Anhydrite is interpreted to have been the principal sulfate present within the Magenta and to have been replaced with or converted to gypsum. It is probable that much of the sulfate within the Magenta originated as detrital grains of gypsum. These gypsum grains were probably replaced by anhydrite prior to maximum burial and later replaced/converted to gypsum. Conversion to gypsum will be discussed in the following section of this report.

Halite pseudomorphs after gypsum swallowtail crystals are common within those anhydrites in contact with halite units. When halite pseudomorphs after gypsum are present, the remaining sulfate rock consists of anhydrite with no, or very little, gypsum. Unlike anhydrite, halite appears to only pseudomorph coarsely crystalline gypsum, leaving the ground mass/matrix unreplaced. Thin sections of anhydrite pseudomorphs after gypsum swallowtail crystals indicate that the anhydrite within the surrounding material is micro- to finely crystalline while the anhydrite within the swallowtail crystal form is also finely crystalline (slightly larger than the ground mass). Halite is interpreted to have replaced/pseudomorphed the gypsum crystals prior to, or synchronous with, the replacement of gypsum with anhydrite. The energy required to replace a large crystal is less than that required to replace microcrystalline material. After the gypsum was replaced by anhydrite the whole rock was finely crystalline. If halite had replaced anhydrite, there would have been little reason for the halite to have

preferentially replaced the swallowtails. Halite replacement would have more readily occurred when the rock was gypsum.

Halite replaced aragonite allochems in the carbonate-rich unit equivalent to the bioturbated clastic zone of the unnamed lower member. Shells and shell fragments are the most common allochem affected by halite replacement. In many places, the halite content in the matrix is volumetrically much greater than the carbonate. As the allochems did not collapse within these zones, the halite could not have been a void filling cement, but instead, was a replacement.

Anhydrite replaced halite along the margins of crystals within anhydrite and halite psuedomorphs after vertically grown gypsum crystals. Long, thin blades of anhydrite project into the crystals of halite. They are interpreted to be replacements as the space occupied by the halite could not have remained open while the anhydrite crystals grew into a void.

Elongate dolomite crystals occur within halite pseudomorphs after gypsum crystals in the unnamed lower member of H-12. These crystals could not have grown into void space, as the void would have collapsed. A replacement origin is proposed for the elongate dolomite crystals. Other authors (e.g., Hovorka, 1985a) have interpreted multifaceted dolomite crystals in halite as replacements.

Dolomite replaced some detrital and authigenic quartz grains within the Culebra. Some quartz crystals with irregular and embayed margins have ghost margins within the dolomite. Other quartz grains display irregular or embayed margins without any evidence of replacement. Some authigenic crystals and grains with euhedral overgrowths also exhibit corroded margins. The authigenic quartz crystals and quartz grains with overgrowths formed prior to dolomitization. The dolomicrite ground mass has partially replaced the quartz grains and crystals.

8.5 RECRYSTALLIZATION

Recrystallization occurs when crystals, under increased temperatures and pressures during burial, change their morphology to minimize energy. Recrystallization results in equigranular crystals with few inclusions as foreign material is purged to the crystal margin. Annealing textures in halite yield triple junctions at angles of roughly 120 degrees. Depositional textures are usually disturbed/destroyed by recrystalliztion of evaporite minerals.

Halite at several locations within the Rustler is interpreted to have been recrystallized. Triple junctions, purged inclusions, and equigranular grains showing no depositional fabrics all occur within that part interpreted to be recrystallized. These textures are found within zones H-1b and H-3. The recrystallization is probably the result of pressure caused by loading rather than increased temperature during burial as the geothermal gradient within the Delaware Basin has been considered low.

Recrystallized gypsum occurs at several locations within the Rustler section. The base of A-5 is recrystallized at the waste handling shaft (Holt and Powers, 1984). Some of the coarsely crystalline gypsum found in the lower part of A-2 and A-3 is interpreted to be recrystallized. The finely crystalline gypsum was reorganized in the presence of fluids at the lithologic contacts.

8.6 CALCIUM SULFATE STABILITY

The relationship between anhydrite and gypsum is complex. The stability of each depends upon temperature, pressure, and the ionic strength of fluids in contact with the minerals. When both are present, one is metastable. The actual processes of either replacement or conversion are not well understood. Anhydrite pseudomorphs after gypsum have yet to be reported from modern evaporite deposits. The volume problem associated with the conversion of one to another at lithostatic pressure has yet to be adequately addressed. However, one feature is suggested here to be indicative of, but not unique to, the simple hydration of anhydrite to gypsum or dehydration of gypsum to anhydrite. Unless the sulfate was only a minor constituent within the sediment, primary depositional features within the sediment would be destroyed during the simple conversion of one to another via the addition or subtraction of water from the crystal structure. Gypsum or anhydrite that has undergone simple conversion retains no primary depositional structures. They are all be severely deformed if not destroyed by the volume change.

The majority of the Rustler sulfate studied macroscopically and microscopically preserves primary sedimentary structures and shows no evidence of either expansive or implosive textures. This indicates that replacement, not simple conversion, was the main process of change between the two

sulfates. Anhydrite pseudomorphing gypsum indicates replacement. Several highly gypsiferous zones, however, preserve fewer original depositional textures than are preserved elsewhere where replacement of gypsum with anhydrite clearly has occurred. These zones are thin and located at the base of A-2, A-3, A-4, and A-5 and at the top of A-3. These zones may have seen the conversion of anhydrite to gypsum in the presence of fluids.

Several authors (e.g. Snyder, 1984) have proposed that increased thicknesses within the Rustler in the vicinity of Nash Draw are the result of the "jacking up" of the section due to the volume change during the hydration of gypsum. Detailed description of cores from the Rustler within Nash Draw reveals an abundance of primary features preserved within the Rustler anhydrites. So, it is unlikely that a large scale simple conversion of anhydrite to gypsum in the presence of fluids occurred. In addition, the Rustler section within Nash Draw is brecciated. The breccia originates within the Salado Formation indicating removal of volume from within the Salado. The brecciation has lengthened the Rustler section giving rise to an apparent increase of thickness within Nash Draw. This apparent thickness adjustment affects nearly all of the units within the Rustler, not just the sulfates.

Not all of the gypsum in the Rustler is secondary. Some of the Rustler gypsum is primary and was never converted to or replaced by anhydrite. Gypsum overgrowths on clastic gypsum grains are preserved within M-3 at WIPP-19. The internal texture of these grains would not be preserved had they been converted from anhydrite to gypsum. Other primary fabrics occur in gypsum from mudstone (M) units. Incorporative gypsum crystals are common. Isolated, twinned, stellate, and palmate crystal forms are present. Lenticular gypsum is rare as the proper organic compounds required to form lenticular gypsum (Cody, 1979) were not present in the depositional system. Most Rustler gypsum is diagenetic. Anhydrite precursors for gypsum are common. Primary gypsum occurs only in the mudstone (M) units. Perhaps the mudstone units protected some gypsum during diagenesis.

8.7 FRACTURES

Much of the Rustler and the overlying Dewey Lake is extensively fractured, with many of the fractures filled with fibrous gypsum. Within competent rocks, the majority of the fractures are horizontal or

subhorizontal and parallel to bedding planes. Sub-vertical and vertical fractures are less common. Gypsum fracture fillings usually indicate separation along a single fracture. Several episodes of crosscutting relationships show that the fracture style changed through time. Gypsum-filled fractures occasionally parallel slickensided surfaces in the mudstone units. This occurs at the exhaust shaft, where arcuate gypsum-filled fractures have slickensided surfaces. The slickensides probably developed as the mudstone units deformed due to loading and unloading.

These fractures are dissimilar to fracturing associated with solution collapse (e.g. Middleton, 1961). Solution collapse breccias vertically decrease clast separation to give way to a series of fractures, hairline fractures and cracks, and then undisturbed beds. Within WIPP cores and shafts, fractures are commonly, but not exlusively, horizontal. They occur in zones that are not well interconnected or continuous in the vertical. This fracture style persists through the Dewey Lake. There is no apparent relationship of WIPP fracturing to dissolution at the site area. A vertical to sub-vertical minimum principal stress in indicated by the horizontal to sub-horizontal fractures. The orientation of the least principal stress was somewhat variable, as suggested by variable fracture orientations. The data are consistent with an unloading origin for Rustler fractures. Differential unloading is considered responsible for the majority of the Rustler fractures.

8.8 FRACTURE FILLINGS

Fracture filling materials are very common through the Rustler. Two types of fracture fillings occur within the Rustler: halite and gypsum.

Halite-filled fractures appear to be contained within those zones containing halite (H-1, H-3, and H-4) and within the lower part of the unnamed lower member between H-1 and the Rustler/Salado contact. Most of the halite fracture fillings are fibrous and may be clear, white, orange or blue. A few of the fracture fillings are color zoned (e.g. WIPP 19) in the clastic units located stratigraphically below H-1. Within the halite-bearing units, the halite fracture fillings are considered to be syntaxial, while in the clastic units below H-1, they are syntaxial and antitaxial (after Durney and Ramsay, 1973).

Gypsum-filled fractures commonly occur above the H-1 unit where that unit is present. The gypsum fracture fillings are clear to white and fibrous and are both syntaxial and antitaxial. Pieces of the wall-rock material are commonly included within the fracture filling. Most of the larger fibrous fracture fillings observed within the Rustler appear to have a "suture" line which always parallels the fracture surface of the host material. The suture line is the site of a moderate to abundant amount of inclusion of wall rock material. Most of the fibrous fracture fillings are parallel to host rock. However, some are tilted away from the perpendicular, and in rare cases, some are sigmoidal.

Fibrous fracture fillings result from growth of the individual fibers as the fracture opens in small increments. When the fracture initially opens, this creates a void and a zone of low pressure. Intercrystalline or pore fluid migrates to the site of low pressure. The pressure decrease coupled with newly created void space is conducive to solute precipitation along the fracture surface. If the fluid is near saturation for a particular mineral, the pressure decrease associated with fracturing can drive the fluid to become saturated with that mineral and precipitation can occur. If the wall rock and the fracture filling contain the same mineral, overgrowth upon grains or crystals of that mineral will occur and the fracture filling is syntaxial (Durney and Ramsay, 1973). If the wall rock does not consist of the same mineral as that precipitating in the void provided by the fracture, then nucleation of the mineral occurs, and the fracture filling is antitaxial (Durney and Ramsay, 1973). The suture line is most visible in antitaxial fracture fillings as small parts of the wall rock are included within the crystals during the initial fracturing and precipitation. The suture line exhibits the same morphology as the fracture surface on the wall rock.

Once the initial fracturing and subsequent precipitation occurs, the fracture filling grows incrementally as the fracture filling mineral precipitates as overgrowths. These overgrowths are constrained by each other in the direction parallel to the fracture surface, so they must grow competitively in the direction perpendicular to the wall rock and away from the seed crystal. This causes a fibrous crystal habit to develop. This habit is visually enhanced when the filling material consists of one of the minerals that are readily twinned (e.g., gypsum).

When the fracturing continues, separation occurs between one side of the fracture filling and the wall rock. Fluids migrate to that point, and precipitation then occurs at the contact between the wall rock and the filling material. So, the youngest part of the filling is next to the wall rock, and the oldest part of the fracture filling is adjacent to the suture line. The width of the fracture on each side of the suture line is related to the availability of chemical nutrients and the frequency of reseparation by fracturing along each side.

The morphology of the fibrous fracture filling is the result of the stress field which produced it (Durney and Ramsay, 1973). Fibers perpendicular to the fracture surface indicate that there was no displacement parallel to the fracture surface at the time of fracturing and subsequent filling. Fibers that are tilted with respect to the perpendicular indicate that there was a component of displacement parallel to the fracture surface and that the component was present throughout the period of fracturing and filling. Sigmoidal morphologies develop when a component of displacement parallel to the fracture surface occurs after the initial fracturing.

The fracture fillings within the Rustler contain information about any changes through time of the chemistry of the precipitating fluid and the stress fields which formed the fracture. Chemical analysis of the minerals contained within the gypsum filled fractures and detailed analysis of the fracture filling morphologies was not part of this study. However, solutes for both halite and gypsum fracture fillings were probably locally derived, as possible sources for all the solutes exist within close proximity to the fractures.

Halite-filled fractures seem to be confined to either zones containing halite or zones adjacent to halitic intervals. Halite-filled fractures within the clastic part of the unnamed lower member appear to occur only when H-1 occupies the stratigraphic interval above the clastic zone. No evidence of the removal of halite from fractures was ever found in the clastic interval when M-1 was present. However, WIPP 30 is the only core through the unnamed lower member where M-1 overlies the clastic interval and the Rustler/Salado contact is in its normal position with a normal appearance, and it is possible that the core did not intersect a halite-filled fracture as they are most often vertical or sub-vertical. The remainder of the cores containing M-1 are located within Nash Draw where some disturbance occurs within the Salado in the vicinity of the Rustler/Salado contact.

Gypsum-filled fractures occur only above the interval H-1, when halite is present. This apparently indicates that gypsum-saturated fluids did not or could not migrate downward below the halite. Lowenstein (1987) believes that porosity in such halitic units is plugged syndepositionally, within a few meters at most. Where M-1 is present, no halite existed and gypsum precipitated in fractures within the mudstone. Gypsum-filled fractures are less common in those cores which have less gypsum within sulfate units. In other words, gypsum-filled fractures are less common when the gypsum to anhydrite ratio of the sulfate rocks is smaller. Less gypsum was observed within the anhydrites (A-units) in the thin sections of H-12. The Rustler at H-12 has seen less fluid capable of precipitating gypsum within fractures.

8.9 DISSOLUTION

Removal of solutes by dissolution occurs when a fluid is present that is undersaturated with respect to the mineral being dissolved and the energy to drive the reaction exists. Dissolution creates void space. Preserved void space or evidence indicating the former presence of void space must be present if dissolution and removal of solutes has occurred. Dissolution porosity varies in scale from intercrystalline to vuggy to cavernous. While preserved porosity is obvious, the former presence of porosity is more difficult to see; it can be recognized by filled void space or features indicating the ductile or brittle mechanical adjustment to the nonuniform stress field caused by the porosity.

Preserved porosity occurs throughout the Rustler. Most of the porosity can be directly attributed to the void space created during the dissolution of soluble minerals. Preserved dissolution porosity occurs within the carbonate, sulfate, and halite-bearing rocks of the Rustler.

8.9.1 Microporosity and Vuggy Porosity

Intercrystalline microporosity and vuggy porosity is common within the Culebra. Neither filled nor open intergranular porosity occurs within the Culebra as the Culebra consists of dense micrite and argillaceous material. Sulfate is not a major constituent within the Culebra. Sulfate occurs as a pore and fracture filling material and locally as a cement. Intercrystalline and vuggy porosity resulted from the dissolution of carbonate, where there is no gypsum precursor. Some vuggy and intercrystalline porosity is

attributable to the dissolution of gypsum. All large scale vugs within the Culebra are interpreted to have contained gypsum. Large, open vugs may have resulted from the dissolution of gypsum. Vuggy porosity is locally well developed in gypsum fracture fillings. Dissolution of gypsum is the last distinguishable event to occur within the Culebra as gypsum dissolution appears to effect gypsum-filled fractures. Dissolved sulfate within the Culebra has a solubility index close to one (Myer, pers.comm.). The sulfate within the Culebra waters is probably partially derived from the gypsum fracture fillings and the apparently related gypsum vug fillings. Further dissolution of sulfate and carbonate within the Culebra is not likely given the present chemical conditions of the waters within the Culebra as they are apparently in equilibrium with gypsum, ordered and disordered dolomite, calcite, and anhydrite in the vicinity of the WIPP site (Myer, pers.comm.). Where fresher fluids have access to the Culebra in Nash Draw, dissolution of carbonate and sulfate can continue.

Dissolution of gypsum is common within the sulfate units across the study area. Intercrystalline porosity was found in thin sections from most of the anhydrite units. Intercrystalline porosity was less common in thin sections from H-12 than WIPP 19 and in both cases appeared to be more abundant near the upper and lower contacts of the anhydrite units. Where present, porosity within the anhydrites was usually less than one percent. Several of the cores from Nash Draw showed the development of vuggy porosity within the sulfate units. Large open vugs, some containing gypsum crystals which grew inward toward the void center, are preserved within some cores. This porosity is interpreted to have originated from the dissolution of sulfate within the Rustler. The presence of large vuggy and cavernous porosity within the Rustler in the vicinity of Nash Draw is interpreted to have formed as the result of dissolution of gypsum by meteoric groundwaters (see also Bachman, 1984 a, 1987 a,b).

Evidence of gypsum dissolution within the Magenta was found in thin sections from H-12 and WIPP 19. Intercrystalline porosity occurs within the gypsum. Small relics of anhydrite remain within the gypsum and appear to be unaffected by the dissolution. Dissolution of gypsum at Magenta outcrops is common.

Intergranular porosity is commonly well developed in halite cemented clastic rocks. M-4 at WIPP 19 is cemented by halite and exhibits microscopic halite crystals. Halite cemented clastic units in the unnamed lower member also exhibit some intergranular porosity.

8.9.2 Caves and Cave Fillings

The only known cavernous porosity encountered in drilling the Rustler near the site was in WIPP 33 (Sandia National Laboratories and U.S. Geological Survey, 1980). There, drilling, logs, and downhole television scanning demonstrated fluid-filled (at the time of drilling) cavernous porosity within the Magenta of undetermined lateral dimensions. Bachman (1980) attributes this porosity to dissolution near the margin of Nash Draw. It is clear that cavernous porosity also is prominent within Nash Draw as part of karst-forming processes.

Ferrall and Gibbons (1978) attribute the laminated claystones found above the Culebra in WIPP 19 to filling of cavernous porosity. This claystone, observed closely in the WIPP shafts, is considered to be partially algal in origin and is believed to be ubiquitous (Ch. 45). The lack of a lower Tamarisk anhydrite clearly leads Ferrall and Gibbons (1970) to consider that dissolution had destroyed that bed, and that a bedded claystone must therefore have formed in cavernous porosity during this dissolution event. In this document, the claystone, which is present even below the lower Tamarisk anhydrite, is considered depositional in origin, and the anhydrite is considered to have been lost very early at WIPP 19 (Ch. 5, 6). Cave fillings found elsewhere sometimes exhibit bedded clastics, but the more common characteristic attributed to cave fillings is the piled to floating, slab-like collapse blocks piled one on another or floating in a matrix. More importantly, on a broader scale, caves and cave fillings are likely to show an upper limit that is well defined and an irregular lower boundary. No feature in cores or shafts is considered likely to be a cave filling.

8.9.3 Dissolution and Collapse Features

As discussed in the previous chapter, overlying competent rocks deform brittely when large volumes of material are removed from stratigraphically distinct zones. The behavior of Rustler materials due to the removal of underlying evaporites can be assessed after observing the cores of the Rustler from Nash Draw.

The upper portion of the Salado Formation within Nash Draw thins dramatically. The depositional environments of the upper Salado give little reason to expect depositional thinning is present in the vicinity of Nash Draw. The stratigraphic units overlying the Salado in Nash Draw are brittely deformed. Upward stoping and downward mixing of clasts derived from overlying stratigraphic units occur within the upper Salado and the Rustler. The upper Salado within Nash Draw is interpreted to have partially dissolved (Vine, 1963; Bachman, 1974). The extent of brecciation varies from borehole to borehole, but in each case is known to include more than a small or isolated zone within the borehole. These breccias are similar to those described previously from the Mission Canyon, for example, in that clasts are generally quite angular, though they may vary in size. These breccias in some cores display the upward decreasing extent of brecciation also described from the Mission Canyon (e.g., Middleton, 1961) and other evaporite solution zones. As the various boreholes in Nash Draw were differentially affected by dissolution of the upper Salado, the apparent loss of Salado salt was tabulated for each of these boreholes (Table 8.1), and the amount of the Rustler section deformed has been estimated (Table 8.1). The ratio of thickness disturbed to the thickness reduction is estimated to be between 1:1 and 1:2. Few previous studies report sufficient data to obtain an equivalent relationship, but there are suggestions of a correspondence. A study such as that by Parker (1967) contains data on the thickness of removed salt, but the logs do not reveal the extent of brecciation and the removal may have been early enough that breccias did not result.

Adjacent boreholes WIPP 29 and WIPP 32 show two important effects related to dissolution. Within the lower unnamed member, WIPP 32 in particular displays brecciated smeared intraclast textures in zones that laterally have halite (see Ch 5). Much of the lower unnamed member in this borehole is brecciated, but the superposition of brecciation over smeared intraclast texture (described in Ch. 5) reveals that the halite in the lower member was dissolved essentially syndepositionally, while the brecciated texture is post-lithification. The brecciated texture is clearly consistent with late removal of salt from the Salado. The upward extent of deformation is not clear as the upper portions of the Rustler have been removed by erosion. The textures in WIPP 29 are similar, but seem much reduced. Though this may partially be due to locally varying processes of dissolution, most of the

difference in this report is attributed to the difference in core diameter between the two boreholes. WIPP 29 is about a 2 inch (5 cm) diameter core while WIPP 32 core is about 4 inches (10 cm) in diameter. The increased diameter is important to the detection and interpretation of these textures.

Collapse, upward stoping, and mixing of clasts derived from various stratigraphic horizons occur in core from WIPP 13 where the deformation is not clearly attributable to Salado dissolution. The lowest deformed unit is A-2. The overlying mudstone (M-3) is also deformed and contains clasts clearly derived from the overlying anhydrite (A-3). A-3 is brecciated and deformed near the base. The center of A-3 was not cored, but core of A-3 below the Magenta displays dipping stratification. The source of at least part of the deformation is within or below A-2, but the originating horizon for the deformation is not clearly identified as the entire Rustler section was not cored at WIPP 13. The extreme deformation of the M-3/A-3 contact does not require that some of the void space originated within the M-3 horizon. However, this cannot be overruled. Dissolution of a large thickness of halite from either the M-2 or M-3 horizon and the collapse of the overlying beds could partially account for the features observed. However, our depositional model generally predicts that halite was not preserved within the M-2 or M-3 stratigraphic interval after the deposition of the overlying units. Our depositional model is based upon the descriptions of several cores and shafts and regional interpretations of geophysical logs, while WIPP 13 is an isolated drill hole. Without more complete Rustler data within the WIPP 13 area, the cause of the structural deformation observed at WIPP 13 cannot be adequately constrained. Therefore, it must be considered an anomaly until more data are available from that area.

Collapse, upward stoping, and mixing of stratigraphic units originating in the M-3 stratigraphic interval occur in the core from borehole H-3b3. M-3 contains readily identifiable clasts and blocks of the overlying rocks. The overlying anhydrite contains dipping and overturned stratification. Our depositional model does not exclude halite within the M-3/H-3 stratigraphic interval at H-3b3. Based upon the apparent distribution of facies, H-3b3 could have contained a small volume of halite. The ratio (1:1 or 1:2) of deformation of the Rustler section within Nash Draw to the volume of Salado removed indicates the thickness of the M-3/H-3 interval may have been reduced by 10 to 30 ft (3 to 9 m).

The M-4 interval at H-3b3 also contains a large block of anhydrite, presumably downdropped, and a clay-filled fracture at the M-4/A-5 contact. A small amount of halite may have been removed from the M-4/H-4 stratigraphic interval. This would also be consistent with the depositional model of that interval. Actual volume reduction could have been at most several feet.

The M-3/A-3 contact at H-11b3 is brecciated. The claystone and the underlying thin sulfate unit are brecciated, but the breccia clasts are confined to the top of the M-3. Minor amounts of subvertical fracturing occurs within the extreme lower part of A-3. This disruption could have resulted from the dissolution of a very thin section of halite. Our depositional model for the M-3/H-3 interval supports the occurrence of halite at H-11b3.

Dissolution of halite is not a unique explanation for the features occurring at the M-3/A-3 contact. Brittle deformation at the contacts of brittle and ductile materials can occur when the ductile material flows (e.g., McKnight and Fischer, 1970).

As described by McKnight and Fischer (1970), incompetent beds between stronger units may show brecciation due to tectonic events. They described plucking of blocks from an overlying chert by a less competent carbonate. Within the Rustler, it is quite possible that some breccia, local in extent, could be attributed to this mechanism as the contrast in competence is large for several beds. As McKnight and Fischer (1970) point out, the movement on adjacent beds may be very small to produce these features. From shaft mapping, slickensides and minor deformation may be consistent with a small amount of lateral movement taken up by incompetent beds. Though it seems likely that some breccia (or deformation) may be formed in such a manner, no feature has been uniquely attributed to the process. It may only be possible to do so where the affected units are exposed along drifts, as in the MVT PB-ZN deposits examined by McKnight and Fischer (1970).

There exists within the shaft, and possibly within some core material, rare and isolated slightly brecciated areas. These areas, as in the Culebra in the exhaust shaft (Holt and Powers, 1986a), have throughgoing stratification underlying and overlying the brecciated area. There is no justification for interpreting these as evidence of broader dissolution, although in the case of the Culebra, extremely local solution of carbonate may have caused such a feature.

Borehole	Approximate Thickness Reduction in the Upper Salado	Approximate Thickness of Rustler Section Disrupted
WIPP 25	115 ft	280 ft
WIPP 27	155 ft	Entire Section
WIPP 29	455 ft	Entire Section
WIPP 30	0 ft	-
WIPP 32	460 ft	Entire Section
WIPP 33	0 ft	-

Table 8.1. Thickness of Rustler section disrupted versus thickness reduction by dissolution in the upper Salado in the vicinity of Nash Draw.

9.0 CONCLUSIONS

The Rustler Formation is the last evaporite deposit of the Permian Ochoan Series in the Delaware Basin. The depositional environments and distribution of the Rustler vary considerably from the older Castile and Salado Formations. The Rustler exhibits abundant primary depositional features permitting detailed reconstruction of facies relationships and depositional environments. Most of the major units of the Rustler thicken in an area east and south of the WIPP site. Resting over and outside of the Capitan reef which restricted earlier deposits, this area served as a depocenter that had shifted east and north of the earlier Castile depocenter. The Rustler formed from environments ranging from shallow lagoons and subtidal environments to shallow saline pans and environments marginal to the saline pan. These environments changed laterally over distances of a few miles, resulting in observable lithofacies changes within cores and shafts at the WIPP site.

The depositional environments of various Rustler units have been reconstructed using a sedimentological approach. Observable bedding, primary features, and certain secondary features (such as pseudomorphs after primary gypsum textures) were described and placed in stratigraphic sequence. Lithologic units and their features have been compared to facies models constructed from modern and ancient analogs. For some features and their associations, such as pedogenic clay skins on clasts and intraclasts in some mudstone units, modern evaporite analogs have not been reported. Nonetheless, soil and paleosol features are well known independently and can be linked readily to the environmental setting of the Rustler. As is common in such studies, new features and associations were described and interpreted from the geological context established from better-known features. Smeared intraclasts and crushed pseudomorphs are expected to become established, independently interpretable features as modern analogs are found and described. In this manner, facies and environmental models are constructed and refined with modern and ancient examples.

Parts of the Rustler formed when fresher water, possibly marine, transgressed rapidly over very low topography, depositing clastics, carbonates, or subaqueous sulfates. A marine transgression over the Salado is the initial example. The transgressing water evaporated to increase salinity and deposit halite. Halite and clastics were reworked along margins, and halite was concentrated in the depocenter, maintaining low topography. A rapid transgression of fresher water terminated halite

precipitation in the depocenter. Several shallowing-upward or desiccating-upward sequences comprise most of the Rustler (Fig. 9.1). Because the upper boundaries are abrupt and are overlain by widespread units of sulfates or carbonates of nearly uniform thickness, these contacts are thought to be nearly isochronous surfaces.

Halite units are lenticular with the thickest part south and east of the WIPP site, in the depocenter. Sulfate units are more nearly uniform in thickness from depocenter outward, indicating either an increase in sedimentation rate or a decrease in subsidence rate. Here it is suggested that sedimentation or accumulation rates may have been relatively greater for sulfates and carbonates as halite accumulation rates were controlled by syndepositional dissolution. The Culebra is somewhat thicker in the depocenter, generally corresponding to mudstone and halite unit patterns.

The halite and mudstone units vary most in lithofacies and thickness from depocenter to margins. Five major facies were deposited, from depocenter outward, in the study area in these generalized depositional environments: mud-poor halite pan, mud-rich halite pan, halite saline mudflat, gypsum saline mudflat, and mudflat. Clastic sediments were distributed mainly around the margins as the capacity and competence of the hydrologic system decreased toward the depocenter. Flooding events introduced clastics and moved them toward the depocenter. Transgressions, or a rise in the base level, caused larger areas to be covered with water that was very likely to be undersaturated with respect to halite. Halite was dissolved around the margins as a consequence. The water became more saline and contracted as evaporation continued. Halite was concentrated in the depocenter as the edges of the brine contracted. During lower water levels (lower base level) additional halite was cannibalized and moved toward the depocenter by rainwater or the encroaching lens of shallow groundwater. Unless subsidence rates varied dramatically during deposition of halite and mudstone units, halite and mudstone accumulated slowly relative to sulfates and carbonates.

Halite was dissolved syndepositionally from halite and mudstone beds at small to large scales. In the Rustler, the sedimentary sequence was drastically modified by large scale dissolution in response to various conditions: a transgression or freshening event that raised the water table or base level, a lowering of the watertable or base level due to evaporation or subsidence, or a changing in the lateral position of saline groundwaters.

Halite was dissolved by less saline water after a transgression. Dissolution continued in some cases after the overlying sediment was deposited, deforming and slumping this sediment. Subsidence or evaporation lowered the water table at the margins, subjecting halite to dissolution by meteoric water in the vadose zone and redepositing it in the depocenter (soluble mineral cannibalism). Incipient soil features formed in the vadose zone of the marginal mud-rich sediments. This hypothesis differs greatly from previous ideas of dissolution of halite from mudstone units. Several features demonstrate that halite was removed from marginal saline pan to mudflat environments before lithification and before the overlying sulfates were deposited. This contrasts with explicit and implicit ideas that Rustler salt was dissolved long after the Rustler was deposited. In addition, the cumulative thickness of halite removed from mudstones is considered here to be much less than the thickness of halite in equivalent zones.

Rustler sediments have also been alterred since deposition. Halite and gypsum cements are common. Some transported grains have been overgrown by authigenic minerals. Overgrowths on some clastic gypsum grains indicate that gypsum-anhydrite-gypsum alteration did not occur. This implies that other gypsum may be primary.

Halite pseudomorphs after gypsum occurred early, prior to or synchronous with the replacement of gypsum with anhydrite. Halite also replaced carbonate allochems. Both dolomite and anhydrite replace halite locally. Quartz grains with overgrowths were partly replaced by dolomite in the Culebra.

Implosive or expansive textures resulting from a volume change, associated with the direct conversion of gypsum to anhydrite or anhydrite to gypsum, do not occur within the sulfate units of the Rustler. Anhydrite pseudomorphs after gypsum are volume-for-volume replacements of gypsum. Gypsum within anhydrite exhibits no evidence of expansion due to a volume increase and is interpreted to also be a volume-for-volume replacement (not pseudomorphous). Snyder (1984) proposed, on the basis of geophysical log interpretations, that the the Rustler section thickens in Nash Draw due to the hydration and subsequent jacking up of the section. However, core from Nash Draw was examined in detail, revealing that the Rustler section is elongated by brecciation originating in the Salado, not by hydration.

A detailed literature review indicates that two major styles of dissolution exist: karst processes at, and relatively near, the surface and bed-controlled dissolution at greater depths. Near-surface dissolution and karst has poor stratigraphic control, an irregular lower boundary, and an upper boundary that is well-defined by subsequent deposits. Solution breccia beds and related features resulting from the dissolution of soluble materials at depth are stratigraphically controlled by the soluble unit. Where a zone of soluble material near the surface is mostly dissolved, the zone may be bounded below by undisturbed, relatively insoluble material and overlain by a post-dissolution deposit with little or no disruption. The mudstone units in the vicinity of the WIPP have undergone complete syndepositional dissolution of halite and show these relationships. Large scale dissolution of soluble rocks at depth creates breccia beds or strata-bound deposits consisting of angular blocks with a variable matrix. The block size and packing increase upward until the separation between blocks decreases to fractures and, finally, microcracks before disappearing. As dissolution proceeds, collapse occurs when the overlying material can no longer bridge the newly created void. Clasts and blocks are displaced downward from their stratigraphic position and mixed with clasts and blocks from other stratigraphic positions.

The Rustler section in Nash Draw is brecciated at various scales due to dissolution of halite and collapse in the upper Salado. Breccias and downward disruption of a lesser scale were found in several cores. Significant features include collapse, upward stoping, and mixing of clasts derived from various stratigraphic horizons. The borehole WIPP 13 exhibits this style of deformation through A-2, M-3, and A-3, but the zone in which the disruption originates was either not cored or is not apparent in the existing core. In the general sedimentological framework proposed in this study, halite in the Rustler is not expected to have survived deposition at this location. As incomplete core data are present at WIPP 13 and other core data in the vicinity are very limited, the disruption observed in the WIPP 13 core is considered an anomaly. Further interpretation of its origin will be reserved until additional drilling in the vicinity is completed and core can be described. Disruption is present in cores from H-3b3 and to a much lesser extent H-11. These boreholes lie in a boundary zone surrounding the zone now containing halite. As it is very possible that halite survived deposition within this boundary zone, the deformation in H-3b3 is attributed to

dissolution and collapse. The deformation at H-11 is minor. Dissolution is not a unique explanation for the features observed at H-11, as brittle beds bounding a less competent unit may show brecciation due to tectonic events.

The fractures in the Rustler and the Dewey Lake are dominantly horizontal and persist in vertically isolated zones. They are not similar to fractures caused by dissolution and are attributed to unloading. Many of the fractures are filled with fibrous gypsum of both syntaxial and antitaxial types.

Minerals dissolved at varying scales throughout the Rustler. Microporosity and vuggy porosity have been created by dissolution of carbonate and sulfate in both the Culebra and Magenta Dolomite Members. Some porosity was created in the sulfate units by dissolution. Halite cements have been dissolved creating intergranular porosity in clastic rocks. Cavernous porosity was encountered in the sulfate units during the coring of WIPP 33 near Nash Draw. Bedded claystone at WIPP 19, interpreted by Ferrall and Gibbons (1980) as cave filling, is here interpreted as syndepositional.

REFERENCES

Adams, J. E., 1944, Upper Permian Ochoan Series of Delaware Basin, west Texas and southeast New Mexico: Am. Assoc. Pet. Geol. Bull., v. 28, p. 1596-1625.

Adams, J.E., Cheney, M.G., DeFord, R.K., Dickey, R.I., Dunbar, C.O., Hills, J.M., King, R.E., Lloyd, E.R., Miller, A.K., and Needham, C.E., 1939, Standard Permian section of North America: Am. Assoc. Pet. Geol. Bull., v. 23, p. 689-700.

Adams, J. E., Frenzel, H. N., Rhodes, M. L., and Johnson, D. P., 1951, Starved Pennsylvanian Midland Basin: Am. Assoc. Pet. Geol. Bull., v. 35, p. 2600-2607.

Adams, S. S., 1969, Bromine in the Salado Formation, Carlsbad Potash District, New Mexico: Bull. New Mex. Bur Mines and Min Res., v. 93, 122 p.

Anderson, E. J., Goodwin, P. W., and Sobieski, T. H., 1984, Episodic accumulation and the origin of formation boundaries in the Helderberg Group of New York State: Geology, v. 12, p. 120-123.

Anderson, R. Y., 1978, Deep dissolution of salt, northern New Mexico: report to Sandia National Laboratories, 106 p.

Anderson, R. Y., 1981, Deep seated salt dissolution in the Delaware Basin, Texas and New Mexico: New. Mex. Geol. Soc., Spec. Pub. 10, p. 133-145.

Anderson, R.Y., 1982, Deformation-dissolution potential of bedded salt, Waste Isolation Pilot Plant site, Delaware Basin, New Mexico: in Lutze, W., Ed., Scientific basis for Radioactive Waste Management - V, p. 449-458.

Anderson, R. Y., Dean, W. E., Jr., Kirkland, D. W., and Snider, H. I., 1972, Permian Castile varved evaporite sequence, west Texas and New Mexico: Geol. Soc. Am. Bull., v. 83, p. 59-86.

Anderson, R. Y., Kietzke, K.K., and Rhodes, D. J., 1978, Development of dissolution breccias, northern Delaware Basin, New Mexico and Texas: New Mex. Bur. Mines and Min. Res., Circ. 159, p. 47-52.

Anderson, R. Y., and Kirkland, D. W., 1966, Intrabasin varve correlation: Geol. Soc. Am. Bull., v. 77, p. 241-256.

Anderson, R. Y., and Kirkland, D. W., 1980, Dissolution of salt deposits by brine density flow: Geology, v. 8, p. 66-69.

Anderson, R.Y., and Powers, D.W., 1978, Salt anticlines in Castile-Salado evaporite sequence, northern Delaware Basin, New Mexico: New Mex. Bur. Mines and Min. Res., Circ. 159, p. 79-83.

Anderson, S. B., 1966, A look at the petroleum potential of southwestern North Dakota: N. Dak. Geol. Survey Rpt. Inv. 42, 3 sheets.

Arakel, A. V., 1980, Genesis and diagenesis of Holocene evaporitic sediments in Hutt and Leeman Lagoons, Western Australia: Jour. Sed. Pet., v. 50, p. 1305-1326.

Arthurton, R. S., 1973, Experimentally produced halite compared with Triassic layered halite-rock from Cheshire, England: Sed., v. 20, p. 145-160.

Bachman, G. O., 1974, Geological processes and Cenozoic history related to salt dissolution in southeastern New Mexico: U. S. Geol. Survey OFR 74-194,81 p.

Bachman, G. O., 1976, Cenozoic deposits of southeastern New Mexico and an outline of the history of evaporite dissolution: J. of Res., v. 4, p. 135-149, U. S. Geol. Survey.

Bachman, G. O., 1980, Regional geology and Cenozoic history of Pecos region, southeastern New Mexico: U. S. Geol. Survey OFR 80-1099.

Bachman, G.O., 1981, Geology of Nash Draw, Eddy County, N.M.: U.S. Geol. Survey OFR 81-31.

Bachman, G. O., 1984a, Assessment of near-surface dissolution in the vicinity of the Waste Isolation Pilot Plant: SAND84-7178, Sandia National Laboratories, Albuquerque, NM, 87185.

Bachman, G.O., 1984b, Regional geology of Ochoan evaporites, northern part of Delaware Basin: New Mex. Bur. Mines and Min. Res., Circ. 184, 22 p.

Bachman, G.O., 1987a, Evaporite karst in the Pecos drainage, southeastern New Mexico: Guidebook 18, El Paso Geol. Soc., p. 118-123.

Bachman, G.O., 1987b, Karst in evaporites in southeastern New Mexico: SAND86-7078, Sandia National Laboratories, Albuquerque, New Mexico, 87185, 82 p.

Bachman, G.O., Johnson, R. B., and Swenson, F. A., 1973, Stability of salt in the Permian salt basin of Kansas, Oklahoma, Texas and New Mexico: U.S. Geol. Survey, OFR USGS-4339-4, 62 p.

Baker, M. R., 1987, Quantitative log interpretation using probabilistic internally consistent inversion (PICI): Proc. of Geoscience Coll., Univ. of Texas at El Paso, P. 49-60.

Beales, F.W., and Hardy, J.L., 1977, The problem of recognition of occult evaporites with special reference to southeast Missouri: Econ. Geol., v. 72, p. 487-490.

Belloni, S., Martinis, B., and Orombelli, G., 1972, Karst of Italy: in Herak and Stringfield (1972), p. 85 - 128.

Billo, S.M., 1986, Petroleum sedimentology of the Ochoa Group (sic), Texas and New Mexico: Abstr., 12th Int. Sed. Congress, Canberra, Australia, p. 30-31.

Bleahu, M.D., 1972, Karst of Rumania: in Herak and Stringfield (1972),p. 341 - 353.

Bodine, M.W., Jr., 1978, Clay-mineral assemblages from drill core of Ochoan evaporites, Eddy County: New Mex. Bur. Mines and Min. Res., Circ. 159, p. 21-32.

Boeglie, A., 1980, Karst Hydrology and Physical Speleology: Springer-Verlag, Berlin, 284 p.

Borns, D.J., Barrows, L.J., Powers, D.W., and Snyder, R.P., 1983, Deformation of evaporites near the Waste Isolation Pilot Plant (WIPP) site: SAND82-1069, Sandia National Laboratories, Albuquerque, New Mexico, 87185, 143 p.

Borns, D.J., and Shaffer, S-E., 1985, Regional well-log correlation in the New Mexico portion of the Delaware Basin: SAND83-1798, Sandia National Laboratories, Albuquerque, New Mexico, 87185, 73 p.

Bowles, C. G., and Braddock, W. A., 1963, Solution breccias of the Minnelusa Formation in the Black Hills, South Dakota and Wyoming: Art. 83, U. S. Geol. Survey Prof. Paper 475-c, p. C91-C95.

Bretz, J.H., 1950, Origin of the filled sink-structures and circle deposits of Missouri: Geol. Soc. Am. Bull., v. 61, p. 789-833.

Brodzikowski, K., and Van Loon, A. J., 1985, Penecontemporaneous non-tectonic brecciation of unconsolidated silts and muds: Sed. Geol., v. 41, p. 269-282.

Brokaw, A.L., Jones, C.L., Cooley, M.E., and Hays, W.H., 1972, Geology and hydrology of the Carlsbad potash area, Eddy and Lea Counties, New Mexico: U.S. Geol. Survey, OFR USGS-4339-1, 86 p.

Butler, G. P., 1969, Modern evaporite deposition and geochemistry of coexisting brines, the sabkha, Trucial Coast, Arabian Gulf: Jour. Sed. Pet., v. 39, p. 70-89.

Butler, G. P., Harris, P. M., and Kendall, C. G. St. C., 1982, Recent evaporites from the Abu Dhabi coastal Flats: in Depositional and Diagenetic Spectra of Evaporites - A Core Workshop, SEPM Core Workshop no. 3, p. 33-64.

Carozzi, A. V., 1962, Observations on algal biostromes in the Great Salt Lake, Utah: Jour. Geol., v. 70, p. 246-252.

Christiansen, E. A., 1971, Geology of the Crater Lake collapse structure in southeastern Saskatchewan: Can. J. Earth Sci., v. 8, p. 1505-1513.

Cody, R. D., and Hull, A. B., 1980, Experimental growth of primary anhydrite at low temperatures and water salinities: Geology, v. 8, p. 505-509.

Cooper, J.B., and Glanzman, V.M., 1971, Geohydrology of Project Gnome site, Eddy County, New Mexico: U.S. Geol. Survey Prof. Paper 712-A, 24 p.

Cornell, 1984, Pers. Comm. to Dennis Powers.

Cys, J.M., 1978, Transitional nature and significance of the Castile-Bell Canyon contact: New Mex. Bur. Mines and Min. Res., Circ 159, p. 53-56.

Davies, P. B., 1983, Structural characteristics of a deep-seated dissolution-subsidence chimney in bedded salt: Sixth Int. Symp. on Salt, v. I, p. 331-350.

Dean, W. E., Davies, G. R., and Anderson R. Y., 1975, Sedimentological significance of nodular and laminated anhydrite: Geology, v. 3, p. 367-372.

Demicco, R. V., 1983, Wavy and lenticular-bedded carbonate ribbon rocks of the Upper Cambrian Conochocheague Limestone, Central Appalachians: Jour. Sed. Pet., v. 53, p. 1122-1132.

DeMille, G., Shouldice, J.R., and Nelson, H.W., 1964, Collapse structures related to evaporites of the Prairie Evaporite Formation, Saskatchewan: Geol. Soc. Am. Bull, v. 75, p. 307-316.

Dilamarter, R.R., and Csallany, S.C., eds., 1977, Hydrologic Problems in Karst Regions: Western Kentucky University, Bowling Green, Kentucky, 481 p.

Donegan, B., and DeFord, R.K., 1950, Ochoa is Permian: Am. Assoc. Pet. Geol. Bull., v. 34, p. 2356-2359.

Doveton, J. H., 1986, Log Analysis of Subsurface Geology - Concepts and Computer Methods: Wiley-Interscience, New York, 273 p.

Durney, D. W., and Ramsay, J. G., 1973, Incremental strains measured by syntectonic crystal growths: in Gravity & Tectonics, eds., K. A. DeJong and R. Scholter, p. 67-96.

Eager, G. P., 1983, Core from the lower Dewey Lake, Rustler, and upper Salado Formation, Culberson County, Texas: Permian Basin Section SEPM Core Workshop #2, p. 273-283.

Elliot, C. L., 1976, An experimental detailed resistivity survey of Hills C and D, Eddy County, New Mexico: report to Sandia National Laboratories, Albuquerque, New Mexico, 13 p.

Eugster, H. P., and Hardie, L. A., 1975, Sedimentation in an ancient playa-lake complex: The Wilkins Peak Member of the Green River Formation of Wyoming: Geol. Soc. Amer. Bull., v. 86, p. 319-334.

Eugster, H. P., and Hardie, L. A., 1978, Saline Lakes: in Lerman, A., ed., Lakes - Chemistry, Geology, Physics, Springer-Verlag, New York, p. 237-293.

Ferrall, C. C., and Gibbons, J. F., 1980, Core study of the Rustler Formation over the WIPP site: SAND79-7110, Sandia National Laboratories, Albuquerque, New Mexico, 87185, 81 p.

Fracasso, M. A., and Hovorka, S. D., 1986, Cyclicity in the Middle Permian San Andres Formation, Palo Duro Basin, Texas panhandle: Texas Bur. of Econ. Geol., Report of Investigations no. 156, 48 p.

Fracasso, M.A., and Kolker, A., 1985, Later Permian volcanic ash beds in the Quartermaster-Dewey Lake Formations, Texas Panhandle: Bull. West Texas Geol. Soc., v. 24, no. 6, p. 5-10.

Friedman, G. M., Amiel, A. J., Braun, M. and Miller, D. S., 1973, Generation of carbonate particles and laminites in algal mats-example from sea-marginal hypersaline pool, Gulf of Aqaba, Red Sea: Am. Assoc. Pet. Geol. Bull., v. 57, p. 541-557.

Gard, L.M., Jr., 1968, Geologic studies, Project Gnome, Eddy County, New Mexico: U.S. Geol. Survey Prof. Paper 589, 33 p.

Garrison, R. E., Schreiber, B. C., Bernoulli, D., Fabricius, F. H., Kidd, R. B., and Melieres, F., 1978, Sedimentary petrology and structures of Messinian evaporitic sediments in the Mediterranean Sea, Leg 42A, Deep Sea Drilling Project: Initial Reports of the Deep Sea Drilling Project, Volume XLII, Part 1, Washington, p. 571-611.

Gebelein, C. D., 1969, Distribution, morphology, and accretion rate of recent subtidal algal stromatolites, Bermuda: Jour. Sed. Pet., v. 39, p. 49-69.

Gendzwill, D.J., and Hajnal, Z., 1971, Seismic investigation of the Crater Lake collapse structure in southeastern Saskatchewan: Can. J. Earth Sci., v. 8, p. 1514-1524.

Gillett, S.L., 1983, A probable cave breccia in Middle Cambrian limestone, southern Nevada: Jour. Sed. Pet., v. 53, p. 221-229.

Glazek, J., Dabrowski, T., and Gradzinski, R., 1972, Karst of Poland: in Herak and Stringfield (1972), p. 327 - 340.

Goldstein, A.G., and Collins, E.W., 1984, Deformation of Permian strata overlying a zone of salt dissolution and collapse in the Texas panhandle: Geology, v. 12, p. 314-417.

Gonzalez, D. D., 1982, Fracture flow in the Ruster Formation: Waste Isolation Pilot Plant (WIPP), southeast New Mexico: SAND82-1012, Sandia National Laboratories, Albuquerque, New Mexico, 87185.

Goodwin, P.W., and Anderson, E.J., 1980, Punctuated aggradational cycles; A general hypothesis of stratigraphic accumulation: Abstr. Geol. Soc. Am., v. 12, p. 436.

Gornitz, V. M., and Schreiber, B. C., 1981, Displacive halite hoppers from the Dead Sea: some implications for ancient evaporite deposits: Jour. Sed. Pet., v. 51, p. 787-794.

Gorrell, H.A., and Alderman, G.R., 1968, Elk Point Group saline basins of Alberta, Saskatchewan, and Manitoba, Canada: in Mattox, R.B., ed., Saline Deposits, Geol. Soc. Am. Spec. Papers, no. 88, p. 291-317.

Griswold, G. B., 1977, Site selection and evaluation studies of the Waste Isolation Pilot Plant (WIPP), Los Medanos, Eddy County, New Mexico: SAND77-0946, Sandia National Laboratories, Albuquerque, New Mexico, 87185.

Gustavson, T.C., 1986, Geomorphic development of the Canadian River Valley, Texas panhandle: an example of regional salt dissolution and subsidence: Geol. Soc. Am. Bull., v. 97, p. 459-472.

Gustavson, T.C., Finley, R.J., and McGillis, K.A., 1980, Regional dissolution of Permian salt in the Anadarko, Dalhart, and Palo Duro Basins of the Texas panhandle: Texas Bur. Econ. Geol., Report of Investigations no. 106, 40 p.

Handford, C. R., 1981, Coastal sabkha and salt pan deposition of the Lower Clear Fork Formation (Permian), Texas: Jour. Sed. Pet. v. 51, p. 761-778.

Handford, C. R., 1982, Sedimentology and evaporite genesis in a Holocene continental-sabkha playa basin-Bristol Dry Lake, California: Sed., v. 29, p. 239-253.

Handford, C. R. and Fredricks, P. E., 1980, Facies patterns and depositional history of a Permian Sabkha complex: Red Cave Formation, Texas Panhandle: Texas Bur. Econ. Geol., Geol. Circ. 80-9, 38 p.

Hardie, L. A., 1968, The origin of the Recent non-marine evaporite deposit of Saline Valley, Inyo County, California: Geochimica et Cosmochimica Acta, v. 32, p. 1279-1301.

Hardie, L. A., and Eugster, H. P., 1971, The depositional environment of marine evaporites: a case for shallow, clastic accumulation: Sed., v. 16, p. 187-220.

Hardie, L. A., Smoot, J. P., and Eugster, H. P., 1978, Saline lakes and their deposits: a sedimentological approcah: Spec. Publs. Int. Assoc. Sed., v. 2, p. 7-41.

Hayes, P. T., 1964, Geology of the Guadalupe Mountains, New Mexico: U.S. Geol. Survey. Prof. Paper No. 446

Hedberg, H.D., 1976, International Stratigraphic Guide: A guide to stratigraphic classification, terminology, and procedure: John Wiley & Sons, New York, 200 p.

Herak, M., and Stringfield, V.T., eds', 1972, Karst: Important Karst Regions of the Northern Hemisphere: Elsevier, Amsterdam, 551 p.

Hills, J.M., 1963, Late Paleozoic tectonics and mountain ranges, western Texas to southern Colorado: Am. Assoc. Pet. Geol. Bull., v.47, p. 1709-1725.

Hills, J. M., 1972, Late Paleozoic sedimentation in west Texas Permian basin: Am. Assoc. Pet. Geol. Bull., v. 56, p. 2303-2322.

Hills, J. M., 1984, Sedimentation, tectonism, and hydrocarbon generation in Delaware basin, west Texas and southeastern New Mexico: Am. Assoc. Pet. Geol. Bull., v. 68, p. 250-267.

Hills, J.M., and Kottlowski, F.E., coordinators, 1983, Southwest/southwest mid-continent region: Am. Assoc. Pet. Geol., Correlation Chart Series.

Hoffman, P., 1974, Shallow and deepwater stromatolites in Lower Proterozoic Platform-to-basin facies change, Great Slave Lake, Canada: Am. Assoc. Pet. Geol. Bull., v. 58, p. 856-867.

Holt, R. M., and Powers, D. W., 1984, Geotechnical activities in the waste handling shaft: WTSD-TME-038, U.S. Dept. of Energy, Carlsbad, New Mexico.

Holt, R. M., and Powers, D. W., 1986a, Geotechnical activities in the exhaust shaft: DOE-WIPP-86-008,U.S. Dept. of Energy, Carlsbad, New Mexico.

Holt, R.M., and Powers, D.W., 1986b, Rustler Formation: evaporite end stanges of a continental basin: Abstr., 12th Int. Sed. Congress, Canberra, Australia, p. 141-142.

Holt, R.M., and Powers, D. W., 1987, The Permian Rustler Formation at the WIPP site, southeastern New Mexico: Guidebook 18, El Paso Geol. Soc., p. 140-148.

Hovorka, S. D., 1983a, Sedimentary structures and diagenetic modifications in halite and anhydrite, Palo Duro Basin: Texas Bur. Econ. Geol., Geol. Circ. 83-4, p.49-57.

Hovorka, S. D., 1983b, Dissolution and recrystallization fabrics in halite and interpretation of the timing of their development, Palo Duro Basin: Texas Bur. Econ. Geol., Geol. Circ. 83-4, p.58-65.

Hovorka, S. D., in press, Depositional environments of marine-dominated banded halite, Permian San Andres Formation: Sed.

Hovorka, S. D. and Granger, P. A., in press, Subsurface to surface correlation of Permian evaporites: San Andres-Blaine-Flowerpot relationships, Texas Panhandle: Midcontinent SEPM Symposium on the Permian of the Midcontinent.

Jennings, J. N., 1971, Karst: M.I.T. Press.

Johnson, K.S., 1981, Dissolution of Salt on the east flank of the Permian Basin in the southwestern U.S.A.: Jour. Hydrol., v. 54, p. 75 - 93.

Jones, C.L., 1954, The occurrence and distribution of potassium minerals in southeastern New Mexico: Guidebook to Southeastern New Mexico, New Mex. Geol. Soc., p. 107-112.

Jones, C. L., 1972, Permian basin potash deposits, southwestern United States: in Geology of saline deposits, UNESCO, Earth Sci. Ser., No. 7, p. 191-201.

Jones, C.L., Bowles, C.G., and Bell, K.G., 1960, Experimental drill hole logging in potash deposits of the Carlsbad District, New Mexico: U.S. Geol. Survey, OFR 60-84, 22 p.

Jones, C.L., Cooley, M.E., and Bachman, G.O., 1973, Salt deposits of Los Medanos area, Eddy and Lea Counties, New Mexico: U.S. Geol. Survey, OFR 4339-7, 67 p.

Jones, C. L., and Gonzales, J. L., 1980, Geologic data for borehole WIPP 19, Ch. 3: in Basic data report for drillhole WIPP-19 (Waste Isolation Pilot Plant - WIPP): SAND79-0276, Sandia National Laboratories, Albuquerque, New Mexico, 87185.

Kelley, V.C., 1971, Geology of the Pecos country, southeastern New Mexico: N.Mex Bur. Mines and Min. Res., Mem. 24, 75 p.

Kendall, A.C., 1984, Evaporites: in Facies Models, 2nd Ed., Geoscience Canada Reprint Series 1, p. 259-296.

Kendall, C. G. C., and Skipwith, P. A., 1968, Recent algal mats of a Persian Gulf lagoon: Jour. Sed. Pet., v. 38, p. 1040-1058.

Kinsman, D. J. J., 1976, Evaporites: relative humidity control of primary mineral facies: Jour. Sed. Pet., v. 46, p. 273-279.

Kirkland, D.W., and Anderson, R.Y., 1970, Microfolding in the Castile and Todilto evaporites, Texas and New Mexico: Geol. Soc. Am. Bull., v. 81, p. 3259-3282.

Kirkland, D. W., and Evans, R., 1976, Origin of limestone buttes, Gypsum Plain, Culberson County, Texas, and Eddy County, New Mexico: Am. Assoc. Pet. Geol. Bull., v. 60, p. 2005-2018.

Lambert, S. J., 1983, Dissolution of evaporites in and around the Delaware Basin, southeastern New Mexico and west Texas: SAND82-0461, Sandia National Laboratories, Albuquerque, New Mexico, 87185.

Landes, K. K., 1945, Ch. 3 - The Mackinac Breccia: in Landes and others, 1945, p. 123-153.

Landes, K.K., Ehlers, G.M., and Stanley, G.M., 1945, Geology of the Mackinac Straits region and subsurface geology of northern southern Peninsula: Pub. 44, Geol. Series 37, Geol. Survey Div., Michigan, 204 p.

Lang, W. B., 1935, Upper Permian formation of Delaware Basin of Texas and New Mexico: Am. Assoc. Pet. Geol. Bull., v. 19, p. 262-276.

Lang, W.B., 1939, Salado Formation of the Permian Basin: Am. Assoc. Pet. Geol. Bull., v. 23, p. 1569-1572.

Lang, W. B., 1942, Basal beds of Salado Formation in Fletcher potash core test near Carlsbad, New Mexico: Am. Assoc. Pet. Geol. Bull., v. 26, p. 63-79.

Lee, W. T., 1925, Erosion by solution and fill (Pecos Valley, New Mexico): U. S. Geol. Survey, Bull. 760-c, p. 107-121.

Logan, B. W., 1961, Cryptozoon and associate stomatolites from the recent, Shark Bay, Western Australia: Jour. Geol., v. 69, p. 517-533.

Logan, B. W., Rezak, R., and Ginsburg, R. N., 1964, Classification and environmental significance of algal stromatolites: Jour. Geol., v. 72, p. 68-83.

Lowenstein, T.K., 1982, Primary features in a potash evaporite deposit, the Permian Salado formation of west Texas and New Mexico, in Handford, C.R., Loucks, R.G., and Davies, G.R., eds., Depositional and diagenetic spectra of evaporites -- a core workshop: SEPM Core Workshop No. 3, Calgary, Canada, p. 276-304.

Lowenstein, T.K., 1987a, Depositional cycles in the Permian Salado Formation, southeastern New Mexico: Guidebook 18, El Paso Geol. Soc., p. 124-132.

Lowenstein, T. K., 1987b, Evaporite depositional fabrics in the deeply buried Jurassic Buckner Formation, Alabama: Jour. Sed. Pet. v. 57, p. 108-116.

Lowenstein, T. K., 1987c, Post-burial alteration of the Permian Rustler Formation evaporites, WIPP site, New Mexico: textural, stratigraphic and chemical evidence: EEG-36, DOE/AL 10752-36, Environmental Evaluation Group, 54 p.

Lowenstein, T. K., and Hardie, L. A., 1985, Criteria for the recognition of salt-pan evaporites: Sed., v. 32, p. 627-644.

Maley, V. C., and Huffington, R. M., 1953, Cenozoic fill and evaporite solution in the Delaware Basin, Texas and New Mexico: Geol. Soc. Am. Bull, v. 64, p. 539-546.

Mazzulo, S. J., 1981, Facies and burial diagenesis of a carbonate reservoir - Chapman deep (Atoka) field, Delaware County, Texas: Am. Assoc. Pet. Geol. Bull., v. 65, p. 850-865.

McGowen, J. H., Granata, G. E., and Seni, S. J., 1983, Depositional setting of the Triassic Dockum Group, Texas Panhandle and Eastern New Mexico: in Mesozoic Paleogeography of West Central United States, eds., M. W. Reynolds and D. Dolly, Rocky Mountain Section S.E.P.M., p. 13-38.

McGillis, K. A. and Presley, M. W., 1981, Tansill, Salado, and Alibates Formations: Upper Permian Evaporite/Carbonate Strata of the Texas Panhandle, Texas Bur. Econ. Geol., Circ. 81-8.

McKnight, E.T., and Fischer, R.P., 1970, Geology and ore deposits of the Picher Field, Oklahoma and Kansas: U.S. Geol. Survey Prof. Paper 588, 165 p. + plates.

Mercer, J. W., 1983, Geohydrology of the proposed Waste Isolation Pilot Plant site, Los Medanos area, southeastern New Mexico: U.S. Geol. Surv., Water Resources Inv. Report 83-4016.

Mercer, J.W., 1986, Compilation of hydrologic data from drilling the Salado and Castile Formations near the WIPP site, southeastern New Mexico: SAND86-0954, Sandia National Laboratories, Albuquerque, NM 87185.

Mercer, J.W., and Orr, B.R., 1979, Interim data report on the geohydrology of the proposed Waste Isolation Pilot Plant site, southeast New Mexico: U.S. Geol. Survey Water Resources Investigations 79-98, 178 p.

Middleton, G.V., 1961, Evaporite solution breccias from the Mississippian of southwest Montana: Jour. Sed. Pet., v. 31, p. 189-195.

Miller, D.N., 1955, Hollow sanidine grains, a stratigraphic marker for the Pierce Canyon Formation, west Texas and southeast New Mexico: Jour. Sed. Pet., v. 25, p. 235-237.

Miller, D.N., 1957, Authigenic biotite in spheroidal reduction spots, Pierce Canyon Redbeds, Texas and New Mexico: Jour. Sed. Pet., v. 27, p. 177-180.

Miller, D. N., 1966, Petrology of Pierce Canyon Redbeds, Delaware Basin, Texas and New Mexico: Am. Assoc. Petrol. Geol. Bull., v. 80, p. 283-307.

Myer, J., 1987, Pers. Com. to Robert Holt.

NAS, 1957, Disposal of radioactive wastes on land: National Academy of Sciences - National Research Council, Washington, D. C., Publ. 519.

Neal, J. T., Langer, A. M., and Kerr, P. F., 1968, Giant desiccation polygons of Great Basin playas: Geol. Soc. Amer. Bull., v. 79, p. 69-90.

Neumann, A. C., Gebelein, C. D., and Scoffin, T. P., 1970, The composition, structure and erodability of subtidal mats, Abaco, Bahamas: Jour. Sed. Pet., v. 40, p. 274-297.

Nicholson, A., Jr., and Clebsch, A., Jr., 1961, Geology and ground-water conditions in southern Lea County, New Mexico: N. Mex. Bur. Mines and Min. Res. Ground-water Report 6, 120 p.

Ohle, E.L., 1985, Breccias in Mississippi Valley-type deposits: Econ. Geol., v. 80, p. 1736-1752.

Olive, W.W., 1957, Solution-subsidence troughs, Castile Formation of Gypsum Plain, Texas and New Mexico: Geol. Soc. Am. Bull., v. 68, p. 351-358.

Oriel, S. S., Myers, D. A., and Crosby, E. J., 1967, West Texas Permian Basin region, in Paleotectonic investigations of the Permian System in the United States: U.S. Geol. Surv. Prof. Paper 515, p. 21-60.

Page, L.R., and Adams, J.E., 1940, Stratigraphy, Eastern Midland Basin, Texas: Am. Assoc. Pet. Geol. Bull., v. 24, p. 52-64.

Palmer, A.R., and Halley, R.B., 1979, Physical stratigraphy and trilobite biostratigraphy of the Carrara Formation (Lower and Middle Cambrian) in the southern Great Basin: U.S. Geol. Survey Prof. Paper 1047.

Parker, J. M., 1967, Salt solution and subsidence structures, Wyoming, North Dakota, and Montana: Am. Assoc. Pet. Geol. Bull, v. 51, p. 1929-1947.

Peryt, T. M., and Piatkowski, T. S., 1977, Stromatolites from the Zechstein Limestone (Upper Permian) of Poland: in Fossil Algae, Recent Results and Developments, ed., E. Flugel, International Symposium on Fossil Algae, p. 124-135.

Pfeiffer, D., and Hahn, J., 1972, Karst of Germany: in Herak and Stringfield (1972), p. 189 - 224.

Playford, P. E., and Cockbain, A. E., 1969, Algal stromatolites: Deepwater forms in the Devonian of Western Australia: Science, v. 165, p. 1008-1010.

Powers, D. 1986, Interpretation of geophysical logs to select stratigraphic horizons within the Rustler Formation: App. D, in Winstanley, D. J., and Carrasco, R. C., Annual Hydrogeologic data report: 1985/1986: DOE-WIPP86-004, Dept. of Energy, Carlsbad, NM.

Powers, D.W., and Holt, R.M., 1984, Depositional environments and dissolution in the Rustler Formation (Permian), southeastern New Mexico: Abstr. Geol. Soc. Am., v. 16, no. 6, p. 627.

Powers, D.W., and Hassinger, B.W., 1985, Synsedimentary dissolution pits in halite of the Permian Salado Formation, southeastern New Mexico: Jour. Sed. Pet., v. 55, p. 769-773.

Powers, D. W., Holt, R. M., and Hoffer, J. M., 1987, Preliminary studies of near-surface sediments, Salt Flat graben, west Texas: Guidebook 18, El Paso Geol. Soc., p. 194-194.

Powers, D.W., Lambert, S.J., Shaffer, S., Hill, L.R., and Weart, W.D., eds., 1978, Geological characterization report, Waste Isolation Pilot Plant (WIPP) site, southeastern New Mexico: SAND78-1596, Vols. I and II, Sandia National Laboratories, Albuquerque, N.M., 87185, about 1500 p.

Presley, M. W., and McGillis, K. A., 1982, Coastal evaporite and tidal-flat sediments of the Upper Clear Fork and Glorieta Formations, Texas panhandle: Texas Bur. of Econ. Geol., Report of Investigations 115, 50 p.

Reineck, H. E., and Singh, I. B., 1980, Depositional sedimentary environments: Springer-Verlag, New York-Heidelberg-Berlin, 549 p.

Richardson, G. B., 1904, Report of a reconnaisance in Trans-Pecos Texas north of the Texas and Pacific Railway: Univ. Texas Bull. 23.

Roberts, A.E., 1966, Stratigraphy of the Madison Group near Livingston, Montana, and discussion of karst and solution-breccia features: U.S. Geol. Survey Prof. Paper 526-B, 23 p.

Robinson, J.Q., and Powers, D.W., 1987, A clastic deposit within the lower Castile Formation, western Delaware Basin, New Mexico: Guidebook 18, El Paso Geol. Soc., p. 69-79.

Rogers, R.K., and Davis, J.H., 1977, Geology of the Buick mine, Viburnum Trend, southeast Missouri: Econ. Geol., v. 72, p. 372-280.

Ross, C.A., 1986, Paleozoic evolution of southern margin of Permian basin: Geol. Soc. Am. Bull., v.97, p. 536 - 554.

Sandia National Laboratories and U.S. Geological Survey, 1980, Basic data report for drillhole WIPP 33: SAND80-2011, Sandia National Laboratories, Albuquerque, N.M., 87185, 27 p.

Sando, W.J., 1974, Ancient solution phenomena in the Madison Limestone (mississippian) of north-central Wyoming: Jour. Res., U.S. Geol. Survey, v. 2, p. 133 - 141.

Sares, S.W., and Wells, S.G., 1987 Geomorphic and hydrogeologic development of the gypsum plain karst, Delaware Basin, New Mexico: Guidebook 18, El Paso Geol. Soc., p. 98-117.

Sawkins, F. J., 1969, Chemical brecciation, an unrecognized mechanism for breccia formation?: Econ. Geol., v. 64, p. 613-617.

Schiel, K.A., 1987, Investigations of the Dewey Lake Formation, Delaware Basin, New Mexico: Guidebook 18, El Paso Geol. Soc., p. 149-156.

Schmalz, R.F., 1969, Deep-water evaporite deposition: a genetic model: Am. Assoc. Pet. Geol. Bull., v. 53, p. 798-823.

Schreiber, B. C., 1978, Environments of subaqueous gypsum deposition: in Marine Evaporites, SEPM Short Course notes no. 4, p. 43-73.

Schreiber, B.C., and Schreiber, E., 1977, The salt that was: Geology, v. 5, p. 527-528.

Severson, J.L., 1952, A comparison of the Madison Group (Mississippian) with its subsurface equivalents in central Montana: unpub. Ph.D. diss., Univ. of Wisconsin, Madison.

Shearman, D. J., 1970, Recent halite rock, Baja California, Mexico: Inst. Mining Met., Trans., v. 79. p. 155-162.

Shearman, D. J., 1978, Evaporites of coastal sabkhas: in Marine Evaporites, SEPM Short Course no. 4, p. 6-42.

Smith, A. R., 1978, Sulfer deposits in Ochoan Rocks of southeastern New Mexico and west Texas: New Mex. Bur. Mines and Min. Res., Circ 159, p. 71-77.

Smith, D. B., 1971, Possible displacive halite in the Permian Upper Evaporite Group of northeast Yorkshire: Sed., v. 17, p. 221-232.

Smith, D. B., 1972, Foundered strata, collapse-breccias and subsidence features of the English Zechstein: in Geology of saline deposits, UNESCO, Earth Sci. Ser., no. 7, p. 255-269.

Smith, N.M., Sunderman, J.A., and Melhorn, W.N., 1961, Breccia and Pennsylvanian cave filling in Mississippian St. Louis Limestone, Putnam County, Indiana: Jour. Sed. Pet., v. 31, p. 275-287.

Snyder, R.P., 1985, Dissolution of halite and gypsum, and hydration of anhydrite to gypsum, Rustler Formation, in the vicinity of the Waste Isolation Pilot Plant, southeastern New Mexico: U. S. Geol. Survey OFR Report 85-229, 11 p.

Snyder, R. P., and Gard, L. M., Jr., 1982, Evaluation of breccia pipes in southeastern New Mexico and their relation to the Waste Isolation Pilot Plant (WIPP) site: U. S. Geol. Survey OFR 82-968, 73 p.

Snyder, F.G., and Odell, J.W., 1958, Sedimentary breccias in the southeast Missouri lead district: Geol. Soc. Am. Bull., v. 69, p. 899-926.

Southgate, P. N., 1982, Cambrian skeletal halite crystals and experimental analogues: Sed., v. 29, p. 391-407.

Stanton, R. J., Jr., 1966, The solution brecciation process: Geol. Soc. Am. Bull., v. 77, p. 843-848.

Sweeting, M. M., 1972, Karst Landforms: MacMillan, London.

Till, R., 1978, Arid shorelines and evaporites: in Sedimentary Environments and Facies, ed. by Reading, H. G., p. 178-206.

Toomey, D. F., 1985, Dasyclad Algae within Permain (Leonard) cyclic shelf carbonates ("Abo"), Northern Midland Basin, West Texas: in Paleoalgology, Contemporary Research and Applications, eds., D. F. Toomey and M. H. Nitecki, p. 315-329.

Tucker, R. M., 1981, Giant polygons in the Triassic salt of Cheshire, England: a thermal contraction model for their origin: Jour. Sed. Pet., v. 51, p. 779-786.

Udden, J.A., 1924, Laminated anhydrite in Texas: Geol. Soc. Am. Bull, v. 35, p. 347-354.

Vai, G. B., and Ricci Lucchi, F., 1977, Algal crusts, autochthonous and clastic gypsum in a cannibalistic evaporite basin: a case history from the Messinian of Northern Apennines: Sed., v. 24, p. 211-244.

Valyashko, M. G., 1972, Playa lakes-a necessary stage in the development of a salt-bearing basin: in Geology of saline deposits, UNESCO, Earth Sci. Ser., no. 7, p. 41-51.

Vaughn, F.R., 1978, The origin and diagenesis of the Arroyo Penasco collapse breccia: unpub. M.S. thesis, SUNY Stony Brook, 70 p.

Vine, J. D., 1963, Surface geology of the Nash Draw Quadrangle, Eddy County, New Mexico: U.S. Geol. Surv. Bull. 1141-B.

Walter, J. C., Jr., 1953, Paleontology of the Rustler Formation, Culberson County, Texas: Jour. Paleontology, v. 27, p. 679-702.

Walters, R.F., 1977, Land subsidence in central Kansas related to salt dissolution: Kans. State Geol. Surv. Bull. 214, 82 p.

Wardlaw, N. C. and Schwerdter, W. M., 1966, Halite-anhydrite seasonal layers in the middle Devonian Prarie Evaporite Formation, Saskatchewan, Canada: Geol. Soc. Am. Bull., V. 7, 331-342.

Warren, J. K., 1982a, The hydrological significance of Holocene tepees, stromatolites, and boxwork limestones in coastal salinas in South Australia: Jour. Sed. Pet., v. 52, p. 1171-1201.

Warren, J. K., 1982b, The hydrological setting, occurrence and significance of gypsum in late Quaternary salt lakes in South Australia: Sed., v. 29, p. 609-630.

Wenrich, K.J., 1985, Mineralization of breccia pipes in northern Arizona: Econ. Geol., v. 80, p. 1722-1735.

Valyashko, M. G., 1972, Playa lakes-a necessary stage in the development of a salt-bearing basin: in Geology of saline deposits, UNESCO, Earth Sci. Ser., no. 7, p. 41-51.

Vaughn, F.R., 1978, The origin and diagenesis of the Arroyo Penasco collapse breccia: unpub. M.S. thesis, SUNY Stony Brook, 70 p.

Vine, J. D., 1963, Surface geology of the Nash Draw Quadrangle, Eddy County, New Mexico: U.S. Geol. Surv. Bull. 1141-B.

Walter, J. C., Jr., 1953, Paleontology of the Rustler Formation, Culberson County, Texas: Jour. Paleontology, v. 27, p. 679-702.

Walters, R.F., 1977, Land subsidence in central Kansas related to salt dissolution: Kans. State Geol. Surv. Bull. 214, 82 p.

Wardlaw, N. C. and Schwerdter, W. M., 1966, Halite-anhydrite seasonal layers in the middle Devonian Prarie Evaporite Formation, Saskatchewan, Canada: Geol. Soc. Am. Bull., V. 7, 331-342.

Warren, J. K., 1982a, The hydrological significance of Holocene tepees, stromatolites, and boxwork limestones in coastal salinas in South Australia: Jour. Sed. Pet., v. 52, p. 1171-1201.

Warren, J. K., 1982b, The hydrological setting, occurrence and significance of gypsum in late Quaternary salt lakes in South Australia: Sed., v. 29, p. 609-630.

Wenrich, K.J., 1985, Mineralization of breccia pipes in northern Arizona: Econ. Geol., v. 80, p. 1722-1735.

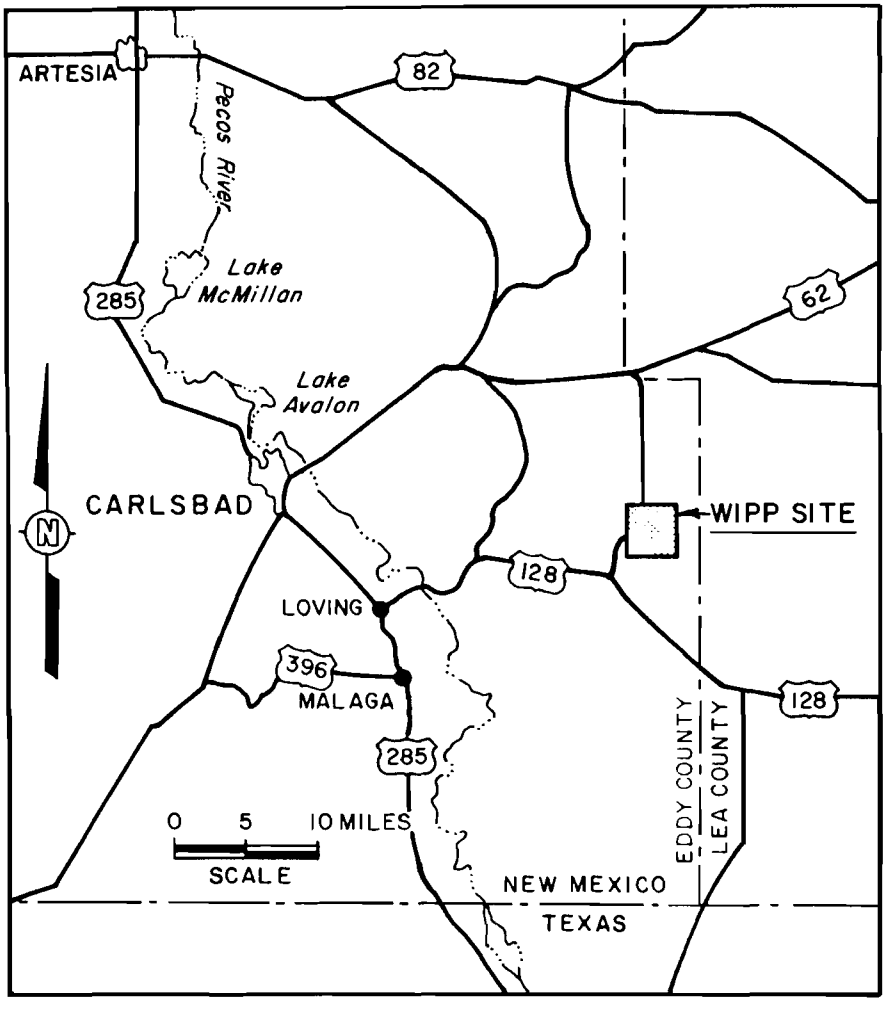

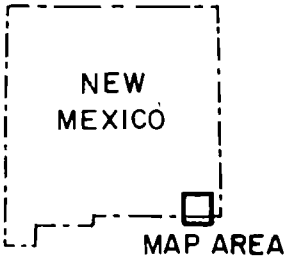

LOCATION MAP

FIGURE 1.1

GENERAL LOCATION
OF THE WIPP SITE

PREPARED FOR

WESTINGHOUSE ELECTRIC CORPORATION
CARLSBAD, NEW MEXICO

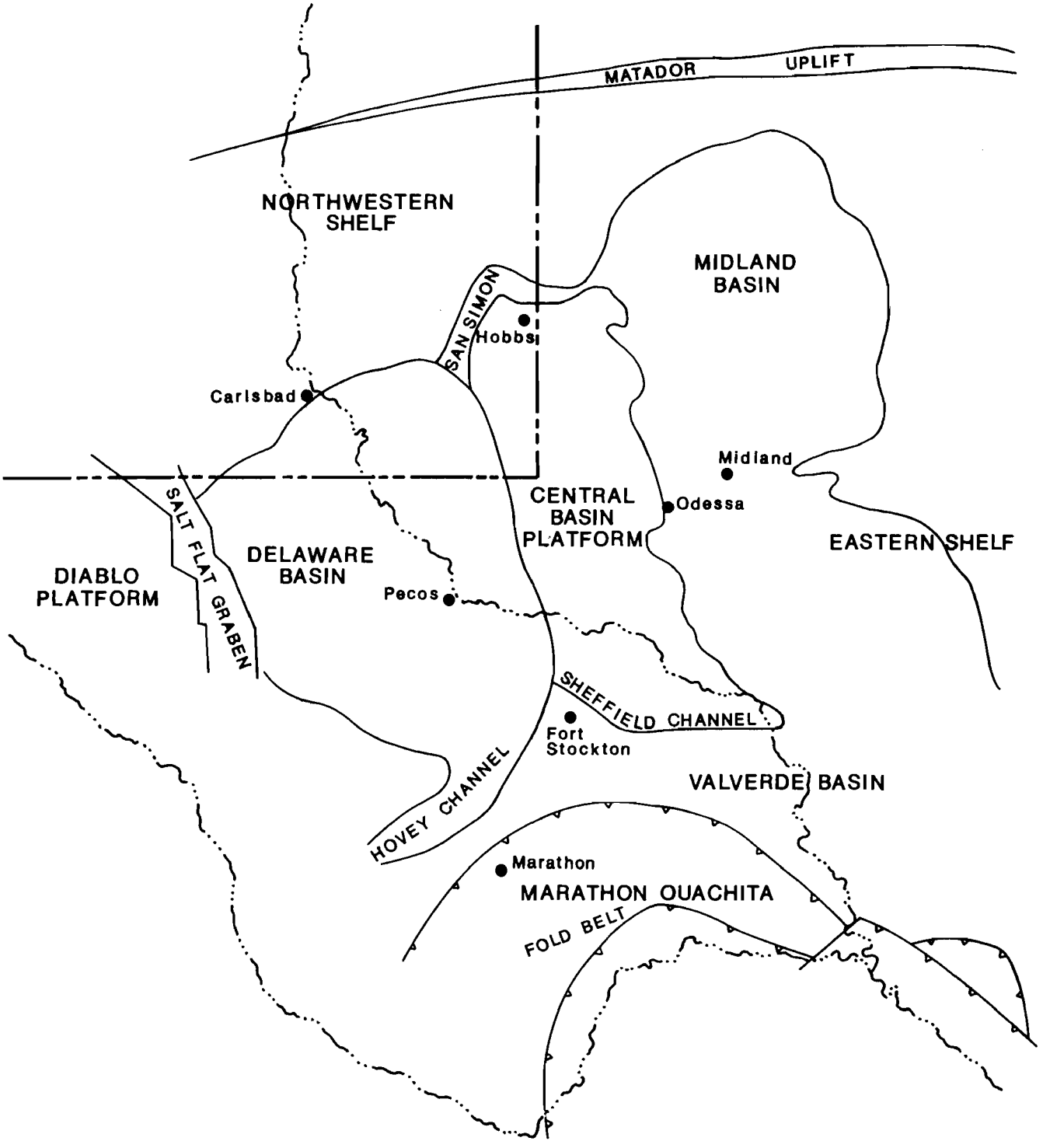

FIGURE 1.2

STRUCTURAL PROVINCES OF
THE PERMIAN BASIN REGION
(After Hills, 1984)

PREPARED FOR

WESTINGHOUSE ELECTRIC CORPORATION
CARLSBAD, NEW MEXICO

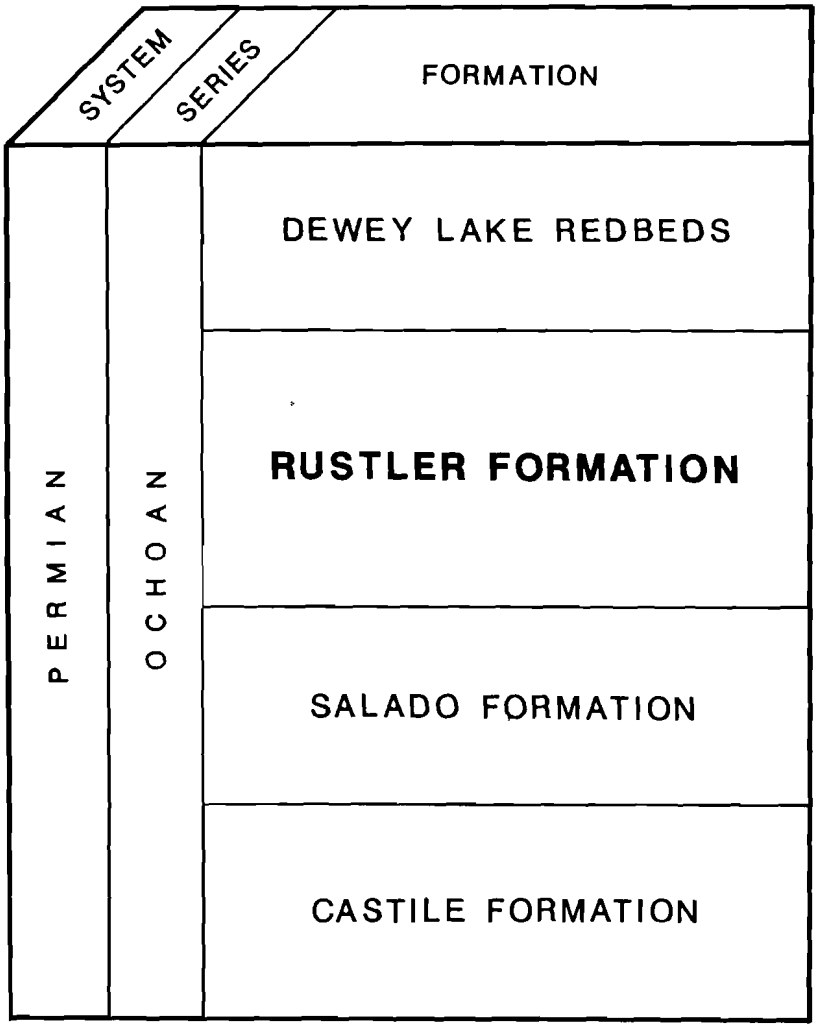

FIGURE 3.1

OCHOAN SERIES IN THE
DELAWARE BASIN

PREPARED FOR

WESTINGHOUSE ELECTRIC CORPORATION
CARLSBAD, NEW MEXICO

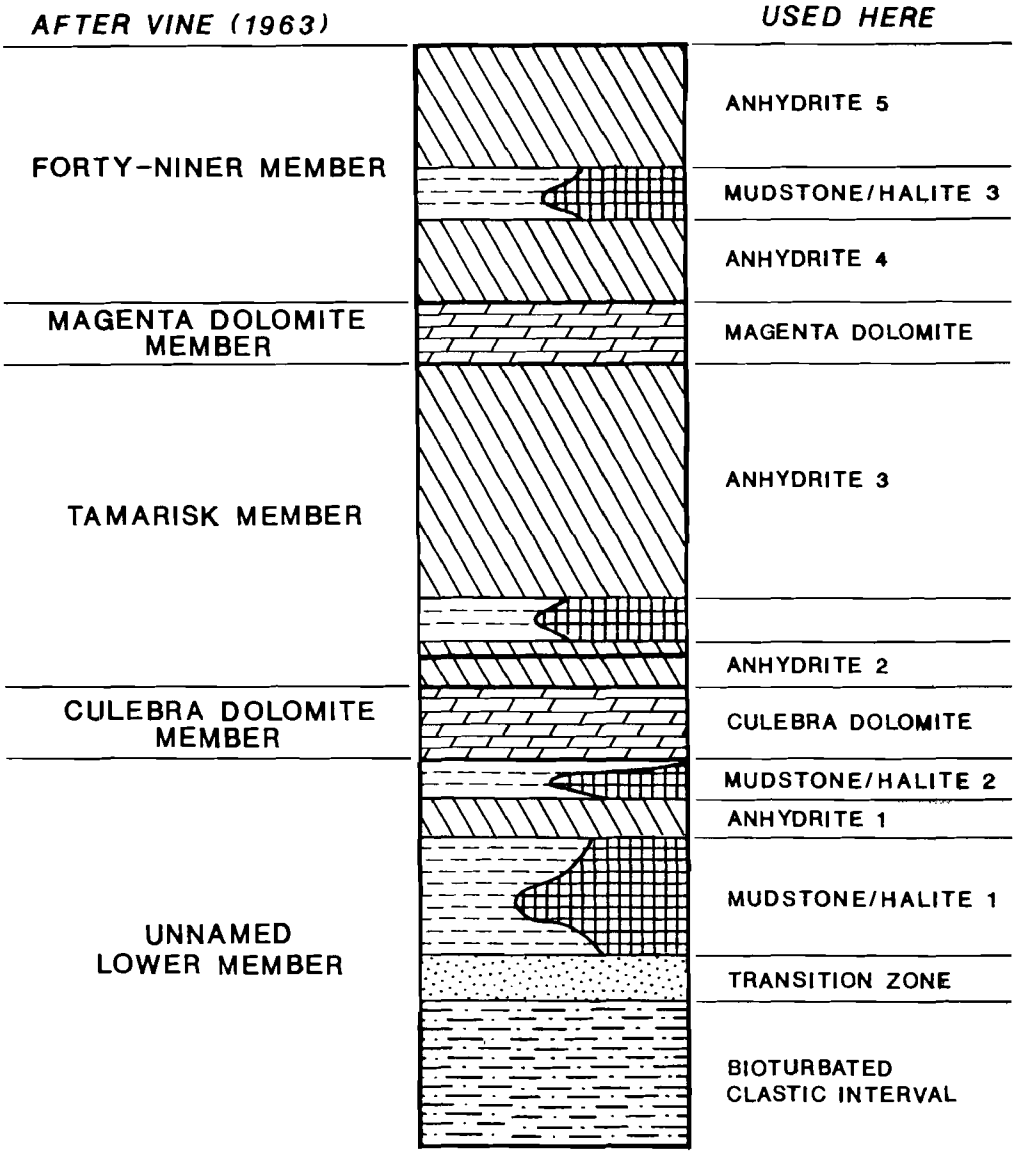

FIGURE 3.2

RUSTLER STRATIGRAPHY

PREPARED FOR

WESTINGHOUSE ELECTRIC CORPORATION
CARLSBAD, NEW MEXICO

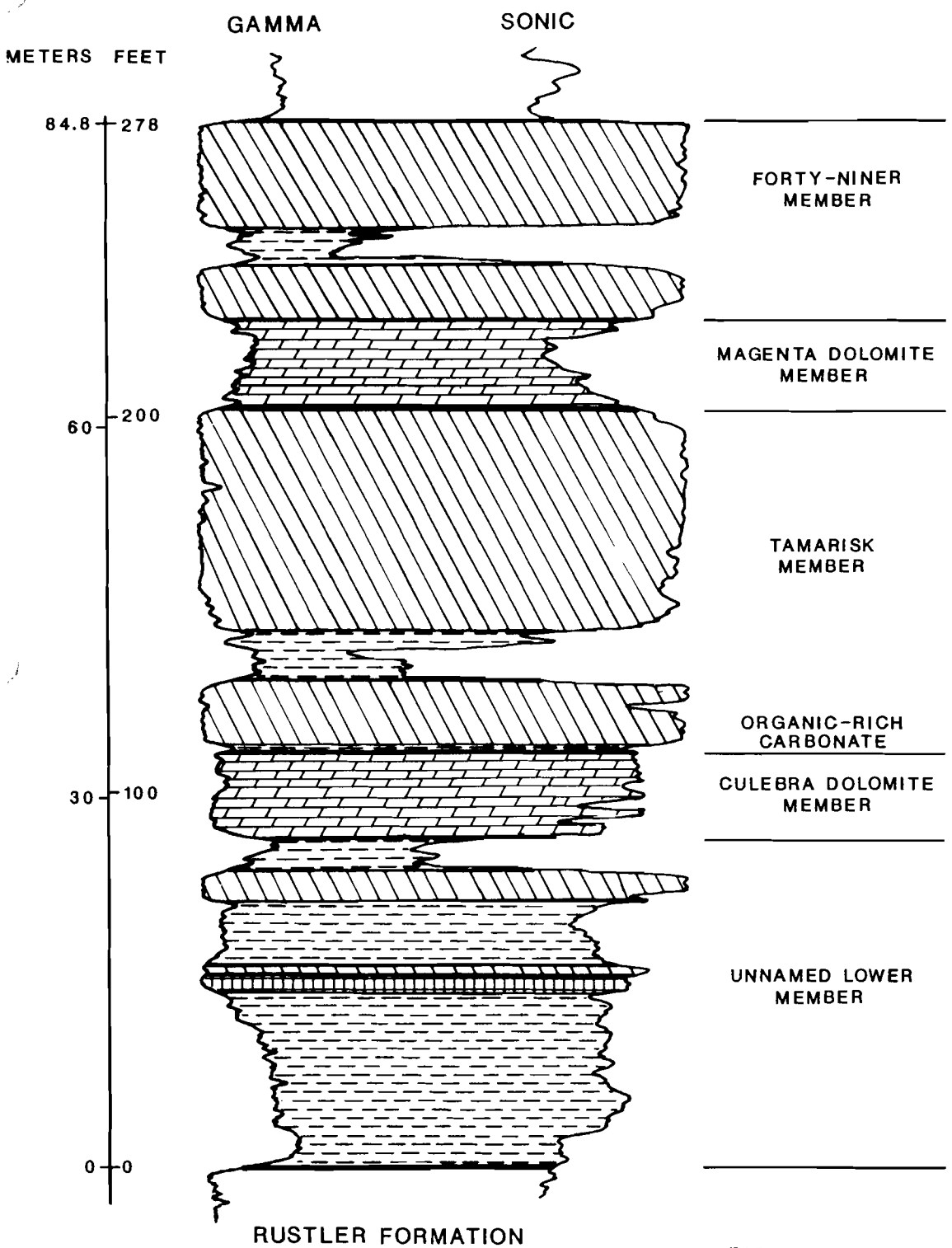

FIGURE 4.1

GENERAL GEOPHYSICAL AND
LITHOLOGIC CHARACTER OF THE RUSTLER

PREPARED FOR

WESTINGHOUSE ELECTRIC CORPORATION
CARLSBAD, NEW MEXICO

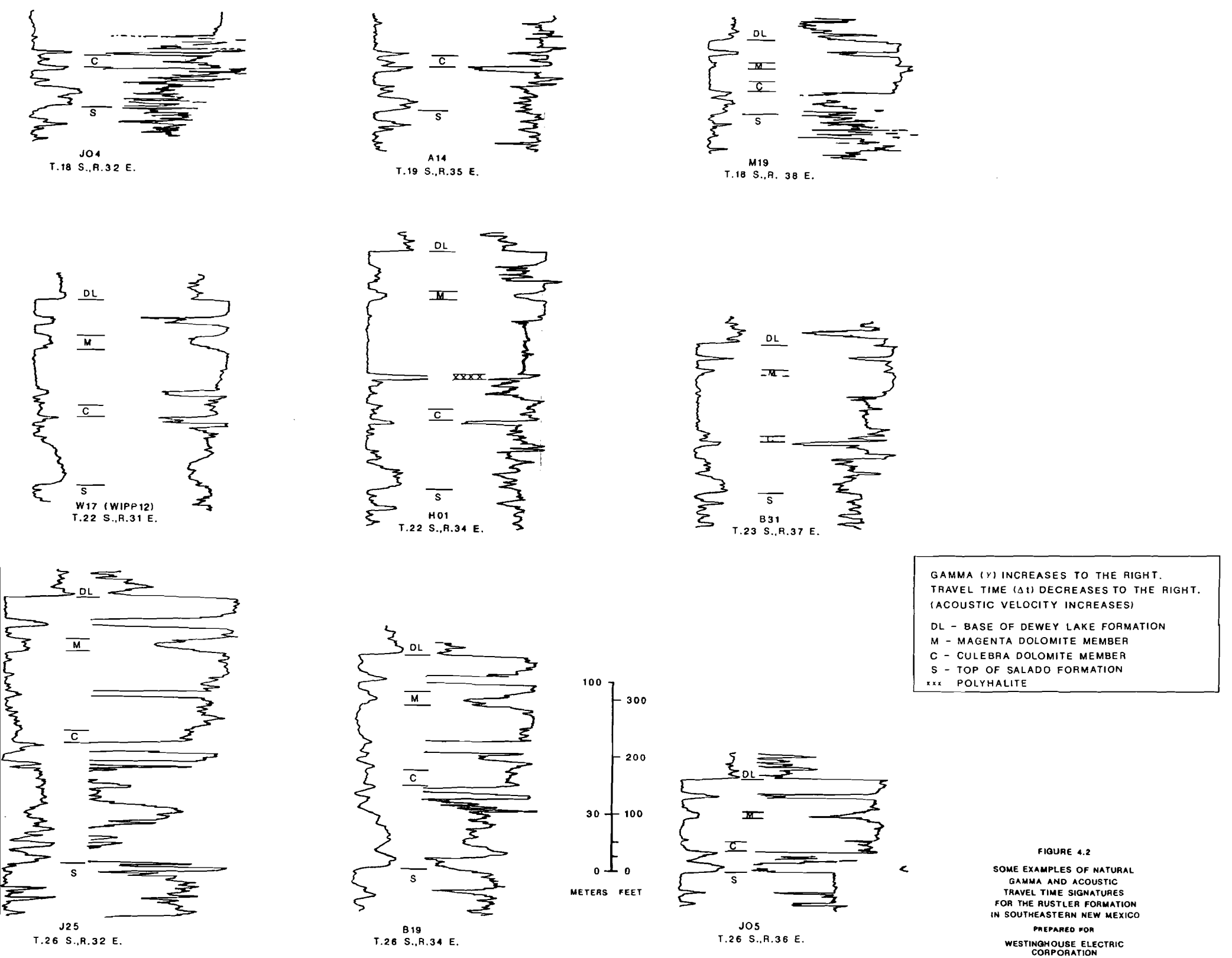

FIGURE 4.2

SOME EXAMPLES OF NATURAL GAMMA AND ACOUSTIC TRAVEL TIME SIGNATURES FOR THE RUSTLER FORMATION IN SOUTHEASTERN NEW MEXICO

PREPARED FOR

WESTINGHOUSE ELECTRIC CORPORATION

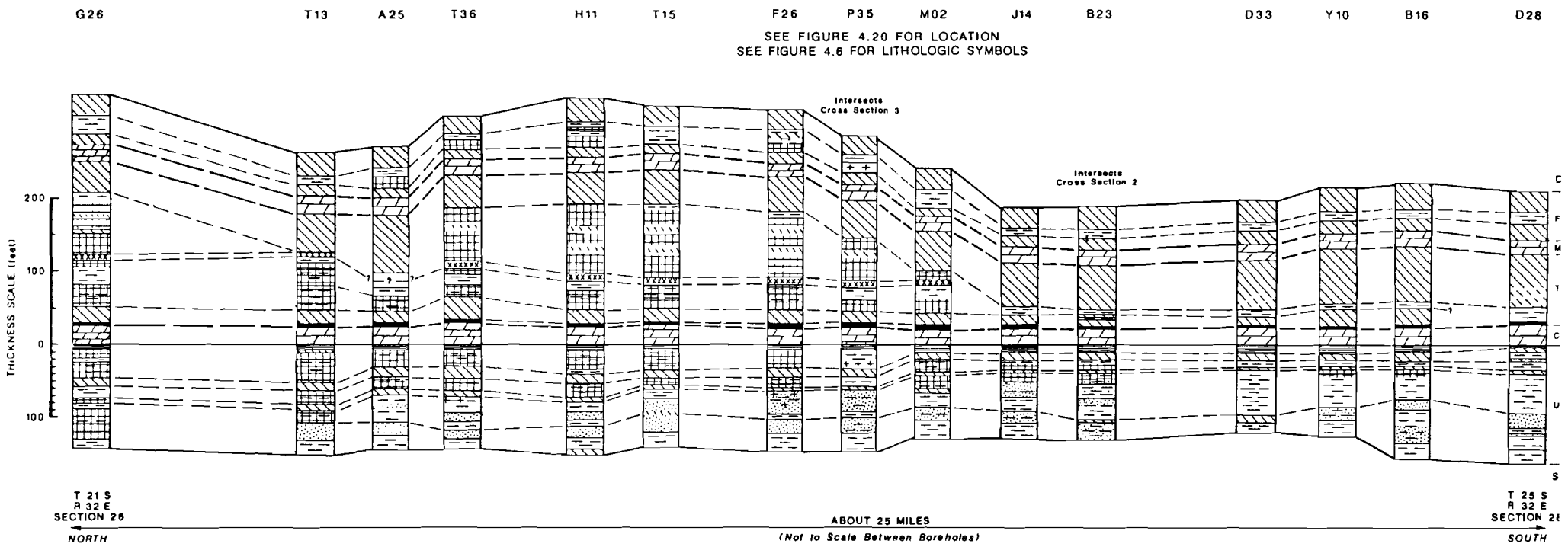
G26
T13
A25
T36
H11
T15
F26
P35
M02
J14
B23
D33
Y10
B16
D28
SEE FIGURE 4.20 FOR LOCATION
SEE FIGURE 4.6 FOR LITHOLOGIC SYMBOLS
Intersects Cross Section 3
Intersects Cross Section 2
THICKNESS SCALE (feet)
200
100
0
100
T 21 S
R 32 E
SECTION 26
NORTH
ABOUT 25 MILES
(Not to Scale Between Boreholes)
T 25 S
R 32 E
SOUTH

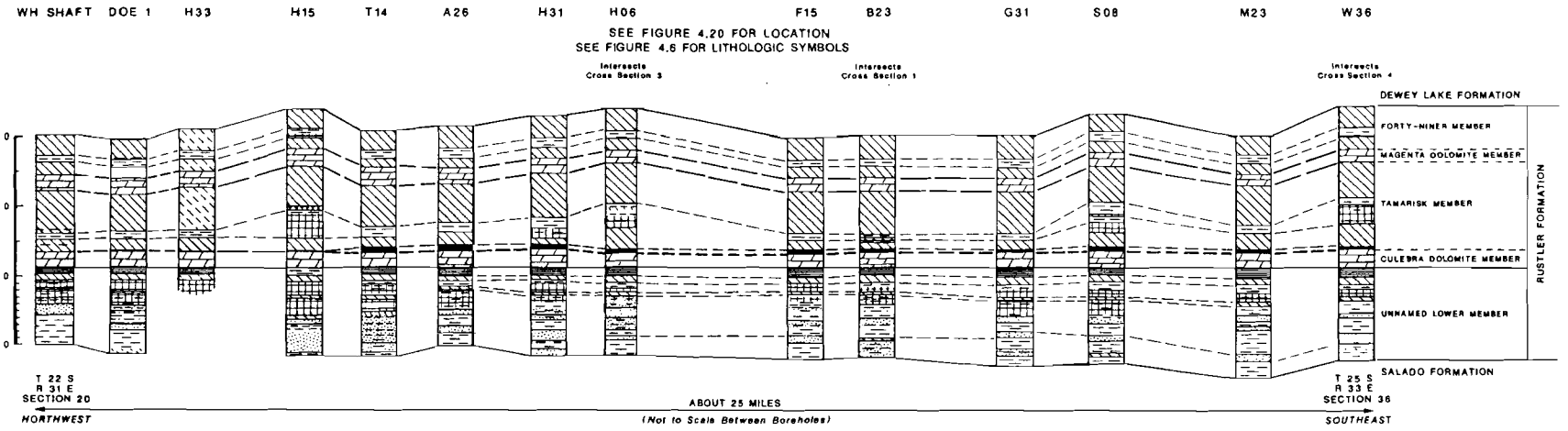

FIGURE 4.4

CROSS SECTION 2

PREPARED FOR

WESTINGHOUSE ELECTRIC CORPORATION
CARLSBAD, NEW MEXICO

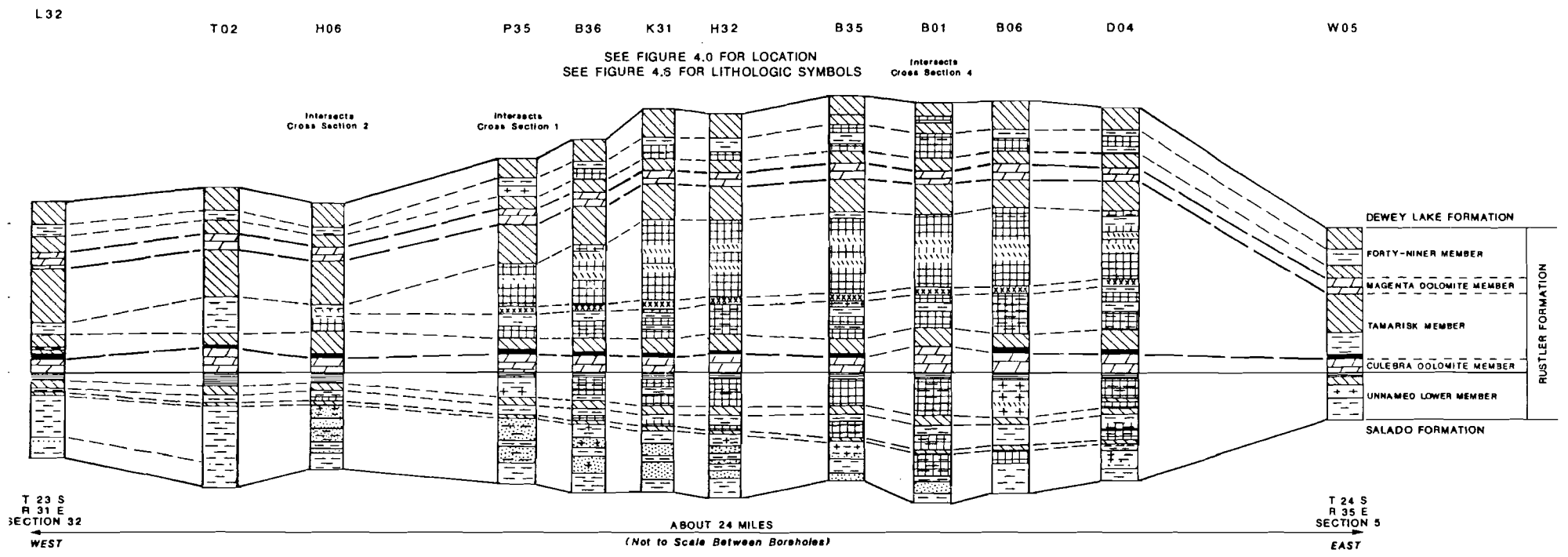

FIGURE 4.5

CROSS SECTION 3

PREPARED FOR

WESTINGHOUSE ELECTRIC CORPORATION
CARLSBAD, NEW MEXICO

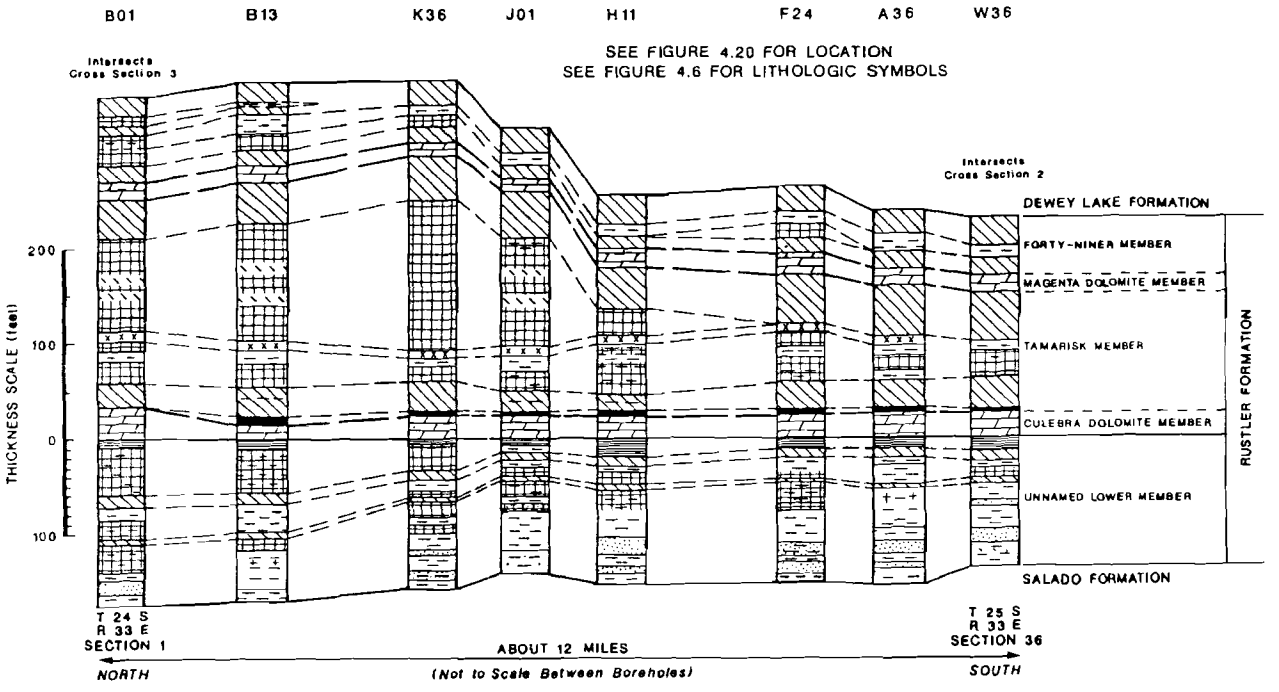

EXPLANATION

- ANHYDRITE OR GYPSUM
- GYPSUM OR GYPSIFEROUS
- POLYHALITE
- DOLOMITE
- ORGANIC-RICH ARGILLACEOUS CARBONATE
- ARGILLACEOUS MUDSTONE TO CLAYSTONE
- MUDSTONE (ARGILLACEOUS IF OVERPRINT)
- SANDY MUDSTONE TO SANDSTONE
- HALITE
- HALITIC ROCK

FIGURE 4.6

CROSS SECTION 4

PREPARED FOR

WESTINGHOUSE ELECTRIC CORPORATION
CARLSBAD, NEW MEXICO

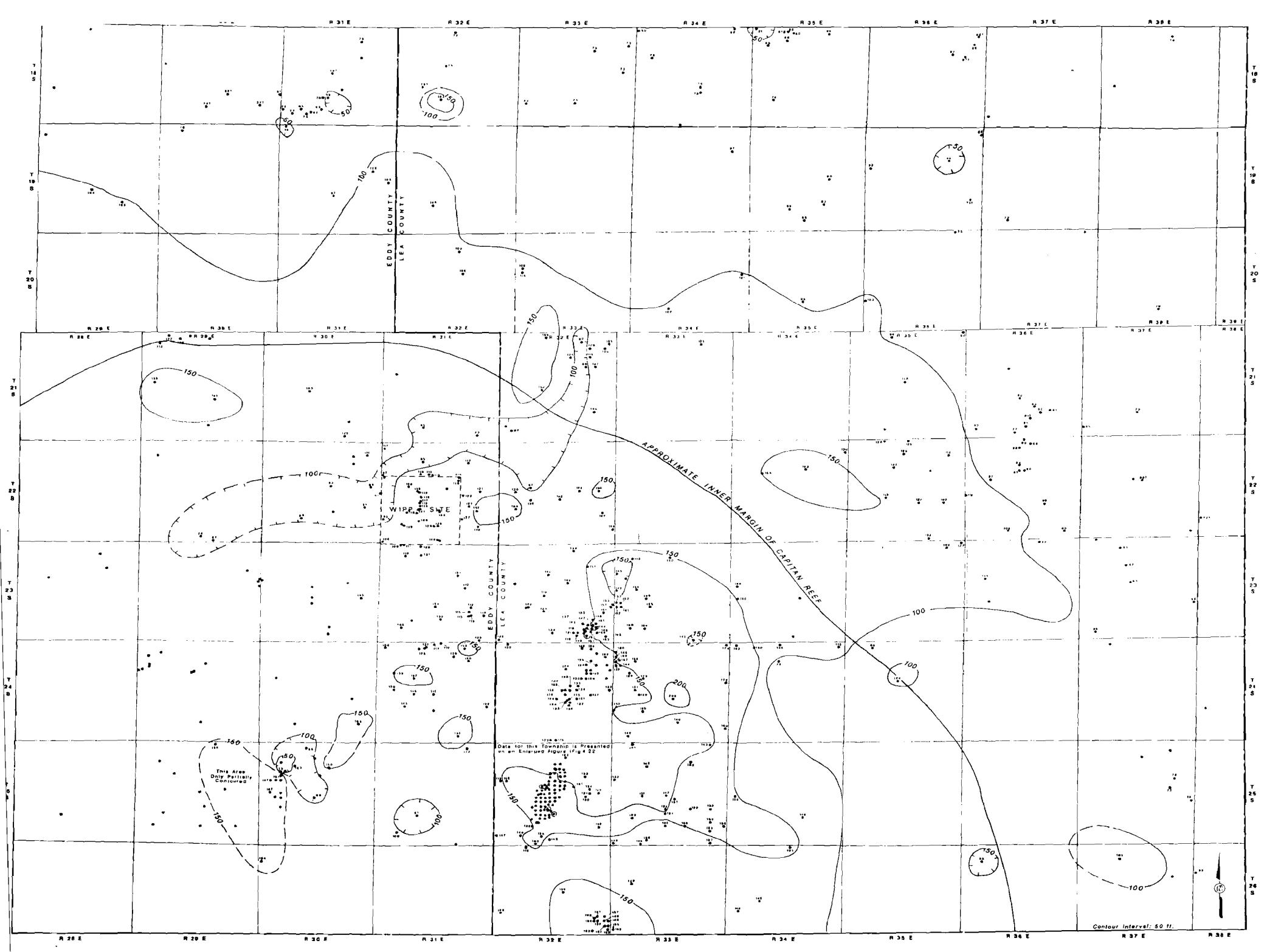
EDDY COUNTY
LEA COUNTY
WIPP SITE
APPROXIMATE INNER MARGIN OF CAPITAN REEF
This Area Only Partially Contoured
Data for this Township is Presented on an Enlarged Figure (Fig 22
Contour Interval: 50 ft.

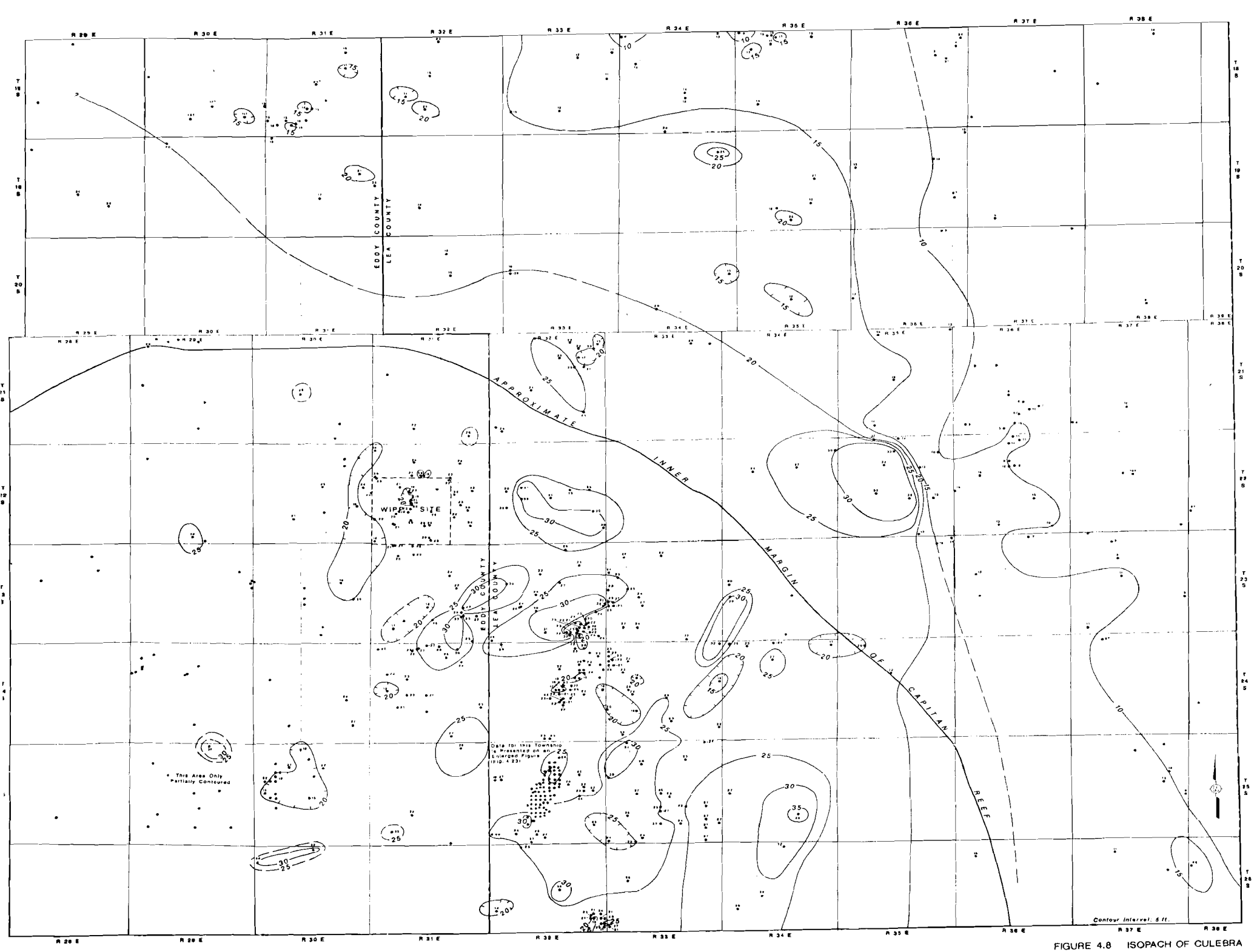

FIGURE 4.8 ISOPACH OF CULEBRA

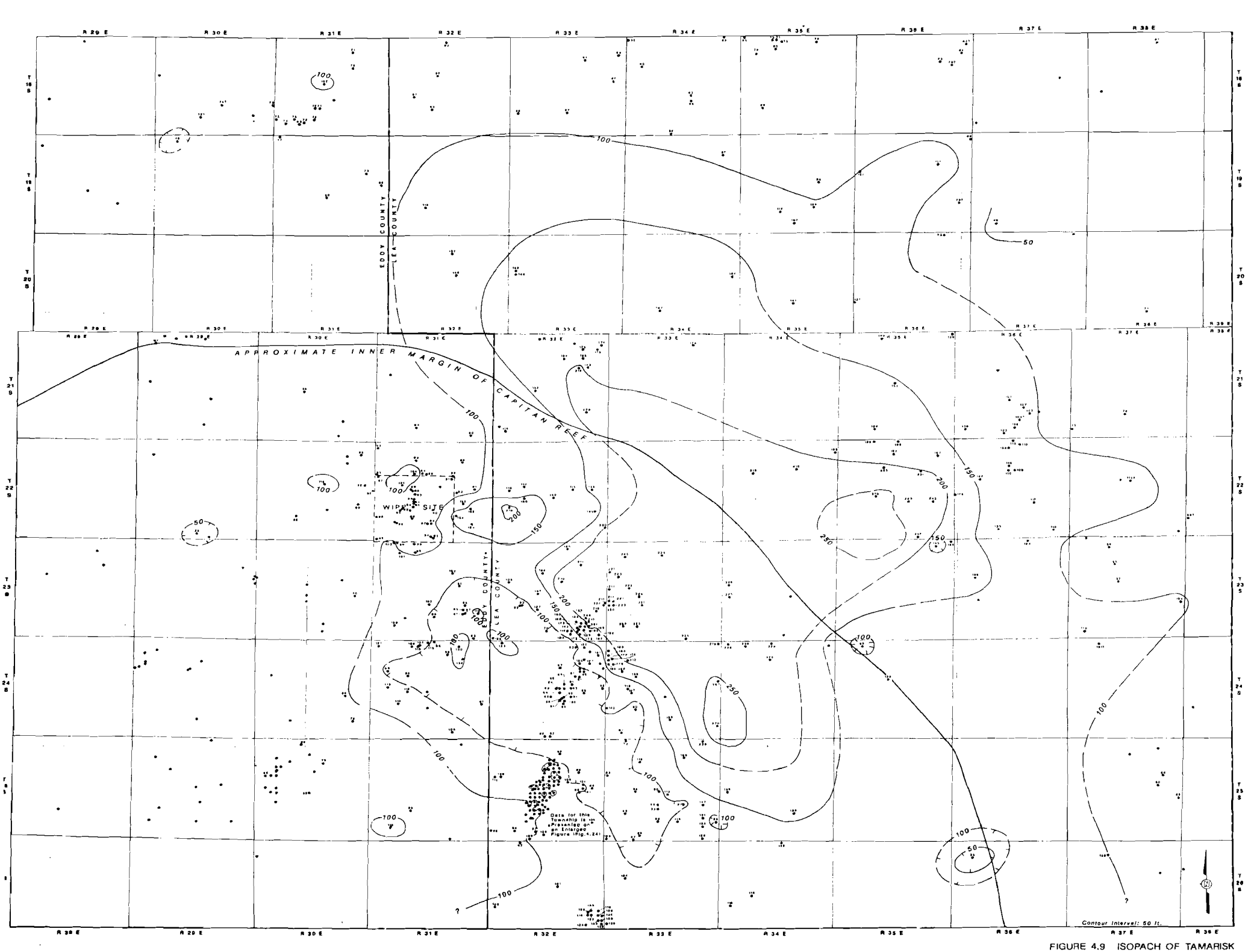

FIGURE 4.9 ISOPACH OF TAMARISK

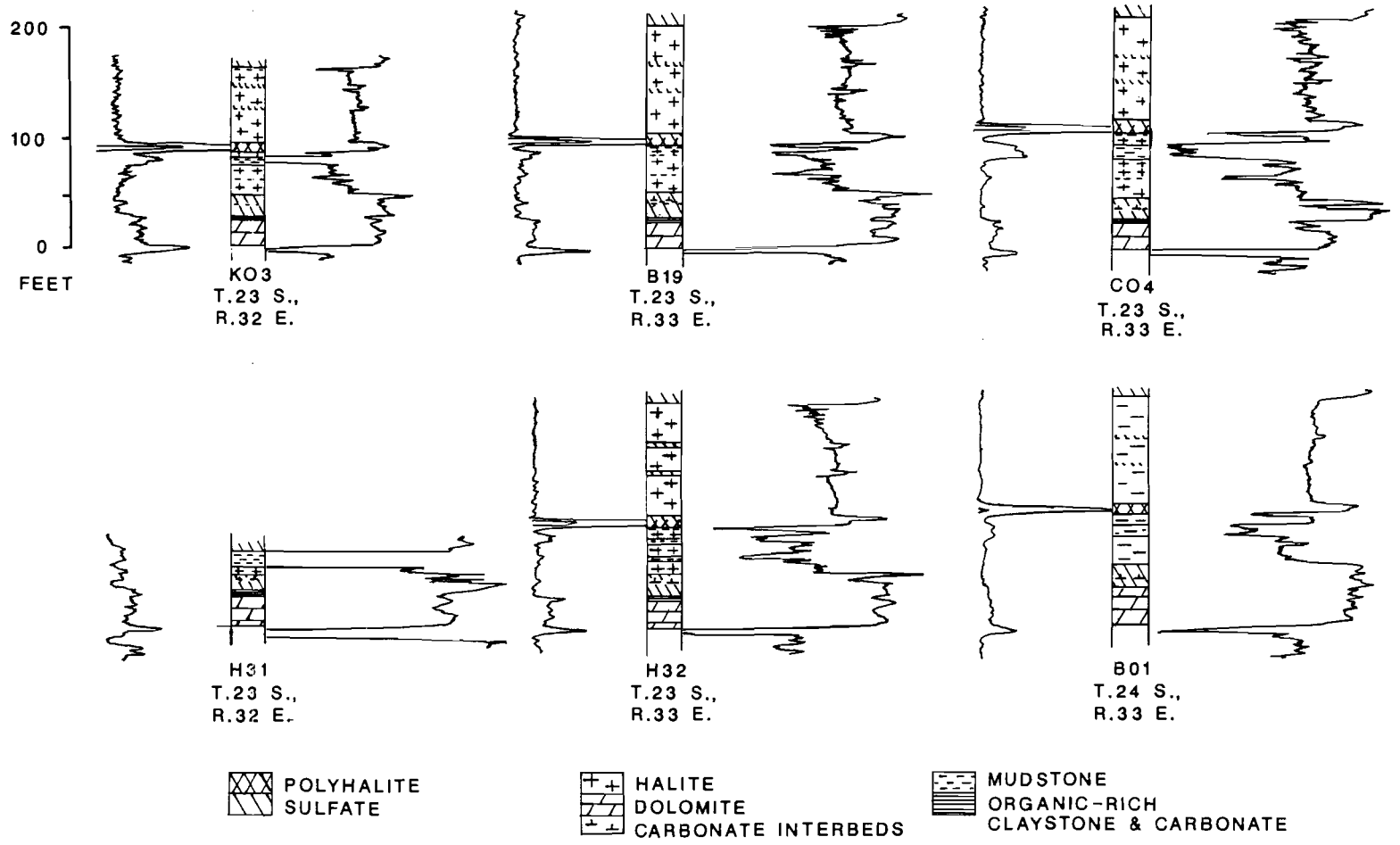

FIGURE 4.10

NATURAL GAMMA (LEFT) AND
ACOUSTIC (RIGHT) LOGS REPRESENTING
THE LOWER TAMARISK MEMBER
AND CULEBRA DOLOMITE MEMBER

PREPARED FOR

WESTINGHOUSE ELECTRIC CORPORATION
CARLSBAD, NEW MEXICO

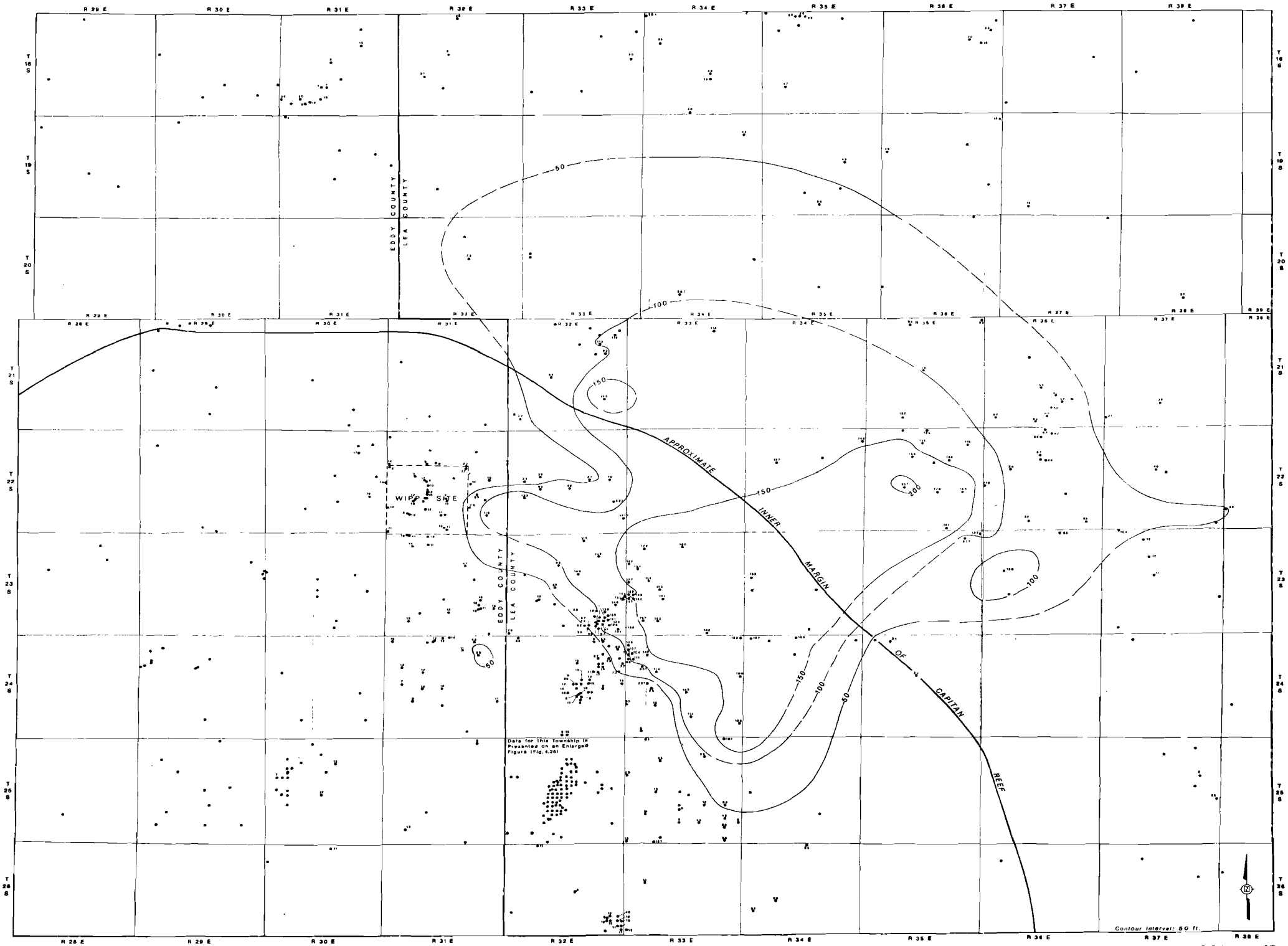

FIGURE 4.11 ISOPACH BETWEEN ANHYDRITES (A2-A3) OF TAMARISK MEMBER

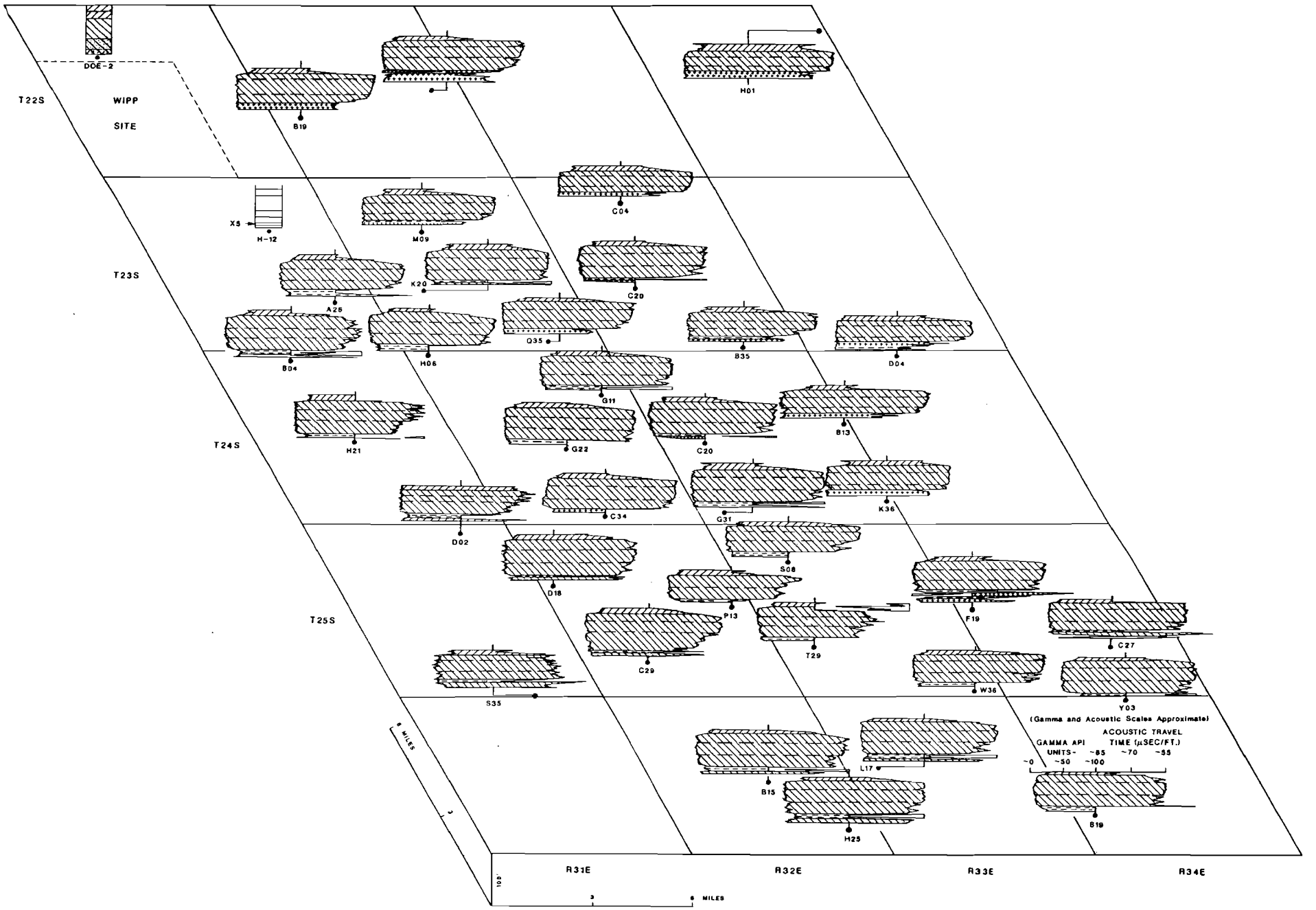

FIGURE 4-12

UPPER ANHYDRITE, TAMARISK MEMBER, RUSTLER FORMATION

PREPARED FOR

WESTINGHOUSE ELECTRIC CORPORATION

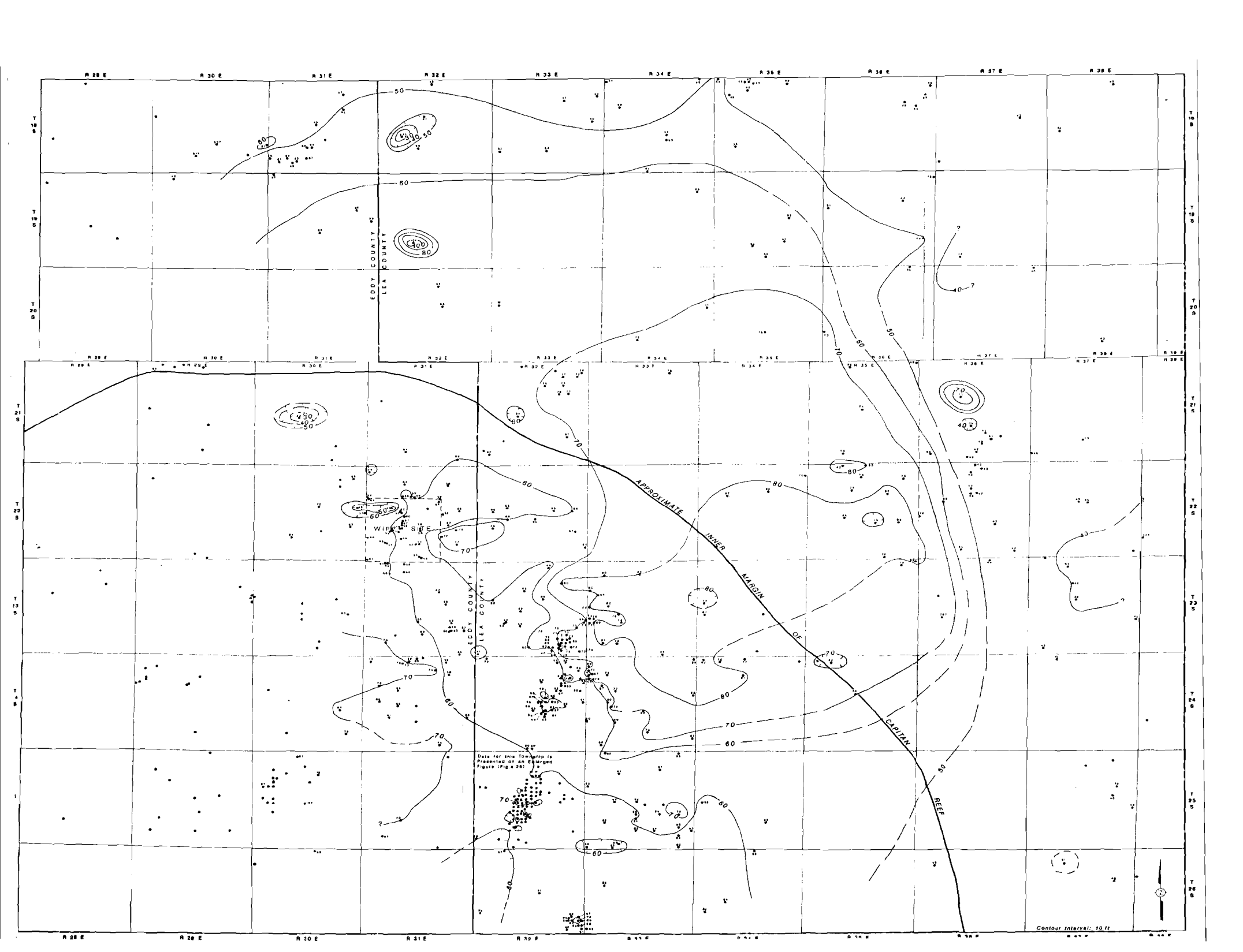
APPROXIMATE INNER MARGIN OF CAPITAN REEF
EDDY COUNTY
LEA COUNTY
WIPP SITE
Data for this Township is Presented on an Enlarged Figure (Fig. 26)
Contour Interval: 10 ft

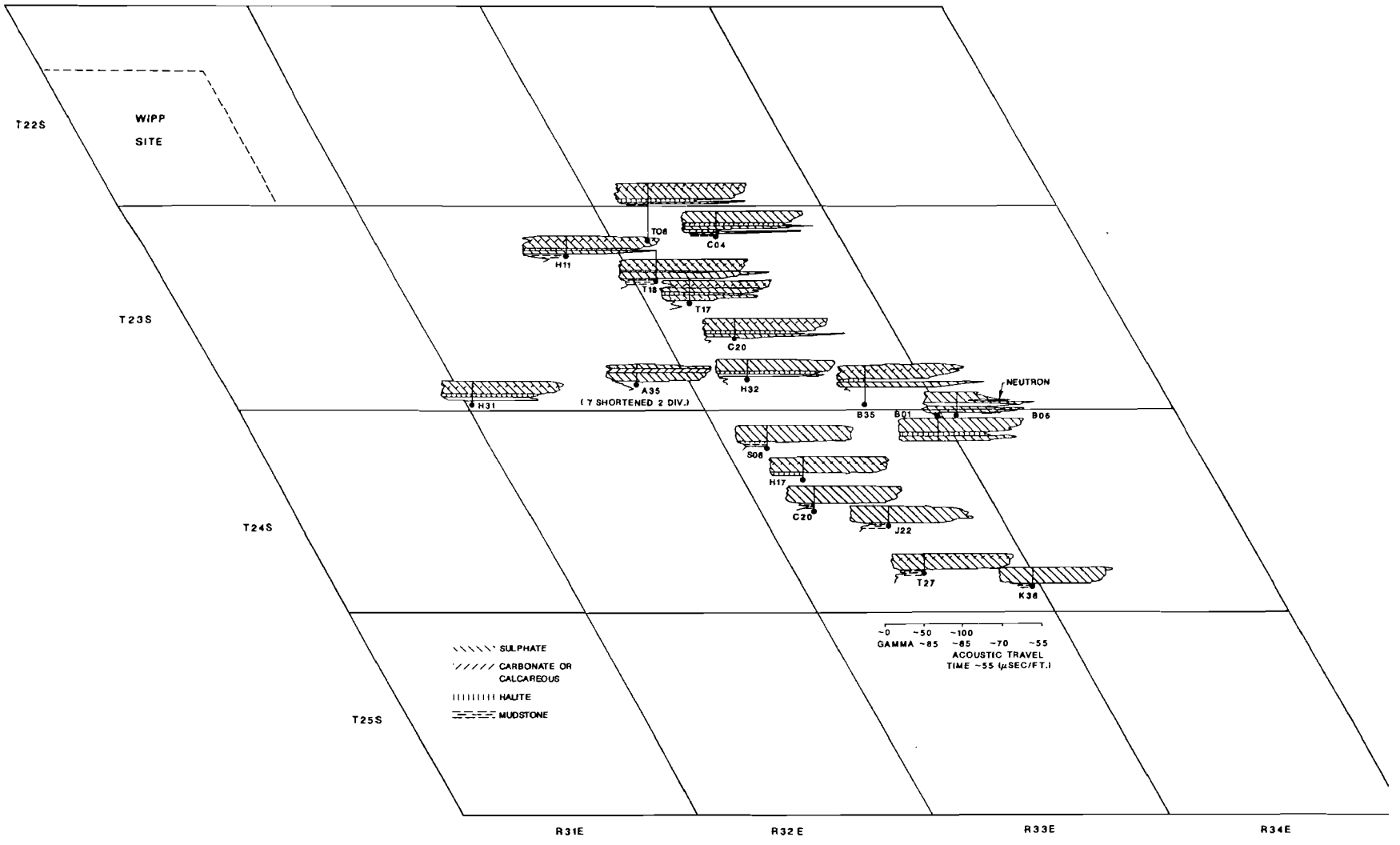

FIGURE 4.14

HALITE BED IN

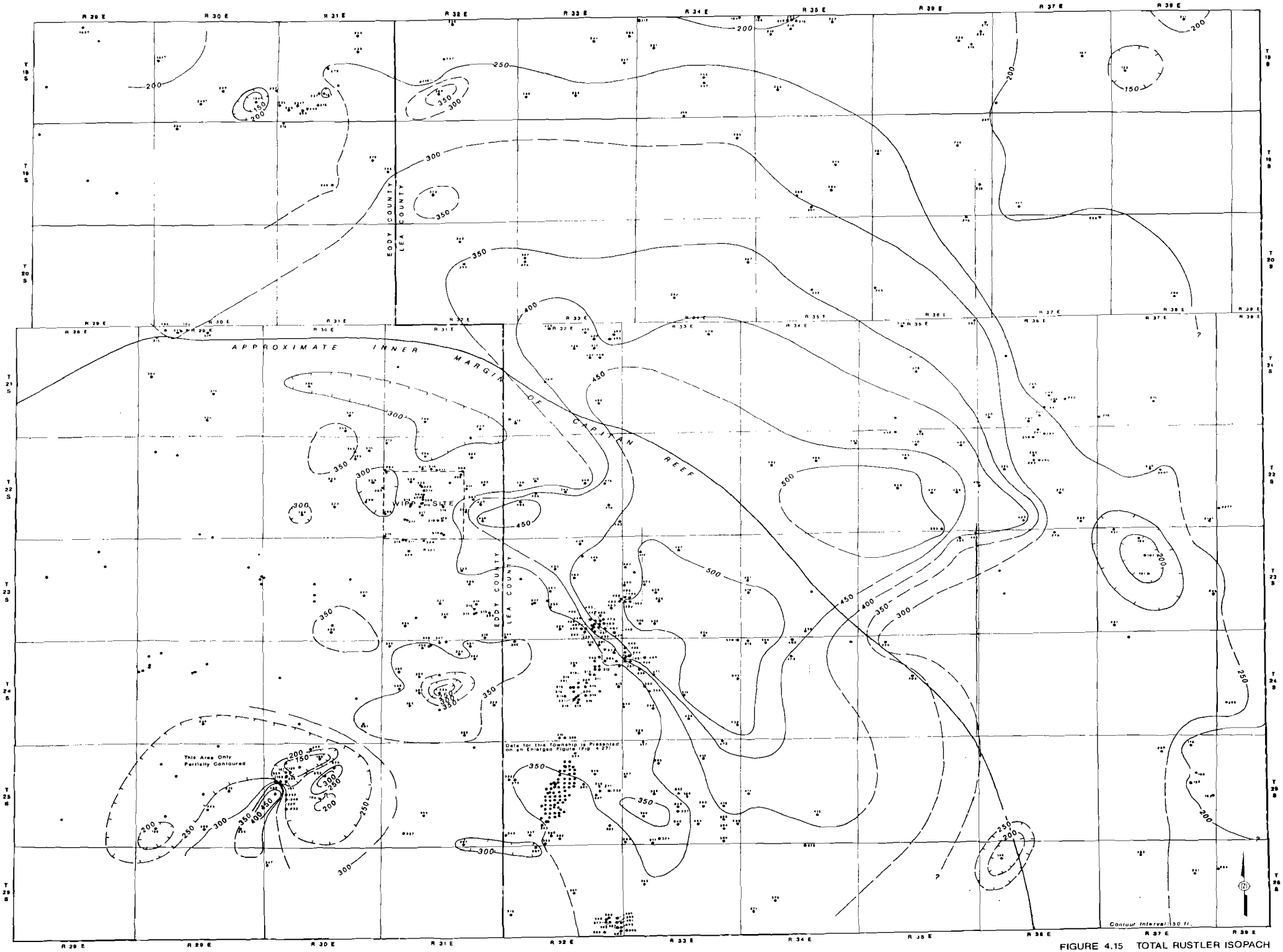

FIGURE 4.15 TOTAL RUSTLER ISOPACH

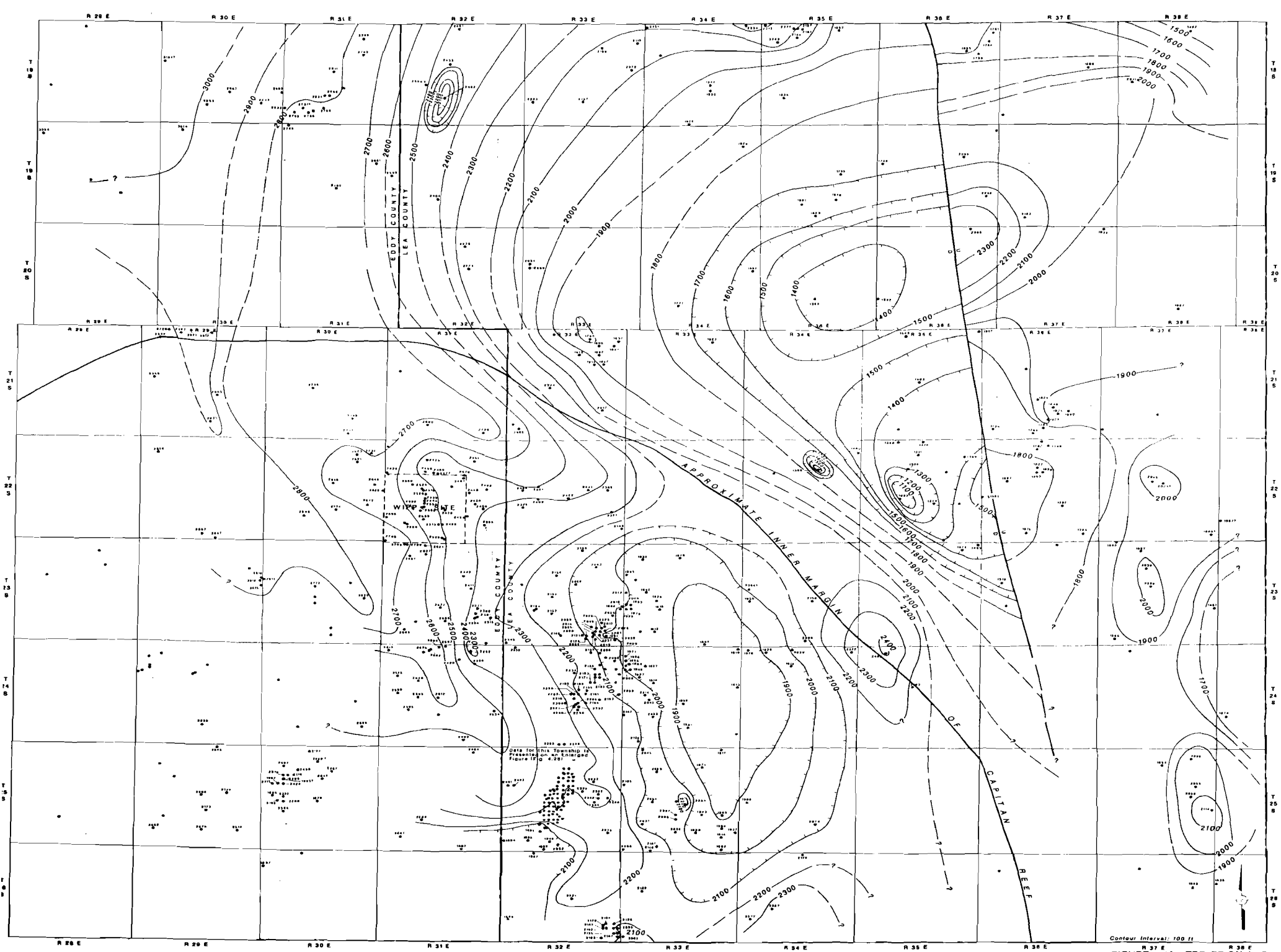

FIGURE 4.16 TOP OF SALADO

FIGURE 4.17 BASE OF CULEBRA

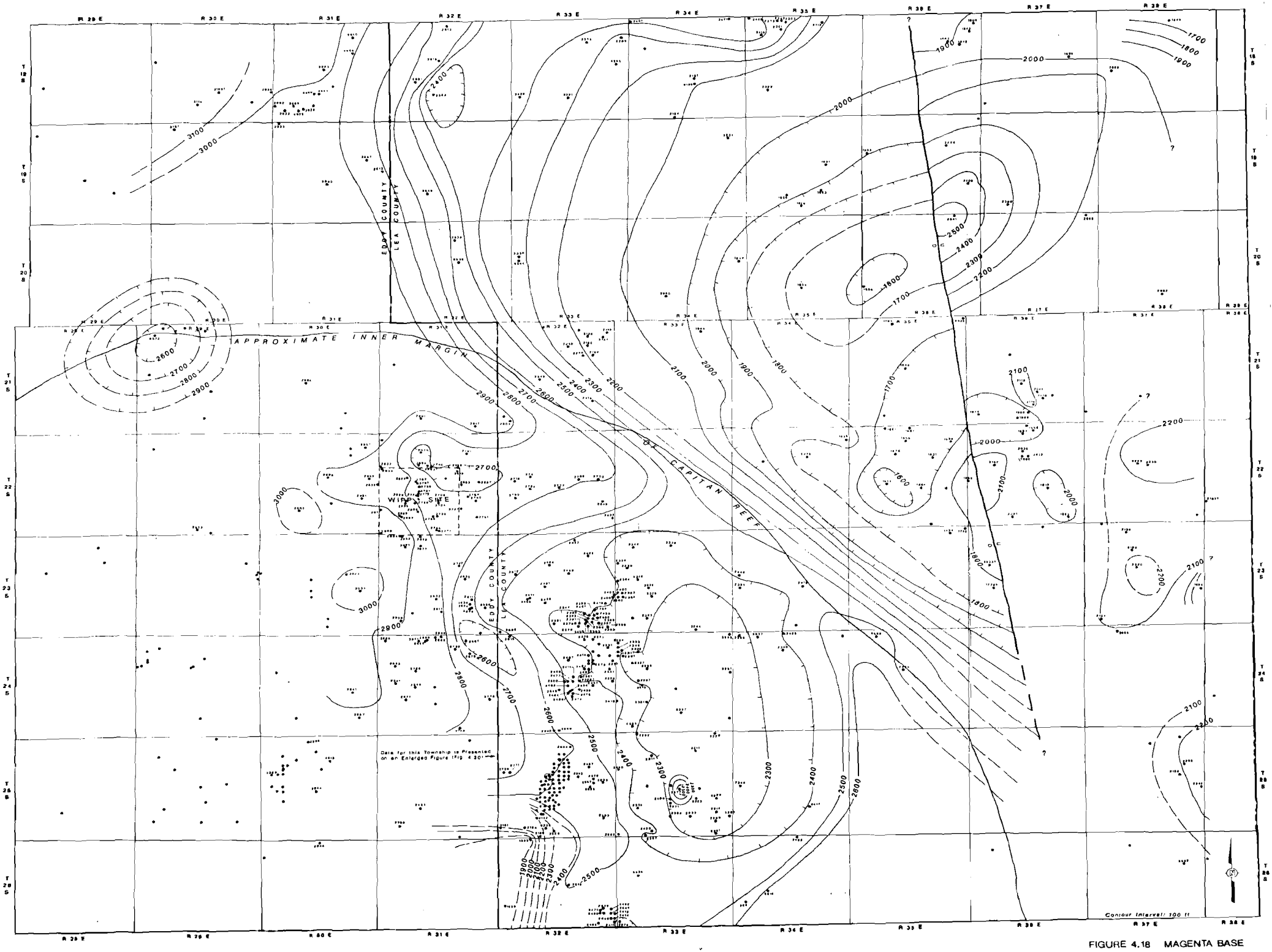

FIGURE 4.18 MAGENTA BASE

FIGURE 4.19 TOP OF RUSTLER

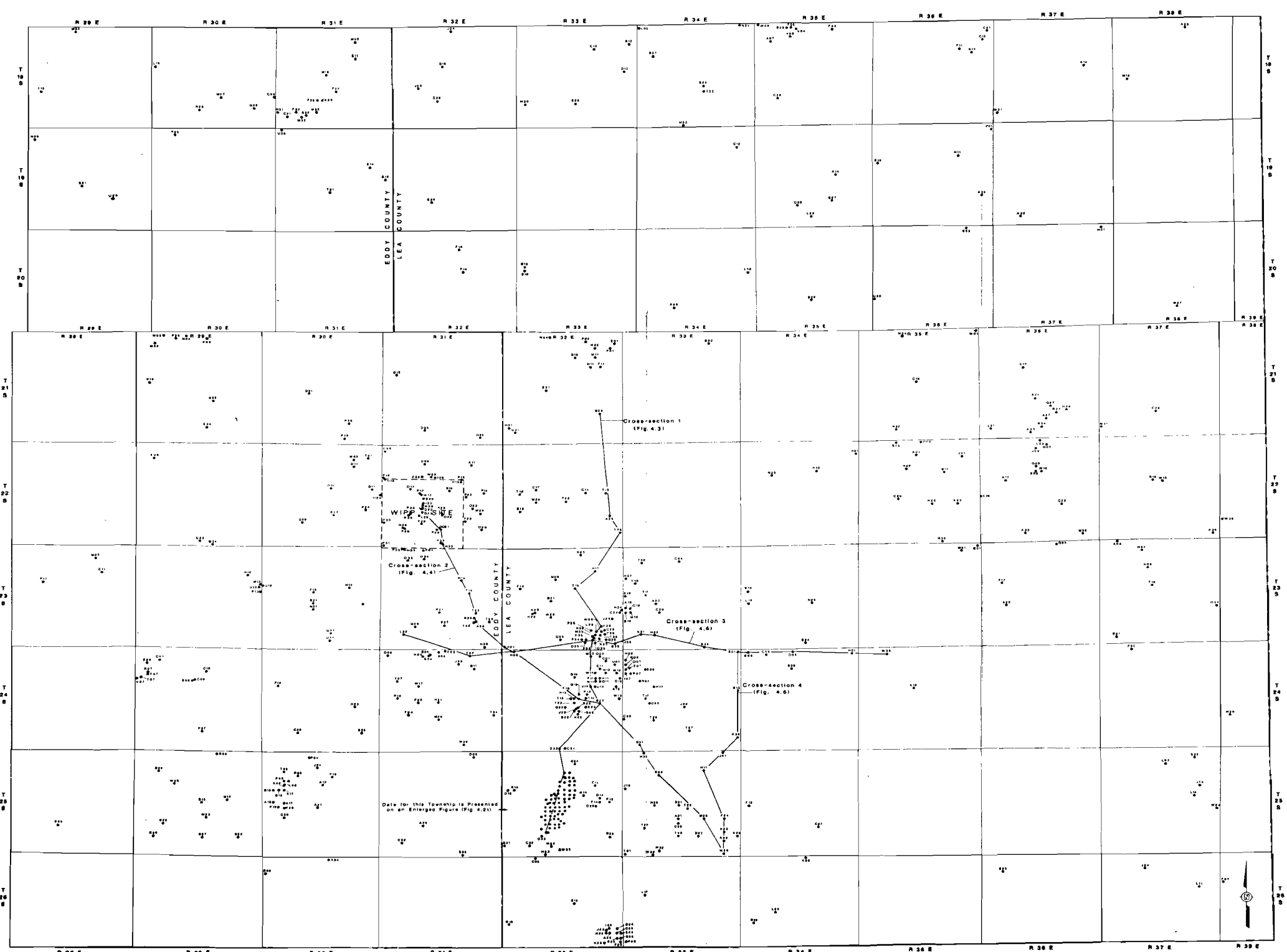

FIGURE 4.20 WELL-CONTROL BASE MAP

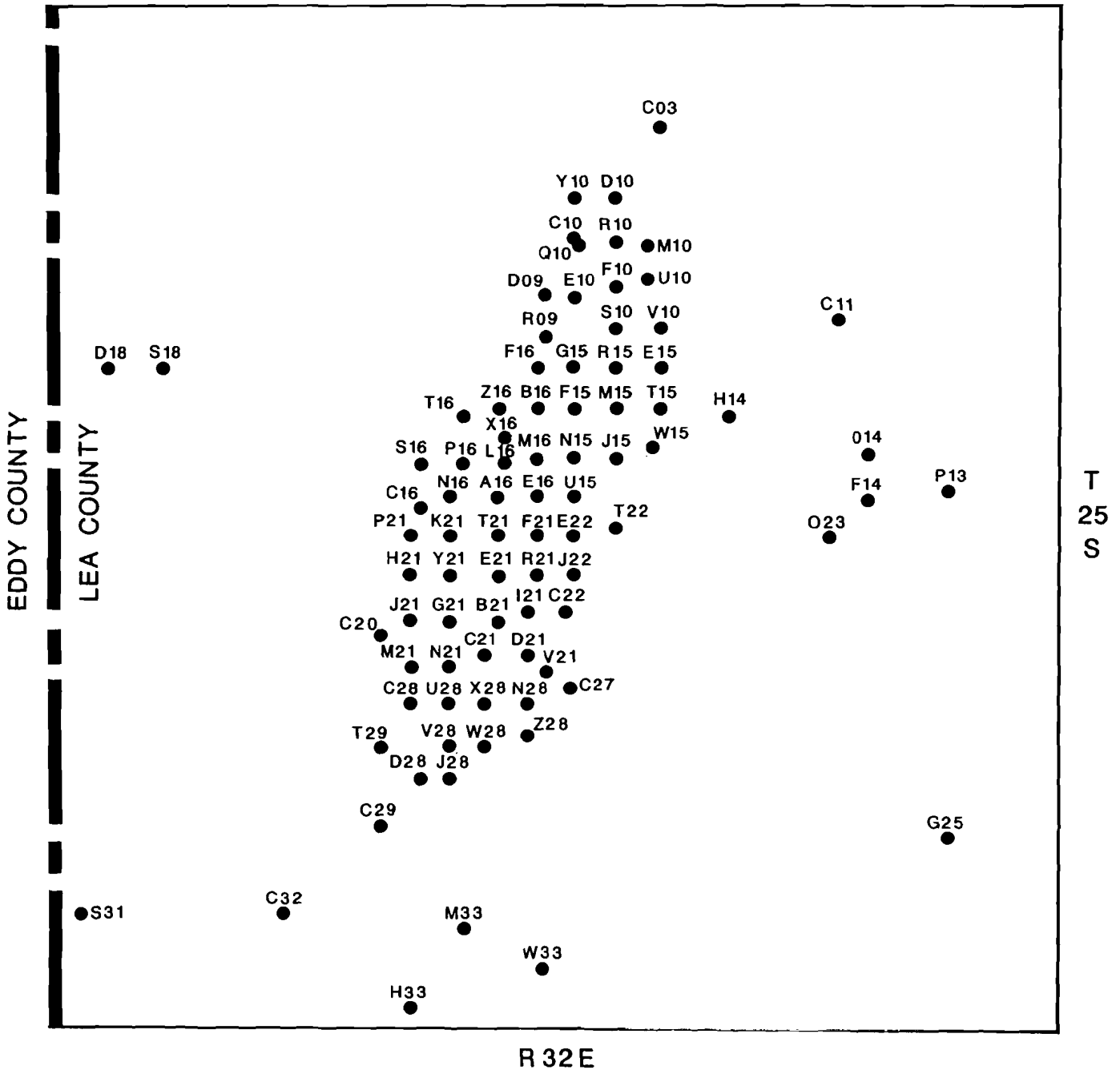

FIGURE 4.21

WELL CONTROL BASE MAP

PREPARED FOR

WESTINGHOUSE ELECTRIC CORPORATION
CARLSBAD, NEW MEXICO

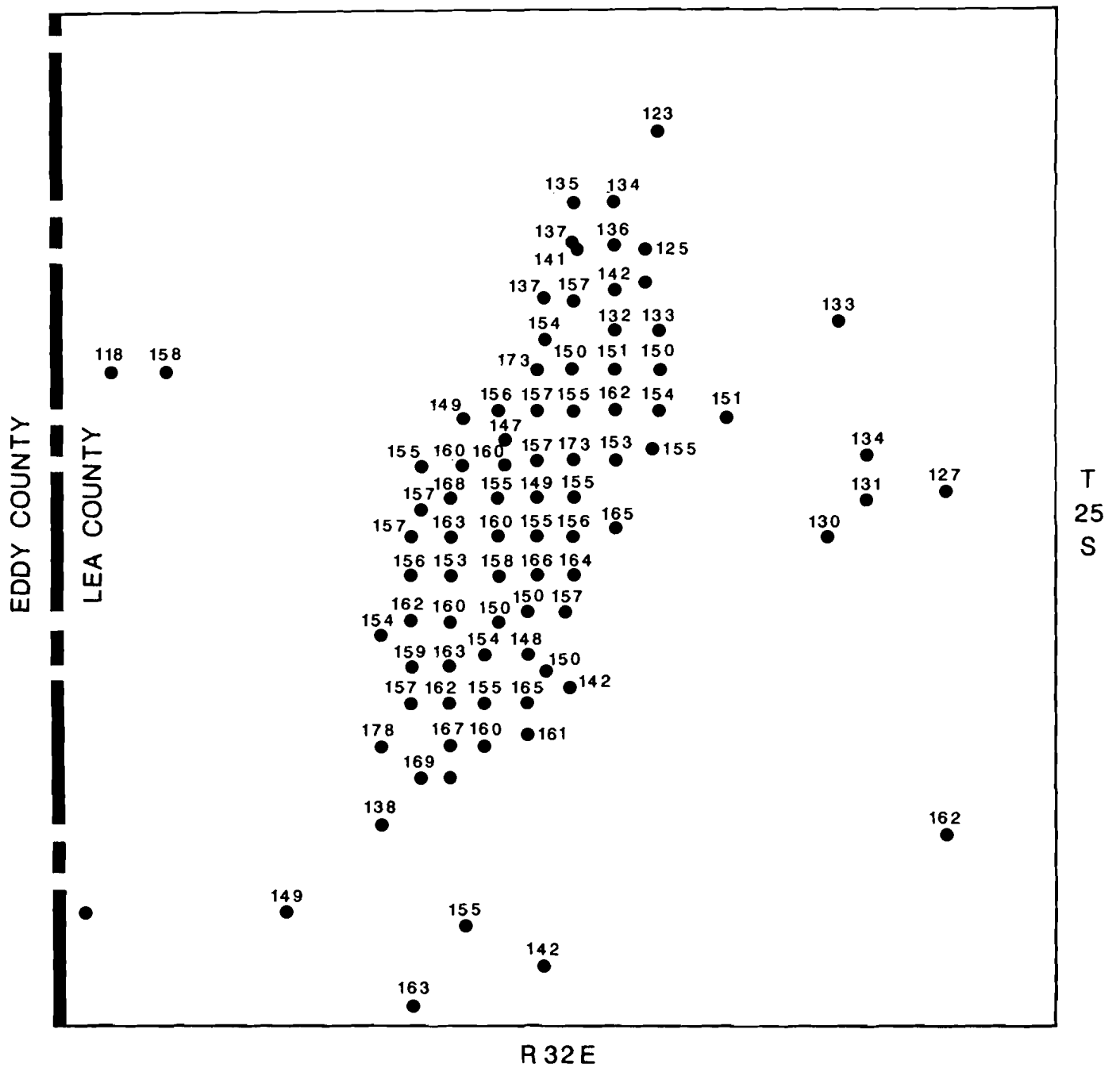

FIGURE 4.22

ISOPACH-LOWER UNNAMED MEMBER

PREPARED FOR

WESTINGHOUSE ELECTRIC CORPORATION
CARLSBAD, NEW MEXICO

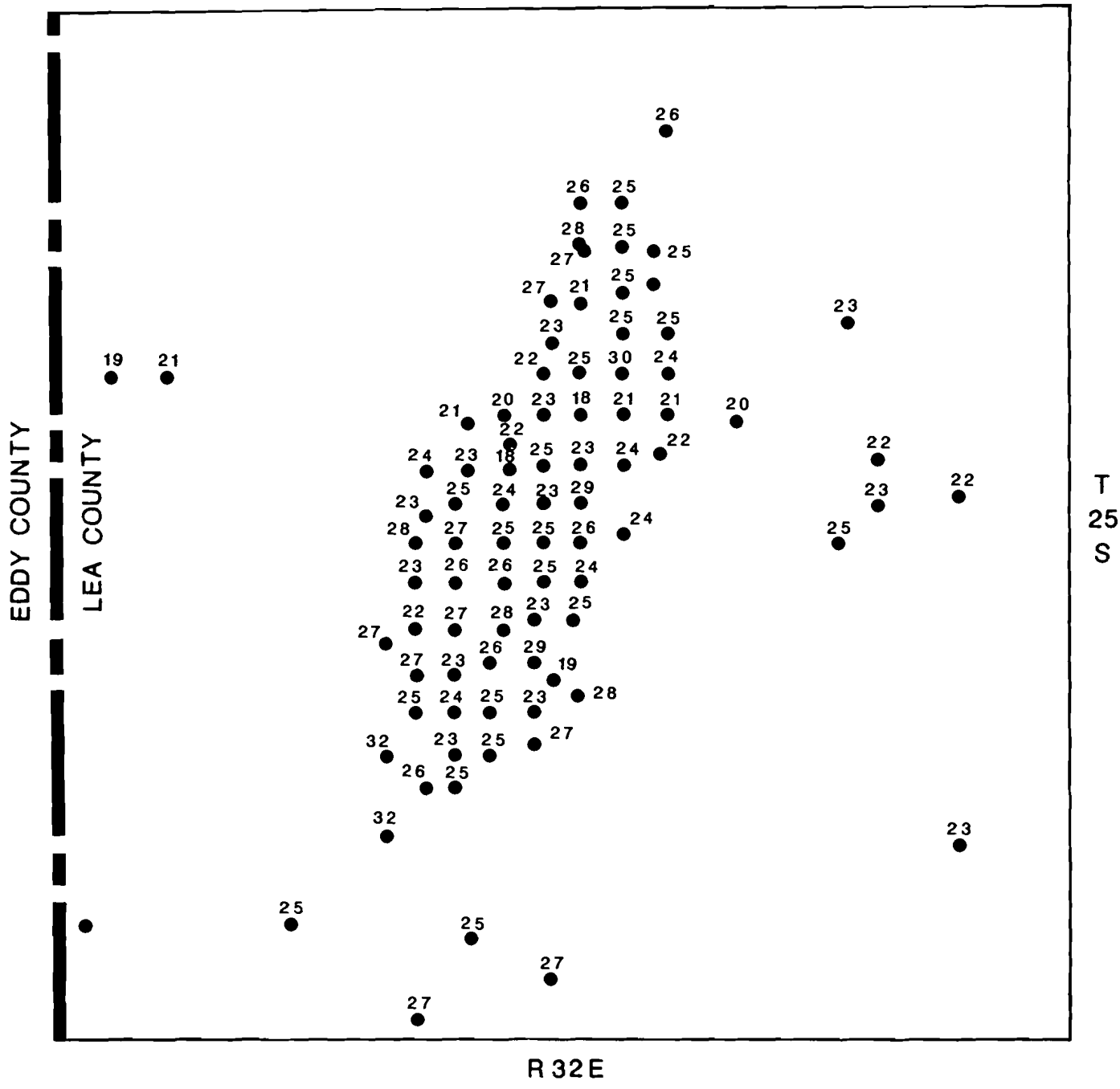

FIGURE 4.23

ISOPACH OF CULEBRA

PREPARED FOR

WESTINGHOUSE ELECTRIC CORPORATION
CARLSBAD, NEW MEXICO

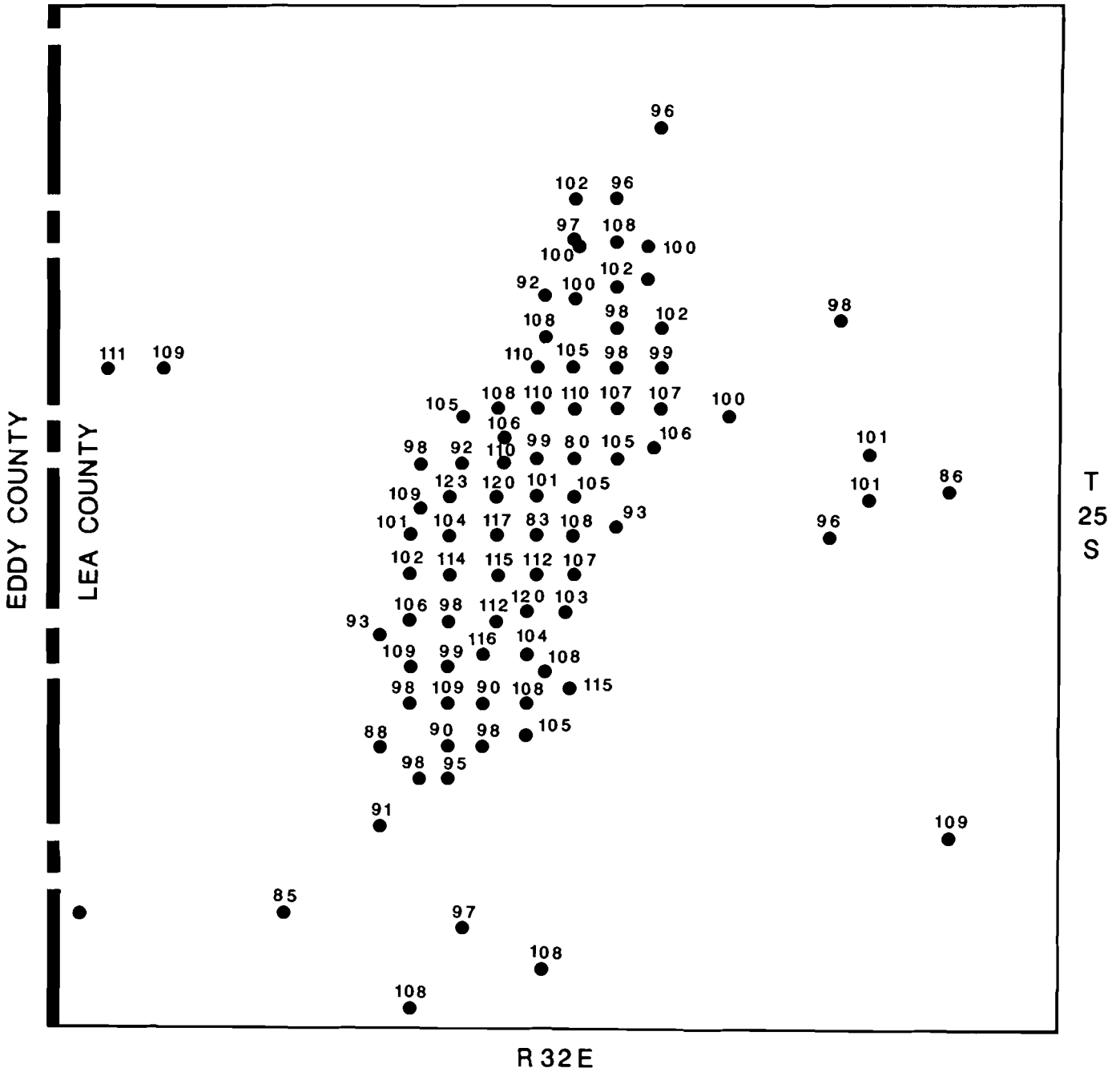

FIGURE 4.24

ISOPACH OF TAMERISK

PREPARED FOR

WESTINGHOUSE ELECTRIC CORPORATION
CARLSBAD, NEW MEXICO

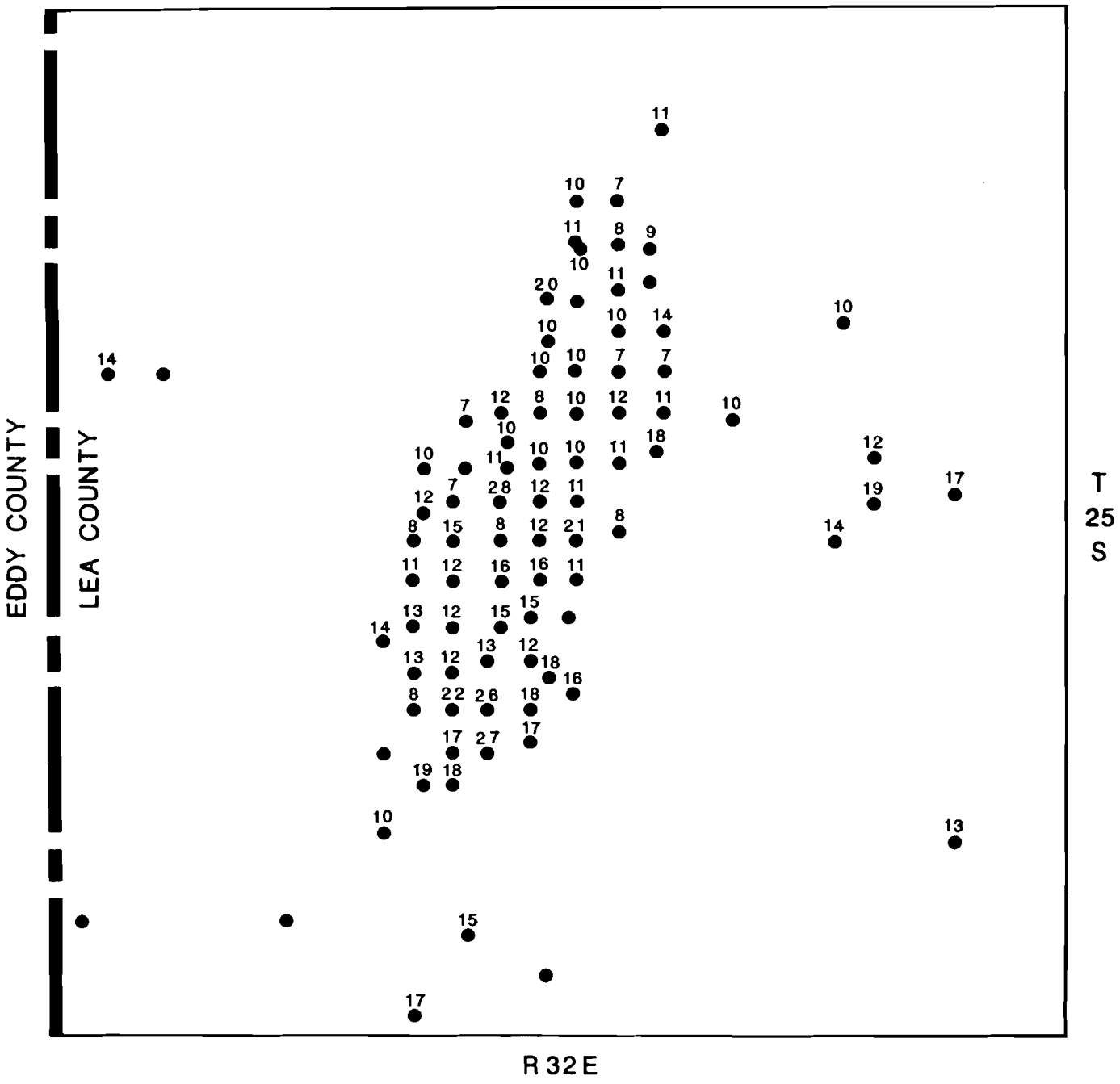

FIGURE 4.25

ISOPACH BETWEEN ANHYDRITES
(A2-A3) OF TAMERISK MEMBER

PREPARED FOR

WESTINGHOUSE ELECTRIC CORPORATION
CARLSBAD, NEW MEXICO

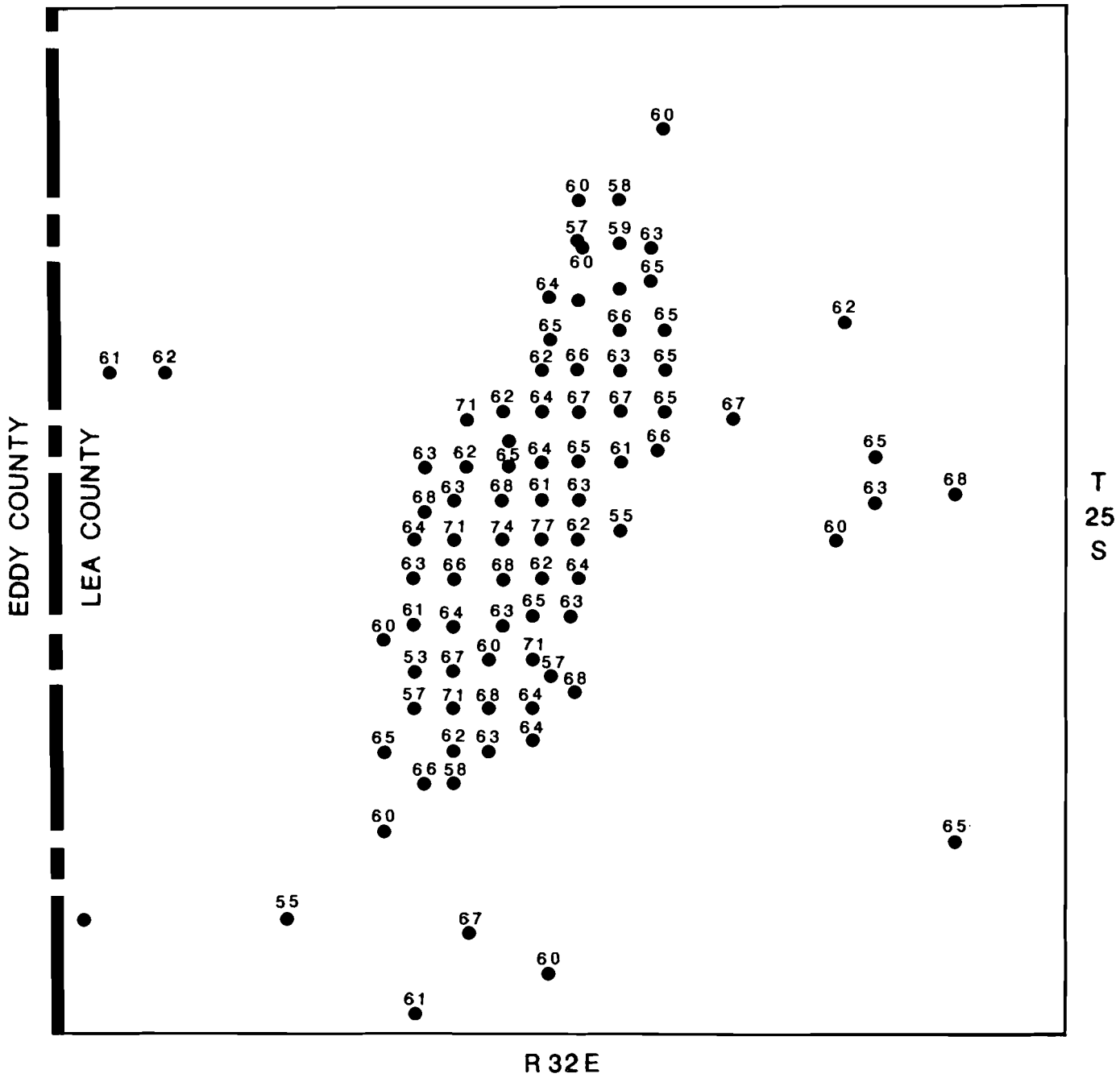

FIGURE 4.26

FORTY-NINER ISOPACH

PREPARED FOR

WESTINGHOUSE ELECTRIC CORPORATION
CARLSBAD, NEW MEXICO

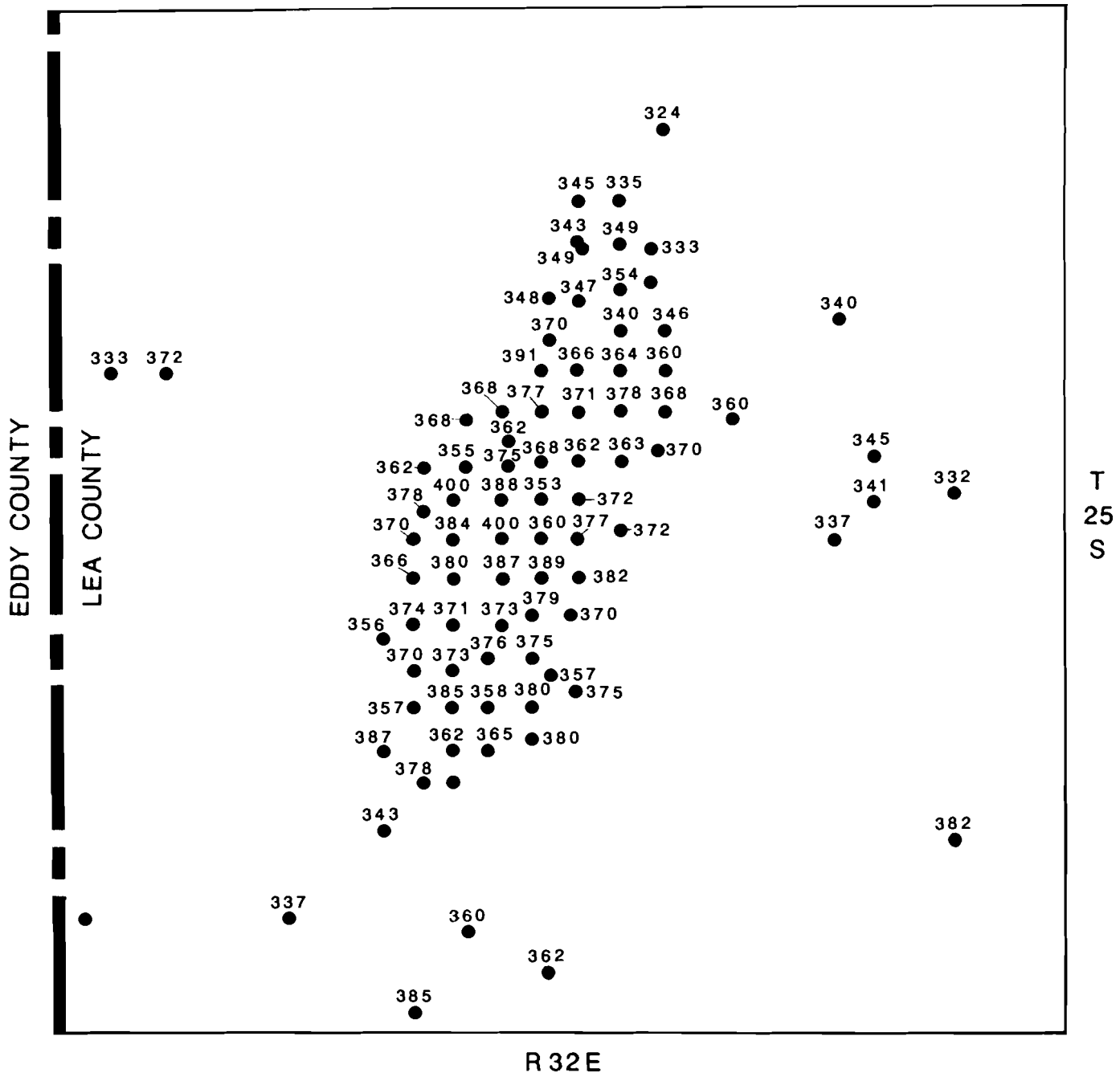

FIGURE 4.27

TOTAL RUSTLER ISOPACH

PREPARED FOR

WESTINGHOUSE ELECTRIC CORPORATION
CARLSBAD, NEW MEXICO

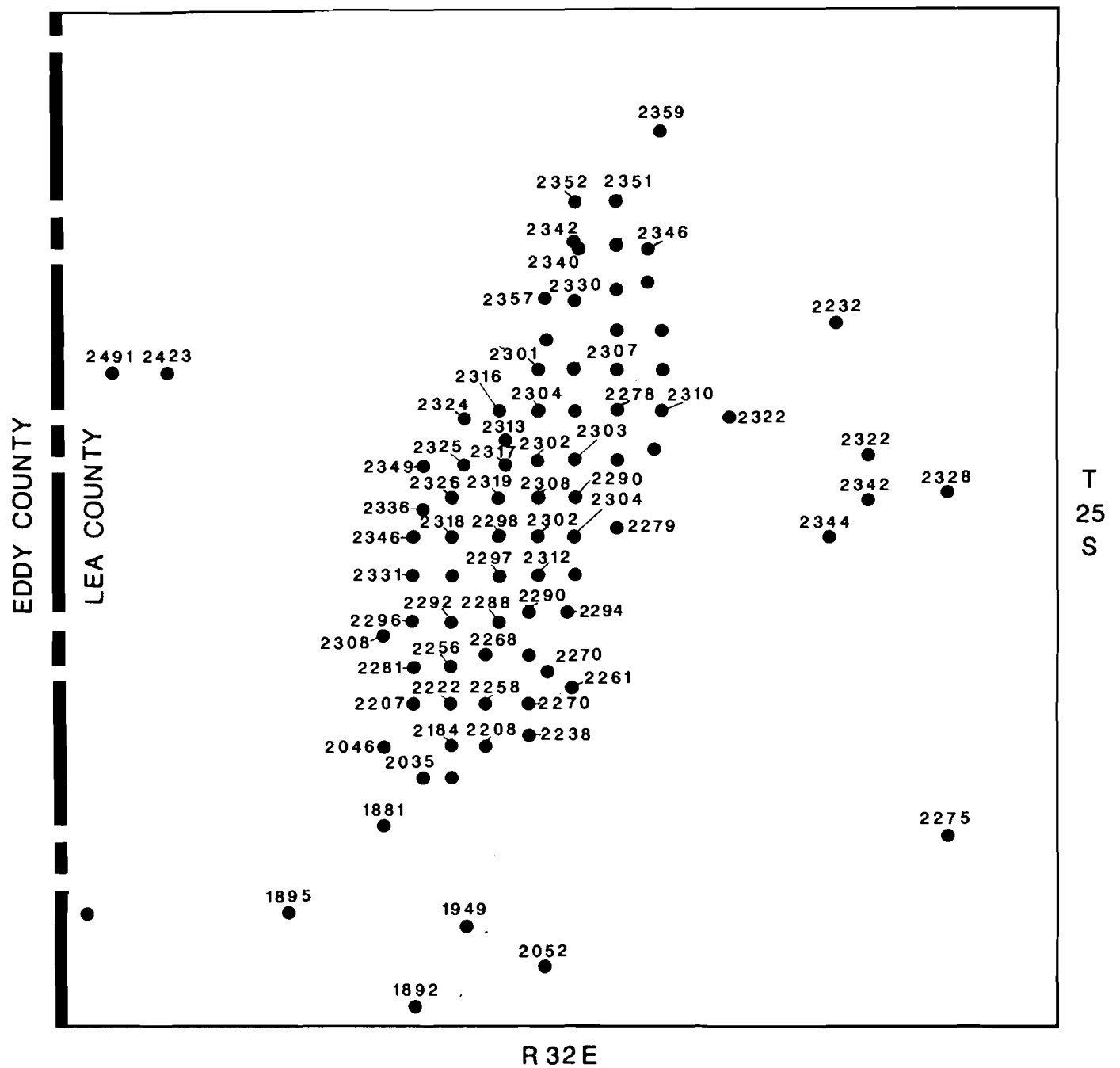

FIGURE 4.28

TOP OF SALADO

PREPARED FOR

WESTINGHOUSE ELECTRIC CORPORATION
CARLSBAD, NEW MEXICO

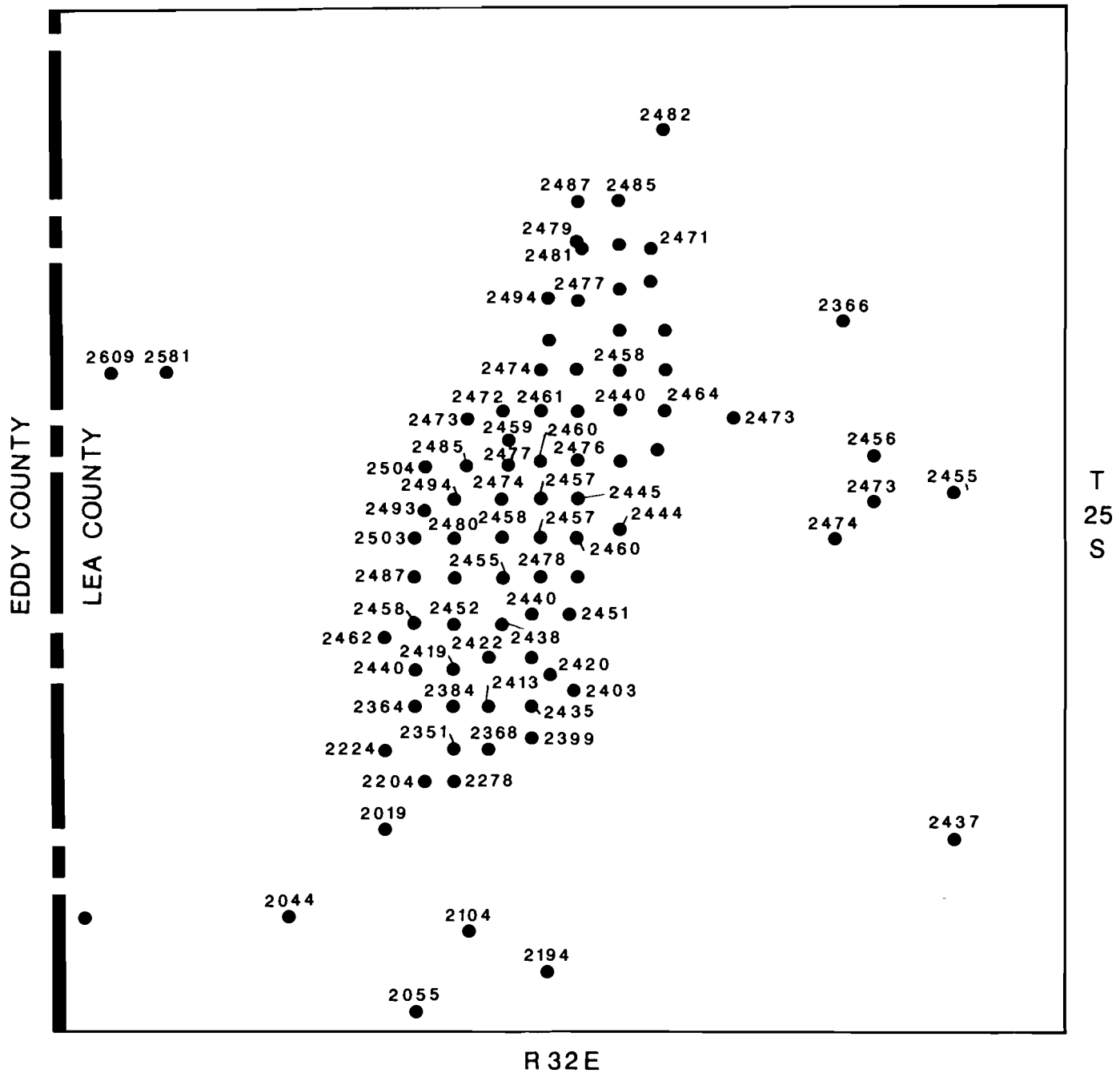

FIGURE 4.29

BASE OF CULEBRA

PREPARED FOR

WESTINGHOUSE ELECTRIC CORPORATION
CARLSBAD, NEW MEXICO

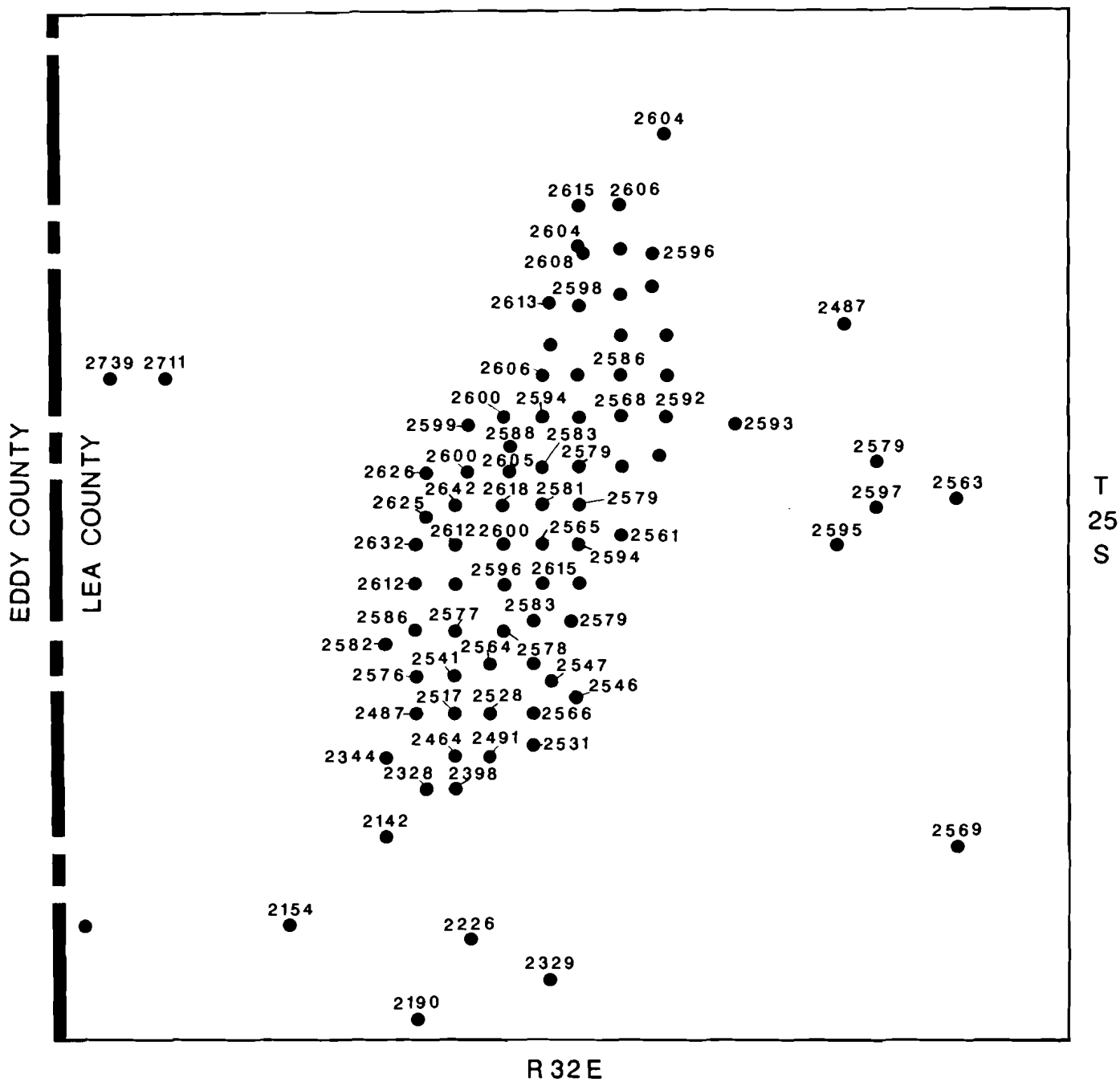

FIGURE 4.30

MAGENTA BASE

PREPARED FOR

WESTINGHOUSE ELECTRIC CORPORATION
CARLSBAD, NEW MEXICO

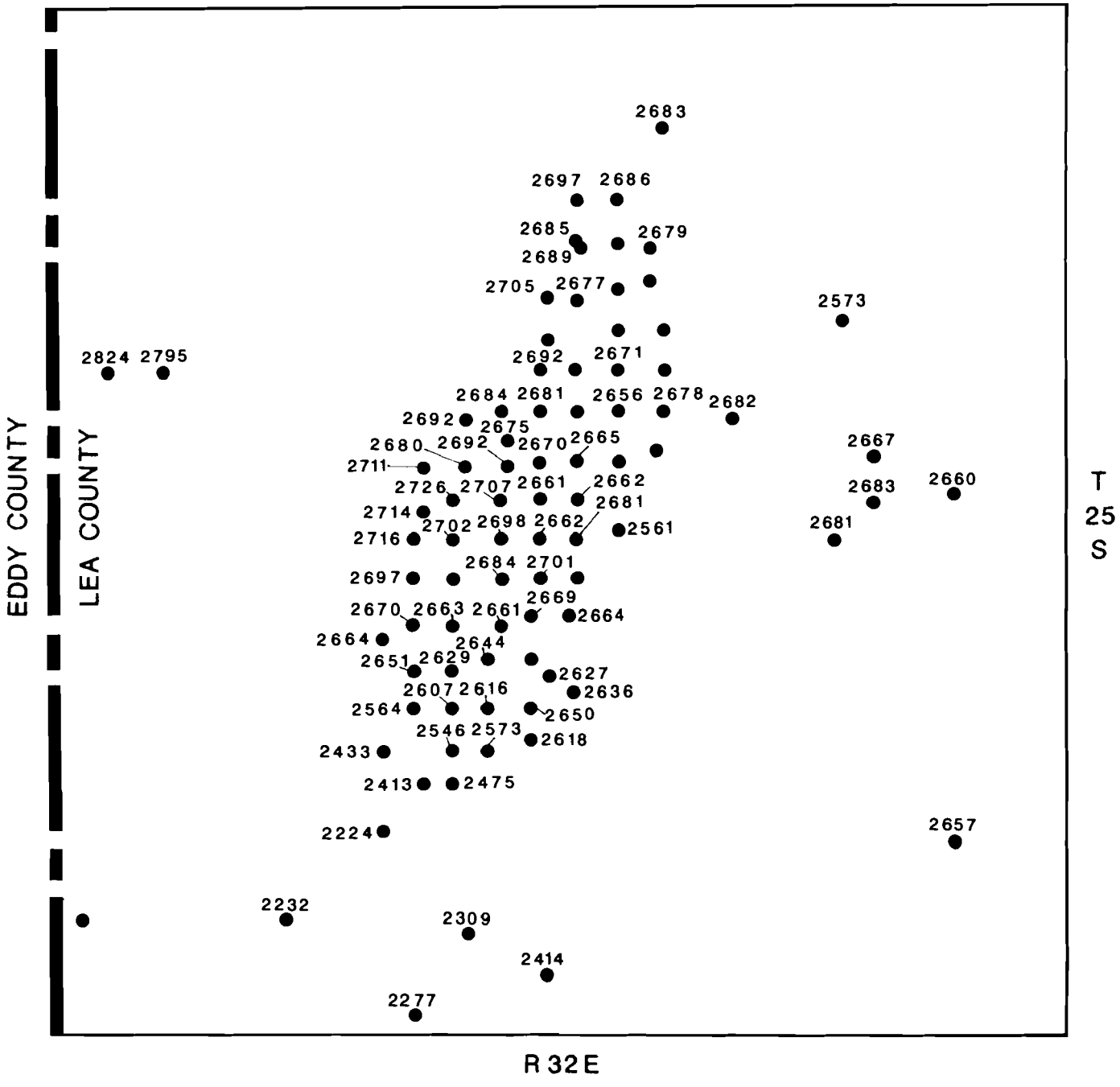

FIGURE 4.31

TOP OF RUSTLER

PREPARED FOR

WESTINGHOUSE ELECTRIC CORPORATION
CARLSBAD, NEW MEXICO

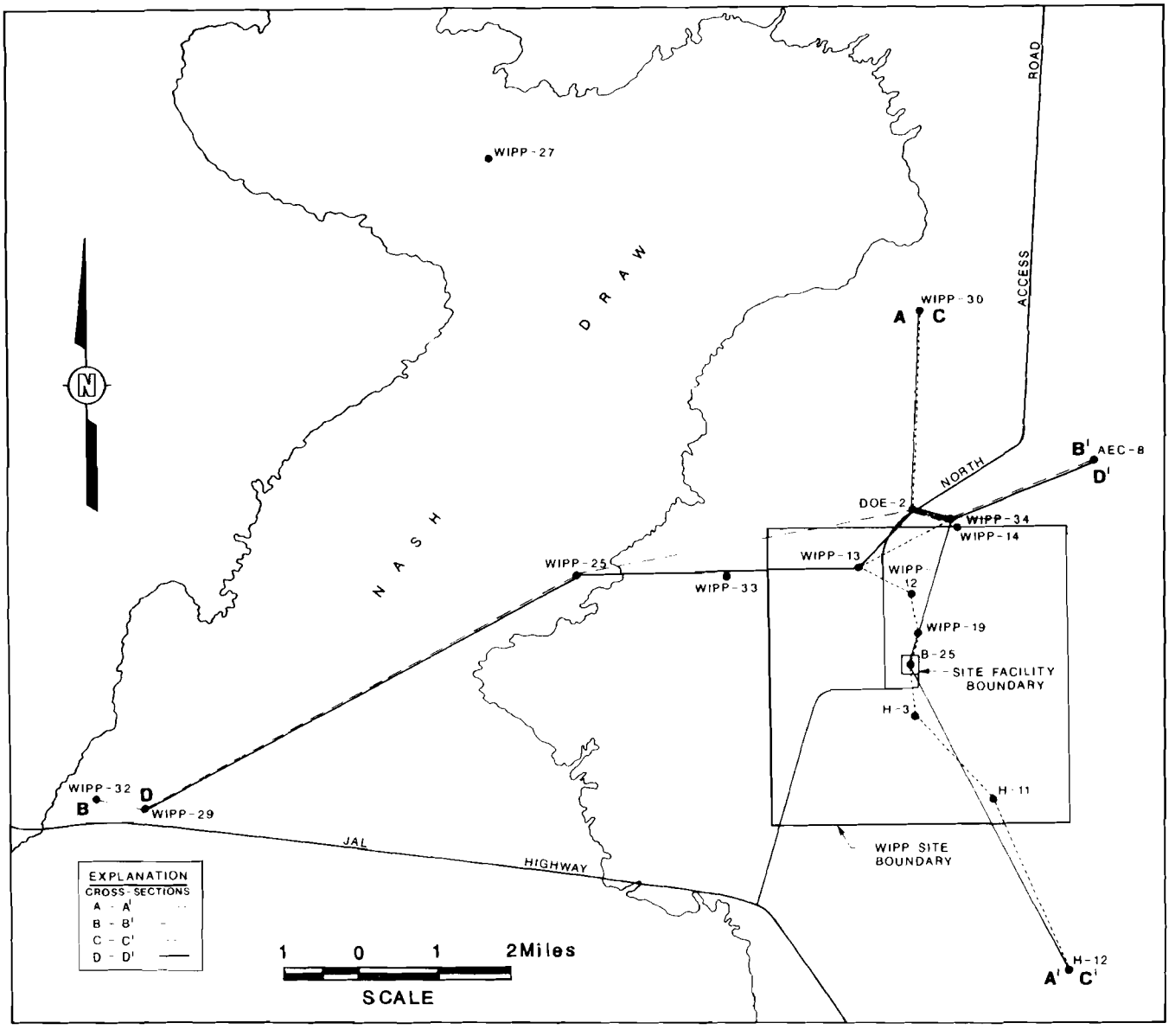

FIGURE 5.1

BOREHOLE AND CROSS SECTION
LOCATION MAP
RUSTLER CORE STUDY

PREPARED FOR

WESTINGHOUSE ELECTRIC CORPORATION
CARLSBAD, NEW MEXICO

EXPLANATION

STRATIFICATION TYPES

- CONTINUOUS
- DISCONTINUOUS
- FLAT LAMINAE
- WAVEY LAMINAE
- CONTORTED LAMINAE
- DIPPING STRATIFICATION
- CROSS-LAMINATIONS
- OVERTURNED STRATA
- WAVEY TO LENTICULAR BEDDING
- E EROSIONAL SURFACE
- St STROMATOLITIC LAYERING
- DISPLACED STRATA

CLASTS

Shape		Clast Type		Allochems	
O	ROUNDED		CARBONATE		OOLITE
Δ	ANGULAR		GYSUM		FOSSIL FRAGMENTS
R	TABULAR RIP-UP CLASTS		MUDSTONE		
∞	SMEARED INTRACLAST				

HALITE TEXTURES

- INCORPORATIVE/DISPLACIVE HALITE
- HALITE CRYSTAL AGGREGATE
- INTERLOCKING HALITE CRYSTALS WITH LITTLE OR NO MATRIX

SULFATE TEXTURES

- PSUEDOMORPHS AFTER VERTICALLY ORIENTED PRISMATIC GYPSUM CRYSTALS
- NODULAR
- BEDDED NODULAR
- CRUSHED PRISM TEXTURE
- ROSETTES/RADIAL GYPSUM CRYSTALS
- INCORPORATIVE GYPSUM
- RADIAL GYSUM IN SULFATE
- N GYPSUM/ANHYDRITE NODULE

BIOGENIC FEATURES

- MOTTLING
- BURROWING/BIOTURBATION

VUGS

- V OPEN VUG
- V GYPSUM-FILLED VUG

OTHER SEDIMENTARY STRUCTURES

- PRISM CRACKS
- SMALL ROTATED BLOCKS
- LARGE ROTATED BLOCKS

OTHER SIDE NOTES

S	SLICKENSIDES	C	POSSIBLE CUTAN		ROTATION
CF	CLAYFILLED FRACTURES	10°-15°	DIPPING STRATA, ANGLE OF DIP 10°-15°	30°-40°	ROTATION, 30°-40°

LITHOLOGIC SYMBOL	ROCK TYPE
	MUDSTONE/CLAYSTONE
	CLAYSTONE BED
	SILTSTONE
	SANDSTONE
	ANHYDRITE/GYPSUM
	DOLOMITE
	CARBONATE
	HALITE

MINOR CONSTITUENTS

- CARBONATE
- HALITE AND SILTSTONE CURVE INDICATES RELATIVE AMOUNTS OF EACH
- SULFATE
- CLAYSTONE

FIGURE 5.2
SHEET 1 OF 5
CROSS-SECTION EXPLANATION
PREPARED FOR
WESTINGHOUSE ELECTRIC CORPORATION
CARLSBAD, NEW MEXICO

A

WIPP 30

DOE 2

WIPP 34

WIPP 19

B25

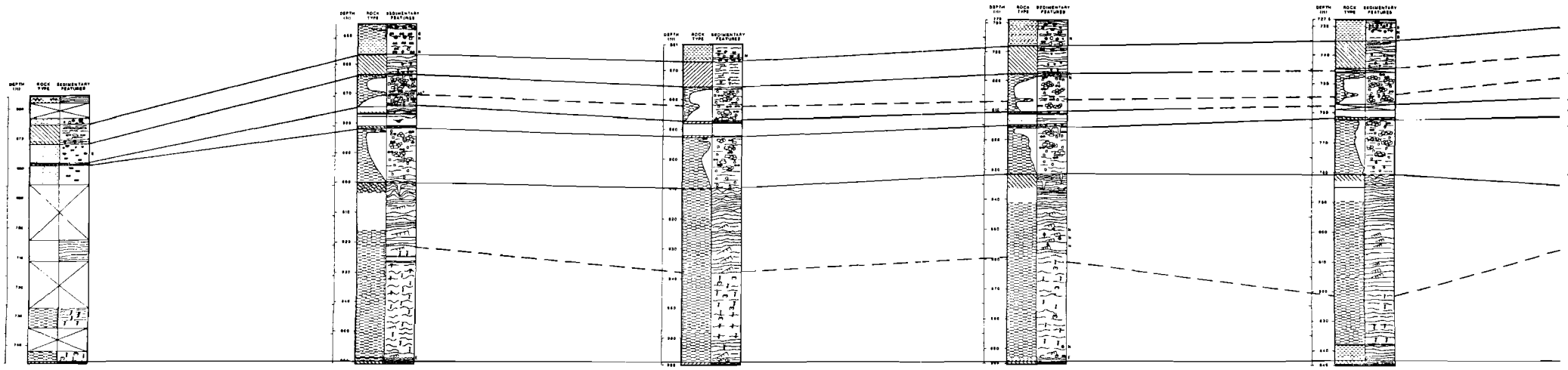

B

WIPP-32 WIPP-29 WIPP-25 DOE-2 WIPP-34

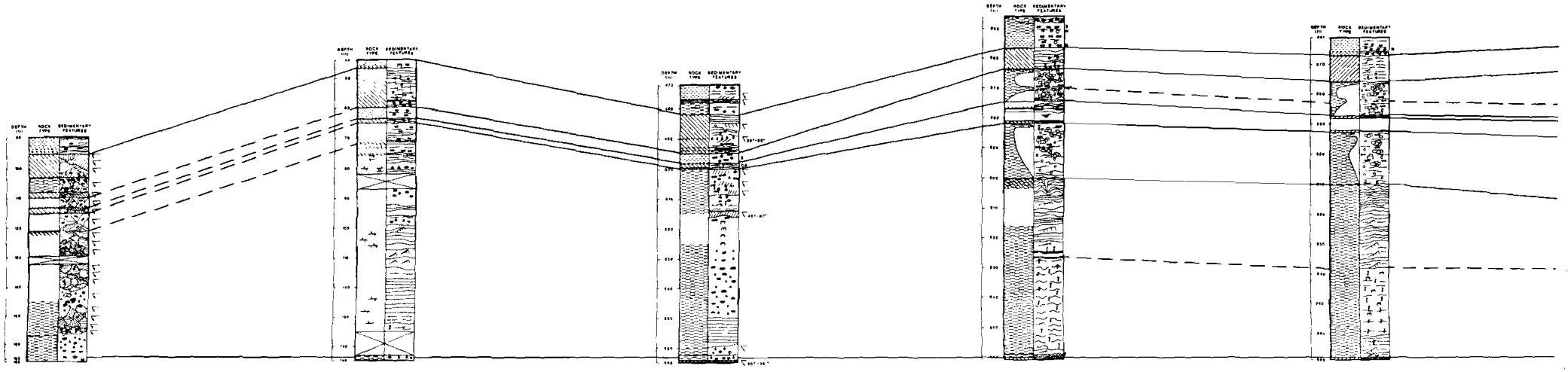

FIGURE 5.2
SHEET 1 OF 5

UPPER RUSTLER FORMATION

PREPARED FOR

WESTINGHOUSE ELECTRIC CORPORATION
CARLSBAD, NEW MEXICO

D

WIPP 29

WIPP 25

WIPP 13

DOE 2

WIPP 34

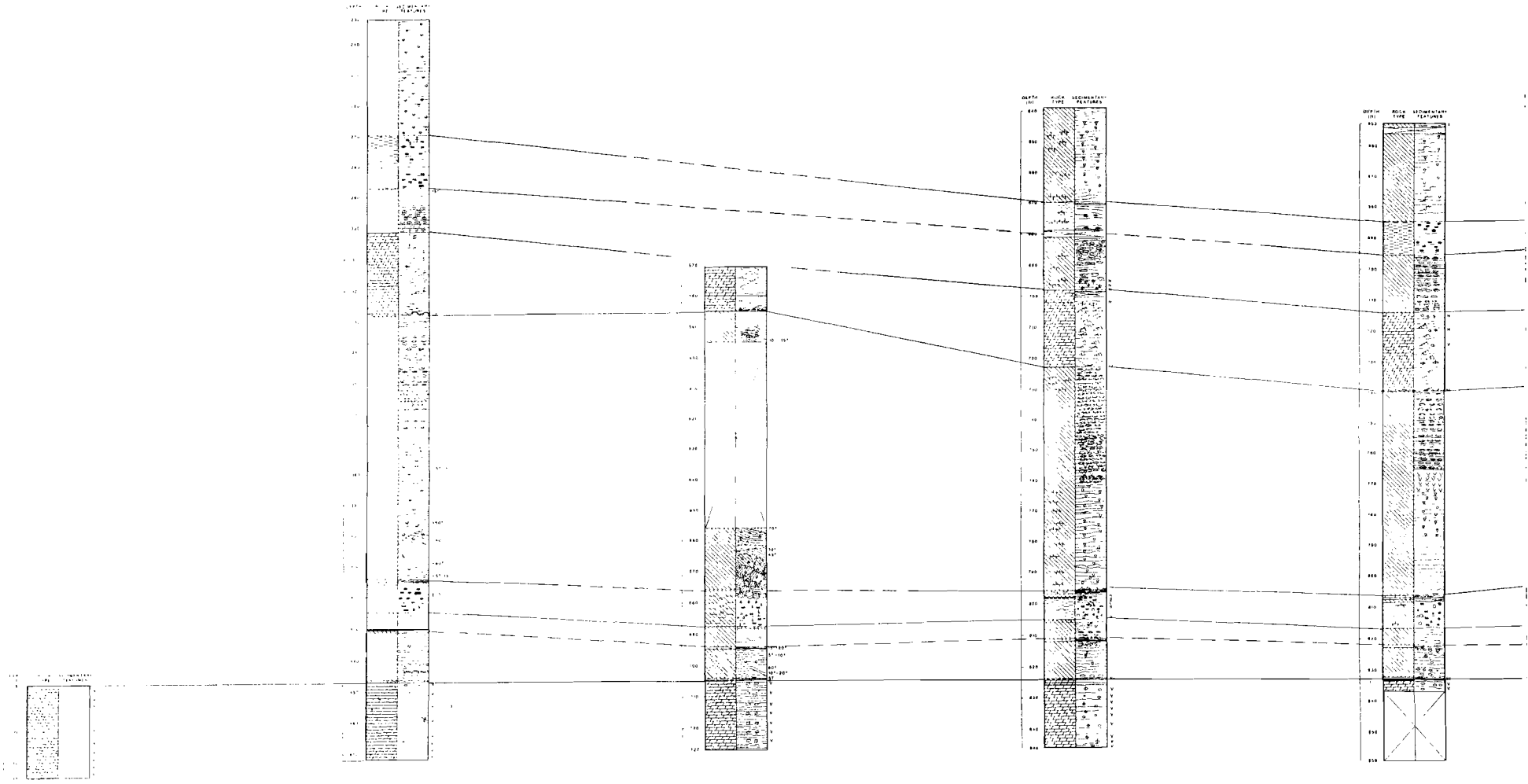

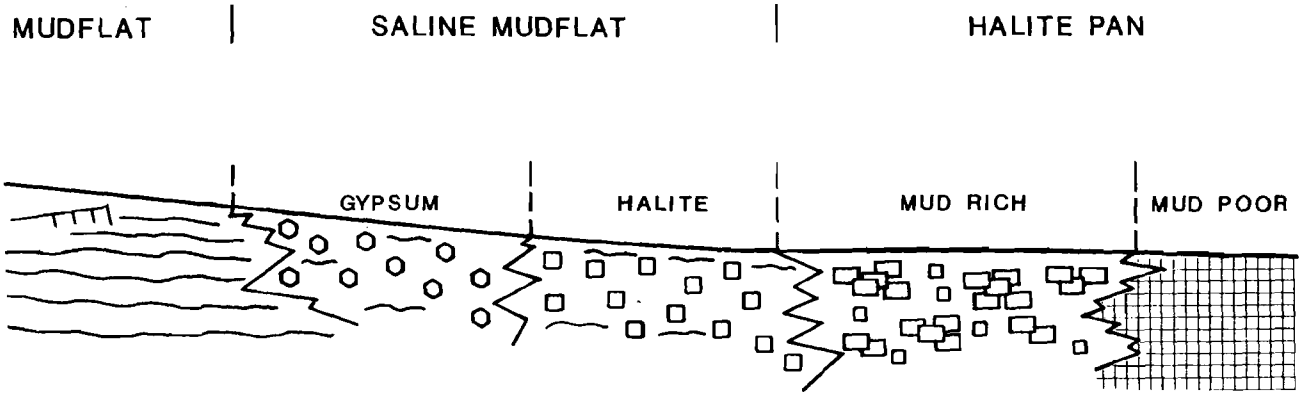

FIGURE 6.1

HALITE PAN AND MARGINAL
DEPOSITIONAL ENVIRONMENTS

PREPARED FOR

WESTINGHOUSE ELECTRIC CORPORATION
CARLSBAD, NEW MEXICO

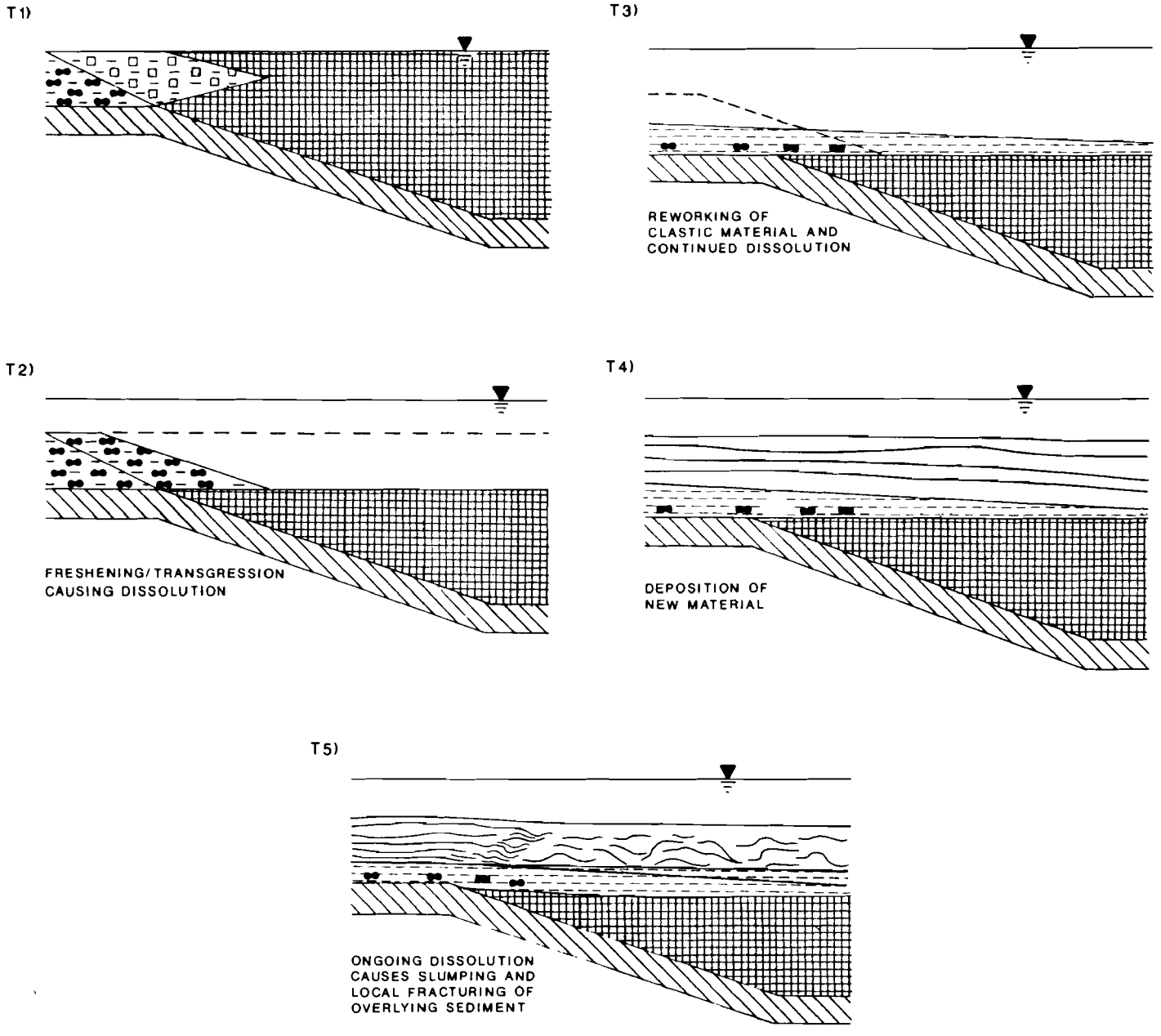

FIGURE 6.2

SYNDEPOSITIONAL DISSOLUTION
DURING A MAJOR FLOOD
OR TRANSGRESSIVE EVENT

PREPARED FOR

WESTINGHOUSE ELECTRIC CORPORATION
CARLSBAD, NEW MEXICO

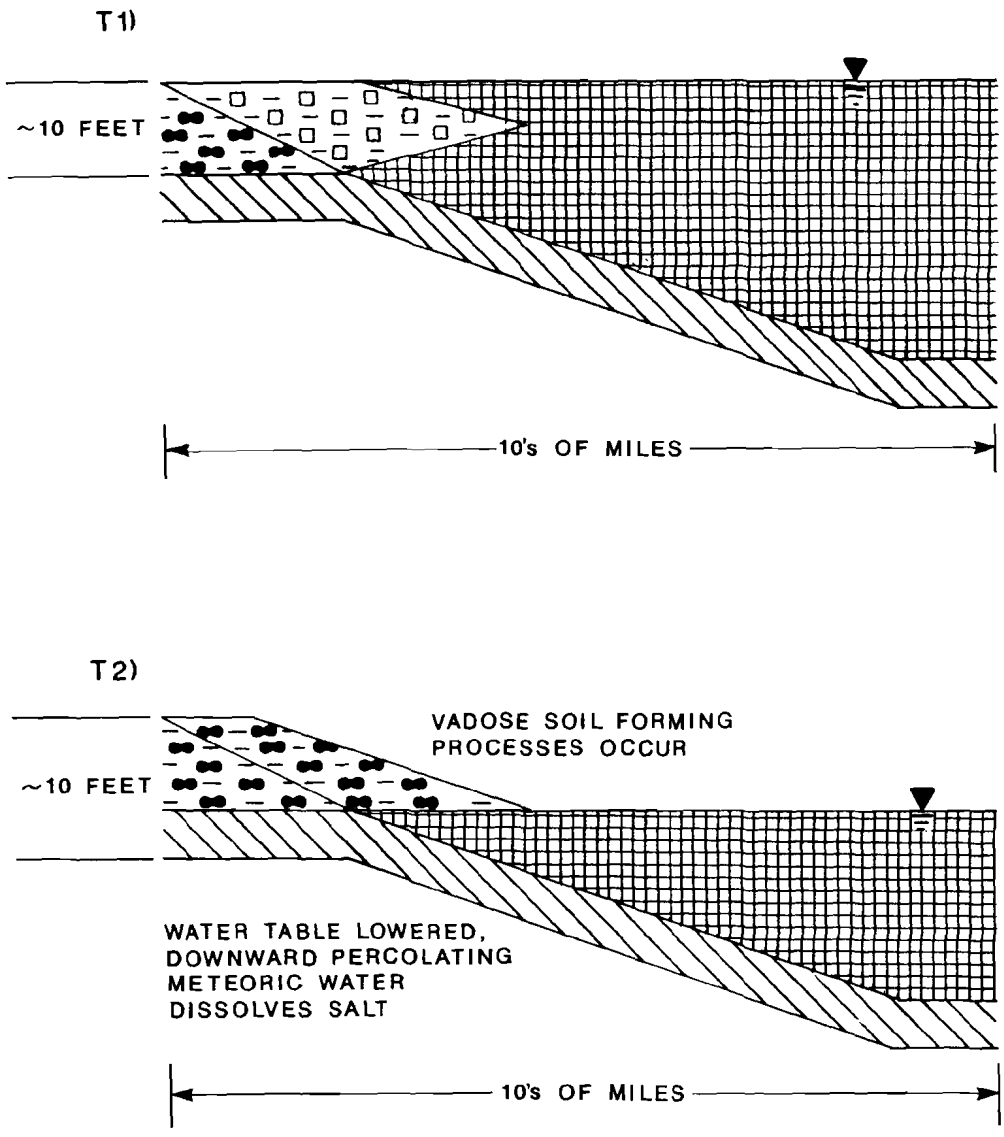

FIGURE 6.3

SYNDEPOSITIONAL DISSOLUTION
CAUSED BY LOWERING THE WATER TABLE

PREPARED FOR

WESTINGHOUSE ELECTRIC CORPORATION
CARLSBAD, NEW MEXICO

T1)

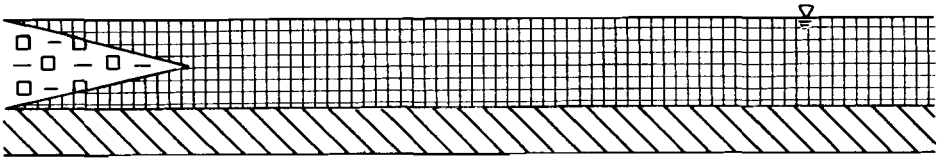

T2)

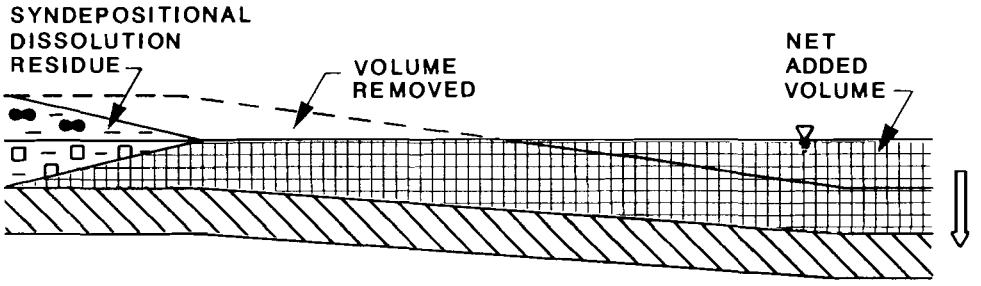

T3)

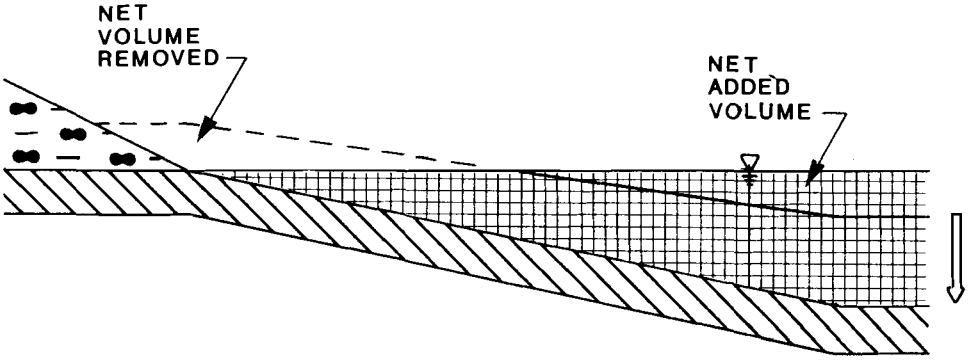

FIGURE 6.4

SUBSIDENCE-CONTROLLED
MODEL FOR SYNDEPOSITIONAL
DISSOLUTION AND REDISTRIBUTION OF HALITE FROM
THE BASIN MARGIN TO THE DEPOCENTER

PREPARED FOR

WESTINGHOUSE ELECTRIC CORPORATION
CARLSBAD, NEW MEXICO

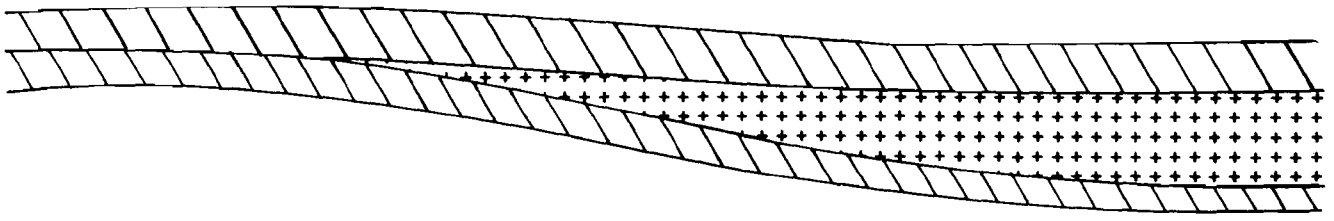

CONSISTENT DIPS, GRADUAL? THINNING: DEPOSITIONAL MARGIN

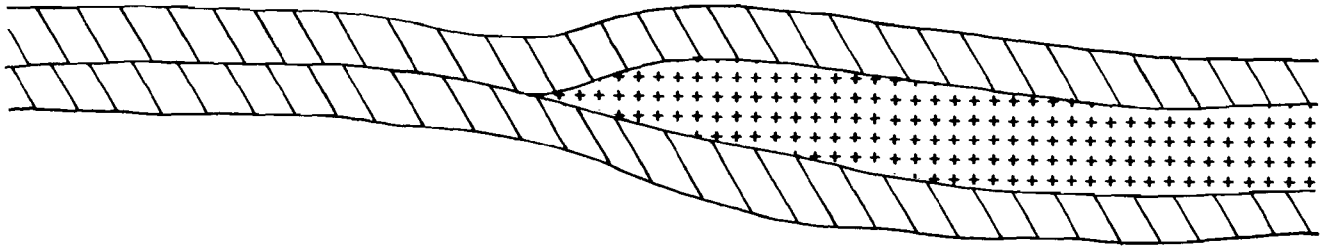

REVERSAL OF DIPS, MORE ABRUPT THINNING: DISSOLUTION MARGIN

After Gorrell and Alderman (1968)

FIGURE 7.1

GENERAL BASIN MARGIN RELATIONSHIPS:
DEPOSITIONAL vs DISSOLUTION

PREPARED FOR

WESTINGHOUSE ELECTRIC CORPORATION
CARLSBAD, NEW MEXICO

a. KARST

UPPER HORIZON CONTROLLED, BRECCIATION MAY INCREASE UPWARD, MIXING OF STRATA IN CLASTS, TRUNCATED UPPER SURFACE BOUNDING AGE

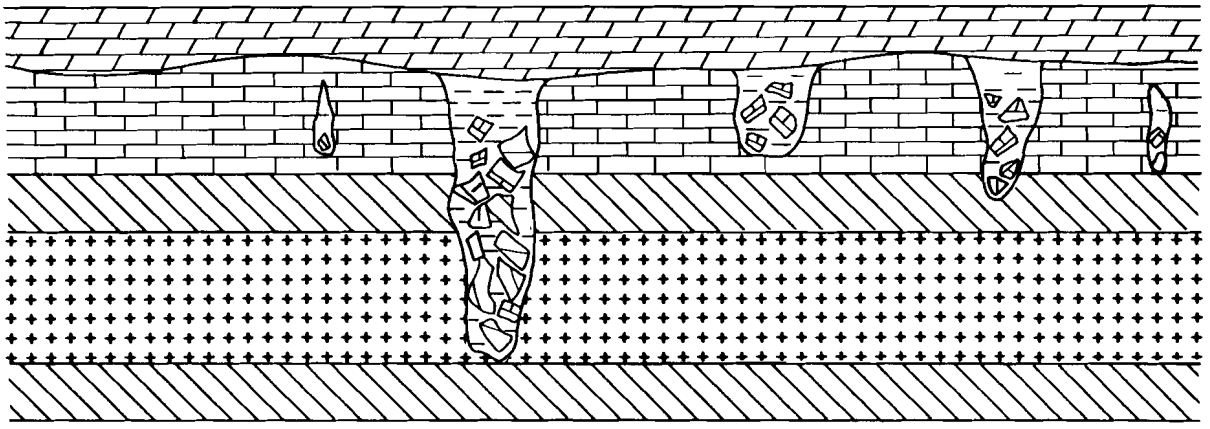

b. SOLUTION

LOWER HORIZON-CONTROLLED, BRECCIATION DECREASES UPWARD, STRATIGRAPHIC RELATIONS INTACT, POST-DEPOSITIONAL, POST-LITHIFICATION SOLUTION ("LATE")

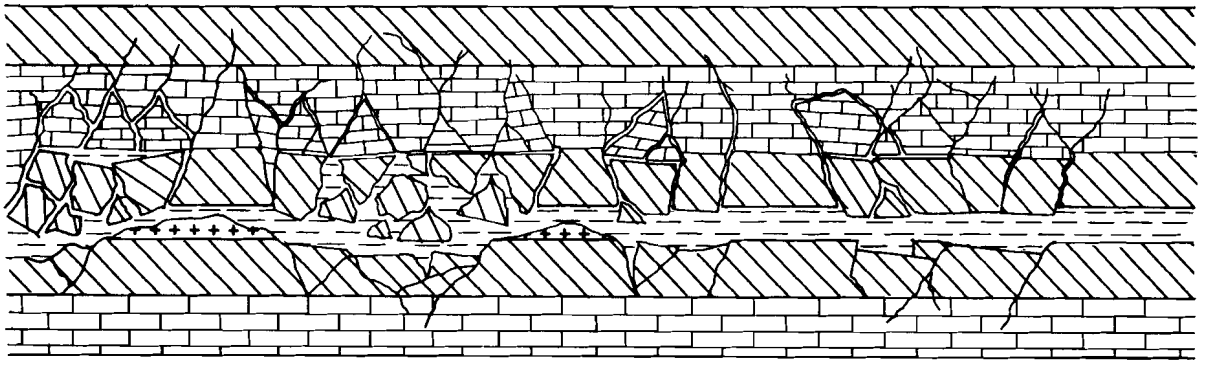

(NOT TO SCALE)

NOTE: SYMBOLS DO NOT REPRESENT SPECIFIC LITHOLOGY

FIGURE 7.2

GENERAL MID-STAGE FEATURES PRESERVED FOR KARST AND SOLUTION AT DEPTH

PREPARED FOR

WESTINGHOUSE ELECTRIC CORPORATION
CARLSBAD, NEW MEXICO

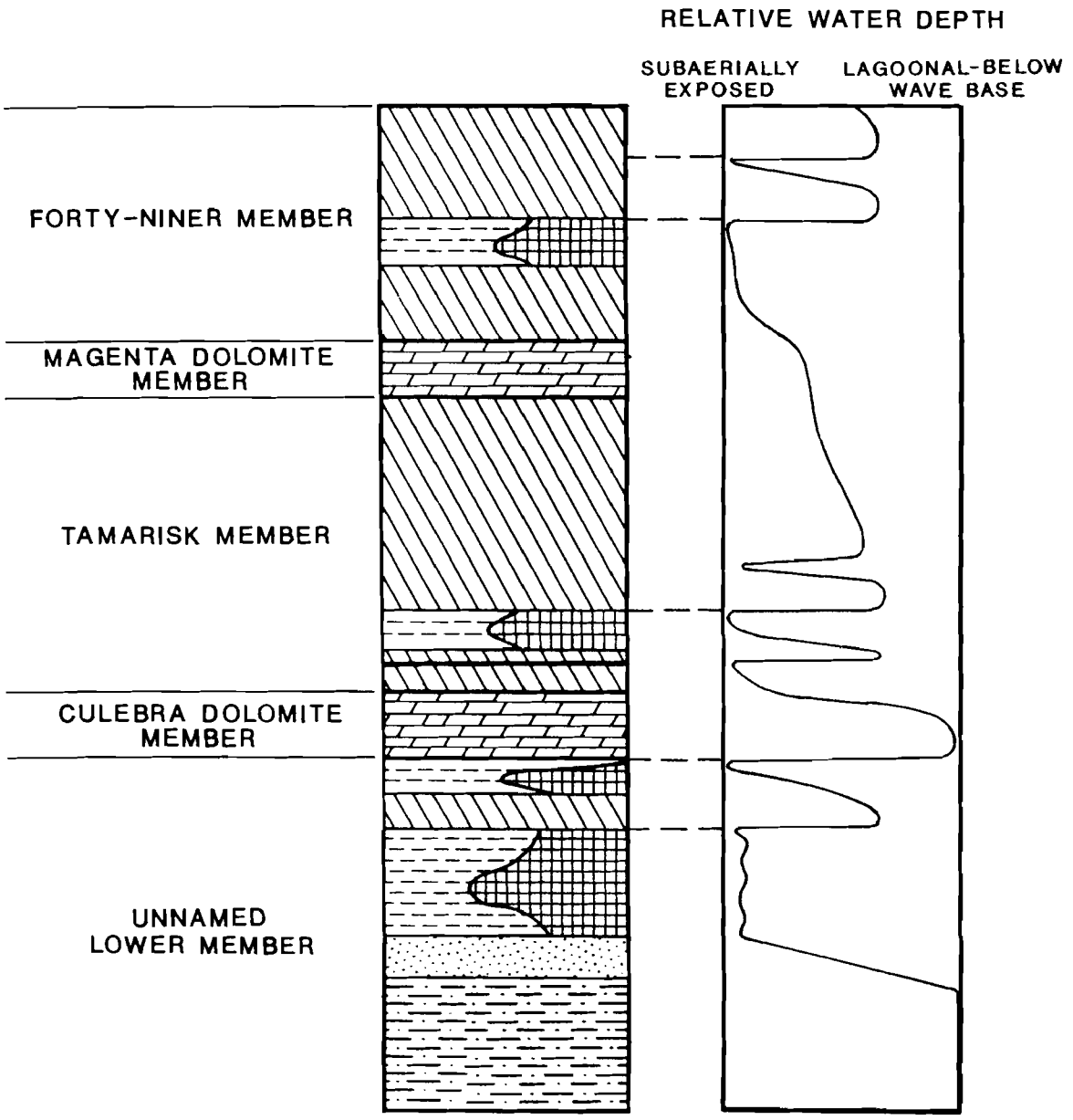

FIGURE 9.1

VARIATION IN
RUSTLER WATER DEPTH

PREPARED FOR

WESTINGHOUSE ELECTRIC CORPORATION
CARLSBAD, NEW MEXICO

Plate 1. Brecciation within the unnamed lower member showing vertical translation of rocks derived from various stratigraphic intervals. Clasts from the bioturbated clastic interval, M-1, and A-1 are all in close proximity.

Plate 2. Displacive halite in siltstone from M-1.

Plate 3. Displacive halite crystals that have coalesced and are tightly packed.

Plate 4. A pod containing an aggregate of halite crystals.

1

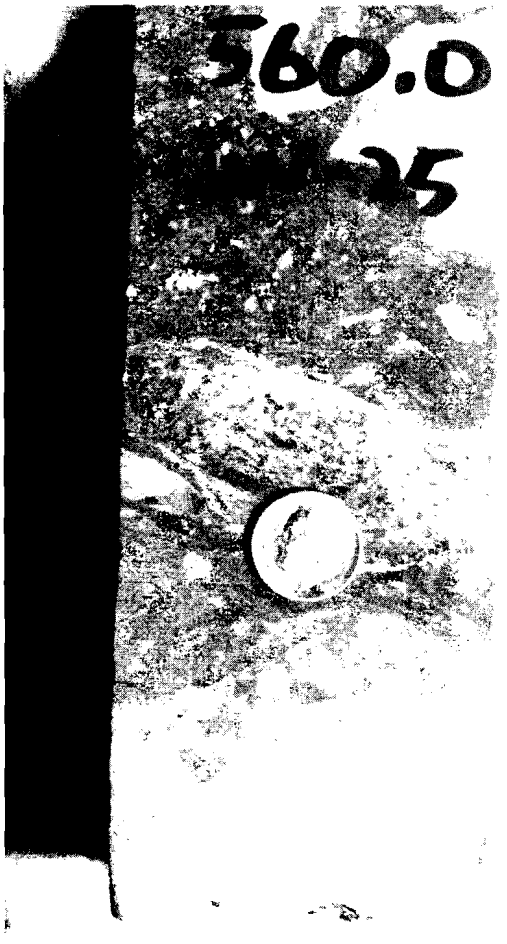

2

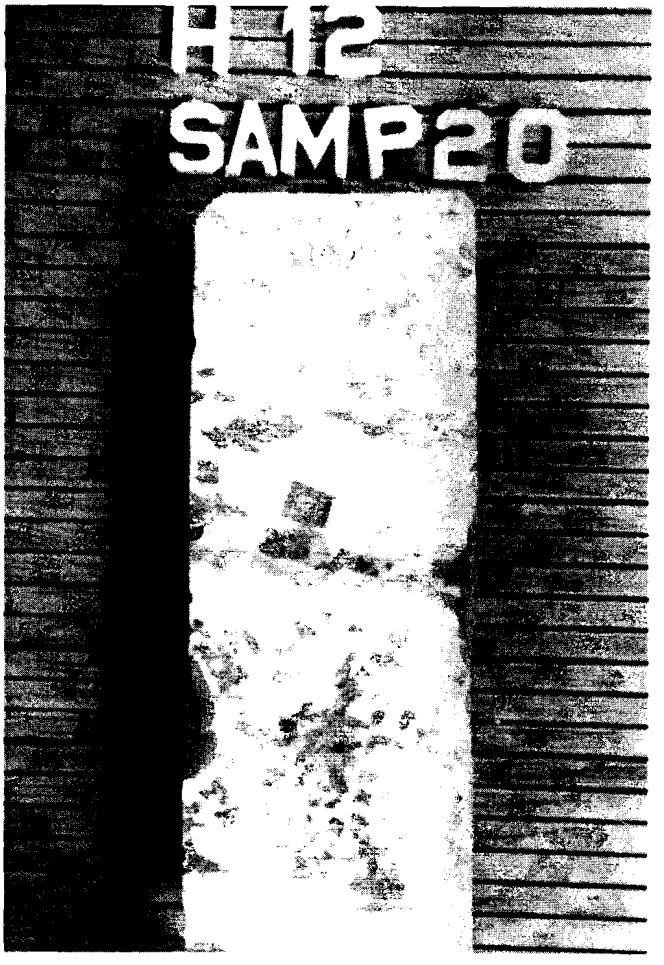

3

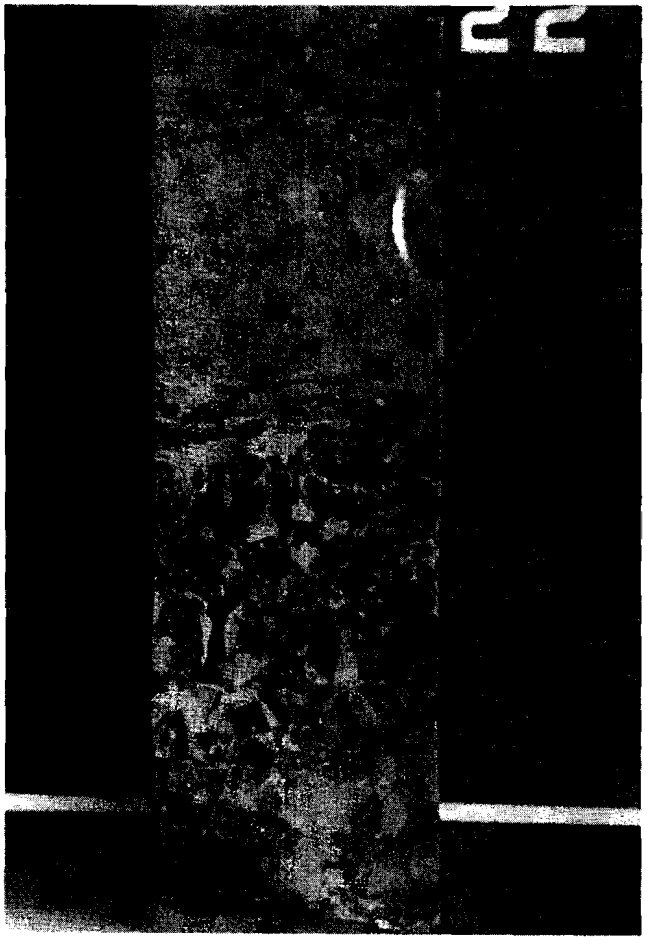

4

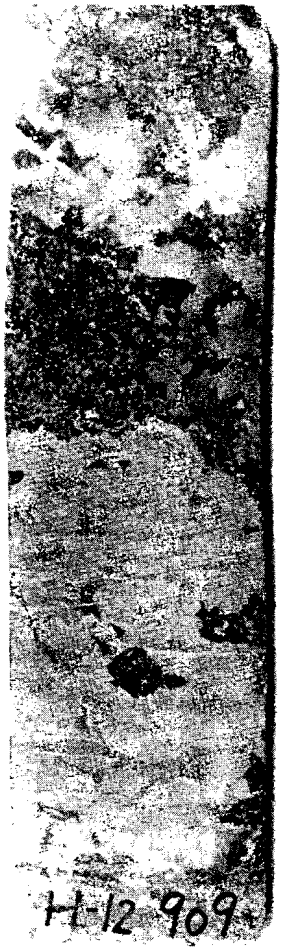

Plate 5. Clastic material contained within halite exhibiting the smeared intraclast/laminae texture.

Plate 6. Siltstone and mudstone from M-1 exhibiting the smeared intraclast/laminae texture.

Plate 7. Smeared intraclast/laminae texture from M-1.

Plate 8. Brecciation in Nash Draw showing vertical translation of clasts derived from A-1 into the stratigraphic position of M-1. Note the clast in the lower center of the photograph is a derived from a gypsum fracture filling.

5

6

7

8

Plate 9. Breccia clasts and blocks of M-1 from Nash Draw. Note the clasts and blocks exhibit the smeared intraclast/laminae texture.

Plate 10. Halite pseudomorphs after gypsum swallowtail crystals, A-1.

Plate 11. Sediment-incorporative gypsum crystals in M-2.

Plate 12. Photomicrograph from M-2 showing oriented clay skins and cutans on mudstone particles.

9

10

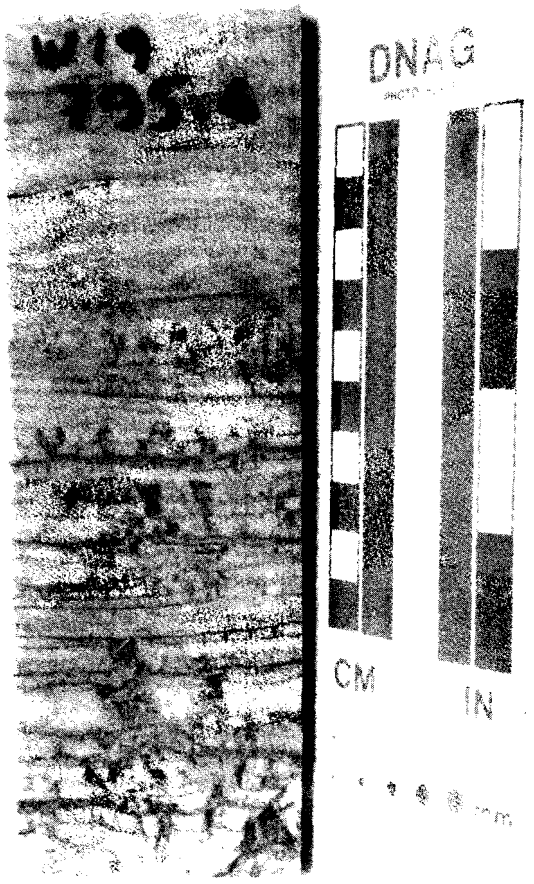

11

12

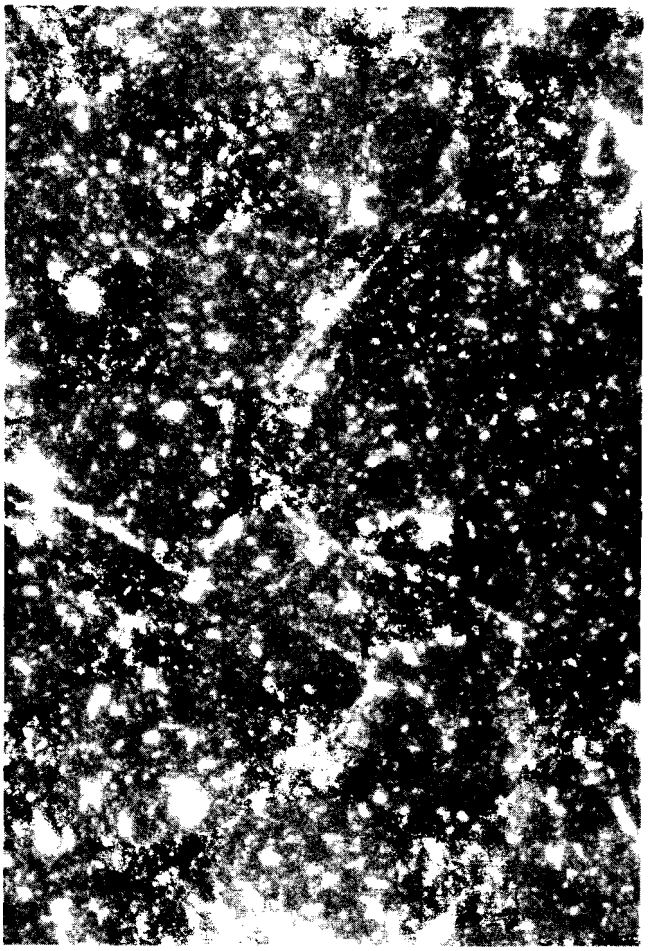

Plate 13. Pebbles of carbonate overlain by subhorizontal laminae in the upper part of M-2.

Plate 14. The upper contact of A-2 with M-3 in the waste handling shaft showing three feet of relief.

Plate 15. Photomicrograph of gypsum overgrowths on detrital gypsum grains, from M-3.

Plate 16. Siltstone and claystone pebble conglomerate in the lower part of M-3 at WIPP 19.

13

14

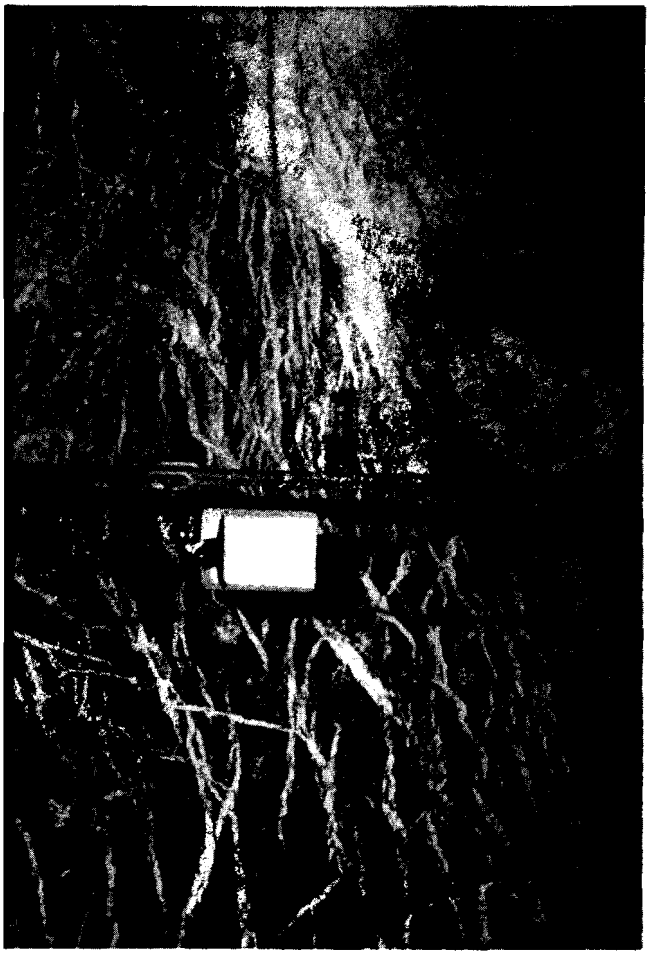

15

16

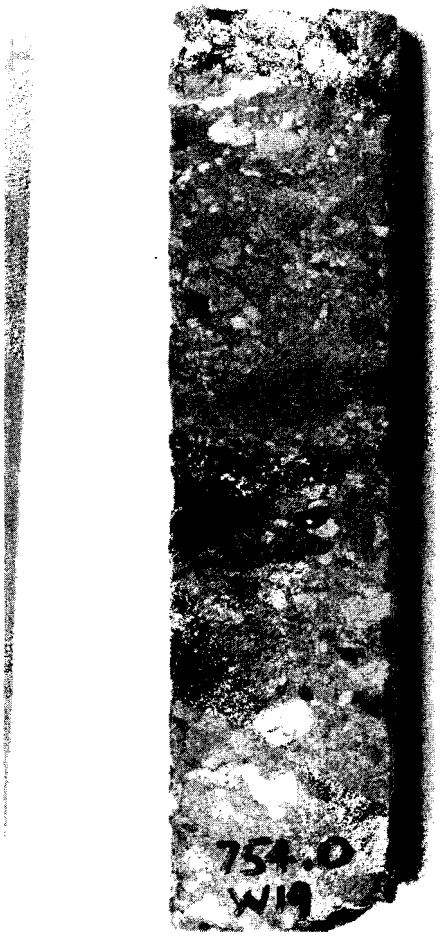

Plate 17. The upper contact of M-3 with A-3.

Plate 18. Tipped and slumped anhydrite pseudomorphs after gypsum swallowtail crystals near the base of A-3.

Plate 19. Incipient development of the crushed prism texture. Note relict halite pseudomorphs after gypsum swallowtail crystals have reduced volume.

Plate 20. Middle stage in the development of the crushed prism texture.

17

18

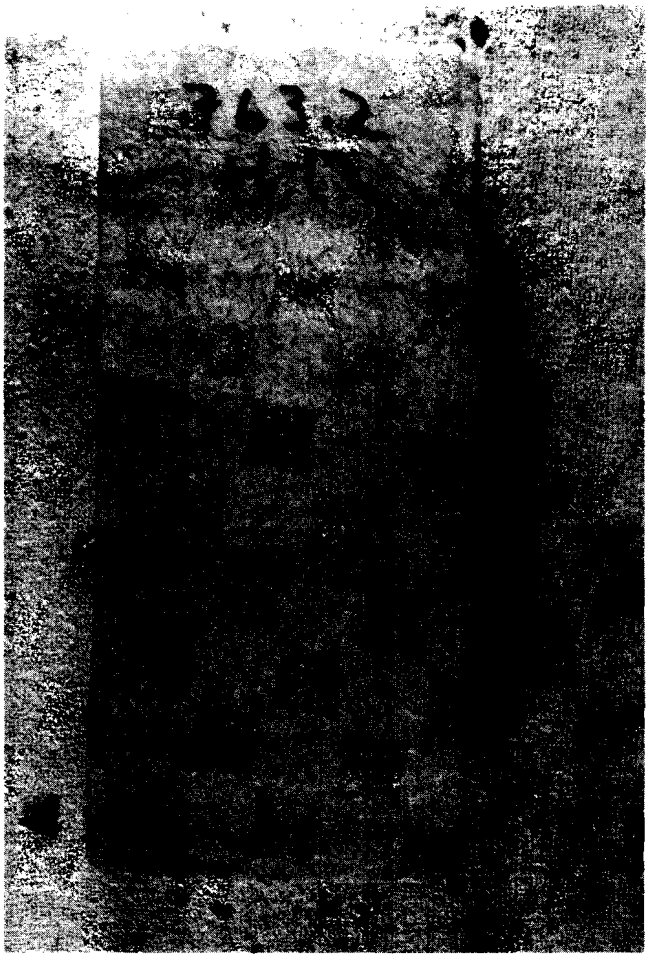

19

20

Plate 21. End-stage in the development of the crushed prism texture.

Plate 22. Bedded nodular texture in A-3. Note nodules containing small pseudomorphs after gypsum swallowtail crystals.

Plate 23. Photomicrograph of M-4 siltstone and sandstone from WIPP 19 with crossed nicols. Halite cement and incipient displacive halite crystals black.

Plate 24. Upper contact of M-4 with A-5.

21

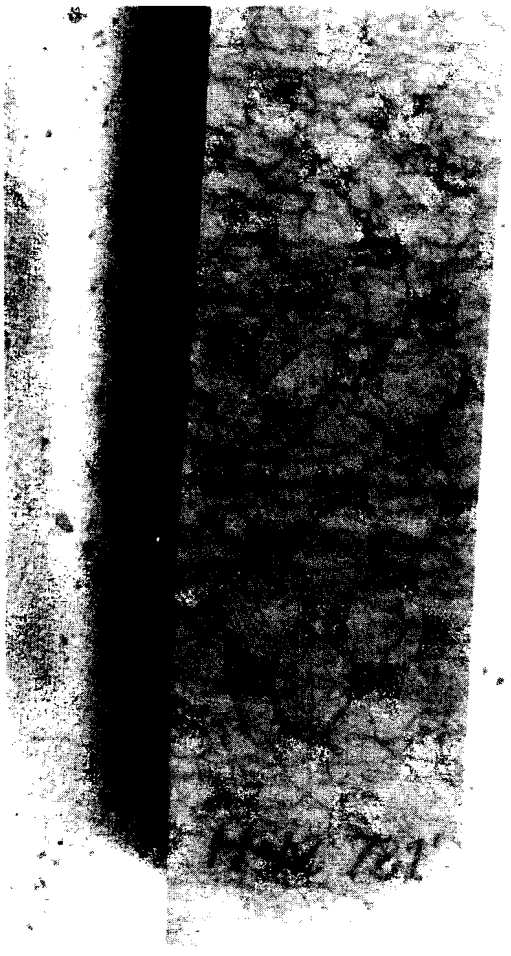

22

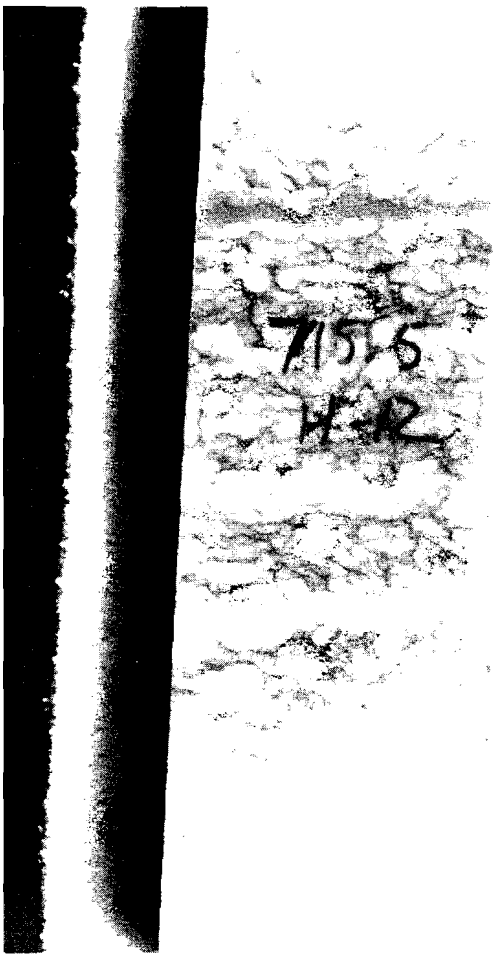

23

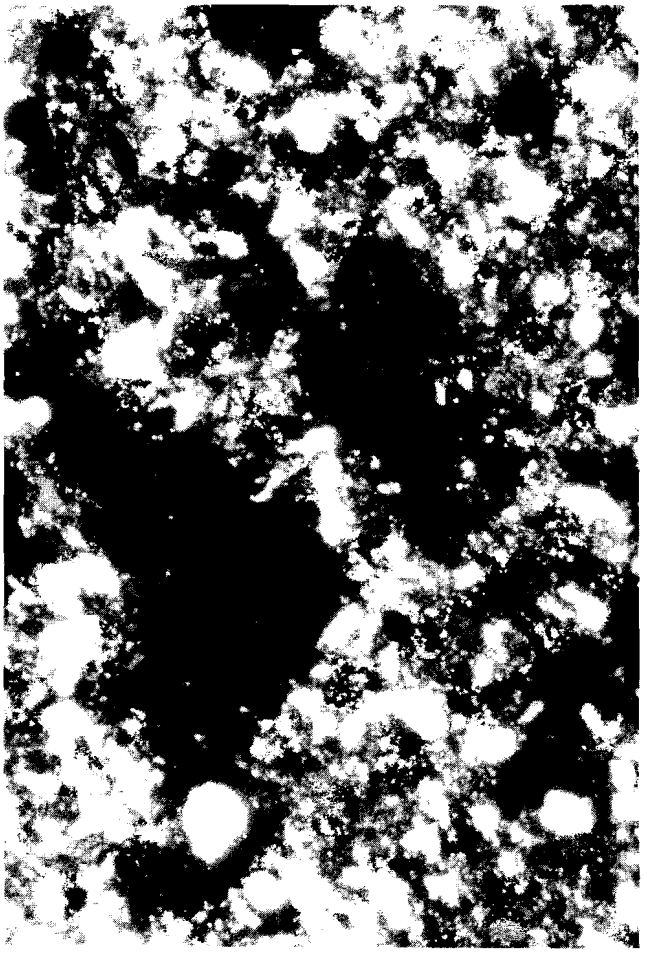

24

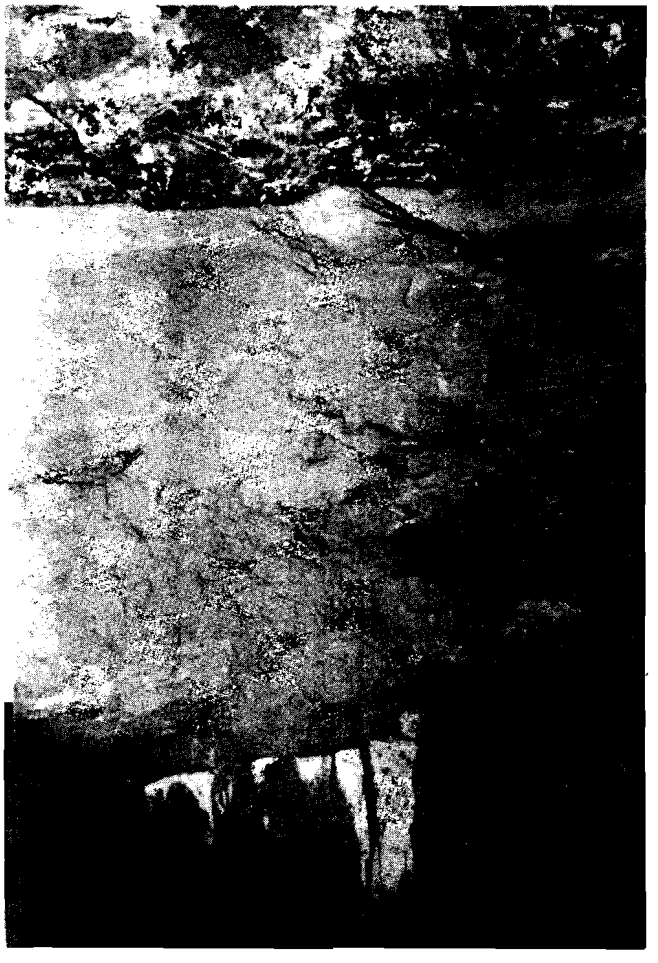

Plate 25. Irregular stratification in M-4 from WIPP 19.

Plate 26. Irregular stratification in mudflat sediments from Saline Valley, California.

Plate 27. Irregular subhorizontal stratification in M-4 at the waste handling shaft.

Plate 28. Irregular subhorizontal stratification in mudflat sediments from Saline Valley, California.

25

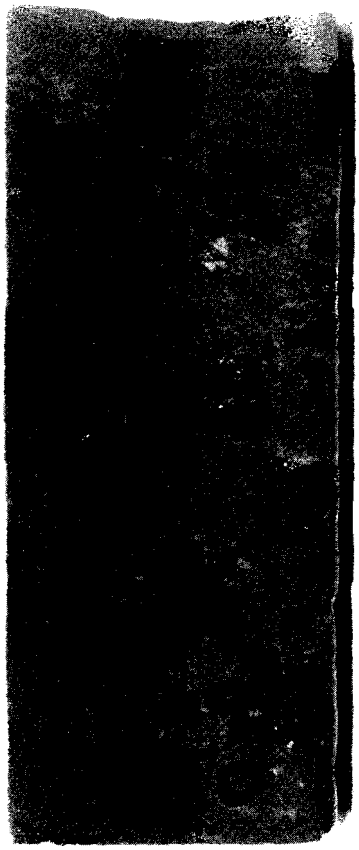

26

27

28

APPENDIX I

Interpretation of Geophysical Logs to Select Stratigraphic Horizons Within the Rustler Formation

INTERPRETATION OF GEOPHYSICAL LOGS TO SELECT STRATIGRAPHIC HORIZONS WITHIN THE RUSTLER FORMATION

Depth and Thickness Information

Geophysical logs from various boreholes for the WIPP project have been interpreted to represent the following stratigraphic markers: Rustler/Salado contact; base and top of Culebra Dolomite Member; base and top of Magenta Dolomite Member; and Rustler/Dewey Lake contact. For the Tamarisk Member, the contacts at the top of the lower anhydrite (A2) and base of upper anhydrite (A3) show regional thickness changes in a halite/mudstone unit of geological significance; we include these data as well (Ch. 4). Here we discuss the bases of our log interpretation for both stratigraphic and lithologic information and some factors that affect the accuracy and precision of the interpretations. The stratigraphy of the Rustler Formation is based on Vine (1963). Details of the Rustler vary, based on shaft mapping (Holt and Powers, 1984, 1986a) and this work.

The basic geophysical log for interpreting the Rustler stratigraphy is the natural gamma ray log (Fig. 4.1). Throughout much of the northern Delaware Basin, the contacts and members can be picked with confidence and good precision based on this log alone. In some areas, acoustic or sonic logs, for example, provide a sharp and significant response where the gamma log is not as sharp. In these interpretations, the gamma ray log was used as consistently as possible because it is the most common usable log and to avoid small registration problems that occur between logs, especially if the final log was a composite of two logs obtained at different times.

Lithologic Information

Specific lithologies may be interpreted through cross-plots of geophysical data for an interval. This procedure is well-known within the petroleum industry, and is adapted for computer with modern borehole geophysical records. A similar, though less mechanical, approach has been used for this report because we have only analog records. For more detailed lithological interpretation, we combined the natural gamma log with acoustic or sonic logs, density logs, or neutron logs, permitting most of the common lithologies to be discriminated. For the Delaware Basin proper, gamma ray-sonic was used nearly exclusively. Over parts of the Central Basin Platform, combined gamma ray-neutron logs are much more common. Gamma

ray-density logs are much less common in the region than at the site and were sparingly used. The common lithologies and their signatures for the Rustler are given in Table 1.

In the vicinity of the WIPP site, log signatures may be matched with descriptions from shafts (Holt and Powers, 1984, 1986a), basic data reports (e.g. Sandia National Laboratories and U. S. Geological Survey, 1980), and redescribed cores from holes with geophysical logs. Examples of the match between detailed logs and core and shaft descriptions form a "type" against which most log interpretations were made. Some of the interpretations here vary from those made previously (Borns and Shaffer, 1985; Griswold, 1977) because of differences in criteria and the details of lithology now available (Ch. 5).

Accuracy and Precision

For stratigraphic interpretation, copies of logs at a scale of 1" = 100 feet were most commonly available and were used, providing a consistent data base. Lines drawn to mark contacts cover about 1 foot, and precision associated with these lines can probably be no better than about 1 foot. The numbers presented are visual interpolations representing a variation estimated at about $\pm$ 1 ft., not allowing for other sources of "error".

The sum of geologic variations and "errors" has been assessed empirically by examining the cluster of data points in T.25S., R.32E. (Ch. 4). The isopachs of four members and part of one member provide data to calculate average thickness as well as sample standard deviation s (Table 2). A plot of thickness vs s partially reveals the effects of these errors (Fig. 1). The relative standard deviation generally decreases as thickness increases. This reflects the compensating effects of sedimentation over time for small, possibly random, local variations in depositional processes. The standard deviation is less than 10 % of the total thickness for the four thicker intervals. For the two intervals averaging less than 25 ft thickness, the standard deviation exceeds 10%. A least squares regression of s (Y) on average thickness (X) (Fig. 1) provides an intercept (b_o) of 3.5 on Y. This intercept is consistent with "errors" of about $\pm$ 1 foot on each contact as previously described. The remaining difference (that part > 3.5 ft) is more likely attributable to geological processes. Though a linear regression of standard deviation on thickness has been calculated, the data points are

probably also consistent with the idea expressed above that greater thickness is related to exponentially smaller standard deviations as a consequence of compensating sedimentologic conditions over a longer period of time.

We may not truly generalize about thicknesses of individual members for the region from the example above, as as it is obvious that some units (e.g. between A2 and A3 of the Tamarisk) vary greatly over the region compared to T.25S., R.32E. However, the "error" associated with picking an individual contact is estimated. An "error" of the type where a mistake in elevation or zero point occurs is not analyzed in this example, as the data are the difference between two successive contacts and will be immune to those two types of errors.

Powers (1986) examined geophysical logs from hydrologic holes at and near the WIPP site, showing that interpreted stratigraphic picks of a horizon from various logs of the same borehole usually vary by 2 feet or less. There is no assurance in some of these cases which is the more accurate depth. For the most part, these small variations from log to log can be attributed to several types of factors such as differences in zero depth point. This kind of variation is usually unimportant for geological interpretations of either isopachs or structure contours. A $\pm$ 2 ft variation on both contacts could conceivably result in an 8 ft discrepancy in thickness between adjacent boreholes. This is unlikely, as common practice here and elsewhere is to compare adjacent logs frequently to minimize such discrepancies. Elevation/depth discrepancies are more important to resolve for the subtle questions of possible hydrologic transport in the Rustler.

Lithologic interpretations are not significantly affected by questions of accurate depths. A more important, and difficult to consider, problem is registration, especially if the log associated with gamma is a composite. Where there is no obvious problem with this particular log, the gamma ray with compensated acoustic (sonic) or compensated density is chosen as the standard over the combination gamma ray with neutron because the lithologic information from the first two combinations is usually more helpful than with neutron.

Geophysical logs contain inherent uncertainties. Stretch in the cable is usually predictable, about 1 foot/1000 feet. This is the same order of magnitude as the resolution for the tools (e.g. natural gamma and acoustic) which operate over a discrete interval or sample a certain volume. The

sharpness of a log response to a sharp change in geophysical properties is a function of this interval, the rate at which the tool is drawn through the borehole, and time constants for data acquisition. Gradual lithologic transitions decrease the sharpness of the response further. In general, lithologic transitions and sampling interval have been dealt with arbitrarily by picking a contact at the midpoint of the geophysical response, and by attempting to make a consistent log response the standard for each "pick." Inconsistent application of standard log signature or criteria leads to error. All logs were interpreted by one person (DWP) to minimize operator to operator inconsistencies in establishing the intervals and contacts, though operator bias may be unchecked by this procedure.

Several "random" factors contribute to errors. Incorrect placement of the logging tool relative to a reference elevation (the zero point referred to above) appears to have occurred on some logs (e.g. compensated neutron, gamma ray for H-9c; Powers, 1986). Incorrect base elevations and locations may occur, but only gross errors will be detected in this study. Log reading errors may occur; they are most easily found through multiple logs of a single borehole and through structure contour and isopach map anomalies.

Further Remarks

No attempt has been made to rectify differences with other interpretations. Minor differences on picks are here of little consequence. Major anomalies may be resolved as necessary by re-examining logs and picks or by obtaining additional logs from the vicinity of the anomaly.

Geophysical well log data are used routinely within industry to infer rock properties. Doveton (1986) summarizes common approaches to log interpretations, but the limitations and problems associated with precision and accuracy of interpretation are not well addressed. The mechanical precision associated with the geophysical tool is commonly considered. For the hydrological studies of the WIPP, the uncertainties beyond mechnical precision can be important, and here we have presented information and analysis of log information that should provide perspective on this problem. Baker (1987) examines methods of quantitative interpretation that integrate geological and geophysical log data. Such approaches will be very helpful in assessing data, and the associated uncertainties, that will be used in complicated numerical codes for hydrologic modeling.

TABLE 1

General Log Responses for Rustler Lithologies

lithology	natural gama (std API units)	sonic travel time (micro-sec/ft)	neutron (API units)
anhydrite	low (<10 API)	high (50)	high
salt	low (<10 API)	medium (70)	variable
dolomite	variable (10-50)	variable (50-90)	variable
siltstones	variable (10-50)	low (>70)	low
gypsum	low (<10)	medium (70-80)	low
polyhalite	very high (50-150)	med to high (50)	med to low

TABLE 2

Statistical Summary of Isopach Data, T.25S., R.32E.

Isopach Interval Name	Number of Data Points	Average Thickness (ft)	Sample Standard Deviation(s)
Forty-niner	83	63.7	4.12
Tamerisk	82	102.8	8.55
A2-A3 of Tamerisk	78	13.0	4.58
Culebra	83	24.5	2.76
1. unnamed mbr.	82	151.9	12.3
Rustler	82	364.6	16.8

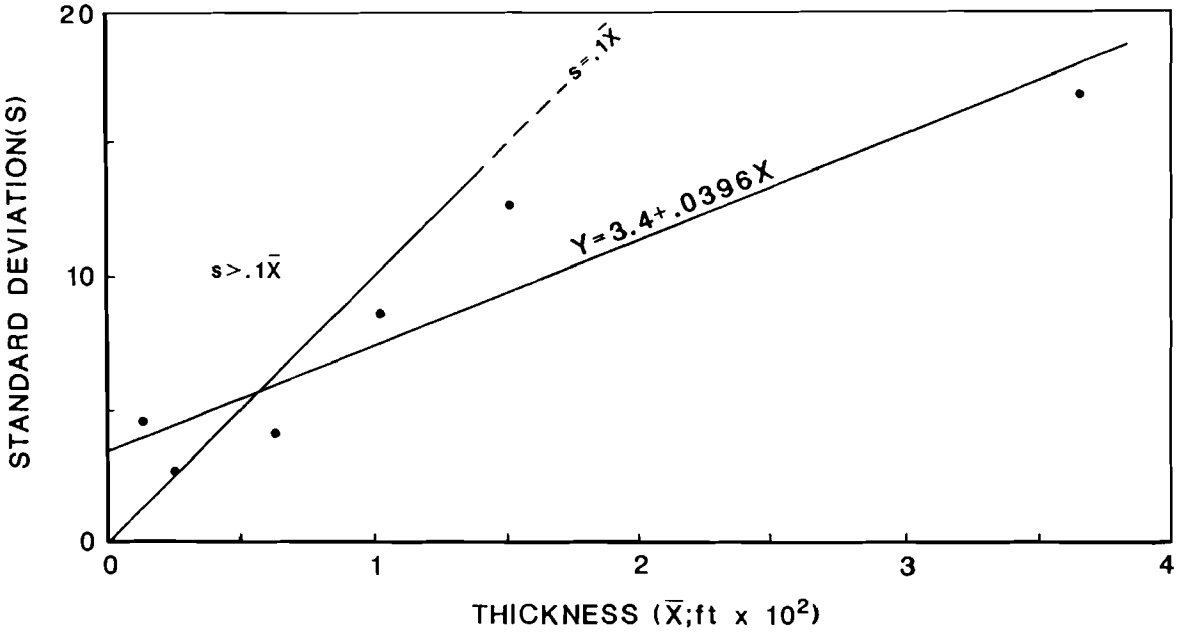
20
10
0
0
1
2
3
4
STANDARD DEVIATION(S)
THICKNESS ($\bar{X}$;ft x 10^2)
$s=.1\bar{X}$
$s>.1\bar{X}$
$Y=3.4+.0396X$

GEOPHYSICAL LOG DATA

Well Identifier	Name of well	Location	Ref. Elev.	Top S	Top u.l.	Top C	Top T	Top M	Top F-N
		T18S, R29E							
W04	Roach Drlg, West. Dev. Miller No. 1	s4,1980fnl,1980fwl	?	278	?	?	?	?	118
T19	Yates, Travis Fed.2	s19,660fsl,1980fel	3568	?	?	?	?	?	?
		T18S, R30E							
L18	Newmont, Loco Hills 21-B-6	s18,1650fnl,924fwl	3510	316	?	?	?	?	164
C25	Yates, Creek"AL"#1	s25,990fnl,330fel	3618	736	675	660	582	565	504
G26	Hanson, Ginsberg Fed. No. 11	s26,990fsl,330fel	3466	624	587	576	?	?	500
M27	Texaco, L.R. Manning "B" NCT-1 Well #20	s27,990fnl,1651fwl	3554	587	525	508	434	411	358
R28	Texaco, L.R. Manning Fed. "B" #4	s28,330fsl,1491fel	3510	557	483	468	396	375	314
		T18S, R31E							
M02	W. S. Montgomery, Magnolia State #1	s2,330fsl,660fwl	3766	1017	942	927	856	841	794
S11	Hudson&Hudson, Shugart B-1	s11,660fsl,660fwl	3733	990	913	902	824	808	757
M16	M. R. Voltz, Magnolia State 2	s16,1980fel,660fsl	3651	840	754	730	628	606	561
F22	Gulf, Fed. LIttlefield #1	s22,660fsl,660fwl	3648	?	?	?	?	?	?
F28	Gulf, Fed. Keohane et al "B" No. 1	s28,660fwl,1980fnl	3624	790	720	706	634	619	563
K28	Gulf, Fed. Keohane etal "B" #3	s28,1980fnl,1980fwl	3631	775	736	721	650	632	578
C31	Campana, Pure Fed. #1	s31,1980fnl,1980fel	3551	785	708	692	618	596	545
H31	R. M. Hall, Pure Fed. #1	s31,330fnl,844fwl	3568	735	663	648	576	555	500
M32	Chambers & Kennedy, Monterey State #4	s32,1980fnl,1980fwl	3566	810	734	720	640	622	574
S32	Sunray, State "Y" #1	s32,2310fel,1650fnl	3580	830	748	732	660	638	590
P32	L. T. Pate, Monterrey State #5	s32,330fwl,330fnl	3571	840	775	760	682	665	606
W33	V. S. Welch, Shugart No. 5-B	s33,330fnl,330fwl	?	828	775	759	687	670	613
		T18S, R32E							
J04	B. M. Jackson, Fed. #2	s4,1650fnl,990fel	3885	1394	1322	1302	1222	1207	1158
G16	Gulf, Lea State "HS" #3	s16,1980fnl,1980fwl	3783	1350	1275	1260	1168	1150	1103
J20	J. M. Beard, Young Fed. #5	s20,2310fsl,990fwl	3751	1247	1168	1157	1060	1044	1017
C28	Texaco, C. D. Unit No. 53	s28,1980fnl,660fwl	3382	1300	1137	1112	1019	996	940
		T18S, R33E							
C10	Carper, Corbin R #1	s10,1980fnl,660fel	4027	1828	1755	1743	1652	1634	1587
B12	Miller, B.A.State #2	s12,660fnl,1980fel	4104	1988	1915	1904	1815	1797	1753
D13	O'Neill, Dorothy Swigart #1	s13,1650fsl,2310fwl	3952	1880	1807	1796	1699	1682	1633
S28	Sunray, Fed. "E" #1	s28,center NE of SE	3800	1663	1588	1576	1479	1460	1407
H30	Penzoil, Hudson "29" Fed. #3	s30,1980fsl,1980fwl	3779	1546	1462	1447	1351	1330	1278

GEOPHYSICAL LOG DATA
(Continued)

Well Identifier	Name of well	Location	Ref. Elev.	Top S	Top u.l.	Top C	Top T	Top M	Top F-N
		T18S, R34E							
N01	Texaco, State of NM "M" #5	s1,560fnl,760fwl	4011	1677	1615	1602	1540	1525	1483
L06	Phillips, Lea No. 17	s6,989fnl,330fwl	4098	1843	1783	1774	1694	1675	1631
B07	Richardson & Bass, State of NM #1	s7,660fsl,660fel	?	2026	1947	1932	1842	1824	1775
S22	Cont., State V-22 #2	s22,1980fsl,1980fwl	4023	2075	1999	1985	1892	1872	1820
T22	Cont., State V-22 #1	s22,1980fwl,330fsl	4000	2050	1972	1960	1870	1852	1793
M33	Tom Brown, Marathon State #1	s33,330fsl,1980fwl	3957	1983	1905	1885	1793	1775	1714
		T18S, R35E							
F03	Phillips, Santa Fe No. 114	s3,2310fsl,330fel	3920	1968	1900	1885	1807	1794	1745
V04	Vac. Edge Unit #2	s4,1980fnl,660fwl	3961	1810	1750	1733	1658	1645	1600
F05	Phillips Pet., Santa Fe No. 111	s5,1650fnl,990fel	3962	1765	1705	1690	1619	1604	1562
S05	Phillips Pet., Santa Fe No. 93	s5,1650fnl,2285fel	3968	1744	1683	1668	1595	1580	1535
V05	Standard Oil of Tx, Vac Edge #19	s5,990fsl,990fel	3958	1814	1748	1737	1657	1643	1598
W06	Ohio Oil, State Waren Acct 2 #9	s6,330fsl,913fwl	3991	1678	1653	1647	1582	1566	1512
A07	Tidewater Oil, State AN #1	s7,330fnl,990fel	3980	1720	1657	1640	1562	1547	1501
C29	Carper, Carper-Luthy No. 1	s29,1980fnl,660fwl	3948	2112	2036	2022	1926	1908	1853
		T18S, R36E							
C01	Cactus Drilling, Catron "B" No. 2	s1,1980fsl,1980fel	3789	2038	1948	1945	1883	1870	1825
K11	J. M. Kelly, State J.J. #1	s11,660fsl,660fel	3816	2030	1943	1940	1870	1855	1811
P11	J. M. Kelly, State PE #1	s11,1980fsl,1980fwl	3822	2137	2050	2042	1969	1958	1909
C12	Cactus Drilling, Amerada State #1	s12,660fnl,1980fwl	3783	1997	1908	1904	1840	1828	1783
		T18S, R37E							
A14	Amerada, State W. H. "B" #2	s14,1650fsl,2310fwl	3698	1810	?	?	1700	1685	1643
W31	Amerada Pet., State WM "E" #3	s31,1980fnl,660fwl	3750	?	?	?	?	?	?
		T18S, R38E							
A03	O. D. Alsabrook, Saunders #1	s3,1980fsl,1980fel	3660	2168	2090	2084	2017	2007	1965
M19	Shell, Mckinley A-19 #1	s19,2310fsl,1650fel	3664	1653	?	?	1572	1560	1520
		T19S, R29E							
N06	Shamrock Drlg., Nix & Curtis #1	s6,1980fsl,1765fwl	3399	305	?	?	?	?	?

GEOPHYSICAL LOG DATA
(Continued)

Well Identifier	Name of well	Location	Ref. Elev.	Top S	Top u.l.	Top C	Top T	Top M	Top F-N
S21	W. J. Spears, Stout State #1	s21,2015fnl,1880fel	?	218	114	90	?	?	?
U26	W. J. Spears, Union State #1	s26,NW/4 of NW/4	?	245	142	120	?	?	?
		T19S, R30E							
P05	Yates, Perkins "AD" 3	s5,1980fnl,330fwl	3402	388	310	290	245	223	183
		T19S, R31E							
U06	Texaco, USA Fed. #1	s6,330fnl,1650fwl	3529	740	692	673	596	576	524
S13	Phillips, Simon "A" No. 1	s13,660fsl,1980fel	3577	978	873	853	764	745	682
S14	Phillips, Simon "A" #2	s14,660fsl,660fel	3559	898	796	775	702	685	619
T21	Texas Crude, Tenn. Fed. # 1-21	s21,1980fsl,660fel	3526	746	683	666	586	565	497
		T19S, R32E							
E29	Epng, Southern Cal. Fed. #1	s29,1980fnl,660fel	3576	1172	1064	1045	927	906	802
		T19S, R34E							
C12	Carper, U.S. Smelting State #1	s12,660fnl,660fwl	3974	2150	2063	2037	1940	1920	1855
		T19S, R35E							
A14	Atlantic Ref., State AU #1	s14,660fsl,660fwl	3815	2080	2000	1979	1884	1867	1805
S27	Shell, Allen Estate A #1	s27,1980fnl,660fel	3723	2045	1963	1944	1840	1822	1761
C28	Cabot Carbon, State G #1	s28,1980fsl,660fwl	3743	2052	1966	1950	1838	1818	1753
L33	Lea State BG #8	s33,1980fnl,660fel	3703	2080	1995	1970	1863	1845	1779
		T19S, R36E							
P01	Pan Amer., State "B" #1	s1,1980fnl,330fel	?	1680	1614	1604	1538	1525	1480
H11	Humble, N.M. State AO#1	s11,660fsl,1980fwl	3759	1704	1660	1650	1533	1517	1474
S18	Tom Brown, Sunray Bryan #1	s18,1980fnl,1980fwl	3744	2038	1955	1942	1841	1828	1777
A25	Amerada Pet., State "T" No. 4	s25,NE/4 of NW/4	3702	1446	1371	1363	1293	1280	1230
		T19S, R37E							
A32	Amerada, May Love Unit #1	s32,1980fsl,1980fel	3580	1397	1325	1320	1272	1257	1220
		T20S, R32E							
F10	Shell, Perry Fed. #1	s10,330fnl,990fwl	3448	1170	1068	1052	915	892	828
P15	Phillips, Plata Deep Unit #1	s15,1980fsl,1980fwl	3510	1236	1128	1112	972	949	883
		T20S, R33E							
B18	R. F. Montgomery, Bass STate #1	s18,660fnl,2080fwl	3524	1470	1362	1343	1194	1172	1103
S18	R. F. Montgomery, Bass State #2	s18,1650fnl,1650fwl	3509	1450	1335	1314	1165	1140	1076
		T20S, R34E							
L13	Marathon, Lea Unit #3	s13,1980fsl,1980fel	3677	2110	2009	1994	1830	1814	1743
F29	E.G. Colton, Fed. #1	s29,1980fsl,330fel	3720	1949	1847	1827	1660	1639	1567

GEOPHYSICAL LOG DATA
(Continued)

Well Identifier	Name of well	Location	Ref. Elev.	Top S	Top u.l.	Top C	Top T	Top M	Top F-N
		T20S, R35E							
B28	W. H. Black, Phillips State No. 1	s28,660fnl,660fel	3701	2315	2220	2208	2067	2048	1973
		T20S, R36E							
S02	Superior Oil, State "A" No. 2	s2,660fnl,1980fel	3603	1218	1143	1135	1062	1050	1005
U30	Union Oil of Cal, Sims State 1-30	s30,660fnl,660fwl	3662	2330	2227	2210	2073	2058	1985
		T20S, R37E							
H01	Humble Oil, N. M. State "AG" No. 6	s1,990fnl,1650fwl	3604	1671	?	?	1516	1505	1465
		T20S, R38E							
W27	Cont. Oil, Warren Unit "BT" No. 26	s27,660fsl,660fwl	3542	1635	1559	1551	1480	1470	1427
		T21S, R29E							
P03	Pan Amer., Big Eddy Unit #18	s3,1980fnl,1980fwl	3412	495	?	?	?	?	187
N04	Union Oil, Cowden Fed. #1	s4,4620fsl,1980fwl	3471	500	?	?	?	?	200
P05	Meadco, Harris-Bell #1	s5,1980fnl,600fel	3472	550	410	?	?	?	255
M05	Meadco, Harris-Bell #2	s5,980fnl,1880fwl	3468	740	608	?	?	?	445
M06	Meadco, Harris 6 #1	s6,3147fnl,660fel	3487	1145	1032	1012	915	895	830
P18	Pan Amer, Big Eddy Unit #16	s18,1980fsl,1980fel	3309	450	291	?	?	?	146
B22	P. R. Bass, Big Eddy Unit #40	s22,1980fnl,1980fel	3458	655	490	?	?	?	345
E34	Bass, Big Eddy No. 38	s34,660fnl,1980fwl	3444	505	?	?	?	?	200
		T21S, R30E							
D21	WIPP 27	s21,90fnl,1485fwl	3177	421	318	292	193	175	152
P26	Phillips, James "D" 1	s26,660fsl,1980fwl	3250	502	?	?	?	?	160
P35	Phillips, James "C" 1	s35,1980fsl,660fwl	3218	485	356	?	?	?	130
		T21S, R31E							
D18	WIPP 28	s18,99fnl,2401fel	3347	?	?	?	?	?	?
D33	WIPP 30	s33,667fnl,177fwl	3427	748	653	631	537	513	449
Q35	ERDA 6	s35,2152fsl,910fel	3540	811	739	713	623	598	538
		T21S, R32E							
F01	Kimball, Fed. #1	s1,660fsl,1980fwl	3792	1945	1840	1820	1645	1622	1550
E01	Phillips, ETZ Fed. #1	s1,3255fnl,1972fel	3748	1890	1785	1772	1598	1575	1505
P02	Amini, Pubco Fed. #1	s2,3300fnl,660fwl	3740	1950	1860	1838	?	?	1530
H02	Phillips, Hat Mesa "A" #1	s2,660fsl,1980fel	3793	1988	1862	1840	1665	1645	1568
N04	Amini, N.M. Fed. #1	s4,1683fnl,1650fwl	3668	1765	1570	1545	?	?	1345
G10	Superior, Government "H" Com. #1	s10,1980fnl,1980fel	3800	1885	1760	1734	1550	1525	1450
F11	Gackle, Fed. 1	s11,SE/4 of SE/4	3862	2005	1858	1837	1664	1642	1565
H11	Phillips, Hat Mesa 2 #2	s11,660fsl,1980fwl	3861	1947	1858	1833	1617	1593	1515

GEOPHYSICAL LOG DATA
(Continued)

Well Identifier	Name of well	Location	Ref. Elev.	Top S	Top u.l.	Top C	Top T	Top M	Top F-N
M11	Phillips, Hat Mesa #1	s11,1980fnl,1980fel	3834	1972	1857	1840	1654	1630	1555
S21	Skelly, Salt Lake South Unit #1	s21,660fnl,660fwl	3679	1455	1303	1282	1130	1110	1056
G26	Gulf, San Simon #1	s26,1980fnl,660fel	3798	1781	1635	1610	1382	1360	1293
H31	Gulf, H. T. Mattern #10	s31,660fnl,1980fwl	3504	?	?	?	?	?	?
U31	Union Carbide, AEC-7	s31,2040fnl,2040fel	3662	982	896	872	758	732	670
		T21S, R33E							
S02	C. Read, Sinclair State #1	s2,2310fsl,2310fwl	3802	2180	2055	2032	1858	1838	1760
		T21S, R35E							
W01	Amerada, State WE "F" #3	s1,660fnl,660fel	3565	1758	1668	1655	1526	1504	1455
N04	British Amer, N.M. State "F" #1	s4,1902fnl,660fwl	3638	2095	1997	1983	1843	1825	1757
C16	Cosden, Cosden State D #1	s16,660fsl,660fel	3603	2200	2092	2074	1917	1900	1825
R32	Resler & Sheldon, Phillips State "C" No. 2	s32,1650fnl,660fel	?	?	2105	2094	1896	1880	1804
		T21S, R36E							
C17	Atlantic Ref., Coleman #1	s17,1650fwl,990fnl	?	?	?	?	?	?	?
A21	Gulf, Arnott Ramsey "C" No. 5	s21,SE/4 of SW/4	3593	1670	1590	1582	1475	1464	1425
H26	Humble Oil, N. M. State "G" #14	s26,1980fnl,1980fwl	3550	1660	1579	1572	?	?	1420
A27	Gulf, Arnott Ramsey "C" No. 5	s27,SE/4 of SW/4	3593	1670	1589	1583	1478	1466	1426
R27	Gulf, W.A. Ramsey #39	s27,1980fsl,510fel	3545	1720	1640	1630	1527	1517	1486
G27	Gulf, W. A. Ramsy NCT A #42	s27,650fnl,1980fel	3568	1720	1640	1634	1527	1517	1476
L31	Late Oil, Rector A #1	s31,1980fnl,1980fel	3635	1900	1807	1799	1661	1642	1580
A33	Gulf, Arnett Ramsey NCT-D #2	s33,1980fsl,1980fel	3581	1817	1740	1735	1612	1600	1560
R34	Gulf, W.A. Ramsey #38	s34,1980fnl,660fwl	3580	1817	1732	1722	1614	1597	1555
		T21S, R37E							
C28	Gulf, J. N. Carson C#9	s28,2085fsl,765fel	?	1377	1305	1295	1219	1210	1167
M31	Gulf, N. T. Mattern (NCT) No. B-12	s31,1980fnl,660fwl	?	1368	1283	1275	1200	1190	1150
		T22S, R29E							
E06	Hudson, Eddy Fed. #1	s6,660fsl,660fel	3304	495	?	?	?	?	?
D33	WIPP 32	s33,1673fsl,29fel	3023	166	90	61	36	19	surf
D34	WIPP 29	s34,404fsl,1824fel	2977	130	43	-	-	-	-
		T22S, R30E							
T01	Tropora, Cabana #1	s1,990fsl,1980fwl	3357	625	515	495	400	380	315
M02	Phillips, James "A" #1	s2,665fsl,2006fel	3193	520	?	?	?	?	170
D11	Phillips, James "E" #1	s11,1980fnl,1980fel	3221	600	?	?	?	?	275
D13	WIPP 33	s13,1762fsl,2426fwl	3323	677	578	550	468	449	401
D15	WIPP 25	s15,1852fsl,2838fel	3212	565	472	447	328	302	232
P24	P - 14	s24,312fsl,613fwl	3358	686	595	576	477	452	387
O24	P - 12	s24,167fnl,195fel	3376	747	656	636	544	519	462
B27	Richardson & Bass, Fed. Legg #1	s27,660fnl,2003fel	3309	535	?	?	?	?	215

GEOPHYSICAL LOG DATA
(Continued)

Well Identifier	Name of well	Location	Ref. Elev.	Top S	Top u.l.	Top C	Top T	Top M	Top F-N
D29	WIPP 26	s29,2232fnl,12fel	3152	306	208	187	99	79	12
		T22S, R31E							
C06	B. McKnight etal, Campero No. 1	s6,1980fnl,660fwl	?	708	591	572	479	454	395
Z08	DOE 2	s8,698fsl,122fel	3418	962	849	828	724	700	641
D09	WIPP 11	s9,712fnl,294fwl	3439	964	881	857	764	740	676
I09	WIPP 14	s9,97fsl,2104fel	3249	952	836	817	729	707	639
W09	WIPP 34	s9,202fsl,1000fwl	3433	973	860	834	740	716	657
A11	AEC 8	s11,935fnl,1979fwl	3541	990	873	848	750	727	668
P14	P - 20	s14,794fsl,103fel	3553	1100	979	957	866	839	780
B15	C. W. Williams, Badger Unit - Fed. No. 1	s15,1980fsl,1980fwl	3496	?	?	?	?	?	?
H15	H - 5c	s15,1006fnl,134fel	3508	1041	922	900	809	784	732
P15	P - 21	s15,852fnl,150fel	3510	1040	924	904	812	786	734
D17	WIPP 13	s17,2564fsl,1727fwl	3405	845	725	704	583	564	517
P17	P - 5	s17,202fsl,164fel	3472	946	827	808	710	685	623
W17	WIPP 12	s17,175fsl,84fel	3484	966	848	825	727	703	641
H18	H-6c	s18,209fnl,375fwl	3349	-	632	612	515	492	427
P18	P - 13	s18,125fnl,116fwl	3345	720	628	608	513	490	426
D20	WIPP 21	s20,1451fsl,10fel	3417	867	752	732	641	617	559
I20	WIPP 19	s20,2986fsl,50fel	3433	894	777	756	672	647	590
S20	WIPP 18	s20,4306fsl,50fel	3457	928	810	791	698	674	614
W20	WIPP 22	s20,2547fsl,50fel	3426	885	763	742	654	630	574
Q20	ERDA 9	s20,267fsl,177fel	3420	860	739	716	632	608	550
P20	P - 3	s20,3122fel,103fsl	3382	783	665	645	553	528	468
O23	P - 19	s23,2330fwl,1652fsl	3546	1116	995	972	839	816	759
P23	P - 11	s23,175fnl,177fwl	3506	1058	938	916	823	799	746
W23	Texas Crude, Wright Fed. #1-23	s23,330fsl,330fel	3596	1190	1038	1018	856	830	755
O26	P - 18	s26,797fel,134fsl	3479	1084	936	912	728	703	626
P26	P - 10	s26,2315fnl,339fwl	3508	1084	957	935	781	758	686
P28	P - 4	s28,1487fel,146fsl	3441	928	802	782	685	662	610
O28	P - 2	s28,172fel,125???	3478	1008	884	864	774	748	690
DOE 1	DOE 1	s28,182fsl,610fel	3473	977	851	829	745	722	668
H29	H-14	s29,372fsl,562fwl	3345	-	-	-	446	422	357
L29	H-1	s29,623fnl,1083fel	3398	7	?	?	?	?	?
P29	P - 1	s29,551fwl,327fsl	3345	676	567	546	448	424	359
R29	H-2c	s29,770fnl,3584fel	3377	-	647	627	542	516	457
Y29	H-3	s29,3200fnl,140fel	3395	826	700	680	590	565	509
P30	P - 6	s30,199fwl,2767fsl	3354	656	560	540	442	418	358
P31	P - 15	s31,184fwl,398fsl	3310	542	436	420	322	296	232
H33	H-11	s33, ?, ?	3409	-	754	731	638	613	557
P33	P - 9	s33,143fel,1493fsl	3409	880	758	738	644	617	562
		T22S, R32E							
T13	Ray Smith, B&H Fed. 1	s13,660fsl,660fel	3644	1275	1125	1100	942	920	860
C14	Carper Drilling, #2 Red Tank Unit	s14,660fsl,1980fwl	3731	1290	1165	1140	1025	1005	950
C17	Cleary Pet, Fed. 1-17	s17,1980fsl,1980fel	3701	1200	1103	1072	960	940	885

GEOPHYSICAL LOG DATA
(Continued)

Well Identifier	Name of well	Location	Ref. Elev.	Top S	Top u.l.	Top C	Top T	Top M	Top F-N
T18	J.H. Trigg, Fed. Jennings 1-18	s18,660fsl,660fel	3696	1230	1110	1090	980	955	900
B19	R. Lowe, Bass Fed. #1	s19,660fsl,660fel	3620	1245	1090	1070	860	835	760
M20	R.J. Zonne, #1 Federal	s20,1980fnl,1980fel	3640	1240	1110	1080	920	895	835
T22	J. Trigg, Fed. Red Tank Unit # 1-22	s22,1980fnl,660fwl	3687	1265	1125	1100	960	935	870
A25	Gulf, Covington "A" Fed. #1	s25,660fnl,1980fwl	3789	1462	1315	1285	1140	1115	1048
T36	Richardson&Bass,State "AQ" #1	s36,660fnl,660fel	3756	1608	1460	1430	1230	1210	1145
		T22S, R34E							
H01	Humble, N.M. State BS #1	s1,1980fsl,660fel	3640	2160	2030	2000	1805	1785	1715
N08	Sunry, N.M. State "AE" No. 1	s8,660fsl,1980fel	?	2092	1942	1918	1700	1682	1600
H10	Allison Fed. No. 1	s10,1980fnl,660fel	3573	2185	2032	2005	1795	1778	1690
		T22S, R35E							
J01	British Amer, Jalmat Deep #1	s1,660fsl,660fwl	3611	2225	2112	2102	1915	1900	1822
D03	Western Drilling, Donegan State No. 1	s3,660fnl&660fwl	3613	2285	2160	2148	1952	1936	1856
A04	Ashmun & Hilliard, Skelly State No. 1 "U"	s4,660fsl,660fel	3611	2300	2175	2142	1955	1935	1860
S05	Skelly Oil, State "U" #1	s5,660fnl,660fel	3623	?	?	?	?	?	?
H09	Hudson, Humble State #1	s9,1980fsl,1980fwl	3581	2275	2142	2110	1905	1885	1810
B11	British Amer., Hall State "F" #9	s11,990fwl,660fsl	3610	?	2193	2180	1979	1960	1877
C20	Carper, Carper Aztec No. 1	s20,1980fnl,660fel	3533	2470	2322	2290	2020	2005	1920
H22	C. Hankamer, Humble State #1	s22,1980fel,1980fsl	3571	2292	2165	2130	1910	1890	1815
A23	Atlantic Ref., State "A" No. 1	s23,330fel,1980fsl	?	2210	2108	2098	1855	1840	1755
G35	J.M. Kelly, Gulf State 1-A	s35,660fsl,660fwl	?	2275	2142	2125	1877	1860	1770
		T22S, R36E							
L03	Gulf, H. Leonard No. 9	s3,660fnl,660fwl	?	1825	1735	1724	1611	1603	1560
G03	Gulf, H. Leonard No. 10	s3,1980fnl,1980fwl	3571	1822	1734	1722	1612	1603	1560
J04	Gulf, J.F. Janda NCT F#15	s4,1980fsl,660fel	3587	1825	1739	1728	1620	1610	1567
S09	Sinclair, State 157 A #3	s9,660fsl,660fel	3540	1687	1600	1590	1480	1472	1424
G09	Sinclair, State 157 A #4	s9,1980fsl,660fel	3552	1725	1641	1632	1517	1508	1465
W10	Western Natural Gas, Record #2	s10,560fsl,660fwl	3560	1735	1645	1637	1528	1517	1475
A17	Cont., Arrowhead Deep Unit #1	s17,1980fnl,1980fwl	3582	1685	1588	1572	1430	1420	1360
C19	Cities Svc., Closson "B" #14	s19,660fnl,330fwl	3589	2008	1890	1875	1700	1678	1602
C23	Shell, Christmas #A-2	s23,660fsl,660fwl	3507	1805	1715	1700	1588	1578	1535
A33	Atlantic Ref., J. L. Selby No. 2	s33,1980fnl,1830fwl	3498	1683	1575	1562	1427	1415	1360

GEOPHYSICAL LOG DATA
(Continued)

Well Identifier	Name of well	Location	Ref. Elev.	Top S	Top u.l.	Top C	Top T	Top M	Top F-N
M36	Ohio Oil, State McDonald A/C 1-B #11	s36,2310fnl,330fwl	3469	1684	1594	1584	1474	1466	1422
		T22S, R37E							
W15	Amerada Pet., E. W. Walden No. 4	s15,NW/4 of SW/4	3410	1385	1305	1295	1180	1170	1125
R16	E. P. Campbell, R. E. Cole #1	s16,2310fsl,1650fel	3405	1360	?	?	1182	1173	1130
A36	Aztec Oil, State BD 36 #1	s36,1980fsl,1980fel	3316	1408	?	?	?	?	1190
		T22S, R38E							
W30	Western Oil Fields, Gulf Drinkard #2	s30,990fsl,330fwl	3337	1350	1268	1259	1170	1160	1123
		T23S, R28E							
M02	N. H. Wills, Martin & Pardue #1	s2,1560fsl,330fwl	?	?	?	?	?	?	?
C11	N. H. Wills, C. P. Pardue #1	s11,2316fsl,2390fwl	?	?	?	?	?	?	?
P17	Cities Serv., Polk "A" #1	s17,660fnl,2310fel	3045	?	?	?	?	?	?
		T23S, R29E							
N12	Mesa Pet., Nash Unit #3	s12,1980fsl,1980fwl	2996	?	?	?	?	?	?
M13	Mesa Pet., Nash Unit #4	s13,990fnl,330fel	3014	195	?	?	?	?	?
P13	Mesa Pet., Nash Unit #5	s13,2310fsl,330fel	3027	212	?	?	?	?	?
U13	Mesa Pet., Nash Unit #1	s13,1980fnl,660fel	3024	212	?	?	?	?	?
		T23S, R30E							
H14	H - 7C	s14,2595fnl,2471fwl	3163	283	274	237	140	117	87
F16	Skelly Oil, Forty Niner Ridge Unit #1	s16,1980fsl,1980fel	3197	425	?	?	?	?	?
U18	Mesa Pet., Nash Unit #6	s18,1980fnl,330fwl	3028	217	?	?	?	?	?
N21	Skelly Oil, Forty Niner Ridge Unit 2	s21,1980fsl,1980fel	3215	?	?	?	?	?	?
S21?	Skelly Oil, Forty Niner Ridge Unit 2	s21,1980fnl,1980fel	3215	?	?	?	?	?	?
S24	Phillips, Sandy Unit #1	s24,1980fnl,660fwl	3290	470	325	305	235	210	150
Q34	ERDA 10	s34,200fnl,2327fel	3371	?	?	?	?	?	?
U34	Atomic Energy Comm, U.S.G.S. Test Hole #1	s34,center of sec	?	710	?	?	?	?	310
		T23S, R31E							
O04	P - 17	s4,1351fsl,395fwl	3339	713	582	562	463	438	382
P04	P - 8	s4,642fnl,96fwl	3336	715	587	565	477	450	391
H05	H - 4C	s5,447fnl,719fwl	3335	626	515	493	403	377	315
P05	P - 7	s5,513fnl,396fwl	3332	627	521	500	398	373	312
O05	P - 16	s5,951fwl,1629fwl	3323	642	523	503	402	376	316
T14	Texas Amer., Todd Fed. "14" No. 1	s14,1980fsl,1980fwl	3511	1100	990	968	876	850	794
H15	H-12	s15,NE1/4,NE1/4,NE1/4	3425	976	849	825	703	678	621
P21	Patoil, Muse-Fed. #1	s21,660fsl,660fel	3374	797	663	645	542	520	460
T23	Texas Amer, Todd "23" Fed. No. 1	s23,660fsl,1650fel	3461	1090	978	945	850	830	775
T25	Skelly, Todd 25 Fed. #1-Z	s25,1980fnl,1970fwl	3506	1190	1072	1050	940	922	865

GEOPHYSICAL LOG DATA
(Continued)

Well Identifier	Name of well	Location	Ref. Elev.	Top S	Top u.l.	Top C	Top T	Top M	Top F-N
A26	Texas Amer, Todd Fed 26 #2	s26,1980fnl,1650fel	3454	1063	950	927	830	810	750
T26	Texas Amer, Todd Fed "26" No. 1	s26,1980fnl,1980fel	3464	1070	955	922	835	814	758
B26	Texas Amer, Todd Fed. #4	s26,660fnl,1980fel	3458	1060	945	920	825	806	750
P27	Patoil, Wright-Fed. #1	s27,1980fsl,660fwl	3402	837	705	680	585	560	497
M29	El Paso Nat. Gas, Mobil Fed. #1	s29,1980fsl,1980fel	3374	?	?	?	?	?	?
L32	J.A. Leonard, Cont. State No. 1	s32,660fnl,660fwl	3358	695	587	570	450	430	360
H36	C. P. Miller, P. Harrison State #1	s36,sw/4 of sw/4	?	1095	975	950	860	835	780
		T23S, R32E							
K03	O.B. Kiel, Fed. #1	s3,1980fnl,660fel	3727	1584	1445	1420	1235	1213	1155
M09	McBee, Cont. Fed. #1-9	s9,1980fel,660fsl	3699	1545	1405	1383	1215	1195	1140
H11	Hill & Meeker, Matthews "11" #1	s11,1980fnl,1980fel	3723	1680	1529	1505	1294	1275	1195
T15	J.H. Trigg, Fed. Cont. 1-15	s15,1980fnl,1980fel	3722	1640	1500	1473	1263	1243	1178
F18	Skelly, Fed. Sand 18-1	s18,1980fnl,660fel	3622	?	1245	1215	1110	1085	1025
H20	H-10c	s20,381fsl,1978fel	3699	-	1402	1376	1294	1270	1217
K20	Kirklin, Fed. Estill AF-1	s20,660fsl,1980fel	3696	1512	1392	1368	1285	1262	1210
G21	C. Hankamer, Gulf-Fed. "A-A" #1	s21,660fnl,1980fwl	3701	1517	1401	1377	1240	1215	1163
H24	HL Johnson, Conoco-Fields Fed. #1	s24,1650fsl,330fel	3720	1710	1557	1526	1315	1294	1225
C24	Cont., Fields Fed. No. 1	s24,660fsl,660fel	3725	1727	1570	1532	1325	1308	1235
C25	Cont., Fields No. 2	s25,990fsl,330fwl	3700	1683	1532	1510	1300	1280	1208
J25	H.L. Johnson, Wehrli-Fed. #1	s25,990fnl,2310fwl	3720	1695	1544	1520	1302	1282	1212
W26	J. Trigg, Fed. "WL" #3-26	s26,330fsl,330fel	3698	1678	1525	1500	1315	1295	1225
P26	P.M. Drilling, Fed. Field #1	s26,660fsl,1980fwl	3658	1630	1493	1472	1312	1292	1222
F26	P.M. Drilling, Fed. James No. 4	s26,1980fsl,330fel	3705	1680	1532	1512	1306	1288	1215
L26	J.H. Trigg, No. 4-26 Fed. WL	s26,330fsl,1650fel	3713	1667	1520	1496	1312	1296	1225
W28	M. Wilson, Cont. Fed. No.1	s28,660fnl,1980fwl	3687	1535	1415	1385	1258	1236	1180
H31	C. Hankamer, Hankamer No. 1 Cont. Fed.	s31,660fsl,660fwl	3551	1206	1078	1050	945	923	862
C33	C. Hankamer, Holder Fed. #1	s33,1980fnl,660fel	3666	1520	1386	1355	1285	1260	1200
P34	Pure Oil, Fed. "K" No. 1	s34,1980fsl,330fel	3629	1508	1387	1365	1250	1230	1170
A35	J.H. Trigg, Fed. WL 1-35	s35,1650fnl,2310fel	3694	1657	1506	1483	1298	1282	1206
T35	P.M. Drilling, Fed. James No. 1	s35,660fnl,660fel	3675	1675	1527	1507	1308	1290	?

GEOPHYSICAL LOG DATA
(Continued)

Well Identifier	Name of well	Location	Ref. Elev.	Top S	Top u.l.	Top C	Top T	Top M	Top F-N
R35	P.M. Drilling, Fed. James No. 2	s35,660fnl,1980fel	3669	1655	1512	1490	1300	1282	1210
D35	P.M. Drilling, Fed. Payne No. 3	s35,1980fsl,330fwl	3630	1505	1387	1355	1252	1233	1183
M35	P.M. Drilling, Payne No. 2	s35,990fnl,2310fwl	3700	1635	1495	1475	1302	1281	1215
J35	J. Trigg, Fed. "WL" No. 2-35	s35,1650fnl,990fel	3691	1653	1498	1475	1293	1275	1205
F35	P.M. Drilling, Payne Fed. No. 4	s35,1980fnl,660fwl	3663	1567	1448	1425	1282	1263	1200
P35	P.M. Drilling, Fed. Payne No. 1	s35,2310fnl,2310fwl	3689	1623	1475	1453	1280	1262	1193
Q35	P.M. Drilling, Fed. James No. 3	s35,1980fsl,1980fel	3670	1623	1472	1453	1278	1260	1187
B36	Pure Oil, Brinninstool Deep Unit #1	s36,1980fsl,1980fel	3689	1680	1517	1493	1296	1280	1210
P36	Penroc, Triste State #1	s36,330fnl,330fwl	3694	1670	1526	1496	1295	1276	1207
G36	D. Fasken, Gulf State #1	s36,1980fnl,660fwl	3664	1673	1517	1495	1297	1278	1206
		T23S, R33E							
C04	Cabeen Exp., Cont. Fed #1-P	s4,660fsl,660fel	3636	1657	1507	1485	1260	1240	1160
T06	Hudon, Shell Fed. #1-6	s6,330fsl,330fel	3704	1772	1622	1600	1355	1340	1260
H07	Hudson, Fed. 7 well #1	s7,660fsl,660fwl	3722	1757	1612	1588	1367	1350	1270
T17	P.M. Oil, Texaco State No. 1	s17,660fsl,660fwl	3715	1773	1615	1590	1367	1350	1268
S18	Helbing & Podeschan, #1 "A" Shell State	s18,660fsl,660fwl	3722	1710	1568	1545	1328	1310	1230
T18	Tenneco, Skelly State #1	s18,660fnl,1980fel	3726	?	1635	1610	1387	1370	1290
B19	Cont, I.J. Marshall 19-1	s19,660fsl,660fwl	3720	1735	1573	1550	1330	1310	1233
C19	Cont., Marshall #19-2	s19,1980fsl,1910fwl	3703	1720	1568	1541	1320	1303	1225
M19	Cont., Marshall #3	s19,660fsl,1980fwl	3711	1732	1571	1550	1327	1310	1230
A19	Cont., Marshall #4	s19,1980fsl,625fwl	3713	1710	1553	1530	1313	1296	1222
A20	Amer., Quaser, Brinninstool #1	s20,1980fnl,1980fel	3713	1790	1634	1610	1385	1364	1285
C20	Cont., Levick Fed. #1	s20,660fsl,660fel	3701	1785	1620	1597	1376	1358	1280
K31	Kirklin, Lea State #1	s31,660fnl,660fel	?	1760	1600	1577	1349	1333	1252
H32	El Cinco, Humble State 1-32	s32,660fnl,1980fel	3683	1770	1606	1582	1360	1343	1268
B35	G. L. Buckles, State 1-35	s35,660fsl,660fwl	3659	1815	1672	1650	1415	1395	1310
		T23S, R34E							
B18	Cont., Bell Lake #9	s18,1980fsl,1980fwl	3533	1469	1330	1310	1084	1066	988
L19	Cont., Bell Lake Unit #10	s19,1980fnl,1980fwl	3555	1605	1455	1425	1200	1182	1095
N22	Shell, N. Antelope Ridge Unit #1	s22,1980fnl,1980fel	3425	1275	?	?	1006	984	912
S34	Shell, Antelope Ridge Unit 34-1	s34,1980fsl,1650fwl	3490	1400	?	?	?	?	944

APPENDIX II

Geophysical Log Data

GEOPHYSICAL LOG DATA
(Continued)

Well Identifier	Name of well	Location	Ref. Elev.	Top S	Top u.l.	Top C	Top T	Top M	Top F-N
		T23S, R35E							
M01	Schermerhorn, Malco Fed. No. 1	s1,2310fsl,330fwl	3494	2020	1900	1885	1740	1725	1655
E01	Kenwood, Ehrman Fed. #1	s1,660fnl,660fel	3515	2030	1903	1888	1723	1708	1625
		T23S, R36E							
G03	A. Gackle, Sinclair State #7	s3,660fnl,660fel	?	1663	1577	1570	1446	1437	1393
F17	Cont., Farney A-17 No. 3	s17,1650fnl,990fwl	3468	1950	1837	1824	1635	1625	?
S20	Sinclair Oil, Fed. 714 #4	s20,1980fsl,1980fwl	3459	?	?	?	1683	1672	1593
		T23S, R37E							
H04	Samedan Oil, Hughes A-1 #6	s4,1980fsl,660fwl	3324	1337	1252	1244	1188	1176	1143
K06	R. Lowe, King "B" #5	s6,330fnl,330fel	3383	1493	?	?	?	?	1262
H09	Skelly Oil, Harrison B-10	s9,1980fsl,1980fwl	3317	1287	1200	1192	1137	1130	1090
T16	The Texas Co., #3 State of N.M. "BZ" NCT-8	s16,1980fsl,1980fel	3317	1228	1165	1154	1097	1086	1047
O24	E.M. Craig, Ohio State #1	s24,660fel,660fsl	3282	1620	1531	1522	1418	1410	1365
B31	Texaco, E.E. Blinberry A NCT 1-2	s31,1980fsl,660fel	3320	1435	1340	1329	1219	1214	1168
		T24S, R29E							
C05	Chase Pet., Valley #1	S5,1650fsl,660fwl	2968	?	?	?	?	?	?
E06	El Capitan Oil, Fed. Reid No. 1	s6,330fsl,2510fel	2984	?	?	?	?	?	?
F07	Southern Cal. Pet., Fed. Reid #1	s7,2310fsl,2310fel	?	?	?	?	?	?	?
V07	Tenn. Prod., Valley Land Comp. #2	s7,990fsl,330fwl	?	?	?	?	?	?	?
R07	Southern Cal. Pet., Fed. Reid #2	s7,2310fnl,2310fel	?	?	?	?	?	?	?
T07	Tenn. Prod., Valley Land #3	s7,1650fsl,1650fwl	?	?	?	?	?	?	?
C09	Skelly, Cedar Canyon #1	s9,770fsl,770fel	2969	?	?	?	?	?	?
S09	Skelly, Cedar Canyon 9D#1	s9,660fsl,1980fel	2941	?	?	?	?	?	?
C10	Skelly, Cedar Canyon #10-1	s10,1980fwl,2180fnl	2997	?	?	?	?	?	?
P27	Pennzoil, Mobil-Fed. "27" #1	s27,660fsl,660fwl	2924	696	?	?	?	?	450
		T24S, R30E							
P18	P. R. Bass, Poker Lake #45	s18,460fnl,660fel	3179	?	?	?	?	?	?
H23	H-8	s23,2059fnl,1420fel	3433	-	614	589	492	467	400
B25	Hill & Meeker, Bass Fed. #1 - 25	s25,660fsl,660fwl	3429	840	675	650	572	552	473
C29	Ford Chapman, Fed. - Nettles No. 1	s29,660fsl,660fel	3266	?	?	?	?	?	?
		T24S, R31E							
T02	Skelly, Todd "2" State #1	s2,1980fnl,1980fwl	3502	1250	1095	1065	935	912	853
J03	M. Wilson, Jennings Fed. No. 1	s3,660fsl,660fel	3500	1010	880	852	762	750	676

GEOPHYSICAL LOG DATA
(Continued)

Well Identifier	Name of well	Location	Ref. Elev.	Top S	Top u.l.	Top C	Top T	Top M	Top F-N
F03	J.L. McClellan,Jennings Fed. No. 1	s3,660fnl,660fwl	3432	835	725	696	600	578	?
B04	Sundance, Betty Fed. #1	s4,1659fnl,2310fwl	3414	812	675	648	545	522	453
H04	H-9c	s4,2482fnl,193fwl	3406	-	687	665	565	535	465
S04	Texaco, M.M. Stewart Fed. #1	s4,660fnl,660fel	3436	832	715	688	573	553	485
E04	El Paso Nat. Gas, Sundance Fed. #1	s4,1980fnl,1980fwl	3430	805	680	658	548	528	455
D06	Amer. Quasar, Dunes Unit Fed. #1	s6,1980fwl,1980fnl	3438	826	720	700	573	550	478
Y07	Ambassador, Fed. "Y" #1	s7,660fsl,660fel	3535	960	810	790	692	670	600
G11	Gulf, Fed. Littlefield "CT" #1	s11,660fnl,1980fel	3528	1130	1010	986	850	826	768
W17	W.J. Weaver, Cont. Fed. #1	s17,660fnl,660fel	3553	1025	873	850	755	730	665
R18	C. B. Read, Ritchie Fed. #1	s18,660fsl,660fel	3514	915	795	780	667	645	576
P20	Pauley, Jennings Fed. #1	s20,660fnl,660fel	3530	965	820	800	690	670	605
F20	D. Fasken, Poker Lake #40	s20,660fsl,1980fwl	3490	895	750	729	619	597	530
H21	Hill & Meeker, Carper Fed. #1-21	s21,660fnl,660fel	3535	923	813	792	?	?	693
T24	Texas Co., T. Heflin-Fed. #1	s24,660fsl,1980fel	3551	1017	895	872	775	755	695
M28	Pan Amer., Poker Lake Unit #36	s28,660fsl,660fel	3502	?	?	?	?	?	595
M35	Texaco, C. D. Unit No. 67	s35,1980fsl,660fwl T24S, R32E	3508	1010	855	828	722	702	628
U01	Union Oil of Cal, Union Fed. "1" #1	s1,660fsl,1980fel	3620	1562	1433	1410	1269	1252	1183
C01	Cabeen Exp., Cont. Fed. #1-L	s1,1980fsl,660fwl	3623	?	?	?	?	?	?
M02	Calco, Marathon St #1	s2,1990fnl,1990fwl	3632	1500	1371	1348	1255	1239	1185
O02	P.M. Drilling, Ohio State No.1	s2,1980fnl,660fel	3631	1533	1408	1388	1255	1238	1172
H06	C. Hankamer, Bondurant Fed. No. 1	s6,1980fel,660fnl	3584	1246	1116	1090	965	947	888
G10	Gulf, Fed. Hanagan D #1	s10,1980fsl,1980fel	3628	1394	1270	1248	1161	1138	1088
C11	Cont., Wimberly #2	s11,660fnl,660fel	3615	?	?	?	?	?	?
H11	Gulf, Fed. Hanagan D #3	s11,1980fsl,660fel	3637	?	?	?	?	?	?
F11	Gulf, Fed. Hanagan D #2	s11,1980fsl,1980fel	3637	?	?	?	?	?	?
W11	Cont., Wimberly #1	s11,1980fnl,1980fel	3640	1502	1378	1352	1227	1210	1157
N11	C. Hankamer, Hanagan Fed. No. 2	s11,660fsl,1980fel	?	?	?	?	?	?	?
G11	C. Hankamer, Gulf Hanagan #1	s11,660fsl,660fel	3637	1504	1372	1352	1264	1247	1192
C12	Cont., Wimberly "12" #2	s12,1980fnl,660fel	3600	1203	1253	1269	?	?	?
H12	C. Hankamer, Hanagan Fed. No. 3	s12,1980fnl,660fwl	?	1495	1370	1347	1220	1201	1130

GEOPHYSICAL LOG DATA
(Continued)

Well Identifier	Name of well	Location	Ref. Elev.	Top S	Top u.l.	Top C	Top T	Top M	Top F-N
W12	Cont., Wimberly 12#1	s12,1980fnl,1650fel	3606	?	?	?	?	?	?
A13	Cont., Wimberly "A" #1	s13,660fnl,1980fel	3599	?	?	?	?	?	?
W13	Westates, Woolley #1	s13,660fsl,660fel	3586	1503	1371	1352	1260	1238	1187
U14	Tenneco, U.S.A. Jennings N.M. Well #3	s14,660fnl,1980fel	3624	1453	1327	1309	1218	1199	1142
J14	Tenneco, #1 USA Jennings	s14,660fnl,1980fwl	3628	1445	1315	1295	1204	1184	1132
T14	Tenneco, U.S.A. Jennings N.M. No. 2	s14,882fsl,882fwl	3588	1437	1308	1283	1200	1182	1122
F14	Tenneco, Jennings Fed. 4	s14,1980fsl,1650fwl	3591	1456	1323	1301	1210	1190	1130
H15	Gulf, Fed. Hanagan "B" #1	s15,660fsl,1980fel	3622	1396	1258	1239	1145	1126	1065
F15	Gulf, Fed. Hanagan "B" #2	s15,660fsl,720fel	3606	1438	1306	1287	1198	1180	1122
G15	Gulf, Fed. Hanagan "B" #3	s15,1980fsl,660fel	3591	1428	1298	1275	1180	1158	1110
T15	Tenneco, Hicks-Fed. #1	s15,660fsl,1980fwl	3602	1340	1208	1191	1102	1083	1025
T22	Tennessee Gas, U.S. Smelting U.S.A. #1	s22,660fnl,1980fel	3602	1384	1246	1225	1140	1125	1066
G22	Tenneco, U.S. Smelting U.S.A. #2	s22,1980fnl,660fwl	3618	1312	1188	1165	1072	1053	998
S22	Tenneco, U.S. Smelting U.S.A. No. 3	s22,1980fsl,660fel	3607	1375	1243	1222	1132	1114	1060
U22	Tenneco, U.S. Smelting USA #4	s22,2310fnl,1650fel	3604	1383	1248	1226	1140	1120	1062
N22	Tenneco, U.S. Smelting U.S.A. No. 5	s22,990fsl,330fel	3591	1362	1223	1201	1118	1100	1047
B22	C. B. Read, Bradley #1	s22,1980fsl,1980fel	3608	1368	1235	1213	1122	1106	1052
R22	C. B. Read, Bradley #2	s22,1980fnl,990fel	3604	1400	1265	1243	1151	1132	1070
E23	C. Hankamer, Ernest Fed. #1	s23,1980fnl,660fwl	3609	1415	1284	1261	1170	1150	1093
B23	C. B. Read, Bradley #3	s23,660fnl,660fel	3605	1412	1275	1253	1168	1148	1088
D33	Texaco, C. D. Unit Well #72	s33,660fsl,660fel	3510	1145	1025	1002	910	890	830
C34	Texaco, C. D. Unit #69	s34,1980fsl,1980fwl	3519	1190	1075	1052	960	940	881
		T24S, R33E							
B01	Cont., Bell Lake Unit #7	s1,660fnl,660fel	3625	1806	1632	1600	1382	1367	1278
G06	Hondo, Gulf State "NW" #1	s6,660fsl,660fwl	3598	1612	1467	1445	1265	1246	1174
H06	Hondo, Gulf N.W. #2	s6,1980fsl,660fwl	3606	1635	1475	1452	1272	1255	1187
T07	T.L. Ingram, State "P" #1	s7,330fnl,1750fwl	3636	1647	1490	1468	1290	1270	1203
O07	T.L. Ingram, State "O" #1	s7,660fnl,660fwl	3590	1635	1475	1452	1273	1257	1184
R07	G.W. Riley, State #1-7	s7,660fsl,660fel	3547	1620	1485	1462	1310	1292	1225
I07	T.L. Ingram, State "O" 2	s7,1980fnl,660fwl	3603	1595	1465	1440	1276	1257	1204
F07	D. Fasken, Gulf State #7-2	s7,2310fnl,2310fwl	3578	1630	1486	1465	1287	1270	1194
S08	Sunray, N.M. State A.G. 1	s8,660fnl,660fwl	3637	1700	1542	1520	1308	1291	1215
B13	B. Bennett, Holland #1	s13,1980fnl,660fel	3598	1785	1613	1600	1347	1330	1245
T17	Tenneco, State Lowe #1	s17,660fsl,660fwl	3554	1540	1409	1385	1267	1250	1190
H17	R.B. Holt, Holly State #1	s17,660fnl,1980fel	3592	1676	1503	1485	1297	1282	1205
C20	Cont., State "BB" 20 No. 1	s20,660fsl,1980fwl	3540	1495	1357	1335	1228	1212	1140
J22	F.R. Jackson, State #1	s22,1980fnl,660fwl	3594	1735	1527	1502	1309	1289	1220

GEOPHYSICAL LOG DATA
(Continued)

Well Identifier	Name of well	Location	Ref. Elev.	Top S	Top u.l.	Top C	Top T	Top M	Top F-N
T27	Tenneco, Sunray State #1	s27,1980fsl,1980fwl	3502	1621	1481	1458	1275	1259	1186
T29	Tidewater, State "AP" #1	s29,660fsl,1980fel	3525	1492	1332	1314	1224	1206	1146
C30	Kirklin, Continental State #1	s30,330fnl,330fwl	3556	1410	1260	1240	1138	1120	1070
G31	A. Gackle, Cont. State 1	s31,1980fsl,660fel	3524	1392	1250	1228	1141	1122	1063
K36	Gulf, #1 Lea St. "GX"	s36,660fnl&660fel	?	1695	1535	1513	1243	1230	1163
		T24S, R34E							
H01	Hanagan, #1 Gerdlag	s1,1980fnl,1980fel	3447	1125	1012	995	?	?	?
D04	Shell, Fed., "BE" #1	s4,1650fel,660fnl	3567	1537	1392	1368	1139	1122	1045
C05	Cont., Bell Lake Unit #14	s5,1650fnl,1650fwl	3619	1690	1540	1517	1282	1263	1185
B06	Cont., Bell Lake Unit No. 3	s6,660fnl,3300fel	3630	1760	1598	1573	1345	1327	1245
S09	Shell, Hall Fed. #1	s9,660fnl,1980fel	3570	1660	1482	1455	1230	1215	1134
		T24S, R35E							
W05	Gulf, Wilson Fed. Com #1	s5,1980fnl,1980fwl	3488	1085	1025	1005	920	900	835
A16	Texas, Aztec State No. 1	s16,1650fnl,1980fel	3378	1186	1062	1040	905	890	820
		T24S, R37E							
F05	Texaco, E. D. Fanning No. 7	s5,1966fnl,1980fel	3295	?	1320	1311	1210	1197	1155
		T24S, R38E							
H30	R. Lowe, Hair #2	s30,535fnl,2310fwl	3156	1482	?	?	?	?	1202
		T25S, R28E							
E28	Gulf, Eddy State FD #1-S	s28,1980fnl,1980fwl	2997	?	?	?	?	?	?
		T25S, R29E							
B03	J. G. Bennett, Superior Fed. #1-3	s3,660fnl,660fel	2985	340	182	147	?	?	?
B08	J. G. Bennett, Superior #1-8	s8,980fnl,660fwl	2921	?	?	?	?	?	?
W08	N. H. Willis, Superior Fed. #1	s8,660fsl,660fel	2923	?	?	?	?	?	?
M14	Mobil, Corral Draw Unit #1	s14,1980fsl,1980fwl	3118	945	?	?	?	?	670
B15	J. G. Bennett, Superior Fed. 15 No. 1	s15,660fsl,660fwl	3041	775	?	?	?	?	?
W22	Mobil, Corral Draw Unit #2	s22,1580fsl,1980fwl	3078	905	?	?	?	?	680
B26	J. G. Bennett, No. 1-26 Superior Fed.	s26,660fsl,660fel	3043	530	?	?	?	?	175
B27	J. G. Bennett, Superior Fed. 1-27	s27,660fsl,660fwl	2990	414	?	?	?	?	115
B29	Bell Pet., Fed. #1	s29,660fnl,1880fwl	2936	?	?	?	?	?	?
B30	Bell, Cities Svc Fed. #1	s30,660fsl,760fel	2945	393	?	?	?	?	260
		T25S, R30E							
J04	Ritchie etal, #1 Hopp Fed	s4,660fsl,660fel	3283	1014	?	?	?	?	888
P04	Pat Oil, R & B Fed. #1	s4,1980fnl,1980fwl	3273	1096	1041	1029	937	915	848
K08	R. Lowe, Poker Lake Superior State #1	s8,663fsl,667fwl	3210	1255	1094	1078	?	?	970
R08	F. Pool, Superior State 1	s8,1980fnl,660fel	3210	760	597	560	?	?	970

GEOPHYSICAL LOG DATA
(Continued)

Well Identifier	Name of well	Location	Ref. Elev.	Top S	Top u.l.	Top C	Top T	Top M	Top F-N
T08	R. Lowe, T&P State #1	s8,660fnl,660fwl	3197	790	?	?	?	?	678
S08	R. Lowe, Superior State 1	s8,1980fsl,1980fwl	3210	1100	?	?	?	?	970
P08	R. Lowe, Poker Lake State #3	s8,1980fsl,660fwl	3190	880	848	820	?	?	699
L08	R. Lowe, Poker Lake State #1	s8,660fsl,660fwl	3199	915	?	?	?	?	745
P10	Bass, Poker Lake #44	s10,2030fnl,2180fel	3317	1050	900	878	809	799	780
A10	Alamo, Poker Lake Unit #5X-1A	s10,660fsl,645fwl	3282	1235	?	?	?	?	900
A17	Alamo, Poker Lake Unit #11A-7	s17,660fsl,660fwl	3219	898	?	?	?	?	640
X17	R. Lowe, #1-X R&B Fed. "A"	s17,610fnl,610fwl	3210	786	?	?	?	?	595
M18	R. Lowe, R&B Fed. #1	s18,660fnl,660fel	3192	1205	?	?	?	?	1050
B18	P. R. Bass, Jennings Fed. No. 1	s18,660fnl,1980fel	3186	1075	908	886	797	782	725
A18	Alamo, Poker Lake #12A-9	s18,660fsl,1980fel	3207	1542	1375	1360	?	?	1053
P19	Central States, Poker Lake Unit No. 38	s19,330fnl,900fel	3209	1100	?	?	?	?	880
F20	P. R. Bass, Cont. Fed. #1	s20,660fnl,660fwl	3204	915	?	?	?	?	675
C20	P. R. Bass, Cont. Fed. #2	s20,1980fsl,660fwl	3184	840	?	?	?	?	608
A21	Alamo, Poker Lake Unit #6-2A	s21,660fnl,660fel	3252	1373	1283	1270	1208	1194	1178
		T25S, R31E							
D02	Texaco, C. D. Unit No. 65	s2,1980fnl,1980fel	3476	1012	870	842	?	?	715
A28	Alamo, Poker Lake Unit 7-A-3	s28,660fnl,660fwl	3348	1123	1032	1010	915	890	820
C32	J. A. Leonard, Cont. State No. 1	s32,660fnl,660fwl	3358	697	588	560	450	427	360
S35	Gold Metals etal, #1 Del. Basin Fed.	s35,660fsl,660fwl	3319	1622	?	?	?	?	1325
		T25S, R32E							
C03	Texaco, C. D. Unit No. 49	s3,1650fsl,1980fel	3486	1127	1004	978	882	863	803
D09	Texaco, C. D. Unit No. 52	s9,1650fsl,330fel	3461	1104	967	940	848	820	756
R09	Texaco, E.F. Ray Nct-2 No. 1	s9,330fsl,330fel	?	1160	1006	983	875	855	790
E10	Tenneco, E. F. Ray U.S.A. 41	s10,1650fsl,660fwl	3470	1140	993	972	872	850	793
C10	Texaco, C. D. Unit No. 39	s10,1980fnl,660fwl	3472	1130	993	965	868	847	787
D10	Texaco, C. D. Unit No. 40	s10,660fnl,1980fwl	3478	1127	993	968	872	850	792
M10	Texaco, C. D. Unit No. 60	s10,2145fnl,2310fel	3464	1118	993	968	868	848	785
S10	Texaco, E.F. Ray Fed. No. 1	s10,660fsl,1980fwl	?	1120	988	963	865	845	780
Q10	Texaco, C. D. Unit #66	s10,2080fnl,760fwl	3480	1140	999	972	872	853	791
F10	Texaco, E.F. Ray-Fed. No. 2	s10,1980fsl,1980fwl	?	1147	1005	980	878	858	793

GEOPHYSICAL LOG DATA
(Continued)

Well Identifier	Name of well	Location	Ref. Elev.	Top S	Top u.l.	Top C	Top T	Top M	Top F-N
V10	Texaco, E.F. Ray- Fed. "B" Well No. 1	s10,660fsl,1980fel	?	1140	1007	982	880	860	794
Y10	Texaco, C. D. Unit No. 63	s10,660fnl,660fwl	3477	1125	990	964	862	840	780
T10	Tennessee, Ray U.S.A. #1	s10,660fnl,660fwl	3460	1122	996	973	866	845	782
R10	Texaco, E.F. Ray Fed. "B" No. 2	s10,1980fnl,1980fwl	?	1123	987	962	854	833	774
C11	Westates, Cont. Fed. #1	s11,sw/4 of se/4	3410	1177	1044	1021	923	899	837
P13	Patoil, Union Fed. #1	s13,660fsl,1980fwl	3468	1140	1013	991	905	876	808
F14	J. O'Neill, Fed. "O" #1	s14,660fsl,660fel	3445	1103	972	949	848	825	762
H14	Hill&Meeker, Ora Hall Fed. 14 #1	s14,2310fnl,330fwl	3455	1133	982	962	862	840	773
O14	J. O'Neill, Fed. "O" #2	s14,1980fsl,660fel	3454	1132	998	976	875	852	787
W15	Texaco, C. D. Unit No. 46	s15,2130fsl,2130fel	?	1150	995	973	867	846	780
F15	Texaco, G.E. Jordan Fed. Well No. 1	s15,1980fnl,660fwl	?	1158	1003	985	875	854	787
J15	Texaco, G.E. Jordan Fed. #2	s15,1980fsl,1980fwl	?	1145	992	968	863	843	782
G15	Texaco, G.E. Jordan-Fed. No. 2	s15,660fnl,660fwl	?	1158	1008	983	878	858	792
M15	Tennessee, G.E. Jordan USA #2	s15,1980fnl,1980fwl	3443	1165	1003	982	875	854	787
R15	Tennessee, G.E. Jordan #3	s15,660fnl,1980fwl	3451	1144	993	963	865	843	780
N15	Tennessee, G.E. Jordan USA 4	s15,1980fsl,660fwl	3441	1138	965	942	862	841	776
T15	Texaco, G. E. Jordan Fed. #6	s15,1980fnl,1980fel	3447	1137	983	962	855	834	769
E15	Texaco, G. E. Jordan Fed. No. 8	s15,660fnl,1980fel	?	1140	990	966	867	845	780
U15	Tenn. Gas, #1 USA G.E. Jordan	s15,660fsl,660fwl	3427	1137	982	953	848	828	765
P16	Tenneco, State Monsanto #6	s16,1650fsl,2310fwl	3423	1098	938	915	823	805	743
Z16	Cont., State Z 16 #1	s16,1980fnl,1980fel	3444	1128	972	952	844	822	760
X16	Shoreline, Cont. State #1	s16,2080fnl,1650fel	3442	1130	983	961	855	836	768
M16	Tennessee, State Monsanto #1	s16,1980fsl,660fel	3439	1137	980	955	856	833	769
E16	Tennesse, Monsanto #2	s16,660fsl,660fel	3433	1125	976	953	852	833	772
C16	Tenneco, State Monsanto #7	s16,330fsl,990fwl	3411	1075	918	895	786	765	697
A16	Tennessee, State Monsanto #3	s16,660fsl,1980fel	3434	1115	960	936	816	795	727
N16	Tennessee, State Monsanto #4	s16,660fsl,1980fwl	3421	1095	927	902	779	758	695
L16	Tenneco, State Monsanto #5	s16,1650fsl,1650fel	3437	1120	960	942	832	810	745
S16	Tenneco, Monsanto State #8	s16,1660fsl,990fwl	3426	1077	922	898	800	778	715

GEOPHYSICAL LOG DATA
(Continued)

Well Identifier	Name of well	Location	Ref. Elev.	Top S	Top u.l.	Top C	Top T	Top M	Top F-N
F16	Tennessee, State Bradley #2	s16,660fnl,660fel	3458	1157	984	962	852	828	766
B16	Tennessee, State E. L. Bradley #1	s16,1980fnl,660fel	3444	1140	983	960	850	827	763
T16	Tenneco, State E.L. Bradley #3	s16,2310fnl,2310fwl	3434	1110	961	940	835	813	742
D18	Texaco, C. D. Unit #64	s18,660fnl,1650fwl	3431	940	822	803	692	668	607
S18	Texas Comp., J. B. Shaw Fed. #1	s18,660fnl,1980fel	3438	1015	857	836	727	705	643
C20	Texaco, C. D. Unit #42	s20,1650fsl,330fel	3394	1086	932	905	812	790	730
P21	Tennessee, E.H. Perry U.S.A. 2	s21,660fnl,660fwl	3408	1062	905	877	776	756	692
H21	Tenneco, E.H. Perry "USA" Well No. 36	s21,1980fnl,660fwl	3404	1073	917	894	792	770	707
T21	Tennessee, E. H. Perry USA #1	s21,660fnl,1980fel	3428	1130	970	945	828	804	730
E21	Tennessee, #3 E.H Perry U.S.A.	s21,1980fnl,1980fel	3422	1125	967	941	826	806	738
F21	Panther City Invest., Perry Fed. #1	s21,660fnl,660fel	3430	1128	973	948	865	845	768
R21	Panther City Invest., Perry Fed. #2	s21,1980fnl,660fel	3421	1109	943	918	806	782	720
G21	Panther City Invest., Perry Fed. No. 5	s21,1980fsl,1980fwl	3408	1117	957	930	832	810	746
Y21	Panther City Invest., Perry Fed. No. 6	s21,1980fnl,1980fwl	?	1106	953	927	813	792	726
K21	Panther City Invest., Perry Fed. No. 7	s21,660fnl,1980fwl	3414	1097	934	907	803	784	713
I21	Panther City Invest., Perry Fed. #27	s21,2310fsl,990fel	3406	1116	966	943	823	802	737
B21	Panther City Invest., Perry Fed. #28	s21,1980fsl,1980fel	3413	1125	975	947	835	815	752
M21	Panther City Invest., Perry Fed. #37	s21,660fsl,660fwl	3398	1117	958	931	822	800	747
N21	Panther City Invest., Perry Fed. #38	s21,660fsl,1980fwl	3404	1148	985	962	863	842	775
V21	P. R. Bass, Perry Fed. #43	s21,330fsl,330fel	3382	1112	962	943	835	812	755
C21	Texaco, C. D. Unit #44	s21,990fsl,2310fel	3400	1132	978	952	836	816	756
D21	Texaco, C. D. Unit #57	s21,990fsl,990fel	?	1115	967	938	834	811	740
J21	Panther City Invest., Perry Fed. #35	s21,1980fsl,660fwl	3396	1100	938	916	810	787	726
E22	Texaco, G. E. Jordan Fed. No. 1	s22,660fnl,660fwl	3419	1115	959	933	825	800	738
T22	Texaco, G. E. Jordan Fed. NCT-1 No. 5	s22,510fnl,1830fwl	3421	1142	977	953	860	825	770
J22	Texaco, G. E. Jordan Fed. #3	s22,1980fnl,660fwl	?	1130	966	942	835	812	748

GEOPHYSICAL LOG DATA
(Continued)

Well Identifier	Name of well	Location	Ref. Elev.	Top S	Top u.l.	Top C	Top T	Top M	Top F-N
C22	Texaco, C. D. Unit no. 48	s22,2310fsl,330fwl	3411	1117	960	935	832	810	747
O23	J. L. O'Neill, Fed. "P" #1	s23,660fnl,1980fel	3429	1085	955	930	834	808	748
G25	Texaco, G. E. Jordan Fed. No. 4	s25,660fsl,1980fwl	3430	1155	993	970	861	838	773
C27	Texaco, C. D. Unit no. 61	s27,330fnl,330fwl	3391	1130	988	960	845	823	755
D28	Tenneco, J. D. Sena Jr. U.S.A. No. 2	s28,2310fsl,990fwl	3370	1335	1166	1140	1042	1023	957
J28	Tenneco, J. D. Sena USA No. 1	s28,2310fsl,1650fwl	3375	?	1097	1072	977	958	900
C28	Texaco, C. D. Unit No. 45	s28,660fnl,660fwl	3382	1175	1018	993	895	875	818
U28	Texaco, C. D. Unit No. 47	s28,660fnl,1980fwl	3392	1170	1008	984	875	856	785
X28	Texaco, C. D. Unit no. 51	s28,660fnl,2310fel	3398	1140	985	960	870	850	782
W28	Texaco, C. D. Unit No. 54	s28,1980fnl,2310fel	3386	1178	1018	993	895	875	813
V28	Texaco, C. D. Unit No. 50	s28,1980fnl,1980fwl	3414	1230	1063	1040	950	930	868
N28	Texaco, C. D. Unit No. 56	s28,660fnl,990fel	3388	1118	953	930	822	802	738
Z28	Texaco, C. D. Unit No. 59	s28,1650fnl,990fel	3386	1148	987	960	855	832	768
T29	Texaco, C. D. Unit No. 58	s29,1980fnl,330fel	3356	1310	1132	1100	1012	988	923
C29	I. W. Lovelady, Conoco Fed. #1-29	s29,990fsl,330fel	3366	1485	1347	1315	1224	1202	1142
S31	R. Smith, Ray Smith #1	s31,1980fnl,660fwl	3311	1417	1270	1242	1150	1132	1072
C32	R.C. Graham, Conoco State No. 1	s32,1980fnl,1980fwl	3307	1412	1263	1238	1153	1130	1075
H33	Hill&Meeker, Hall Fed. "33" #1	s33,660fsl,660fwl	3332	1440	1277	1250	1142	1116	1055
M33	Hill&Meeker, Jennings #33-1	s33,2310fnl,2310fwl	3354	1405	1250	1225	1128	1112	1045
W33	Westates, Jennings #1	s33,1980fsl,560fel	3348	1297	1155	1128	1020	995	935
		T25S, R33E							
J01	P. R. Bass, Fed-Muse #1	s1,660fnl,660fwl	3490	1673	1530	1506	1268	1255	1200
H05	Hill&Meeker, Bass Fed. #1	s5,660fnl,660fel	3478	1433	1292	1258	1186	1168	1106
S08	Santana, A. Bass Fed. #1	s8,1980fsl,660fel	3456	1428	1285	1259	1140	1120	1065
H11	C. Hankamer, Muse Fed. #1	s11,660fnl,660fwl	3424	1550	1395	1372	1213	1195	1138
J18	S. H. Jolliffe, #1 Bass Fed.	s18,660fnl,660fwl	3497	1312	1180	1150	1057	1038	985
H20	C. Hankamer, Fed. Bass #1	s20,660fnl,1980fel	3431	1347	1210	1183	1095	1077	1012
A21	Amer. Quasar, Vaca Draw #1	s21,660fsl,660fel	3392	1335	1209	1184	1092	1075	1006
B21	G. L. Buckles, Fed. Marshall #1	s21,660fnl,660fel	?	1374	1232	1207	1117	1098	1042
T22	Texaco, C. D. Unit No. 18	s22,1650fnl,1650fwl	3414	1130	973	950	837	816	750
M23	Hill & Meeker, Muse Fed. 23 #1	s23,660fsl,660fwl	3353	1410	1250	1227	1130	1114	1060
F24	R. B. Farris, Perry Fed. 1	s24,660fsl,660fwl	3358	1463	1310	1283	1136	1117	1045
K25	King Resources, Pan Amer Fed. #1	s25,1980fsl,660fwl	3342	1435	1285	1258	1127	1105	1047
A25	Ashmun&Hilliard, Fed. No. 1-25	s25,660fsl,660fel	3332	1395	1237	1210	1125	1108	1045

GEOPHYSICAL LOG DATA
(Continued)

Well Identifier	Name of well	Location	Ref. Elev.	Top S	Top u.l.	Top C	Top T	Top M	Top F-N
D27	R. A. Dean, H. Dickson #1	s27,660fsl,660fel	3320	1387	1237	1213	1098	1082	1023
T28	Tidewater, A. R. Bass Fed. #1	s28,660fsl,660fel	3353	1315	1170	1143	1053	1038	975
C28	C. Hankamer, Conley Fed. #1	s28,660fnl,660fel	3344	1339	1188	1167	1074	1056	1002
T29	Tenneco, W.H. Jennings Inc. USA No. 1	s29,1980fnl,660fwl	3422	1385	1196	1171	1083	1060	995
T31	Tennessee, Richardson& Bass USA 1	s31,660fsl,660fwl	3386	1096	951	927	824	800	742
D32	Pure Oil, Red Hills Unit #1	s32,330fsl,2310fel	3332	1192	1067	1042	945	927	875
W32	N. H. Wills, Cont. State No. 1	s32,1980fsl,660fel	3391	1224	1096	1070	971	956	900
W36	M. M. Wilson, Marathon State #1	s36,660fsl,660fwl	3325	1334	1197	1170	1045	1025	965
A36	Ashmun Hilliard, State #1-36	s36,660fnl,660fwl	3346	1432	1277	1250	1117	1102	1038
		T25S, R34E							
F19	Ashmun&Hilliard, Fed. 2-19 No. 5	s19,660fnl,1980fwl	3346	1437	1287	1260	1104	1085	1023
C27	Tenneco, Conoco Fed. #1	s27,1980fnl,660fel	3339	1265	1119	1083	925	905	852
		T25S, R37E							
S02	Cont., State A-2 #2	s2,2310fsl,1650fel	3163	1095	?	?	?	?	917
L03	G. L. Buckles, Liberty Royalty No. 4	s3,330fsl,990fwl	3143	1290	?	?	?	?	1030
J14	Johnson & French, Fed. "A" #1	s14,560fnl,330fel	3123	1068	990	980	920	912	870
L14	Atlantic Ref., Langlie Fed. #2	s14,1650fsl,1650fel	3115	1065	992	979	919	913	873
W24	Western Natural Gas, Wimberly #4	s24,1980fnl,990fwl	3087	973	915	906	838	830	790
		T26S, R30E							
K04	Aztec, Fed. K.W. No. 1	s4,660fnl,660fwl	3179	?	1257	1225	1133	1115	1046
B06	J. G. Bennett, No. 1 Brunson Fed.	s6,660fsl,660fwl	3059	1162	978	948	?	?	815
		T26S, R32E							
C05	F. Pool, Conoco Bradley #1	s5,660fnl,1980fwl	3282	1685	1567	1542	1460	1445	1388
B15	Brown&Krug, Ben Fed. #1	s15,NE/4 of SE/4	3177	956	798	768	667	650	589
R19	Cont., Russell Fed. 19 No. 4	s19,660fsl,1980fwl	3180	1595	1467	1453	1350	1335	1280
F25	Cont., Wilder #12	s25,660fsl,660fel	3113	1006	847	830	702	684	623
E25	Cont., Wilder #10	s25,1980fnl,660fel	3130	1034	874	852	717	698	633
J25	Cont., Wilder #23	s25,990fnl,990fwl	3133	963	794	770	662	643	583
I25	Cont., Wilder #15	s25,660fnl,1980fwl	3131	967	813	792	672	653	587
H25	Cont., Wilder #14	s25,1980fnl,660fwl	3124	967	802	780	664	648	590
A25	Cont., Wilder #6	s25,1980fnl,1980fwl	?	975	816	798	676	656	593
G25	Cont., Wilder #13	s25,1980fsl,660fel	3122	1020	855	828	708	687	625

GEOPHYSICAL LOG DATA
(Continued)

Well Identifier	Name of well	Location	Ref. Elev.	Top S	Top u.l.	Top C	Top T	Top M	Top F-N
B25	Cont., W.W. Wilder No. 7	s25,1980fsl,1980fel	3122	987	825	805	682	665	600
C25	Cont., W.W. Wilder #8	s25,1980fnl,1980fel	3131	994	828	807	687	670	595
D25	Cont., W.W. Wilder Fed. #9	s25,660fnl,1980fel	3130	1005	848	824	708	690	623
K25	Cont., Wilder 25 Fed. No. 1	s25,330fsl,330fwl	3113	930	765	745	620	600	540
		T26S, R33E							
L17	Gulf, Fed. Littlefield DP Optional #1	s17,660fsl,660fwl	3264	1095	956	930	826	808	740
P30	Cont., Payne #3	s30,1980fsl,660fwl	3122	1055	897	876	746	727	659
		T26S, R34E							
Y03	Gulf, Gulf Yates Fed. #1	s3,660fnl,1980fwl	3414	1235	1084	1052	926	915	856
B19	Cont., Bradley 19 #2	s19,1980fsl,1980fel	3392	1115	972	943	830	810	744
L20	M. Wilson, Leonard Fed. No. 1	s20,660fnl,660fel	3332	1005	862	833	714	699	635
		T26S, R36E							
S05	Cities Service, Sand Hills Unit #9-A	s5,660fsl,660fwl	?	1203	1168	1152	1117	1102	1054
		T26S, R37E							
J04	Jal Oil, Farnsworth #6	s4,990fsl,990fwl	?	1265	1156	1145	1045	1034	983
L11	Stanolind, U.S.A. Leonard Oil No. 1	s11,660fsl,660fel	3013	1163	?	?	981	972	932
		T26S, R38E							
F07	Forest Oil, Fed. Lowe #1	s7,1980fsl,660fwl	3032	1194	1102	1082	?	?	970

APPENDIX III

X-Ray Diffraction

X-RAY DIFFRACTION DATA

The interpreted x-ray diffraction (XRD) data for samples distributed throughout the Rustler from WIPP 19 and H-12 are presented in tables attached to this section. The data are only generally semi-quantitative and are limited by procedures (SOP for XRD at end of this Appendix) to major evaporite minerals. Clays have not been included in this investigation.

Two features of this XRD study are somewhat unusual. Quartz occurs more frequently and more abundantly than expected in purer chemical sediments, and dolomite and high magnesium calcite are more ubiguitous than expected. The carbonate phases are apparent through petrography, and XRD confirms the Mg content. Further petrographic study might be necessary to evaluate the significance of carbonate where a dolomite as well as probable high magnesium calcite occur.

X-RAY DIFFRACTION - H-12

NO*	GYPSUM	ANHYDRITE	QUARTZ	HALITE	DOLOMITE	CALCITE	POLYHALITE	OTHER
1				XX				
5	x	?tr	X	tr	x	? Mg calcite		? feldspar
8			X	x	x			? feldspar
10			X	X	x	? Mg calcite		? feldspar
12			X		x	? Mg calcite		
13			X	X	x	? Mg calcite		? feldspar
15		x	X	X	x	x Mg calcite		? feldspar
19		x	X	X				
23			? tr	X				
25		X	tr	tr				
28			x	X				
31		x		X				
33		XX						
36			X	x				
39			X	x	X	x		
41	X				X			
42	X			x	x?			
46		XX						
50		X		x				prob.elec.err
51		X		X				
52		x		X				? magnesite tr
54		tr		X				
58		tr	x	X				
59		tr	x	X				
61		tr	x	X				
62		X		?tr				X magnesite
63		X			x?		?tr	
64		XX					?tr	
65		XX		?				
67		X			x		?	
68		X		x				
71	X		x	tr?	x		?	
73	X		tr	tr?	x	x?		
74	tr	X						
76			x		X			
79		x	X	x	x			
80			X	X	x			
81		X		tr?				
82		X			x			

KEY: XX - sole or overwhelming mineral
X - major
x - minor
tr - trace
? - questionable
Mg calcite - magnesium-rich calcite, generally >20% Mg
*Sample Number

X-RAY DIFFRACTION - WIPP 19

NO*	GYPSUM	ANHYDRITE	QUARTZ	HALITE	DOLOMITE	CALCITE	POLYHALITE	OTHER
1		X	x	x				
2		tr	X	x		? Mg calcite		unidentified
4	x		X		x	? Mg calcite		unidentified
5		tr	X	x	x	?		unidentified
6	tr	tr	X	x	x			
10			X	X	x			
11		x	X	X				
12		X		x				
14		x	x	X				
20	X		x					
23				?	X			
24			x	x?	X			
25			tr		X			
38	X	tr				x		
39	X					x		
40	X	X				tr		
41		XX						
42		X				tr		
43		X	x					
44	x	X	tr		x			
46	X	tr	X		X			
47	?	X			X			
49	X	x						unidentified
50	XX							
55			X		x	?tr		? Feldspars
57	x	tr	X	X		? Mg calcite		
60		XX						
62		XX		tr?	x			
63	x	X			?tr			

KEY: XX - sole or overwhelming mineral
X - major
x - minor
tr - trace
? - questionable
Mg calcite - magnesium-rich calcite, generally >20% Mg
unidentified - unidentified minor peaks
*Sample Number

STANDARD OPERATING PROCEDURE

X-RAY DIFFRACTION ANALYSIS

RUSTLER FORMATION

Dennis W. Powers

Robert M. Holt

October 13, 1986

GENERAL

This procedure is developed for use on samples from the Waste Isolation Pilot Plant (WIPP) project to determine mineralogy and qualitative to semi-quantitative mineral proportions from samples from the Rustler Formation. The techniques presented here are collectively based on experience of the authors and well-known sources such as Mueller (1967) and more recent literature (e.g. Fang and Zevin, 1985).

OBJECTIVES

There are two principal objectives for the X-ray diffraction work on samples from the Rustler Formation:

a) provide a basic comparative mineralogy for the Rustler based on regular sampling procedure from available core, and

b) provide specialized mineral identification (e.g. clays or rare mineral phases) for further interpretive work.

The first objective is met through a sampling program from two boreholes (WIPP 19 and H-12) which provide a general sampling from both near the site center and in an area near the depocenter for parts of the Rustler. Samples were collected at regular spacings to provide a general representation of the mineralogy of the formation. The second objective is met through some initial specialized sampling of minerals and features of particular interest and through separation and/or concentration of mineral phases of interest from these special samples or from regularly spaced samples.

METHODS

Sample Preparation

A sample of the core will be selected for XRD analysis; general samples will usually be about 20-100 gms in weight while specialized samples may be as small as an individual crystal. The sample will be visually selected to be representative of the core specimen or to be a sample consistent with the analytical objective.

The sample will be individually stored in a plastic canister labeled by the sample identifier. The sample will be crushed in a mortar and a smaller amount, as a subsample, will be ground in an agate mortar with an agate pestle to obtain powder of the order of 10Ì in maximum diameter. A small amount of

Si metal or powdered fluorite (CaF_2) will be added to provide an internal standard peak. General mineralogy samples will be approximately unoriented samples obtained by sprinkling powder onto a glass slide with vaseline on the surface.

Specialized samples may be prepared differently. Clay samples may be obtained after concentration of the clay fraction through dissolution of water and/or acid soluble portions (Bodine and Fernalld, 1973; Bodine, 1978). Clay identification will be made on the basis of three general tests (Carroll, 1970; Millot, 1970):

a) oriented sample
b) oriented sample treated with ethylene glycol
c) oriented sample heated to 550°C.

Oriented samples will be made in triplicate by sedimentation onto glass slide from water (with Calgon) suspension or by soaking the sample with acetone on the slide. Samples to be treated for ethylene glycol will be moistened and placed for 24+ hours in a desiccator with liquid ethylene glycol in the bottom. Heated samples will be kept at 550°C for a period of at least 1 hour, and will be X-rayed within four hours of heating. Samples will be kept in a desiccator with desiccant as appropriate during the interval.

Other special techniques of importance will be documented as carried out.

X-ray Diffraction

All XRD work for this project will be done with Cu K_α radiation with a Ni filter to eliminate Cu K_β-radiation. The current and voltage will be set at 18 mA and 30 kV, respectively for all runs. Scaling and time factors will be established each day, and will be as uniform as is reasonably possible. These parameters will be recorded for each trace of any sample.

For general samples, a speed of 2°/minute for the goniometer and a chart speed of 1"/minute will be used. Each sample will be examined through 2-35° 2θ. The trace will be compared to an artificial pattern for common minerals. Peaks not in this set will be identified by satndard methods of comparing peak intensities to patterns within ASTM card files. Peaks not identified by this methods will be noted for possible further work.

Special samples will be characterized through an appropriate range of 2θ and with modified chart and goniometer speeds as appropriate to the type of sample.

Interpretation

All identified minerals will be listed and note taken of unidentified or unidentifiable peaks. The relative intensities of mineral peaks will be used to assigned general abundance descriptors: major, minor, trace. As appropriate, certain mineral combinations, such as gypsum and anhydrite, may be assigned semi-quantitative proportions based on comparison of peak heights with artificial mixes. Records of these mixes will also be kept for checking.

Safety

All operators of XRD equipment will meet Department of Geological Sciences training requirements. All operators are required to wear monitoring badges for exposure to radiation. These badges are checked periodically by the University.

Quality Assurance

All operators are experienced in the use of XRD equipment for mineral analysis. Holt and Powers will provide supervision of the sample preparation and equipment operation periodically to ensure that record-keeping is appropriate.

All samples are marked with unique identifiers. Subsamples and all subsequent slides and traces will be immediately marked with identifying sample numbers and modifiers (e.g. G or H to denote glycolated or heated, respectively) as appropriate. Patterns will be individually marked with equipment operating parameters. Traces will be maintained in a file. An individual worksheet will be prepared with a summary of important information, including mineral identification for each sample (see attached).

REFERENCES CITED

Bodine, M.W., Jr., 1978, Clay-mineral assemblages from drill core of Ochoan evaporites, Eddy County, New Mexico: Circ. 159, New Mexico Bureau of Mines and Mineral Resources, pp. 21-31.

Bodine, M.W., Jr., and Fernalld, T.H., 1973, EDTA dissolution of gypsum, anhydrite, and Ca-Mg carbonates: Jour. of Sedimentary Petrol., v. 43, pp. 1152-1156.

Carroll, D., 1970, Clay Minerals: a guide to their X-ray identification: Spec. Paper 126, Geol. Soc. Am.

Fang, J.H., and Zevin, L., 1985, Quantitative X-ray diffractometry of carbonate rocks: Jour. of Sedimentary Petrol., v. 55, pp. 611-613.

Millot, G., 1970, Geology of Clays: Springer-Verlag, New York, Heidelberg, Berlin, 429 p.

Mueller, G., 1967, Methods in sedimentary petrology: Hafner Publishing Co., New York, London, 283 p.